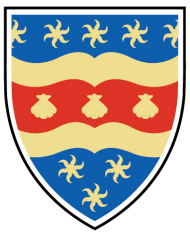

UNIVERSITY OF
PLYMOUTH

Neuronal Network Oscillations in the Control of Human Movement

by

Edward Rhodes

A thesis submitted to the University of Plymouth
in partial fulfilment for the degree of

DOCTOR OF PHILOSOPHY

School of Psychology

February 2019

Acknowledgements

FIRST and foremost, I'd like to acknowledge the supervision and guidance I have received from Professor Stephen Hall. He created a work environment that allowed me to make my own mistakes and produce a body of work that I can be proud of. He was also there when required to remind me that, while data analysis is interesting, this thesis would not write itself. This, I hope, is only the beginning of our research collaboration.

Professor Jonathan Marsden provided an ideal sounding board when it came to deciding the direction this thesis would take. His insightful comments never failed to improve my work.

Two of the studies described in this thesis came from one meeting with Dr. William Gaetz. He has a knack for making the incredibly complex sound simple to achieve. A skill I can now say I am grateful he possesses.

A special thank you goes to my research apprentice Anna Kharko, who not only helped to collect data for the study described in Chapter 3 but also to maintain my sanity throughout the process. A challenge I think only she and I know the true depths of. Also, to the rest of my fellow PhDs, particularly those in the Action Prediction lab, for giving me something to talk about other than work.

Finally and most importantly, I'd like to thank my parents for a lifetime of encouragement and support. Despite them never being quite sure what it is I do, the reason I am able to do so is entirely due to their support and patience. As scientists, we stand on the shoulders of the giants that came before us, and none are so sturdy as those of my family.

Authors declaration

At no time during the registration for the degree of Doctor of Philosophy has the author been registered for any other University award without prior agreement of the Doctoral College Quality Sub-Committee.

Work submitted for this research degree at the University of Plymouth has not formed part of any other degree either at the University of Plymouth or at another establishment.

Word count for the main body of this thesis: **51,461**

Signed: E. RHODES

Date: 24/07/18

Publications:

Rhodes, E., Kharko, A., Gaetz, W.C. & Hall, S.D (2017) *Does post-movement beta rebound inhibit future movement?* Movement Disorders, 32(S2), S1465, DOI: 10.1002/mds.27087

Rhodes, E., Gaetz, W.C., Marsden, J & Hall, S.D. (2018) *Transient alpha and beta synchrony underlies preparatory recruitment of directional motor networks* Journal of Cognitive Neuroscience, 30(6), 867–875 DOI: 10.1162/jocn_a_01250

Posters and conference presentations:

International Congress of Parkinson's Disease and Movement Disorders, Movement Disorders Society, Vancouver, BC. Poster presentation: *Does PMBR inhibit future movement?* 2017.

Cognition Institute Conference, Plymouth University, Plymouth. Invited talk: *Neural oscillations of motor control.* 2016.

7th Annual School of Psychology Conference, Plymouth University, Plymouth. Poster presentation: *Neural oscillations of motor control.* 2015.

Abstract

THE overarching aim of this thesis was to use neuroimaging and neuromodulation techniques to further understand the relationship between cortical oscillatory activity and the control of human movement. Modulations in motor cortical beta and alpha activity have been consistently implicated in the preparation, execution, and termination of movement. Here, I describe the outcome of four studies designed to further elucidate these motor-related changes in oscillatory activity.

In Chapter 3, I report the findings of a study that used an established behavioural paradigm to vary the degree of uncertainty during the preparation of movement. I demonstrate that preparatory alpha and beta desynchronisation reflect a process of disengagement from the existing network to enable the creation of functional assemblies required for movement. Importantly, I also demonstrate a novel neural signature of transient alpha synchrony, that occurs after preparatory desynchronisation, that underlies the recruitment of functional assemblies required for directional control.

The study described in Chapter 4 was designed to further investigate the functional role of preparatory alpha and beta desynchronisation by entraining oscillatory activity in the primary motor cortex (M1) using frequency-specific transcranial alternating current stimulation. No significant effects of stimulation were found on participant response times. However, no clear conclusion could be drawn due to limitations of the stimulation parameters that were used.

In Chapter 5, I explored the inverse relationship between M1 beta power and cortical excitability using single-pulse transcranial magnetic stimulation to elicit motor-evoked potentials (MEPs). The amplitude of MEPs collected during a period of beta desynchronisation was significantly greater than during a resting baseline. Conversely, the amplitude of MEPs collected during the post-movement beta rebound that follows the termination of a movement was significantly reduced compared to baseline. This finding confirms the inverse relationship between M1 beta power and cortical excitability.

The study in Chapter 6 explored the effect of experimental context on M1 beta power. When the participant was cued to expect an upcoming motor task, resting beta power was significantly increased, then when the likelihood of an upcoming motor requirement decreased, there was a significant concurrent decrease in resting beta power. This reflects increased coherence and functional connectivity within M1 and other motor areas, to *'recalibrate'* the motor system in preparation for a synchronous input signal to more readily recruit the required functional assembly.

Key words: Motor control, primary motor cortex, oscillations, beta, alpha, electroencephalography, transcranial stimulation

Contents

List of Figures

List of Tables

Abbreviations

5-HT 5-hydroxytryptamine

AIP Anterior intraparietal sulcus

BA Brodmann's area

BCI Brain-computer interface

BNC Bayonet Neill-Concelman

CMAd Dorsal cingulate motor area

CMAr Rostral cingulate motor area

CMAv Ventral cingulate motor area

CNS Central nervous system

cTBS Continuous theta burst stimulation

DBS Deep brain stimulation

ECoG Electrocorticography

EEG Electroencephalography

EMG Electromyography

EPSP Excitatory post-synaptic potential

ERD Event-related desynchronisation

ERP Event-related potential

ERS Event-related synchronisation

FDI First dorsal interosseous

FEF Frontal eye field

FIR Finite impulse response filter

fMRI Functional magnetic resonance imaging

FS Fast-spiking cells

GABA Gamma-aminobutyric acid

GPe Globus pallidus external

GPi Globus pallidus internal

IPL Inferior parietal lobule

IPS Intraparietal sulcus

IPSP Inhibitory post-synaptic potential

LFP local field potential

L1-6 Layers I-VI

LIP Lateral intraparietal area

LS Late-spiking cells

LTS Low-threshold spiking cells

M1 Primary motor cortex

M1h Primary hand area

MAD Median absolute deviation

MEG Magnetoencephalography

MEP Motor-evoked potential

MRGS Movement-related gamma synchronisation

MUAP Motor unit action potential

PCu Precuneus

PD Parkinson's disease

PEF Parietal eye field

PFC Prefrontal cortex

PMBR Post-movement beta rebound

PMC Premotor cortex

PMCd Dorsal Premotor cortex

PMCv Ventral Premotor cortex

PPC Posterior parietal cortex

PRR Parietal reach region

RMT Resting motor threshold

RSNP Regular spiking non-pyramidal cells

RT Response time

rTMS Repetitive transcranial magnetic stimulation

S1 Primary somatosensory cortex

SCD Scalp-current density

SMA Supplementary motor area

SNr Substantia nigra pars reticulata

SPL Superior parietal lobule

STN Subthalamic nucleus

tACS Transcranial alternating current stimulation

tDCS Transcranial direct current stimulation

tES Transcranial electrical stimulation

TMS Transcranial magnetic stimulation

VA Visual angle

Chapter 1

Introduction

To know the brain . . . is equivalent to ascertaining the material course of thought and will, to discovering the intimate history of life in its perpetual duel with external forces.

– Santiago Ramón y Cajal (1852-1934)

THE central purpose of this thesis is to investigate the role of neural oscillations in human motor control. To use neuroimaging and neuromodulation techniques to further understand the relationship between changes in oscillatory power and the preparation and execution of voluntary movement. This chapter provides an overview of the neural systems involved in human movement, the oscillatory nature of those systems and techniques that can be used to externally modulate oscillatory activity.

1.1 Anatomy of the human motor system

Human behaviour ranges from the simple to the complex, from the avoidance of pain to the production of speech and language. No matter how complicated the behaviour, each one shares a common attribute, that its expression is a motor act. A hand is reflexively withdrawn from a painful stimulus, a complicated pattern of tongue and lip movements combine to say “Hello.” The human motor system has evolved beyond that of any other species, forming increasingly complex connectivity patterns and devoting more cortical resources than any of our predecessors (Kaas, 2004).

Since the late 19^{th} century, knowledge of the motor system has advanced dramatically. Year by year, our overall understanding of its anatomy, histology, and physiology grows ever more complex. These advances have furthered our understanding of the connections between subcortical structures, commonly involved in locomotion across mammalia, and cortical structures, unique to humans and non-human primates.

Early animal studies provided the first evidence of the role of specific brain regions in the

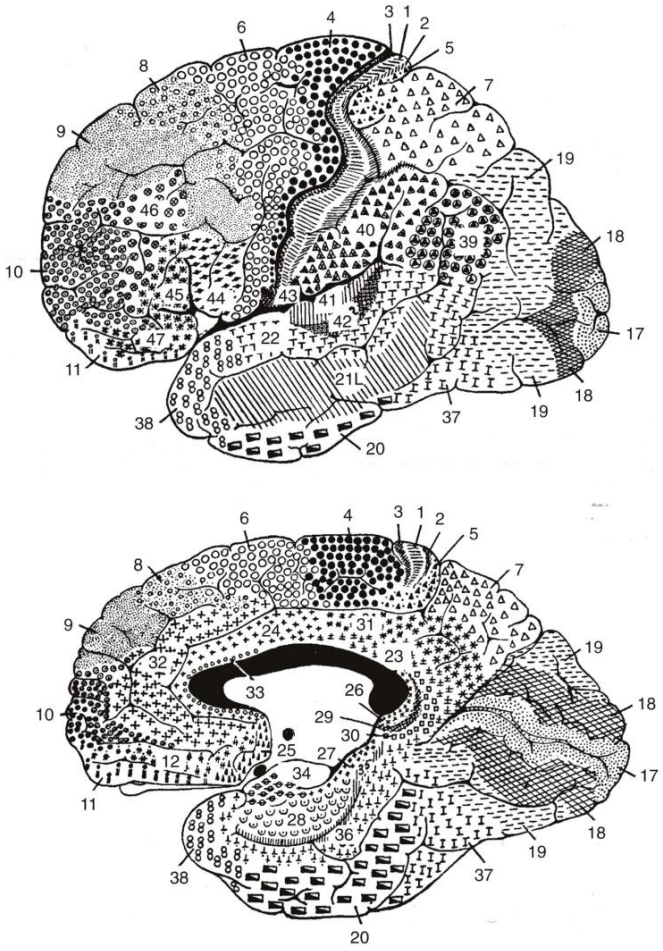

Figure 1.1: Brodmann's (1907) cytoarchitectonic map of the human cerebral cortex. Cortical areas of the lateral (**Top**) and medial (**Bottom**) surfaces. The precentral gyrus, found anterior to the central sulcus, is indicated by black dots and labelled as ***4***. A different pattern represents each distinct cytoarchitectonic region (Brodmann, 1907). BA4 is represented by black circles, while BA6 is represented by white circles.

control of movement by demonstrating that movement deficits can be created by removing cortical tissue from canine (Fritsch & Hitzig, 1870) and monkey (Ferrier, 1876) precentral regions. These early findings, alongside a series of pioneering electrophysiological works by Charles Sherrington and colleagues, in which they stimulated great ape precentral gyri and mapped the elicited motor response, highlighted the importance of precentral regions in motor control (Grunbaum & Sherrington, 1901; Leyton & Sherrington, 1917; Sherrington & Leyton, 1924).

Following identification of the precentral region by Sherrington and colleagues; in 1905, Alfred Campbell tested the hypothesis, that functional specificity of the precentral region is represented histologically. Campbell (1905) took the same tissues Sherrington had operated upon to analyse their cytoarchitecture. The samples' distinct histology led Campbell to conclude: *"it is just as possible to define the motor area on the histological*

bench, as on the operating table" (Campbell, 1905, p. 20).

So confident was Campbell that the cell and fibre architecture he had found in primate brains would equal that of the human cortex, he produced only one map for both primates and humans. Brodmann (1907), a proponent of Darwinian evolution, believed that the human cortex and the primate cortex would share homologous cytoarchitecture, but that the human cortex would have evolved further than that of primates (Zilles & Amunts, 2010). Therefore he produced his separate cytoarchitectonic maps of the primate and the human cerebral cortex (Figure 1.1).

A second research group led by Wilder Penfield also built upon the findings of Sherrington and colleagues by performing electrophysiological investigations of the human precentral gyrus while patients underwent surgery to remove tumours (Penfield & Boldrey, 1937; Penfield & Rasmussen, 1950). They found that, as in apes, humans have a somatotopic organisation with the sites most susceptible to excitation found in the precentral gyrus. They also discovered that hand movement, in particular, was easy to evoke (Figure 1.2). This topographical organisation of the precentral gyrus has since been demonstrated using both electrophysiological (Stoney et al., 1968) and modern neuroimaging techniques (Dechent & Frahm, 2003; Hluštík et al., 2001; Indovina & Sanes, 2001; Zeharia et al., 2015).

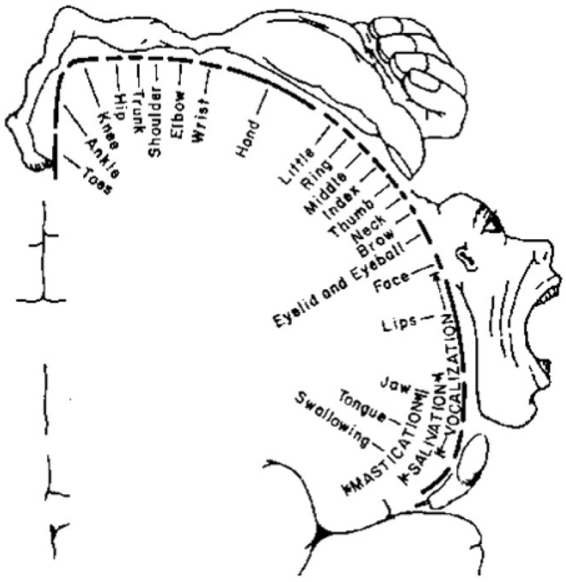

Figure 1.2: Penfield's (1937) motor humunculus. Electrical stimulation of different sections along the precentral gyrus evokes movement of different parts of the body. The body is disproportionately represented in the cortex, with a large volume of cortex devoted to control of the hand.

1.1.1 Cortical motor areas

Brodmann's cytoarchitectonic map (Figure 1.1) distinguished between the precentral and the intermediate precentral cortex, (Brodmann's area (BA)4 and BA6 respectively). Through a series of lesion studies, Fulton (1935) functionally differentiated BA4 from BA6, naming the former the **primary motor cortex** and the latter, the **premotor cortex** (Fulton, 1935). A further subdivision of BA6 was later defined by Woolsey and colleagues (1952) as the **supplementary motor area**, which is found on the medial wall, posterior to the premotor cortex (Woolsey et al., 1952).

In the ensuing years since the work of Fulton and Woolsey, we have developed a greater understanding of the complexity of cortical motor areas. Both animal and human studies have allowed the fractionation of the cortex through characterisation of anatomical, physiological, histological, pharmacological and functional properties. By staining corticospinal projections, Hutchins and colleagues (1988) discovered that the **cingulate cortex** also plays a role in motor control (Hutchins et al., 1988).

Hierarchical connections in motor control

The cortical motor system is hierarchical (Figure 1.3), particularly during the learning, preparation, and execution of complex and novel, goal-directed actions. Prefrontal areas integrate sensory input and abstract information about the schema of the action and its goal. Efferent connections to the supplementary motor area (SMA) and premotor cortex (PMC) then activate neural assemblies for selection of more concrete action before the M1 sequentially innervates, via the pyramidal tracts, the required muscle groups (Badre & D'Esposito, 2007; Koechlin et al., 2003; Koechlin & Summerfield, 2007).

Primary motor cortex

The M1 is named as such because the threshold for evoking movement via electrical stimulation is lower here than in any other region (Dum & Strick, 2004; Penfield & Boldrey, 1937; Sherrington & Leyton, 1924; Woolsey et al., 1952). M1 is located in the precentral gyrus, including the anterior wall of the central sulcus and the anterior part of the paracentral lobule on the medial surface of the hemisphere (see BA4, Figure 1.1). M1 is readily distinguishable from the surrounding cortex as it is the only area that contains giant infragranular pyramidal cells, known as Betz cells, in cortical layer V (Betz, 1874). The size of Betz cell bodies is reported to decrease along a mediolateral

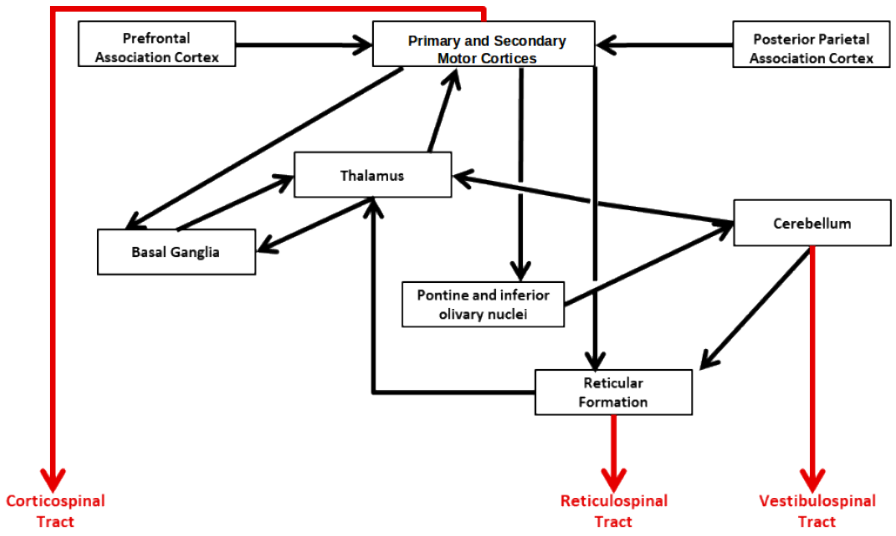

Figure 1.3: A simplified schematic of the hierarchical motor system. The primary and secondary motor cortices receive input from the posterior parietal and frontal association cortices, in order to integrate sensory input and abstract information about the action and its goal. The primary motor cortex innervates, via the pyramidal tracts, the required muscle groups. Sensory and abstract information about the action being performed is then integrated through multiple feedback loops between cortical and subcortical structures.

gradient (von Bonin, 1949; Zilles & Amunts, 2011), in line with the somatotopy found by Penfield and colleagues (Penfield & Boldrey, 1937; Penfield & Rasmussen, 1950). The largest can be located in the foot and leg area of M1 where efferent axons project farthest along the corticospinal tract (Rivara et al., 2003).

Research has consistently shown that while M1 does have a topographic organisation, the theory that there are clear, non-overlapping cortical representations of individual muscles is inadequate. The representations of different body parts are actually intermingled (Cunningham et al., 2013; Donoghue et al., 1992; Park et al., 2001; Sanes & Donoghue, 2000). For example, digits on the hand do not have separate, distinct cortical areas but are represented in an overlapping structure (Olman et al., 2012; Schieber & Hibbard, 1993). It is likely that this representational overlap allows for the functional integration of multiple muscle groups during the execution of a learned behaviour (Nudo et al., 1996). This theory is supported by studies of the macaque cortex which have shown that stimulating the same site results in different combinations of joints and muscle movements depending on the behavioural context at the time of stimulation (Graziano et al., 2002).

Generally, the laminar structure of the cerebral cortex consists of six layers. Until recently, the consensus had been that M1 did not have a layer IV (L4), however, optogenetics has provided evidence of a narrow layer, dwarfed by layers III and V, that is functionally and

histologically consistent with L4 of the primary somatosensory cortex (S1) (Yamawaki et al., 2014). Elsewhere in the cortex, L4 has a dense population of stellate cells which receive afferent sensory input. The lack of such a dense L4 in M1 suggests it receives little afferent sensory information and is indicative of the role it plays as an output station for motor commands.

Layer I

Layer I (L1) contains no excitatory cell bodies (Chu et al., 2003) and approximately 95% of neurons in this layer are inhibitory. The density of these inhibitory neurons was determined using Gamma-aminobutyric acid (GABA) markers (Gabbott & Somogyi, 1986). L1 consists of a prominent horizontal system of axons originating from thalamic and higher order cortical areas (Cauller, 1995; Douglas & Martin, 2004; Sanes & Donoghue, 2000).

Layers II/III

Layer II (L2) and layer III (L3) contain both pyramidal and non-pyramidal cells and receive multiple neurochemical projections including noradrenaline, dopamine, and 5-hydroxytryptamine (5-HT) (Douglas & Martin, 2004). The pyramidal cells receive input from S1 and send axons to layer V pyramidal cells, including Betz cells, and to other pyramidal cells in L2/3. Pyramidal cells in these more superficial layers also project to the contralateral cortex (Cho et al., 2004; Kawaguchi & Kubota, 1997).

There are four subtypes of non-pyramidal cells in L2/3. Fast-spiking (FS), late-spiking (LS), low-threshold spiking (LTS) and regular spiking non-pyramidal (RSNP) cells. These cells are mostly GABAergic with FS and RSNP cells the most common interneuron type (Kawaguchi & Kubota, 1998).

Layer V

As previously mentioned, layer V (L5) of M1 is unique as it contains infragranular Betz cells. These cells can be divided into two subtypes. Type 1 Betz cells project to the striatum, superior colliculus, spinal cord and the basal pons, and exhibit intrinsic burst firing. Whereas, Type 2 Betz cells project to the contralateral cortex or ipsilateral striatum and are regular spiking (Molnár & Cheung, 2006).

L5 receives synaptic input from pyramidal cells in L2/3 (Kaneko et al., 2000) along with dopaminergic projections from the rostral mesencephalon, the nucleus linearis and the ventral tegmental area (Berger et al., 1991; Descarries et al., 1987; Towers & Hestrin,

2008).

Layer VI

The pyramidal cells in layer VI (L6) project to and receive input from the thalamus (Kaneko et al., 2000; Kawaguchi & Kubota, 1997). There is also some reciprocal connectivity between L6 and the deeper laminae of S1 (Douglas & Martin, 2004; Thomson & Lamy, 2007). Both non-pyramidal and pyramidal cells of L6 receive synaptic input from callosal neurons (Karayannis et al., 2006).

Mapping oscillations onto cortical layers

Several studies have begun to investigate the role that specific cortical layers play in the generation of neural oscillations, with the consensus being that more superficial layers are involved in the generation of faster gamma oscillations while slower oscillations originate from deeper cortical layers (Wang, 2010).

Layers L2 and L3, which consist of numerous horizontal connections (Binzegger et al., 2004), have been shown to demonstrate a propensity towards higher frequency gamma-band oscillations (Buhl et al., 1998). The distinction between superficial and deep layers was further demonstrated through the use of in vitro kainate application to the rat S1 (Roopun et al., 2008). This study revealed that after kainate application, distinct rhythms were being generated in different layers: high-frequency gamma in L2 and L3 and slower beta oscillations in L5 (Roopun et al., 2008).

Alpha oscillations, like beta oscillations, appear to be generated within deeper cortical layers. A number of studies have localised alpha synchrony to pyramidal cells within the granular and infragranular layers (Buffalo et al., 2011; Flint & Connors, 1996; Silva et al., 1991; Sun & Dan, 2009). Translaminar studies in dogs and awake macaques have suggested that these L5 cells are the cortical origin of the alpha rhythm (Bollimunta et al., 2008; Silva & Leeuwen, 1977).

It is important to consider the role that laminar structure may play in the generation of different neural oscillations within the brain, and also to consider the role such oscillations play in communication between different cortical layers. Wang (2010) has suggested that, in the light of evidence that beta oscillations are predominantly generated in deeper cortical layers, beta may play a special role in top-down communication. Hypothetically, two reciprocally connected cortical areas, one associated with higher cognitive function and the other with lower sensory function

would share both bottom-up and top-down connections. The 'lower' cortical area would communicate with the 'higher' cortical area through feed-forward projections that originate in the superficial layers, whereas the 'higher' area would mediate the function of the 'lower' area through feedback projections originating from the deeper layers (Barbas & Rempel-Clower, 1997; Douglas & Martin, 2004; Wang, 2010)

Premotor cortex

The term "premotor cortex" was initially coined by Marion Hines (1929) to describe the cytoarchitectonically defined BA6 (Figure 1.1). However, the characterisation of the PMC has been a controversial topic since the early 20^{th} century and has undergone several revisions (Barbas & Pandya, 1987; Dum & Strick, 1991; Fulton, 1935; Wise, 1985; Woolsey et al., 1952). Of all the cortical regions associated with motor control, the PMC appears to be the most evolved in humans when compared to that of the macaque (von Bonin, 1949). The macaque PMC has roughly the same volume as M1, whereas, human PMC is approximately six times larger than M1 (Freund, 2011).

The modern definition of PMC refers only to the lateral PMC; this is because the medial PMC was redefined by Woolsey and colleagues (1952) as the supplementary motor area, an area functionally distinct from the lateral PMC. The lateral PMC can be further divided into the dorsal premotor cortex (PMCd) and the ventral premotor cortex (PMCv) (Rizzolatti et al., 1998). Both PMCd and PMCv lack the giant pyramidal cells found in M1 and can be distinguished from one another by histological analysis of L4. The PMCv is dysgranular with a thin L4 whereas PMCd is agranular (Kaas & Stephniewska, 2002; Shipp, 2005).

The PMC is concerned with the voluntary control of action, dependent on sensory input. It receives input from the parietal and frontal association cortices as well as S1 and projects via pyramidal cells to M1 and the spinal cord. The threshold for stimulation of the PMC is higher than that for M1 and stimulation elicits gross movements that require the coordination of multiple muscle groups (Afifi & Bergman, 2005).

Supplementary motor area

The SMA was first defined by Woolsey and colleagues (1952) and is located on the medial surface of BA6 (Figure 1.1), anterior to the medial extension of M1. The SMA can be further subdivided based on its cytoarchitecture and neurochemistry into the pre-SMA and the SMA (Matsuzaka et al., 1992; Picard & Strick, 2001; Zilles et al., 1995).

The SMA has reciprocal connections with M1 and projects directly to the corticospinal tract (Dum & Strick, 1996; He et al., 1993; Wise, 1996). In contrast, the pre-SMA has sparse projections to the corticospinal tract and no connection to M1 (Luppino et al., 1993, 1994). Both the SMA and the pre-SMA are part of cortico-subcortical loops with the basal ganglia, thalamus and cerebellum (Akkal et al., 2007; Inase et al., 1999; Nambu et al., 1996).

The SMA holds a somatotopic map of the whole body, arranged along a rostrocaudal gradient, with hindlimb representations in the caudal sites, and forelimb and orofacial representations in rostral sites (Fried et al., 1991; Matsuzaka et al., 1992; Mitz & Wise, 1987). Increased activity is consistently seen in the SMA immediately prior to hand movements (Nambu et al., 1996; Tanji & Kurata, 1982; Wilson et al., 2014b). Scalp recordings have also revealed a slowly increasing negative potential centred over SMA known as the *Bereitschaftspotential* or 'readiness potential' (Deecke & Kornhuber, 1978). The Bereitschaftspotential is greater preceding self-initiated movement than externally cued movement, suggesting SMA plays more of a role in voluntary movement than in response to external stimuli (Nachev et al., 2008; Tanji & Kurata, 1982).

Electrical stimulation of the pre-SMA rarely evokes movement, except in areas closer to the border with SMA, which evoke forelimb movements. This is likely due to pre-SMA contributing very little to the corticospinal tract (Luppino et al., 1993, 1994) compared to SMA which provides approximately 10% of corticospinal cells (Dum & Strick, 1991; He et al., 1993; Wise, 1996). Neuroimaging studies have shown greater activation in pre-SMA during self-initiated movement than externally-cued movement (Cunnington et al., 2002; Deiber et al., 1999; Jenkins et al., 2000). Both pre-SMA and SMA appear to play an important role in the planning and execution of sequential movements with greater neural response found in the former (Shima & Tanji, 2000; Sohn & Lee, 2007; Tanji & Shima, 1994).

Cingulate cortex

The cingulate cortex is located along the medial wall of the cerebral hemisphere, ventral to the SMA and M1, and spans both BA23 and BA24 as well as sections of the medial portion of BA6. In the macaque, three distinct subdivisions of the cingulate cortex have been found. A rostral motor area (CMAr) and two caudal motor areas: one located on the ventral bank of the cingulate sulcus (CMAv) and the other on the dorsal bank

(CMAd)(Paus, 2001). Picard and Strick (2001) performed a meta-analysis of numerous imaging studies of the human cingulate cortex and concluded that there are human homologues for each of these three motor areas. A finding later confirmed by modern functional magnetic resonance imaging (fMRI) (Amiez & Petrides, 2012).

These three cingulate motor areas all appear to contain somatotopic representations of the body (Dum & Strick, 1991; Luppino et al., 1991; Morecraft et al., 1996; Wang et al., 2001). CMAr contains a face, hand and leg representation, CMAv contains a hand and leg representation, and CMAd contains two arms and a leg representation (Amiez & Petrides, 2012; Dum & Strick, 1993; Luppino et al., 1991).

Beckmann and colleagues (2009) investigated the probabilistic connectivity of the cingulate cortex using magnetic diffusion tractography. They identified nine distinct clusters, three of which likely correspond to the three described cingulate motor areas. Clusters 4, 5 and 6 represent CMAr, CMAd, and CMAv respectively. Their study revealed that each cingulate motor area is interconnected as well as having projections to and receiving input from the PMC, SMA, M1 and the dorsal striatum (Beckmann et al., 2009). CMAd and CMAv both have reciprocal connections with the parietal association cortex while CMAr has a reciprocal connection with the frontal association cortex.

Frontal association cortex

The frontal association cortex, or prefrontal cortex (PFC), is the most rostral portion of the neocortex; located anterior to SMA, PMC, and M1, and constitutes nearly a third of the total volume of the neocortex. The PFC consists of BA8, 9, 10, 11, 12, 13, 44, 45, 46 and 47 (Brodmann, 1907; Petrides & Pandaya, 1994). It is mostly granular, except for the agranular BA44 and the dysgranular BA11 and 47 (Amunts et al., 1999, 2003).

Electrophysiological studies have implicated several regions of the PFC in the control of action. The frontal eye field (FEF) is located on the border of BA8 and the PMC, and when stimulated elicits conjugated eye movements (Bruce & Goldberg, 1985; Chouinard et al., 2003; Ferrier, 1873; Penfield & Boldrey, 1937; Pierrot-Deseilligny et al., 2004). Stimulation of the FEF can also elicit more complex movement associated with attending to stimuli, such as head rotation and pupil dilation. The FEF, therefore, is often implicated in anticipatory and goal-directed actions, for which ocular motility is essential (Fuster, 2015). The FEF receives both proprioceptive and visual information and has reciprocal connections with both primary and secondary motor cortical and subcortical

regions (Sawaguchi et al., 1989).

Single-unit recordings of primate PFC have allowed researchers to investigate the extent of prefrontal involvement in the execution of complex motor plans. Averbeck and colleagues trained macaques to copy geometric shapes. They found multiple cell assemblies that encode shape, the trajectory of movement and the sequence of movements required to draw the selected shape (Averbeck et al., 2003, 2006; Averbeck & Lee, 2007). Additional evidence that PFC assemblies encode complex sequences of action was found by Shima and colleagues (2007).

Posterior parietal cortex

The posterior parietal cortex (PPC) is located in the parietal lobe, anterior to the visual cortex and posterior to the S1. It is therefore ideally situated to receive both visual and somatosensory input. The PPC is divided by the intraparietal sulcus (IPS) into the superior parietal lobule (SPL) and the inferior parietal lobule (IPL) (Damasio, 2005). Several subdivisions have been identified in the macaque PPC that relate to motor functions. For example, the lateral intraparietal area (LIP) has been implicated in the control of eye movements, the parietal reach region (PRR) in the control of reaching and pointing and the anterior intraparietal sulcus (AIP) in the control of hand grasping actions (Culham et al., 2006).

In the macaque, the LIP is activated when a monkey plans a saccade to or attends to a location in the receptive field (Colby, 1998). It also appears to code space in retinotopic coordinates and updates the receptive fields of its neurons in anticipation of an upcoming saccade (Andersen et al., 1985; Cohen & Andersen, 2002; Duhamel et al., 1992). In humans, parietal lesions have been correlated with a slowness of eye movement (Pierrot-Deseilligny et al., 1991) and neuroimaging studies have suggested the parietal eye field (PEF) as the likely homologue to the macaque LIP (Koyama et al., 2004; Medendorp et al., 2003; Müri et al., 1996).

The PRR consists of two regions of the macaque PPC: the medial intraparietal area and area V6a (Andersen & Buneo, 2002; Buneo et al., 2002). Single-unit recordings of macaque PRR have shown its selectivity for reaching actions (Fattori et al., 2001; Johnson et al., 1996). Perenin and colleagues have suggested that lesions to the human PPC, mainly the SPL and precuneus (PCu), result in optic ataxia (Karnath & Perenin, 2005; Perenin & Vighetto, 1988). Neuroimaging studies are yet to identify a true human

homologue to the macaque PRR, however, there has been some suggestion that the medial IPS responds similarly to the macaque medial intraparietal area (Grefkes et al., 2004; Grefkes & Fink, 2005) and that perhaps, in line with lesion studies, the PCu may be homologous to the PRR (Astafiev et al., 2003; Connolly et al., 2003).

The PPC appears to be involved in integrating sensory information about an object to facilitate the grasping of that object. In particular, the AIP of the macaque has been shown to contain neurons that respond when performing an action to grasp an object, even when that object is not visible, and when a graspable object is viewed in the absence of any action (Gallese et al., 1994; Gardner et al., 2002; Murata et al., 2000; Taira et al., 1990). Lesion studies in humans suggest that an IPS lesion can result in deficits in grasping with the contralateral hand (Binkofski et al., 1998). Neuroimaging studies have confirmed that the anterior IPS is a likely candidate to be the human homologue of the macaque AIP (Binkofski et al., 1998; Creem-Regehr & Lee, 2005; Culham et al., 2003; Frey et al., 2005).

1.1.2 Subcortical motor areas

These structures play an essential role in the human motor system. They receive inputs from both peripheral sensory systems and cortical motor areas. That information is then processed through recurrent feedback loops to provide outputs that contribute to the timing, sequencing, and learning of movement.

Basal ganglia

The term 'basal ganglia' is somewhat of a misnomer as it actually refers to a collection of nuclei located below the cortex, in the forebrain and midbrain. These nuclei include the subthalamic nucleus (STN), the substantia nigra pars reticulata (SNr), the globus pallidus internal (GPi), the globus pallidus external (GPe), and the dorsal striatum, which is made up of the putamen and the caudate nucleus.

The dorsal striatum acts as the main relay for direct, excitatory neocortical inputs. With the vast majority of afferent axons originating from L5 of the primary and secondary cortical motor areas (Dudman & Gerfen, 2015). Over 90% of the striatal neurons that act as targets for these neocortical projections are GABAergic and can be divided into two basal ganglia circuits: 'direct' and 'indirect.' The direct circuit provides input to the GPi and the SNr; whereas, the indirect circuit provides input to the GPe and to the STN, which

then provide excitatory projections to the GPi, SNr and back to the striatum (Gatev et al., 2006; Smith et al., 1998).

The traditional view of these two circuits is that the direct circuit facilitates movement, whereas, the indirect circuit inhibits movement (Gatev et al., 2006; Surmeier et al., 2005). A more recent optogenetic study supports this view. Researchers showed that bilateral excitation of the indirect circuit resulted in a Parkinsonian state, with increased freezing and bradykinesia. On the other hand, excitation of the direct circuit reduced freezing and bradykinesia (Kravitz et al., 2010).

The output nuclei of the basal ganglia are the SNr and the GPi. The SNr projects efferents to the superior colliculus and the thalamus, while the GPi projects to different regions of the thalamus, the centromedian thalamic nucleus and the habenula (Parent & Hazrati, 1995).

Thalamus

The thalamus is the largest region of the diencephalon, caudal to the brainstem and rostral to the cerebral cortex. The motor thalamus receives afferents from the output nuclei of the basal ganglia, GPi and SNr; from the dentate and interposed nucleus of the cerebellum; and from the cerebral cortex (Bosch-Bouju et al., 2013). Efferents from motor thalamic nuclei project to L1, L2, and L5 of the primary and secondary motor cortices (Hooks et al., 2013; McFarland & Haber, 2002). Interestingly, the laminar origin of cerebral input to the thalamic nuclei seems to determine whether a reciprocal or non-reciprocal loop is created. Projections from L5 of primary and secondary motor cortices tend to be reciprocated whereas projections from L6 tend to target nuclei that have efferents to a different cortical region (Fang et al., 2006; Haber & Calzavara, 2009; McFarland & Haber, 2002; Rouiller et al., 1999).

Several studies have shown that lesions in the thalamus can result in both akinesia (Klockgether et al., 1986; Wüllmer et al., 1987) and ataxia (Bornschlegl & Asanuma, 1987) along with deficits in postural maintenance (Jeljeli et al., 2003; Starr & Summerhayes, 1983) and motor learning (Canavan et al., 1989; Goldberg & Fee, 2011).

Cerebellum

In humans, the cerebellum is located in the posterior cranial fossa, contains over half the neurons of the central nervous system and constitutes approximately 10% of total brain

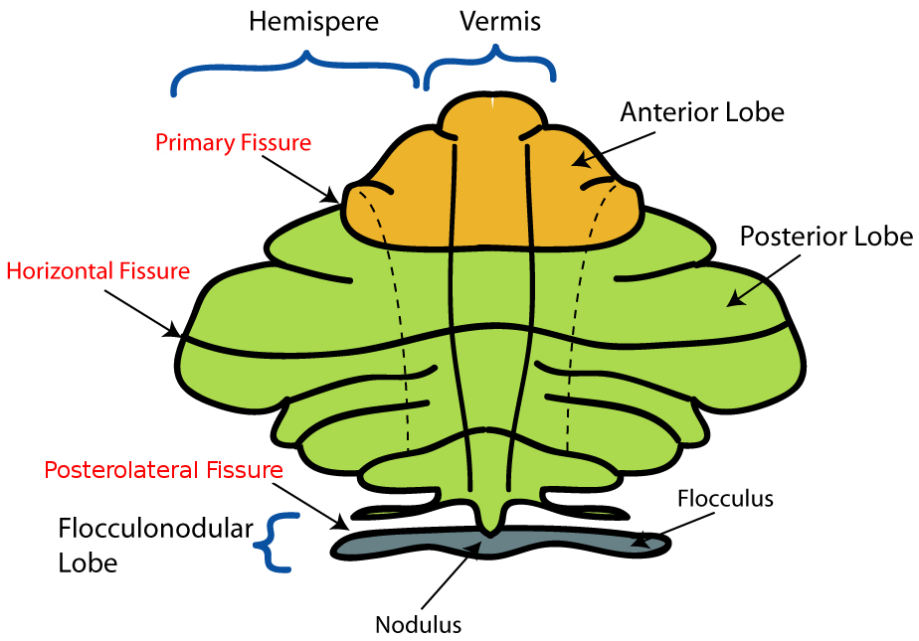

Figure 1.4: An inferior view schematic of the unfolded cerebellum. The schematic shows the location of the vermis and the three lobes of the cerebellum. Figure modified with permission from Nrets, the original uploader at English Wikipedia - Transferred from en.wikipedia to Commons., CC BY-SA 3.0

volume (Molinari, 2002). The cerebellum can be subdivided based on its anatomical markers; the vermis sits between the two hemispheres, then each hemisphere can be divided into three distinct lobes (Figure 1.4). The primary fissure separates the anterior from the posterior lobe, and the posterolateral fissure separates the posterior from the flocculonodular lobe (Larsell, 1970).

The cerebellum is unlike the motor cortex and basal ganglia in that it does not play a primary role in motor function. At least not in the sense that it directly innervates alpha motor neurons. Instead, it acts as a regulator or modulator of motor output through the integration of sensory input (Ghez & Thatch, 2000; Ito, 1984). In essence, a motor plan is received from the primary motor cortex before movement execution. The cerebellum then compares this motor plan to somatosensory, auditory and visual input during the implementation of the planned movement. Once this comparative processing is complete, feedback is outputted to primary and secondary motor cortices to adjust movement accordingly.

1.1.3 Human and non-human primate homologues in hand control

Much of what we know about the human motor system comes from our understanding of the anatomy and physiology of non-human primates. It is important then to evaluate the

similarities between human and primate motor systems in order to assess the efficacy of making assumptions about human motor control from animal studies. Due to the macaque being by far the most common non-human primate to be used in neurological studies most of the discussion below will be a comparison between macaques and humans.

The genetic divergence between macaques and humans is estimated to have occurred around thirty million years ago (Patterson et al., 2006; Steiper et al., 2004), therefore, one would expect there to be significant differences between the anatomy of the two species. However, this difference is not immediately obvious in the musculoskeletal control of action, with both species sharing similar muscle structure of the forelimb and being capable of performing the same hand movements such as precision grip, reaching and grasping.

One very clear and obvious distinction between the human and macaque brain structure is the difference in mass. The human brain is proportionally 4.8 times the size of that of the macaque (MacLeod et al., 2003). This difference in brain size is not simply due to a proportional increase, as neuron size does not easily scale up with body size. Instead, the number of neurons within the human brain is significantly greater than that of the macaque. For example, humans have three to four times the number of descending fibres in the corticospinal tract compared to the macaque (Courtine et al., 2007; Nakajima et al., 2000).

The increase in neural density is also accompanied by an increase in the number of specialised subregions within the brain (Krubitzer & Huffman, 2000; Orban et al., 2004; Saygin & Sereno, 2008). As a result of this increased mass and fractionation, the human neocortex is 35% larger than would be expected in a similarly sized primate (Rilling & Insel, 1999). Within the motor system, a clear distinction can be made between the macaque and human PMC. The macaque PMC has approximately the same volume as M1, whereas, human PMC is approximately six times larger than M1 (Freund, 2011).

Despite these more global differences between the macaque and human brain, a number of studies have demonstrated that there are homologous areas within the motor system of the two species. Human/macaque homolgues have been found within the M1 (Chouinard & Paus, 2006), the PMC (Chouinard & Paus, 2006; Chouinard et al., 2003), the cingulate cortex (Amiez & Petrides, 2012; Picard & Strick, 2001), the parietal cortex (Astafiev et

al., 2003; Frey et al., 2005; Grefkes & Fink, 2005; Koyama et al., 2004; Medendorp et al., 2003; Müri et al., 1996) and the SMA (Picard & Strick, 1996).

The human brain has clearly become more specialised than that of non-human primates, which may explain why humans are capable of executing far more complex movements. However, there are clear similarities between primate species and much can be learned about the human motor system from the study of our closest relatives. Despite differences in overall brain structure, many of the mechanisms that underlie neural communication are identical between species. Primate studies allow researchers to investigate such mechanisms in far greater detail than will ever be possible in human experiments.

1.2 Neural oscillations

Hans Berger, in 1929, was the first to describe neural oscillations in the human brain. He described how alpha wave (~ 8–$12Hz$) oscillatory activity recorded from the scalp was attenuated when the subject's eyes were open compared to closed.

Berger's observations of reduced oscillatory activity during conscious, wakeful behaviour and increased oscillatory power during unconscious states such as anaesthesia and epilepsy, led researchers to dismiss oscillations as having no functional role in cognition (Adrian & Yamagiwa, 1934).

More recently, however, the study of oscillations has once again become a major topic of interest with numerous studies reporting complex oscillatory activity throughout the central nervous system (CNS). Several frequency bands, other than the alpha activity described by Berger, have been associated with various cognitive functions (Table 1.1). This pervasiveness of oscillatory activity at all organisational levels, from single cells to large-scale neural networks, suggests that it is an intrinsic and fundamental property of a functioning CNS and may be the primary mechanism for information processing.

Due to the conductive nature of bone, skin and brain matter, scalp recordings of neural activity lack the spatial resolution required to record individual neurons. Instead, the signals recorded by techniques such as electroencephalography (EEG) and magnetoencephalography (MEG) reflect the activity of a minimum of ten-thousand anatomically-aligned neurons firing in synchrony (Murakami & Okada, 2006; Nunez & Srinivasan, 2006; Srinivasan, 1999). To better understand oscillations on a macroscopic level, we must first understand neural activity at a cellular level.

Table 1.1

Frequency classes of neural oscillations

Frequency Band Name	Frequency Bandwidth (Hz)
Delta (δ)	$0.5 - 3.5$
Theta (θ)	$4 - 7.5$
Alpha/Mu (α/μ)*	$8 - 12.5$
Beta (β)	$13 - 30$
Gamma (γ)	$30.5 - 100+$

**The alpha band is often referred to as the mu rhythm within the sensorimotor system.*

1.2.1 Oscillations at the cellular level

Placing an electrode directly into the axon of a nerve cell allows the monitoring of its membrane potential. The average approximate resting membrane potential is $-70mV$ then, when an action potential is generated, the membrane potential increases to around $40mV$. This change in potential represents the firing of a neuron: the transfer of information via the propagation of an impulse along its axon. The periodic variation in amplitude created by the neuron firing can then be measured as an oscillation.

According to the Hodgkin-Huxley model of action potential generation (Hodgkin & Huxley, 1952), many neurons are individually oscillators. This is because these neurons repetitively fire action potentials at a given frequency in response to a constant current. This periodic activation is mathematically described as a stable oscillatory state.

The firing of a neuron is often referred to as an all-or-nothing response; either the neuron fires or it does not. Extracellular recordings have demonstrated this, showing that the spike in electrical activity generated as the neuron fires has a relatively constant amplitude under stable conditions (Thompson, 1967). The spiking rate of a neuron has been shown to have an intrinsic rhythm which may be generating these measurable oscillations.

There is also evidence to suggest that individual neurons have intrinsic resonant frequencies. The neuron is more likely to fire if it receives an input within a narrow frequency window, its *'eigenfrequency'* (Hutcheon & Yarom, 2000). This eigenfrequency is determined by subthreshold dynamics of the cell membrane potential (Blankenburg et al., 2015). Such subthreshold impedance resonance, as observed in neurons of the inferior olive, have been suggested to act as the neuron's low-pass filter (De Zeeuw et al., 1998; Lampl & Yarom, 1993). In the case of olivary neurons, it is the presence of Ca^{2+} ion channels that allow subthreshold oscillations to be generated (Choi et al.,

2010; Llinás & Yarom, 1986). Recent advancements have now made it possible to determine the history of an individual neuron's firing activity, including its intrinsic resonance, from its gene expression (Tyssowski et al., 2018).

1.2.2 Oscillations at the ensemble level

Generally, several neurons need to fire to cause the reliable firing of an individual neuron (Bruno & Sakmann, 2006; Churchland & Sejnowski, 1999). This also means that when many neurons fire they cause many other neurons to fire. Therefore, ensembles of neurons tend to fire together. Neural ensembles within the same network likely exhibit the same intrinsic resonant frequencies. This is because, if both the sending and receiving ensemble are open to communication during the same narrow frequency window they will be able to effectively communicate (Figure 1.5) (Fries, 2005).

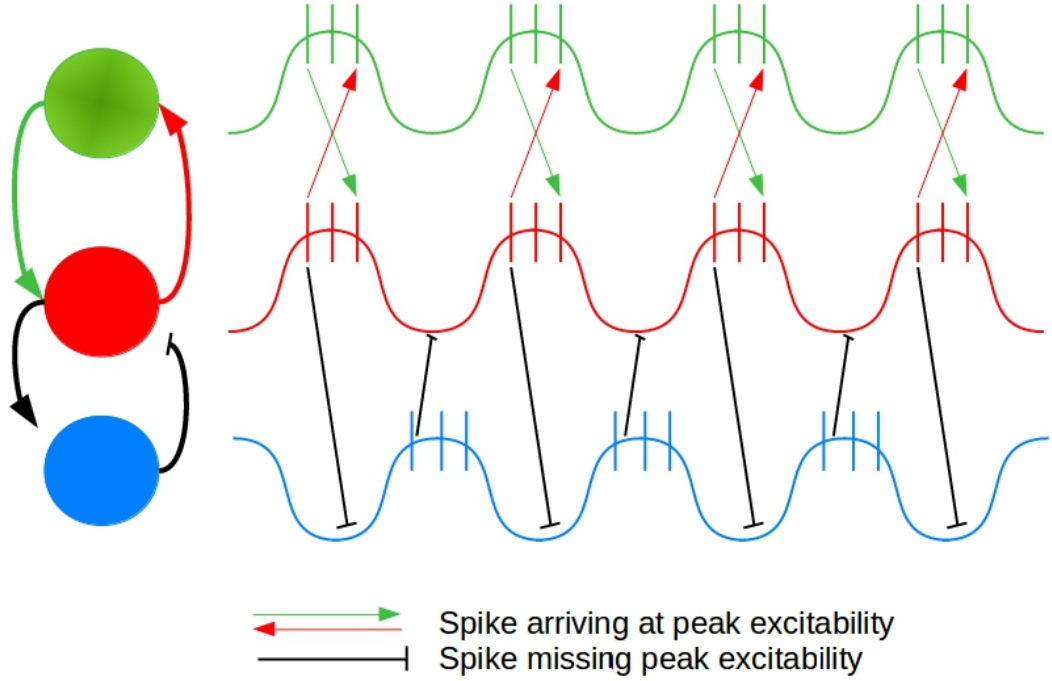

Figure 1.5: Communication through coherence. Red, green and blue circles each represent different neural ensembles. Each wave represents the subthreshold oscillation of the neurons within each ensemble, with the vertical lines representing action potentials. Red and green arrows represent spikes that arrive during peak excitability while black, blunt arrows represent spikes that miss the peak excitability. As the green and red neuronal groups oscillate in synchrony, they are able to communicate effectively. The blue and red neuronal groups are asynchronous and therefore unable to communicate. Adapted from Fries (2005) and Volgushev et al. (1998).

This time window of synchrony is dependent on the distance between ensembles as the spike travelling from sender to receiver must arrive at the excitable phase of the receiver oscillation (Buzsáki & Draguhn, 2004; Schnitzler & Gross, 2005). This is managed by changes in regional myelination along the axonal tree that regulate conduction velocity

to ensure spike arrival is synchronous (Innocenti et al., 1994; Salami et al., 2003). Due to shorter conduction delays, smaller groups of anatomically adjacent neurons tend to exhibit coherent oscillations within the gamma (~ 30–$80Hz$) frequency range (Friedman-Hill et al., 2000; Fries et al., 2002; Maldonado et al., 2000). On a larger scale, neuronal groups within the same networks found in different cortical areas to one another tend to have slower coherent oscillations within the beta (~ 13–$30Hz$) range (Brovelli et al., 2004; Lachaux et al., 2005; Tallon-Baudry et al., 2004).

Within any typical neural circuit, there are two main cell types: excitatory principal neurons and inhibitory interneurons. Three types of synaptic mechanism have been suggested to explain how synchronisation occurs within a circuit: recurrent excitation between principal neurons, mutual inhibition between interneurons and feedback inhibition through the excitatory-inhibitory loop (Wang, 2010).

Recurrent excitation

Synchronisation by recurrent excitation makes intuitive sense. If coupled principal neurons within a network mutually excite one another, then it seems likely that they would do so in synchrony. Support for recurrent excitation as a mechanism of synchrony came when Traub and colleagues demonstrated that blocking synaptic inhibition resulted in robust, synchronous neural firing similar to epileptic discharges (Traub et al., 1989). However, recurrent excitation lacks generalisability across frequency bands. The faster the frequency, the shorter the oscillatory period that synaptic transmission can occur. Synaptic transfer is not fast enough to robustly synchronise principal neurons at faster oscillations, such as gamma.

Mutual inhibition

When the rise time of the synaptic response is longer than the oscillatory period, inhibition generates synchrony rather than excitation (Van Vreeswijk et al., 1994; Wang & Rinzel, 1993; Wang, 2010). Whittington and colleagues used an in vitro study of the rat hippocampus to show that when excitatory glutamate transmission was blocked, $40Hz$ gamma oscillations were observed in pyramidal cells (Whittington et al., 1995). This gamma activity appeared to be generated by GABAergic interneurons, an idea supported by further studies that showed a reduction in frequency once drugs that slowed the kinetics of GABA-A were administered (Traub et al., 1996b; Wang & Buzsáki, 1996; Whittington et al., 1995).

While individual interneurons do not necessarily fire in bursts; when they are coupled they produce alternating patterns of activity (Calabrese, 1998; Wang & Rinzel, 1993; White et al., 1998). This alternation can occur because of spike-frequency adaptation, whereby the presynaptic neuron may reduce its firing rate or stop altogether, releasing the postsynaptic neuron from inhibition. On the other hand, due to intrinsic membrane properties, the inhibited neuron may escape from inhibition and reciprocally inhibit the presynaptic neuron (Marder & Bucher, 2001; Skinner et al., 1994; Wang & Rinzel, 1993).

Excitatory-inhibitory loop

Wilson and Cowan were amongst the first to show that oscillations within a network naturally emerge as a result of reciprocal connections between excitatory and inhibitory neural ensembles (Wilson & Cowan, 1972). Fast excitation increases neural firing to begin an oscillatory cycle; inhibitory interneurons then reduce the level of population activity. Once the excitatory input to the interneurons starts to decrease the network is released from the inhibition, and the next oscillatory cycle begins (Paik et al., 2009; Wang, 2010).

The excitatory-inhibitory loop allows us to understand how coherent oscillations may be generated. For example, FS cells such as those found in layers 2 and 3 of the M1 (Section 1.1.1) and also in thalamic and basal ganglia structures, appear to play a role in the generation of gamma oscillations (Traub et al., 1996a, 1997; Whittington et al., 1995, 2000; Yamada et al., 2016). Extensive networks of FS cells provide synchronous inhibitory post-synaptic potentials (IPSPs) to local excitatory cells (Cardin et al., 2009; Hasenstaub et al., 2005). These IPSPs generate oscillations within the gamma frequency that are then modulated by excitatory feedback from pyramidal neurons (Börgers et al., 2005; Cardin et al., 2009).

In a truly reciprocal network, excitatory inputs drive interneuron firing and, while mutual excitation between principal cells is unable to produce synchronous activity, it amplifies the excitatory activity of the network, enhancing oscillations generated by feedback inhibition (Bathellier et al., 2008; Hansel & Mato, 2003; Wang, 2010). However, synchrony by the excitatory-inhibitory loop is reduced in a network that contains an abundance of mutual inhibition between coupled GABAergic interneurons. This is because the mechanism of mutual inhibition between interneurons is significantly faster (Hansel & Mato, 2003).

1.2.3 Oscillations within a network

As the size of a neural network increases so does the distance between neural ensembles. A better understanding of the complex connectivity properties between these ensembles is key to determining how they can sculpt network oscillations. Several computational models have been put forward to help explain this network architecture. A summary of the more prominent models can be found below.

All-to-all networks

An all-to-all network refers to a hypothetical network; within which every neuron is directly connected with every other. While this is over-simplistic and unrepresentative of the complex neural networks that exist in nature, some useful insights have been formed from its study.

In principle, an all-to-all network should function in the same way as a pair of interconnected neurons, in that when there is zero-phase synchrony between the neurons they will all fire in perfect synchrony. Whereas, if there is a phase shift in the firing of the neurons the resulting network would be entirely asynchronous or consist of a range of complex firing patterns (Wang, 2010).

One such firing pattern that has been observed both computationally (Achuthan & Canavier, 2009; Golomb & Rinzel, 1994; Hansel & Mato, 2001) and in tissue (Bartos et al., 2002), is clustering. This is where the network consists of a number of fixed neural clusters. Within each cluster, the neurons demonstrate zero-phase synchrony, while there is a phase shift between the clusters. The end result is that the neurons in a cluster fire in unison, then different clusters take it in turn to fire. The network oscillation ($\mathbf{F_n}$) can then be calculated as the number of clusters ($\mathbf{C}$) multiplied by the single-cell firing frequency ($\mathbf{F_s}$)

$$\mathbf{F_n} = \mathbf{C} \times \mathbf{F_s} \tag{1.1}$$

Sparse random networks

For a coherent network oscillation to be generated there has to be a minimum level of connectedness. However, due to the sparsity of synaptic connections within the average cortical layer, the probability of two pyramidal cells being connected in either direction is as low as ~ 0.1–0.2 (Lefort et al., 2009; Song et al., 2005; Stepanyants et al., 2007; Wang, 2010).

Modelling studies have shown that there is a non-linear relationship between the number of synaptic contacts a neuron makes in a network and the synchrony of the network. It stands to reason that if the average number of synaptic connections is zero, then each neuron will fire independently; therefore there can be no synchrony within the network. However, it is also not the case that an increase in the number of synaptic contacts increases the overall synchrony. Instead, synchrony can only be achieved once the number of synaptic connections exceeds a certain threshold (Börgers & Kopell, 2003; Wang et al., 1995). Interestingly this threshold seems to remain constant regardless of network size (Albert & Barabási, 2002; Buzsáki, 2006; Wang & Buzsáki, 1996).

This threshold of connectedness varies depending on the network's neuronal composition. This is due to differences between neural types, including intrinsic cellular mechanisms and the biophysics of synaptic interactions (Wang, 2010). For example, in a network of mutually inhibitory, Hodgkin-Huxley type interneurons, the threshold for connectedness is approximately 50 synaptic connections per neuron (Wang & Buzsáki, 1996). If the same network had been made up of 'leaky integrate-and-fire' model neurons, the threshold would be in the thousands (Golomb & Hansel, 2000).

Small world networks

As previously stated, synaptic connections depend on the spatial distance between neurons (see Section 1.2.2), as a result, connectivity cannot be entirely random (Buzsáki et al., 2004; Larimer & Strowbridge, 2008; Morgan & Soltesz, 2008). As the size of the network increases so does the 'path length' (the minimum distance between two neurons through intermediary neurons) and the resulting synaptic delay (Wang, 2010).

The path length can, however, be shortened through the introduction of a small subpopulation of long-range connections between distant parts of the network (Watts & Strogatz, 1998). Buzsáki and colleagues (2004) simulated a network of inhibitory neurons that approximated the rat dorsal hippocampus. They found that network synchrony could be achieved by rewiring 10% of the existing connections from short-range to long-range. Thus, a 'small world network', with a large subpopulation of short-range interneurons interconnected by a small subpopulation of long-range interneurons, is capable of a high rate of synchrony (Lago-Fernández et al., 2000; Buzsáki et al., 2004; Kitano & Fukai, 2007; Yu et al., 2008).

There is, however, a limit to the proportion of long-range neurons in a network. Too few, and distal neural clusters will be asynchronous, too many and the network will be too resource-heavy. Buzsáki et al. (2004) demonstrated little benefit of increasing the proportion of long-range connections above 40%.

Network hubs

A further proposed computational model is that of network 'hubs.' In this model, there are a number of nodes or hubs within the network which are extremely well-connected to the rest of the network (Morgan & Soltesz, 2008). Due to the high degree of connectedness afforded to these hubs they are capable of significantly altering overall network behaviour.

An example can be seen in the GABAergic hub neurons found in rodent hippocampal CA3 networks (Bonifazi et al., 2009). A subpopulation of GABAergic cells were shown to be the top 40% most well-connected neurons in the network. Stimulation of these cells resulted in changes in synchronous network dynamics that did not occur when the other 60% of cells were stimulated (Bonifazi et al., 2009).

The models mentioned above theorise how rhythmogenesis occurs in small, local networks and, therefore, do not necessarily encompass large-scale networks capable of connecting separate brain areas. However, some common themes have emerged. For instance, a network consists of clusters of locally connected, zero-phase neurons; that are interconnected by a small subpopulation of well-connected, long-range cells.

1.3 Neural oscillations of the motor system

There have been several frequency classes of neural oscillations associated with both the resting and active motor system. The most prominent of which are alpha, beta and gamma frequency bands. While the majority of this thesis will investigate lower frequency activity in the alpha and beta ranges, some explanation of the background of gamma activity in the motor system can also be found below.

1.3.1 Alpha

Sensorimotor alpha is often referred to as the mu rhythm thanks to Henri Gastaut who wanted to differentiate the "wicket" rhythm he had found in the rolandic region from the alpha oscillations Hans Berger had observed in the occipital cortex (Gastaut, 1952; Gastaut et al., 1952). However, to avoid confusion, the ~ 8–$12Hz$ rhythm will be referred to as alpha throughout the body of this thesis.

Jasper and Andrews (1938) were the first to demonstrate alpha activity in EEG recordings of the sensorimotor cortex, noting a correlation between a $10Hz$ physiological tremor in the index finger and a $10Hz$ cortical rhythm (Jasper & Andrews, 1938). They also noted that alpha activity appears to be state dependent as the cortical rhythm would disappear when the patient was nervous or agitated, while the tremor still remained.

Gastaut later demonstrated that ongoing rolandic alpha was blocked during reflexive and voluntary movement before subsequently rebounding after the movement (Gastaut, 1952; Gastaut et al., 1952). This movement-related decrease in alpha activity became known as an event-related desynchronisation (ERD) and has since been seen in a range of neuroimaging studies including EEG (Erbil & Ungan, 2007; Leocani et al., 1997; Neuper & Pfurtscheller, 2001a; Pfurtscheller & Aranibar, 1979; Pfurtscheller & Lopes Da Silva, 1999; Stancák & Pfurtscheller, 1996b), MEG (Hari et al., 1997; Jurkiewicz et al., 2006; Salmelin & Hari, 1994) and electrocorticography (ECoG) studies (Crone, 1998a; de Pesters et al., 2016).

Alpha ERD occurs as early as two seconds before movement onset (Crone, 1998a; Leocani et al., 1997; Pfurtscheller & Lopes Da Silva, 1999; Salmelin & Hari, 1994). The onset of the ERD varies dependent on the movement effector, i.e., hand vs. foot. However, the onset is not modulated by the type of movement performed by the same effector, i.e., fast vs. slow finger movements (Stančák et al., 1997). The amplitude of the alpha ERD, in contrast to its onset, does appear to vary with different movement parameters. There was a greater desynchronisation prior to fast finger flexions than slow (Stančák et al., 1997).

Movement-related changes in alpha activity have been seen in bilateral somatosensory and primary motor cortices (McFarland, 2000; Pfurtscheller & Neuper, 1994; Salmelin & Hari, 1994). Similar observations are reported with alpha decreases resulting from somatosensory stimulation; in the absence of movement. Whether it be electrical median nerve stimulation (Nikouline et al., 2000), or tactile stimulation of the finger (Cheyne et al., 2003; Pfurtscheller & Berghold, 1989). These changes tend to have a propensity towards the hemisphere contralateral to the movement/sensation (Arroyo et al., 1993; Hommelsen et al., 2017). There is also evidence to suggest that the early stages of alpha ERD begins more generally across bilateral somatosensory and motor cortices, then becomes more somatotopically focussed in the later stages (Crone, 1998a).

The ERD of alpha power in task-related areas is often accompanied by an event-related synchronisation (ERS) of alpha in motor areas that are not directly required to form the motor output (Fu et al., 2001; de Pesters et al., 2016; Pfurtscheller & Berghold, 1989; Pfurtscheller, 1992). This observation aligns with the *'gating-by-inhibition'* hypothesis (Jensen & Mazaheri, 2010), which suggests that increased inhibition of task-irrelevant areas gates information flow toward the required neural ensemble.

Following the cessation of movement, there is a transient ERS of alpha activity. Unlike the dramatic and exaggerated post-movement ERS of beta discussed below, alpha power slowly returns to its baseline level (Leocani et al., 1997). Again, this finding aligns with the idea that alpha is a correlate of neural inhibition. Desychronising to allow the recruitment of the required neural ensemble, then once the movement is complete, resynchronising the motor network, returning it to a state of readiness (Jensen & Mazaheri, 2010).

1.3.2 Beta

Hans Berger's seminal work was the first to describe the ~ 13–$30Hz$ beta rhythm, describing it as the characteristic frequency of the motor cortex (Berger, 1929). This predominance of beta activity within the motor cortex was then further demonstrated by Jasper and Penfield who, through bipolar recordings of the cortical surface, showed that beta activity, present during rest, was suppressed during voluntary movement (Jasper & Penfield, 1949).

As previously mentioned (Section 1.2.2), the oscillation frequency a network exhibits may be representative of its spatial extent (Kopell et al., 2000; Miller, 2007; von Stein & Sarnthein, 2000). Due to negligible conduction times, faster gamma oscillations generally occur in smaller, local networks (Friedman-Hill et al., 2000; Fries et al., 2002; Maldonado et al., 2000). Whereas, slower oscillations such as beta represent large-scale networks, with longer conduction delays between spatially disparate regions (Brovelli et al., 2004; Lachaux et al., 2005; Tallon-Baudry et al., 2004). It is therefore not unreasonable to assume that the dominant beta activity recorded from the resting motor cortex is generated by the synchronised integration of a large-scale network.

The exact role this high power beta activity plays is still an issue for debate, however, its prevalence during rest and periods of continuous muscle contraction, along with its suppression during phasic movement, is indicative of a preference towards postural constants (Gilbertson et al., 2005; Pastötter et al., 2008; Van Wijk et al., 2008). In

general, the healthy brain is an efficient system and synchronised oscillations are an economical method of driving network activity. The partial synchronisation of the overall network allows for the recruitment of specific ensembles while still firing at a low rate (Baker et al., 1999; Brown, 2000; Hari & Salenius, 1999).

Event-related desynchronisation (ERD)

Prior to and during the execution of a movement, there is a reduction in beta EEG activity relative to the resting baseline. This suppression of cortical beta has been attributed to a desynchronisation of the underlying neural ensembles and has been repeatedly and robustly demonstrated (Cheyne et al., 2006; Engel & Fries, 2010; Gaetz et al., 2010; Neuper & Pfurtscheller, 2001a; Pfurtscheller & Lopes Da Silva, 1999; Zhang et al., 2008). This phenomenon became known as the 'peri-movement beta ERD.'

Beta ERD has been measured during the execution of various different types of movement and is present regardless of the effector, whether it be: finger flexion (Gaetz et al., 2010), shoulder elevation (Stančák et al., 2000), tongue protrusion (Crone, 1998a) or foot dorsiflexion (Crone, 1998a; Pfurtscheller & Lopes Da Silva, 1999). As is the case with alpha ERD, beta ERD onset usually occurs approximately one second before the movement onset and persists until movement cessation (Erbil & Ungan, 2007; Pfurtscheller & Lopes Da Silva, 1999; Stancák & Pfurtscheller, 1995).

During such movements the peak of the ERD power change has been observed bilaterally in the precentral gyri (Alegre et al., 2003; Doyle et al., 2005; Leocani et al., 1997; Pfurtscheller et al., 1996; Stancák & Pfurtscheller, 1996a), predominantly on the contralateral side to the active effector (Jurkiewicz et al., 2006; Salmelin et al., 1995a). The peak of the ERD also appears to follow the classic somatotopic organisation of the M1 (Crone, 1998a; Salmelin et al., 1995b).

During particularly complex movements beta ERD also occurs in other motor areas such as the SMA, PPC and the cerebellum (Cheyne et al., 2006; Heinrichs-Graham & Wilson, 2015; Heinrichs-Graham et al., 2016; Wilson et al., 2010, 2014a). Further studies have also shown that there is a strong coherence between the M1 and secondary motor areas during ERD (Gross et al., 2005; Heinrichs-Graham & Wilson, 2015; Pollok et al., 2008, 2009; Schoffelen et al., 2008). This is indicative of the large-scale, coherent network that underlies movement execution.

The decrease in beta power during ERD does not vary with the type of movement. For

example, when comparing brisk finger movements to slow, the amplitude of the initial ERD prior to movement is identical (Stancák & Pfurtscheller, 1995; Stancák & Pfurtscheller, 1996a). The same is true when contrasting individual index finger movements with all four fingers moving in unison (Salmelin et al., 1995a). There was also no significant difference in beta ERD between different grip types or force manipulations (Pistohl et al., 2012; Stančák et al., 1997). All of the above seems to suggest that if the exact required movement is known by the participant when they receive the 'GO' cue, then the optimal degree of beta desynchronisation can occur.

Beta desynchronisation has also been observed in the absence of any actual physical movement. Several studies have demonstrated that merely observing the actions of others or merely imagining one's own movements is sufficient to cause a beta ERD in the sensorimotor cortex (Avanzini et al., 2012; Pfurtscheller et al., 2005; Schnitzler et al., 1997). Albeit with a reduced amplitude compared to the ERD elicited by movement execution (Babiloni et al., 2016; Duann & Chiou, 2016; Gonzalez-Rosa et al., 2015). Therefore, beta modulation not only occurs ahead of motor output but also before other more abstract forms of sensorimotor activation.

The majority of the studies cited above define the peri-movement ERD as the beta desynchronisation that occurs prior to and during the execution of a movement. However, recent studies have begun to separate this period of desynchronisation into two: the preparatory-phase beta ERD and the response-phase ERD. As stated above the execution of an upper-limb movement results in a robust beta desynchronisation prior to movement onset. The extent of this desynchronisation does not seem to depend on the exact nature of the movement (Pistohl et al., 2012; Salmelin et al., 1995a; Stancák & Pfurtscheller, 1995; Stancák & Pfurtscheller, 1996a; Stančák et al., 1997). This is the response-phase ERD.

The preparatory-phase ERD becomes more apparent when the motor task involves a planning stage prior to the GO cue. Kaiser and colleagues (2001) developed a delayed-response motor paradigm, whereby the participant was first presented with an auditory warning cue that was either spatially relevant to the upcoming movement or contained spatially ambiguous information. After a delay, a second auditory GO cue was presented indicating whether the left or right index finger should be moved. When the warning cue was unambiguous, beta ERD occurred significantly earlier during the planning stage than

the ambiguous cue (Kaiser et al., 2001).

The degree of certainty during this planning stage modulates not only the onset of preparatory ERD but also its amplitude. By introducing a choice of potential directions to which the participant could move, other researchers have demonstrated that a negative relationship exists between directional uncertainty and preparatory-phase ERD amplitude (Grent-'t Jong et al., 2014; Tzagarakis et al., 2010). That is to say, the more certain one is about a movement that one is shortly to perform, the greater the beta desynchronisation that occurs prior to the GO cue.

Post-movement beta rebound (PMBR)

Following beta ERD there is a resynchronisation of the sensorimotor beta that results in a period of elevated amplitude greater in power than that of the relative baseline, termed the post-movement beta rebound (PMBR). The PMBR tends to begin ~ 300–$800ms$ after the cessation of movement and lasts for up to three seconds (Cheyne et al., 2006; Gaetz et al., 2010; Heinrichs-Graham et al., 2014b; Jurkiewicz et al., 2006; Pfurtscheller & Lopes Da Silva, 1999; Wilson et al., 2011).

As is the case with ERD, PMBR peaks bilaterally, with a greater propensity towards the contralateral side to the preceding movement (Alegre et al., 2002; Andrew & Pfurtscheller, 1999). However, PMBR seems to include a more anterior network than that of ERD, including the PMC and PFC along with the sensorimotor cortices and the SMA (Heinrichs-Graham et al., 2014b; Jurkiewicz et al., 2006; Ohara et al., 2000; Wilson et al., 2010). There is also some evidence to suggest that, in the contralateral M1 at least, the source of the PMBR is significantly more focal than that of ERD. Finger movements elicit PMBR predominantly over the M1 somatotopic representation of the finger, whereas the response-phase ERD for the same movement is much more widespread (Stancák & Pfurtscheller, 1995).

The peak frequency of the PMBR may also have some functional relevance. Neuper and Pfurtscheller (2001b) demonstrated that following the cessation of a foot movement the peak rebound frequency was faster ($21.5Hz$) than the rebound frequency of a hand movement ($17.5Hz$). This finding may be indicative of anatomical segregation between the regions, preventing the accidental entrainment of the irrelevant ensemble. However, it may also merely be a by-product of the somatotopic organisation of the M1, in that the hand area is significantly larger, both in terms of physical size and neural mass, than the

foot area and therefore would necessarily have a lower intrinsic frequency.

Unlike the response-phase ERD, which appears to remain constant as motor task parameters change (Pistohl et al., 2012; Salmelin et al., 1995a; Stancák & Pfurtscheller, 1995; Stancák & Pfurtscheller, 1996a; Stančák et al., 1997), the PMBR appears to vary dependent on the preceding movement type (Fry et al., 2016; Parkes et al., 2006; Stančák et al., 1997). For example, when a load is added to apply resistance to a finger extension, the resulting PMBR is greater than when the same movement is performed with no additional mass (Stančák et al., 1997).

Alegre and colleagues (2004a) demonstrated that when two sequential movements are performed in quick succession, the PMBR does not occur until after the cessation of the second movement (Alegre et al., 2004a). This suggests that, rather than occur after each constituent movement, PMBR occurs after the full motor plan has been executed.

There have been several theories put forward for the functional role of the PMBR, each one difficult to disentangle from the other. There is the *'idling theory'* which suggests that once a movement is complete, the motor cortex needs to be reset to its resting state (Pfurtscheller, 1992; Pfurtscheller et al., 1996, 2005; Salmelin & Hari, 1994). Then there is the theory that the rebound reflects sensory feedback about the performed movement (Alegre et al., 2002; Cassim et al., 2001). The evidence for this theory comes from studies of passive movement which showed an M1 rebound following the movement that is then obliterated by an ischemic nerve block (Cassim et al., 2001).

A further explanation may be that the rebound represents a *recalibration* of the sensorimotor network after each movement (Riddle & Baker, 2006). This may also explain why during long periods of sustained static-hold movements underlying beta begins to transiently resynchronise over time, possibly indicating a recalibration to the current motor state (Baker et al., 1997; Sanes & Donoghue, 1993; Spinks et al., 2008).

An alternative hypothesis that has emerged more recently within the literature is that put forward by Tan and colleagues (Tan et al., 2016). They suggest that PMBR indexes confidence in the estimations from internal models. Through the use of EEG, they demonstrated that a history of task-related errors in a simple movement paradigm resulted in an increase in uncertainty in feed-forward estimations derived from the internal model. The amplitude of the resultant PMBR correlated with the uncertainty such that the greater the uncertainty in the feed-forward estimation the lower PMBR

amplitude.

Then there is possibly the simplest explanation of all, that PMBR reflects the termination of movement, the active inhibition or *disengagement* of the motor network to prevent further motor output (Alegre et al., 2004b; Chen et al., 1998; Gilbertson et al., 2005; Leocani et al., 2000; Pastötter et al., 2008). This argument is strengthened by the finding that forced early termination of a movement elicits a greater PMBR response than an expected termination of the planned movement (Heinrichs-Graham et al., 2017).

The role of beta oscillations

In general, high amplitude beta activity is thought to reflect cortical inhibition (Cassim et al., 2001; Gaetz et al., 2011). Therefore a desynchronisation of motor beta activity could represent a gating mechanism, *'switching off'* the inhibition to enable the recruitment of the correct neural ensemble required to initiate a movement (Alegre et al., 2008; Cassim et al., 2001; Pfurtscheller & Lopes Da Silva, 1999; Solis-Escalante et al., 2012). Whereas, the high amplitude beta that occurs during the PMBR may be representative of an active inhibition of the motor network after the performance of a movement (Alegre et al., 2004b; Chen et al., 1998; Gaetz et al., 2011; Gilbertson et al., 2005; Leocani et al., 2000; Pastötter et al., 2008).

Evidence for the relationship between beta amplitude and cortical inhibition comes from studies of motor cortical GABA concentrations (Gaetz et al., 2011; Hall et al., 2010a, 2011; Jensen et al., 2005; Muthukumaraswamy et al., 2013). As previously touched upon (Section 1.2.2), reciprocal connections are formed between excitatory glutamatergic pyramidal cells and GABAergic interneurons. The balance between these two cell types drives oscillatory changes in the network (Murakami & Okada, 2006; Prokic et al., 2015; Rönnqvist et al., 2013; Roopun et al., 2006; Yamawaki et al., 2008).

In animal slice studies, artificial blocking of GABA-A receptors, by bicuculline (Roopun et al., 2006) and picrotoxin (Yamawaki et al., 2008) resulted in the abolition of motor cortical beta. Hall and colleagues (2010a; 2011) demonstrated that the administration of diazepam, a positive allosteric modulator of GABA-A, resulted in increased resting beta amplitude (Hall et al., 2010a) and exaggerated PMBR (Hall et al., 2011). A similar effect was observed when tiagabine, a GABA-reuptake inhibitor, was administered (Muthukumaraswamy et al., 2013).

An earlier pharmacological study also found highly significant increases in sensorimotor

beta activity after the administration of benzodiazepine, along with a reduction in peak frequency (Jensen et al., 2005). Naturally occurring sensorimotor GABA concentration also positively correlates with PMBR power, though in this study no difference in peak frequency was observed (Gaetz et al., 2011). In each of these studies, alpha activity was largely unaffected, suggesting that alpha oscillations are driven by a different mechanism to GABA-A mediated inhibition (Baker & Baker, 2003). However, a study by Rönnqvist et al. (2013) found that, while GABA modulation did not have a significant effect on MEG recorded alpha power, there was an increase in alpha power. Through in-vitro analysis, the authors found that there was indeed a significant increase in alpha power in M1 L3 following zolpidem administration but the amplitude of L3 neurons was too low to significantly alter the MEG recorded response (Rönnqvist et al., 2013).

Neural plasticity has also been linked with GABA concentration, as increased glutamatergic excitation, coupled with decreased GABAergic inhibition tends to increase the plasticity potential of a network (Benali et al., 2008; Hensch, 2005; Stagg, Bachtiar, & Johansen-Berg, 2011). Therefore, motor cortical beta, driven as it appears to be by GABA-A mediated inhibition, may be an indirect correlate of the brains capacity for neuroplastic change (Rossiter et al., 2014).

The theory that beta is a correlate of neural plasticity also helps to explain age-related changes in both spontaneous and movement-related beta amplitude. Rossiter and colleagues (2014) demonstrated increased spontaneous beta power in older adults compared with younger adults (Rossiter et al., 2014). Heinrichs-Graham and colleagues (2018) demonstrated that this relationship is not a simple linear relationship throughout our lifespan. Rather, a quadratic relationship whereby resting beta decreases as children develop into early-adulthood before then significantly increasing from early to late-adulthood (Heinrichs-Graham & Wilson, 2016; Heinrichs-Graham et al., 2018).

A second quadratic relationship was also found when investigating the PMBR response, relative to the resting baseline. In this case, relative PMBR increases in amplitude as children develop into early-adulthood (Gaetz et al., 2010; Wilson et al., 2010), then drastically decreases from early to late-adulthood (Heinrichs-Graham et al., 2018; Labyt et al., 2003; Liu et al., 2017; Rossiter et al., 2014). If one was to compare these two quadratic relationships with the well-established relationship between age and motor performance (Mattay et al., 2002; Smith et al., 1999), then one could conclude that

optimal motor performance requires spontaneous beta activity to be low and relative PMBR amplitude to be high.

Unlike spontaneous beta and relative PMBR, the relative beta ERD appears to increase entirely linearly with age (Gaetz et al., 2010; Heinrichs-Graham & Wilson, 2016; Heinrichs-Graham et al., 2018; Rossiter et al., 2014; Toledo et al., 2016). Therefore, an elderly subject, whose spontaneous beta activity may be threefold that of a younger adult (Rossiter et al., 2014), will exhibit a greater percentage decrease in beta power prior to movement (Heinrichs-Graham & Wilson, 2016; Rossiter et al., 2014) than the younger adult. However, the peak of that desynchronisation will be significantly greater in absolute power for the elder subject because of their significantly greater baseline beta level.

1.3.3 Gamma

Much of our knowledge about gamma (~ 30–$100Hz$) oscillations comes from studies of the hippocampus, which generates high amplitude gamma due to its relatively simple laminar structure (Förster et al., 2006). The actual source of the gamma oscillation appears to be the result of the interaction between reciprocally connected excitatory pyramidal cells and inhibitory interneurons (Buzsáki & Wang, 2012; Bathellier et al., 2008; Hansel & Mato, 2003; Traub et al., 1997; Wang, 2010; Yamada et al., 2016). Though a study by Hall and colleagues (2011) demonstrated that movement-related gamma synchronisation (MRGS) is generated by a non-GABA-A receptor mediated process (Hall et al., 2011).

Throughout the brain, gamma activity is thought to reflect enhanced neural activation, critical for the timing of neural communication and information processing (Bartos et al., 2007; Fries et al., 2007; Jensen et al., 2007). Acting as a mechanism for entraining spontaneously firing neurons into a coherent ensemble to perform a cognitive function (Rodriguez et al., 1999; Schnitzler & Gross, 2005; Singer & Gray, 1995).

An ECoG study by Crone and colleagues (1998b) found that there was a separation of gamma activity into low (30–$50Hz$) and high (75–$100Hz$) frequency bands. After movement onset, concurrent with alpha ERD, there was an ERS of the lower frequency gamma that was sustained until movement cessation. Whereas, a higher frequency gamma ERS occurred prior to movement onset and ended much earlier than movement cessation (Crone, 1998b). Both lower and higher frequency gamma ERS originated from the contralateral M1 and was much more focal than either concurrent alpha or beta

ERD (Crone, 1998a, 1998b). So much so that the authors concluded that ECoG measures of gamma ERS could be used as an additional method to map the motor cortex topographically.

MRGS has been observed at movement onset and lasts for $\sim 300ms$ (Cheyne, 2013; Cheyne et al., 2008; Crone, 1998b; Gaetz et al., 2010; Muthukumaraswamy, 2010). In line with the earlier corticographic study, Cheyne and colleagues (2008) demonstrated that gamma activation was strongly lateralised in the contralateral M1 and appeared to be consistent with somatotopic organisation (Cheyne et al., 2008). Although, later studies suggest that alongside M1, other regions such as the SMA and cerebellum also show significant gamma synchrony at movement onset (Gaetz et al., 2010; Wilson et al., 2010). Even so, MRGS is considered to be both spatially and temporally more congruent with movement onset than movement-related changes in either the alpha or beta band (Miller et al., 2009).

Alpha and beta bands appear to be modulated by movement preparation, both desynchronising prior to the onset of movement (Cheyne et al., 2006; Crone, 1998a; Engel & Fries, 2010; Gaetz et al., 2010; Leocani et al., 1997; Pfurtscheller & Lopes Da Silva, 1999). Whereas, while Crone and colleagues found a synchronisation of higher frequency gamma $(75–100Hz)$ prior to movement onset (Crone, 1998b), most MEG studies do not show MRGS until the onset of movement (Cheyne, 2013; Muthukumaraswamy, 2010). Interestingly, sensorimotor gamma appears to be strongly coupled to alpha during rest, then is released from the alpha phase at movement onset to recruit the correct motor representation (Yanagisawa et al., 2012). This finding supports the theory that sensorimotor alpha is involved more in local information processing and neural recruitment, while beta coordinates the large-scale motor network required to perform and assess one's movements in relation to the outside world (Athanasiou et al., 2018).

A further contrast between MRGS and alpha/beta ERD is that the former has not been observed during indirect motor activities, such as action observation or passive movement (Babiloni et al., 2016; Muthukumaraswamy, 2010). This finding has led to the conclusion that gamma synchrony may be a result of motor system activation to initiate an action. Whereas, alpha and beta modulation may be representative of a more generalised sensorimotor function and integration.

1.3.4 Abnormal oscillations in motor dysfunction

A great deal of the evidence linking neural oscillations with healthy motor function has come from studies of patients who suffer from motor deficits as a result of neurological disorders such as Parkinson's disease and ischemic stroke. Some of the key findings are summarised below.

Parkinson's disease

Parkinson's disease (PD) is a progressive, neurodegenerative disorder, the prevalence of which increases with population age, from 0.04% of 40–49 year-olds to 1.9% of those over 80 (Pringsheim et al., 2014). The neuropathology of PD is the loss of dopaminergic neurons in the basal ganglia, particularly in the SNr, as well as the presence of Lewy bodies and Lewy neurites (Fröhlich, 2016).

The characteristic symptoms of PD are motor deficits such as tremor, muscle rigidity, postural instability, bradykinesia, hypokinesia, and akinesia. The diagnosis of PD comes from clinical observation of these motor symptoms, though it is difficult to confirm this diagnosis until the presence of neurodegeneration is found post-mortem.

Patients with PD often suffer from cognitive deficits alongside the motor symptoms described above, such as attentional deficits, issues with working memory and increased risk of dementia and depression. These cognitive symptoms also aid in the accurate diagnosis of PD, but it is important to establish potential biomarkers of the disease, to allow for earlier diagnosis and to monitor disease progression.

One potential biomarker is oscillatory activity in the basal ganglia, thalamus, and M1. There is increased low-frequency alpha activity (3–$7Hz$) in the basal ganglia of PD patients with tremor and pathological beta activity in those without tremor, particularly in the GPi and STN (Brown et al., 2001; Brown & Williams, 2005; Hutchison et al., 2004; Levy et al., 2000, 2002; Little & Brown, 2012; Wichmann & Soares, 2006). There is also an increase in the coherence of beta oscillations between GPi, STN and cortical motor areas when in the absence of dopamine (Brown et al., 2001; Levy et al., 2002; Pollok et al., 2012; Williams et al., 2002). This increased beta activity is attenuated when patients are treated with dopaminergic medication (Brittain & Brown, 2014; Hammond et al., 2007; Heimer et al., 2006; Kühn et al., 2009; Silberstein et al., 2005).

Pathologically increased beta activity in the basal ganglia has been correlated with

reduced motor performance and response times (Kühn et al., 2004, 2006; Williams et al., 2005). As with cortical motor areas a desynchronisation of basal ganglia beta activity seems to be necessary to perform a voluntary action (Alegre et al., 2005; Fogelson et al., 2005; Joundi et al., 2012). This ERD still occurs in PD patients; however, their resting level of beta synchrony is significantly elevated and is less susceptible to suppression than in the healthy basal ganglia (Courtemanche et al., 2003).

This same relationship between spontaneous and relative beta power has been demonstrated in M1 of PD patients. A study by Heinrichs-Graham et al. (2014a) found that, compared to age-matched controls, PD patients had significantly higher resting M1 beta power. The same authors also found that, during movement, the relative decrease in M1 beta power was significantly reduced in the patient population (Heinrichs-Graham et al., 2014a, 2014b).

Stroke

Stroke is a type of acute cerebrovascular disease that occurs when cerebral blood flow is interrupted and can result in a range of neurological deficits. Due to the extremely heterogeneous nature of stroke origin, the outcome can vary in severity. In the UK the prevalence of stroke has been found to be as high as 3%, not controlling for gender, with associated stroke risk increasing significantly with age (Zhang et al., 2012).

By far the most common form of stroke is an ischemic stroke, caused by an atherothrombotic infarction. This type of infarction is reported to be the cause of 60% of strokes, with 25.1% due to cerebral embolism, 8.3% by intracerebral haemorrhage, 5.4% by subarachnoid haemorrhage, and the remaining 1.2% due to unknown causes (Wolf, 2004).

The nature of cerebrovascular disease means that the affected brain tissue has the potential to be extremely localised to the infarction or almost entirely global; therefore, the outcome of stroke can be extremely unpredictable. However, the most common site of stroke is the middle cerebral artery, the primary blood supply for many major structures of the motor system. As such, symptoms of stroke often include motor issues; for instance, unilateral or bilateral motor and sensory impairment, aphasia, apraxia, ataxia, and forced gaze.

Several MEG studies of patients who have suffered from stroke have investigated the power of neural activity in the affected and unaffected hemispheres. These studies

demonstrate greater cortical alpha (Laaksonen et al., 2013; Tecchio et al., 2006a) and beta power (Hall et al., 2010b; Tecchio et al., 2006b) over the affected hemisphere than over the unaffected hemisphere. A study of stroke patients, who have recovered some or all motor faculties, suggested that clinical recovery correlates with the coherence of resting beta power between the two hemispheres. The more 'normalised' the two hemispheres, the greater the recovery (Tecchio et al., 2006b).

The theory that motor cortical beta power may be a signature of neural plasticity may help to explain these stroke studies (Rossiter et al., 2014). It appears that not only does resting beta increase over the affected hemisphere; there is also a relative decrease of beta power in the unaffected hemisphere (Tecchio et al., 2006b). These changes may be reflective of decreased plasticity within the lesioned hemisphere and an increase in plasticity in the undamaged hemisphere. This may be a result of the brain trying to counter the adverse effect of the stroke by reassigning the neural workload to an undamaged area of the brain. Then as the patient recovers this imbalance between hemispheres decreases.

1.4 Modulating neural oscillations

Oscillations may be a functionally relevant mechanism for information processing and network recruitment, or alternatively, oscillatory activity may simply be a by-product of neural function. Arguably the true role of neural oscillations, whether directly functional or an epiphenomenon of function, is irrelevant. The mere existence of neural synchrony and its correlation with both healthy and pathological brain states means that its study is of great importance. Understanding how oscillations can be modulated can help researchers and clinicians develop treatments and interventions for patients, as well as having far-reaching consequences for fields such as robotics and sports-science.

1.4.1 Pharmacological intervention

As mentioned above (Section 1.3.4), pathological oscillations can be modulated through pharmacological intervention. PD patients who exhibit elevated subcortical beta oscillations have been treated using the dopamine precursor levodopa (L-DOPA). L-DOPA along with other dopaminergic medication suppresses beta synchrony and reduces beta coherence within the motor network (Brittain & Brown, 2014; Hammond et al., 2007; Heimer et al., 2006; Kühn et al., 2006, 2009; Silberstein et al., 2005).

Dopaminergic and GABAergic cells form a complex interaction of excitation and inhibition. The loss of dopaminergic cells in PD patients upsets this balance and as such GABA modulators may also alter oscillatory states. For example, low doses of the GABA-A receptor modulator, zolpidem, has been shown to improve motor function in PD (Y-Y. Chen et al., 2008; Daniele et al., 1997; Hall et al., 2014) and stroke patients (Hall et al., 2010b).

Hall and colleagues (2014) demonstrated that low-dose zolpidem not only improved the motor deficits of PD patients but also reduced the exaggerated beta activity recorded from contralateral M1 (Hall et al., 2014). A further interesting finding from this study was while contralateral beta decreased, ipsilateral beta was increased by zolpidem administration, resulting in an equalisation of interhemispheric power during rest. The authors conclude that the balance between contralateral and ipsilateral M1 beta power may be an intrinsic requirement for healthy motor function. Therefore, an imbalance may act as an additional biomarker for PD (Hall et al., 2014).

Modulation of neural oscillations is not limited to prescribed medication of course; recreational substances such as alcohol have also been shown to affect neural activity. Alcohol, or more specifically, ethanol binds to GABA-A receptor sites (Lobo & Harris, 2008). There have been few, if any, studies investigating the immediate effect of alcohol on oscillatory power. However, studies of patients suffering from alcoholism have demonstrated increased beta activity in motor areas, similar to the pattern seen in PD patients (Costa & Bauer, 1997; Coutin-Churchman et al., 2006; Rangaswamy et al., 2002).

1.4.2 Transcranial electrical stimulation

The idea of electrically modulating the brain is not a new one; humans have been using electricity to try and stimulate the brain since the days of antiquity. The Greek physician Claudius Galen (129–216AD) noted that placing a live torpedo fish on the scalp would relieve the pain of a headache, suggesting the relief came as a result of the strong electric current delivered by the fish (Priori, 2003). In the 1800s, Giovanni Aldini applied galvanic currents to patients, reporting a reduction in melancholia and starting a spate of research into direct current's potential as a neuropsychological treatment (Aldini, 1804). The controversial use of electroconvulsive therapy throughout the mid 20th century (Cerletti, 1940; Shorter & Healy, 2007) somewhat curtailed research into direct current

stimulation. Therefore, it was not until 1980 that Merton and Morton reported the first successful instance of transcranial electrical stimulation (tES) electrically stimulating the cortex (Merton & Morton, 1980).

The methodology has gradually evolved from unidirectional, direct current stimulation between two electrodes to bidirectional, alternating current between focal arrays of multiple electrodes.

Transcranial direct current stimulation

The most basic form of tES is transcranial direct current stimulation (tDCS). This type of stimulation involves passing a low-amplitude direct current, usually no higher than $2mA$, between two large anodal and cathodal electrodes (Nitsche & Paulus, 2011; Stagg & Nitsche, 2011; Stagg, 2014; Zaghi et al., 2009). This non-invasive form of brain stimulation is thought to modulate the excitability of superficial cortical layers, with the effect lasting longer than the period of stimulation (Datta et al., 2009; Kuo et al., 2013; Stagg, 2014; Wagner et al., 2007). The polarity of the stimulation appears to be of physiological importance, as anodal stimulation leads to facilitation of the M1, whereas cathodal appears to be inhibitory (Paulus, 2011).

The relationship between the polarity of stimulation and cortical excitability may also be reflected in changes in oscillatory activity. A study by Zaehle and colleagues (2011) found that anodal stimulation of the PFC led to an increase in theta and alpha activity, alongside an improvement in working memory performance. While cathodal stimulation appears to decrease underlying alpha and beta power and interfere with working memory ability (Zaehle et al., 2011).

Anodal tDCS has also been linked with GABA concentration. Ten minutes of anodal stimulation to the M1 has been shown to decrease GABA concentration (Stagg, Best, et al., 2009). This same relationship has been found by a number of studies in both young (Bachtiar et al., 2015; Kim et al., 2014) and older adults (Antonenko et al., 2017). As mentioned above, GABA plays a role in cortical inhibition and plasticity. Therefore one could conclude that anodal tDCS increases neural plasticity and excitation. The evidence that cathodal stimulation has an opposite effect is less consistent; with one study finding cathodal stimulation reduces glutamate concentration (Stagg, Best, et al., 2009), while another found no effect (Kim et al., 2014).

Transcranial alternating current stimulation

tACS is accomplished by using pulses of rectangular waves, changing polarity with each pulse; or by using sinusoidal waves of stimulation (Moreno-Duarte et al., 2014). tDCS has been shown to modulate the firing rate of neurons by increasing their resting membrane potential (Purpura & McMurtry, 1965; Nitsche et al., 2003), the same is not necessarily true for tACS as it induces a significantly lower cortical current than tDCS. However, it is possible the phasic nature of tACS may induce an oscillatory change in membrane potential, increasing the likelihood of neuronal firing at the stimulation frequency (Bergmann et al., 2009; Stagg & Nitsche, 2011; Stagg, 2014; Zaehle et al., 2010).

Studies have shown a behavioural effect of tACS when applied over the M1. Alpha frequency tACS ($10Hz$) has been shown to facilitate motor learning, while stimulation at 1, 15, 30 and $45Hz$ had no significant effect (Antal et al., 2008). Beta stimulation has, however, also been shown to significantly slow the execution of a voluntary movement (Pogosyan et al., 2009). A finding which may provide evidence for a causal link between increased resting beta activity in PD patients and their bradykinesia symptoms (Gilbertson et al., 2005; Jenkinson & Brown, 2011; Joundi et al., 2012).

Evidence that tACS may be able to entrain neural oscillations has come from investigations of occipital alpha activity. Zaehle and colleagues (2010) used EEG to find each participant's individual alpha frequency within their occipital cortex, then used tACS to stimulate the same region at its intrinsic frequency. Occipital alpha was increased after three minutes of alpha-tACS stimulation compared to sham (Zaehle et al., 2010). A further study replicated this finding, adding that the increase in occipital alpha lasts for up to thirty minutes after stimulation (Neuling et al., 2013). While, computational modelling has also shown that alpha oscillations are only elicited by tACS in a narrow band around the endogenous oscillatory frequency (Merlet et al., 2013).

1.4.3 Transcranial magnetic stimulation

Transcranial magnetic stimulation (TMS), originally developed as a diagnostic tool by Anthony Barker and colleagues in 1985 (Barker et al., 1985), allows for non-invasive stimulation of the cortex. Since its inception, TMS has become a mainstay of neurophysiological research. A simple PubMed keyword search shows that in the past ten years there has been a nearly 15-fold increase in the average number of papers

published per year with TMS in the title (*2008–2017*, $M = 323.2$, $SD = 69.4$); compared to the first ten years after its invention (*1985–1994*, $M = 21.9$, $SD = 14.7$).

Repetitive transcranial magnetic stimulation

Repetitive transcranial magnetic stimulation (rTMS) refers to the delivery of a train of TMS pulses as opposed to a single, isolated pulse. While single-pulse TMS can consist of either a monophasic pulse or one biphasic pulse cycle, the polyphasic waveform of rTMS tends to be generated by a biphasic stimulator. The frequency of different rTMS trains varies; but in general, pulses are delivered at a rate no slower than $1Hz$ and no faster than $50Hz$ (Oberman, 2014).

The parameters of rTMS vary with the train frequency; slower frequencies tend to be delivered continuously for longer durations, whereas faster frequencies are delivered in short duration trains, with relatively longer intertrain intervals (Oberman, 2014). The neural effect of rTMS appears to be frequency-dependent; with lower $1Hz$ stimulation inhibiting neural activity (Taylor & Loo, 2007), while $10Hz$ stimulation has a facilitating effect (Arai et al., 2007). Another difference between rTMS and single-pulse TMS is the duration of the effect of stimulation. While single-pulse TMS elicits an immediate response that stops with the cessation of the pulse, rTMS has been shown to elicit long-term effects (Rotenberg et al., 2014).

TMS and neural oscillations

The potential effect of TMS on neural oscillations has been investigated using simultaneous TMS and EEG recordings. Paus and colleagues found beta oscillations lasting several hundred milliseconds following a single TMS pulse to the M1 (Paus et al., 2001). A follow-up study went on to show that subthreshold rTMS resulted in significantly higher beta amplitudes when centred over M1 than over PMC (Van Der Werf & Paus, 2006). They argue; however, that TMS, instead of eliciting a new neural oscillation, resets the ongoing beta oscillation, time-locking it to the TMS pulse. Studies of tremor in PD patients support this as single-pulse TMS has been shown to reset the ongoing hand tremor, time-locking it to the pulse (Britton et al., 1993).

TMS has also been used to probe the natural frequencies of different cortical areas. A study by Rosanova and colleagues (2009) used single-pulse TMS of varying intensities to stimulate occipital (BA19), parietal (BA7), and frontal (BA6) regions. Each region

appears to have a different natural frequency; alpha oscillations were elicited in the occipital region, beta oscillations in the parietal region and high-frequency beta/low-frequency gamma in the frontal region (Rosanova et al., 2009). They concluded that there was no significant relationship between TMS intensity and the elicited oscillation frequency; however, an earlier study demonstrated that the power of TMS elicited alpha and beta oscillations in the M1 increases with TMS intensity (Fuggetta et al., 2005).

Thut and colleagues (2011b) used an rTMS paradigm to investigate the ability of TMS to directly entrain an intrinsic oscillator (Thut et al., 2011b). Based on their theory of externally driving an oscillator (Figure 2.8, Thut et al., 2011a), they used MEG to find each participant's preferred parietal alpha frequency. Then stimulated the parietal region at the same alpha frequency. They found that alpha oscillations were induced by and synchronised to the alpha-TMS (Thut et al., 2011b).

A high-frequency form of rTMS, continuous theta burst stimulation (cTBS), has been shown to modulate cortical excitability and plasticity (Huang et al., 2005). A combined EEG-cTBS study found that beta synchrony was increased for up to thirty minutes after a 20s train of cTBS (Noh et al., 2012). A later study also demonstrated increased beta power after forty seconds of cTBS which also correlated with delayed response times in a simple motor task (McAllister et al., 2013). However, unlike the earlier study, McAllister and colleagues (2013) found that increased beta power was only observed in half of their participants. This divide led the researchers to theorise that there may be a genetic difference, in the form of brain-derived neurotrophic factor (BDNF), between *'responders'* and *'non-responders'* that alters the mechanism of GABAergic inhibition (McAllister et al., 2013). A theory supported by the finding that cTBS increases M1 GABA concentration (Stagg, Wylezinska, et al., 2009).

1.5 Thesis overview

This thesis is comprised of seven chapters:

- Chapter 2 describes the general methodology used throughout this body of work. Here, the techniques and apparatuses that are used on multiple occasions are described in detail so that the reader can refer back to this chapter when required.
- Chapter 3 examines the role of beta and alpha desynchronisation during both the

preparatory and execution phases of movement. Through the use of an established paradigm (Bock & Arnold, 1992; Churchland et al., 2008; Dorris & Munoz, 1998; Pellizzer et al., 2006; Tzagarakis et al., 2010), directional uncertainty was modulated to investigate whether the magnitude of alpha and beta desynchrony during motor preparation is predictive of motor performance.

I demonstrate that consistent with previous findings, both alpha and beta desynchronisation reflect a process of disengagement from existing networks to enable the recruitment of functional assemblies required to generate motor output. Importantly, I also demonstrate a novel signature of transient alpha synchrony that occurs after preparatory desynchronisation that underlies the synchronous recruitment of those functional assemblies.

Some of the work reported in this chapter appears in Rhodes et al. (2018). I can confirm that I was solely responsible for the data collection and analyses performed for this study and that this contains novel analyses and conclusions.

- In Chapter 4, tACS was applied to M1 during the preparatory phase of the same instructed-delay reaching task used in Chapter 3. This was to further investigate the functional role of preparatory alpha and beta desynchrony in motor performance. For each individual, tACS was applied at peak frequencies to further investigate the frequency-specificity of tACS. No significant effects of tACS on response times were found, though this is likely due to the stimulation parameters used.

- Chapter 5 Investigates the relationship between PMBR and cortical excitability. Several studies have indirectly linked movement-related changes in beta activity with changes in cortical excitability (Chen et al., 1998; Coxon et al., 2006; Leocani et al., 2000; Lepage et al., 2008; Mäki & Ilmoniemi, 2010). In this chapter, the latency of motor-related changes in beta power during a simple motor-task was determined, then single-pulse TMS was applied during beta ERD and PMBR to investigate the relationship between M1 beta and cortical excitability.

  I demonstrate that there is an inverse relationship between M1 beta power and cortical excitability. During beta ERD, TMS measures of cortical excitability were significantly greater than a relative baseline. Conversely, during PMBR following motor termination, cortical excitability is significantly reduced. This finding corroborates previous research that has linked PMBR and M1 beta in general with

cortical inhibition (Chen et al., 1998; Coxon et al., 2006; Leocani et al., 2000).

- Chapter 6 expands on previous findings from Chapters 3 and 5, that suggest that the context of being involved in a motor study can cause a change in M1 beta synchrony. Several resting measures of M1 beta power were recorded throughout the course of a motor experiment. Prior to each baseline measure, the participant received a contextual cue designed to alter their anticipation of an upcoming motor requirement.

  I demonstrate that, contrary to my prediction, M1 beta synchrony significantly increases in power when the participant expects to be involved in a motor study. I also demonstrate that the relative magnitude of movement-related changes in M1 beta power during a single motor trial is significantly altered by the beta power at trial onset.

- In Chapter 7, I discuss the key findings from the work described in this thesis, along with the methodological considerations that became apparent throughout my studies and directions for future research.

Chapter 2

Methodology

If we knew what it was we were doing, it would not be called research.

– Albert Einstein (1879-1955)

THIS chapter contains descriptions and rationales for the recurrent methodology used throughout this body of work. Several apparatuses were used on multiple occasions for multiple studies, and many of the analysis techniques were repeatedly employed.

2.1 Participants

The healthy participants that took part in the studies reported herein were recruited from a local pool of University of Plymouth psychology students and staff, as well as local residents. Participants were all right-handed to limit any variance caused by differences in brain morphology and lateralisation. Before taking part in any study, participants were screened to ensure they had no personal or family history of neurological or psychiatric illness.

All studies that form part of this thesis were approved by the University of Plymouth Faculty of Health and Human Sciences Ethical Committee, in accordance with the Declaration of Helsinki (World Medical Association, 2013).

2.2 Electromyography

Electromyography (EMG), a term first coined by Weddell et al. (1943), is the study and quantification of muscle activity. EMG can be achieved through the use of needle electrodes inserted directly into the muscle, or by placing electrodes on the surface of the skin, to record the bioelectrical activity produced by the muscle fibres beneath. The latter procedure has become known as surface EMG and provides a safe, non-invasive method to clinically and experimentally measure muscle activity (Cram & Kasman, 2010).

Surface EMG signal is generated by the sum of motor unit action potentials (MUAPs) within the muscle of interest. A motor unit consists of a lower motor neuron, its axon, and the muscle fibres that it innervates (Eccles & Sherrington, 1930). The fewer the number of muscle fibres innervated by a single neuron the more precisely the muscle can be controlled (MacDonald et al., 2013). Therefore, muscles such as those in the hand, that are responsible for precise motor output, contain many hundreds of motor units generating MUAPs that can be easily detected by surface EMG.

EMG recordings were made during each of the experimental studies described within this thesis. This allowed for the recording of both transient and event-related changes in the muscle activity of the hand (see Section 2.3.1 for more).

2.2.1 Amplifier and electrodes

A Bagnoli 2-channel hand-held EMG system (DelSys Inc., Boston, USA) was used to collect all EMG recordings. This system is capable of recording from two electrode sites simultaneously, has its own power supply, and amplifies and filters the raw EMG data as it is collected. The amplifier was used to increase the raw signal gain by a factor of 10,000 and to apply a band-pass filter between $20Hz$ and $450Hz$. In combination with a differential electrode, the system provides a common mode rejection of $\approx 92dB$ and an input impedance $> 10^{12}k\Omega$.

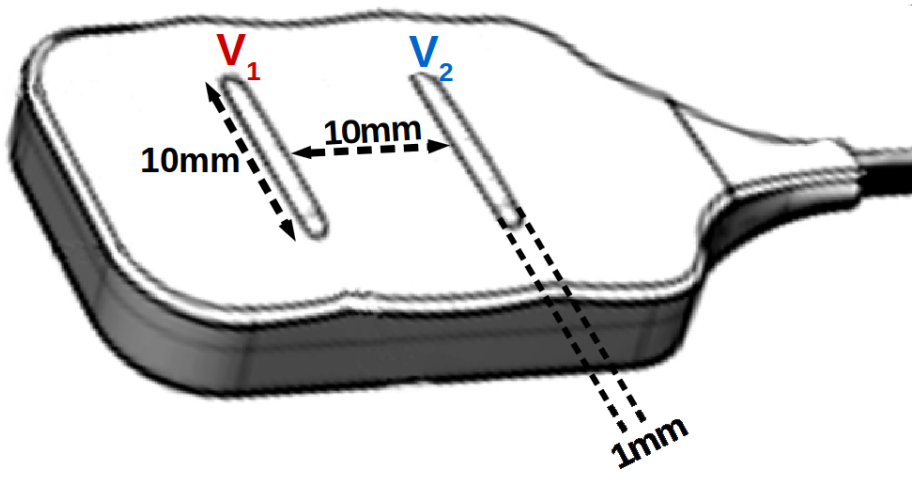

Figure 2.1: The DE-2.1 single differential electrode. Two pure silver sensor bar contacts $(10 \times 1mm)$ are spaced $10mm$ apart. The normalised output signal is calculated by subtracting the raw signal recorded by contact **V_2** from contact **V_1**.

The EMG electrodes used were bipolar single differential surface electrodes (DE-2.1; DelSys, 2017), designed to be compatible with the Bagnoli system. The active electrodes comprised two parallel, $10 \times 1mm$ sensors, spaced $10mm$ apart. These sensor

contacts were made of 99.9% pure silver and encased in an insulated polycarbonate housing (Figure 2.1).

These electrodes are designed to maximise signal stability by subtracting the raw signal measured by the second contact ($\mathbf{V_2}$) from the signal recorded by the first ($\mathbf{V_1}$). The differential between the two electrode contacts is, therefore, a normalised reflection of the underlying muscle activity. The reference signal ($\mathbf{V_{ref}}$) from a distinct, neutral site is then subtracted to create the output signal ($\mathbf{V_{out}}$)

$$\mathbf{V_{out}} = (\mathbf{V_1} - \mathbf{V_2}) - \mathbf{V_{ref}} \tag{2.1}$$

The analogue output signal was amplified 10,000 times and transferred via a Bayonet Neill-Concelman (BNC) cable to the data acquisition interface (Section 2.6). Here the normalised, referenced and amplified EMG signal was digitised and sampled at a rate of $2048Hz$, the same sampling rate as any concurrent EEG recordings.

2.2.2 Electrode placement

The overall aim of this body of work is to investigate the neural control of movement, with a particular focus on simple, hand movements. Therefore, the muscle of interest throughout this thesis was the first dorsal interosseous (FDI), the index finger abductor that is innervated by the ulnar nerve.

The FDI is located in the web space between the index finger and the thumb, parallel to the direction of the finger (Figure 2.2, A). The muscle itself arises from the metacarpus of the thumb and index finger and inserts at the proximal phalanx of the index (Cram et al., 2010). It is mainly responsible for gross movement of the index finger and, as such, is often the muscle of interest in studies of hand movements such as precision grip (Davare et al., 2010; Huesler et al., 1998; Svane et al., 2018) and button-press tasks (Kilner et al., 2004; Klein et al., 2016; Litvak et al., 2012), both of which are integral to the motor paradigms employed in this thesis.

To aid in the identification of the FDI, each participant was asked to perform a simple pincer grasp, whereby pressure is applied to the thumb by the index finger. This contraction of the muscle causes it to stand out and allows it to be palpated to help locate the muscle belly. Once located, the DE-2.1 single differential electrode was affixed to the skin surface using a 2-slot adhesive interface (DelSys Inc., Boston, USA),

ensuring the two sensor bars are parallel to the FDI muscle fibres beneath (Figure 2.2, B).

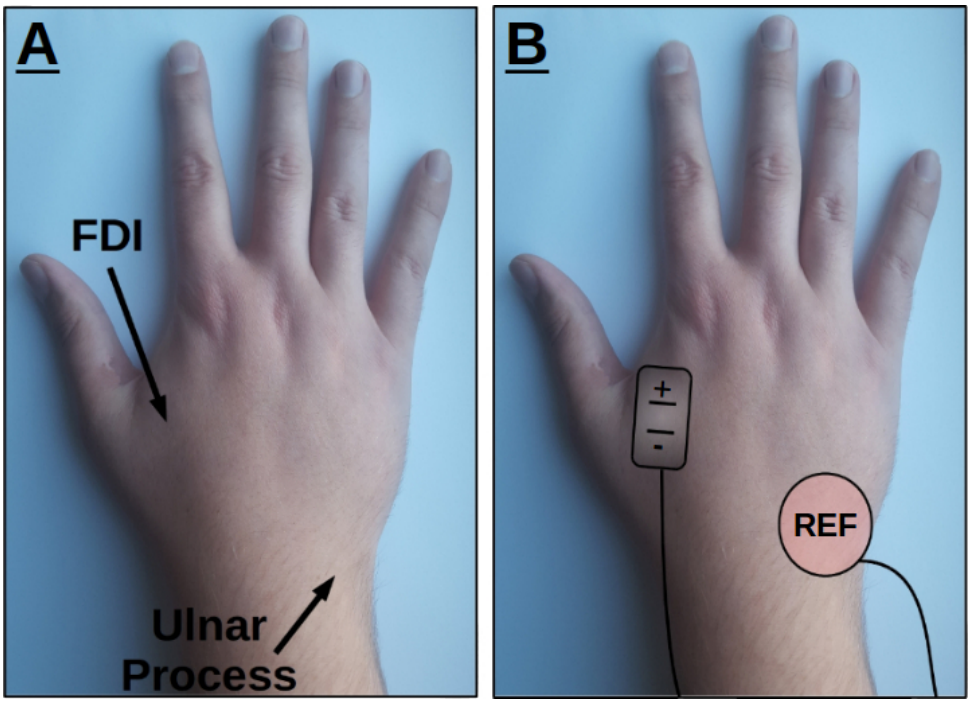

Figure 2.2: EMG electrode placement ***A.*** The FDI is located in the web space between the thumb and index finger, while the ulnar process is located at the junction between the ulnar and the wrist joint ***B.*** The single differential electrode is placed over the FDI, while the reference electrode is placed over the ulnar process.

The reference electrode; a single-use, conductive adhesive electrode patch, with a $5cm$ diameter (Dermatrode, American Imex, CA, USA), was placed over the ulnar process of the wrist. The ulnar process was chosen as the reference site, rather than other commonly used sites such as the fingertip or the metacarpophalangeal joint, as it has been shown to produce more reproducible results (Sanchez et al., 2016; Seror et al., 2011).

2.2.3 Maximising the signal-to-noise ratio

There are a number of factors that can dampen the signal or introduce noise into the recording of electrophysiological measures such as EMG and EEG. These include external factors, for example, electrical interference from other devices, and movement artefacts; as well as internal factors, such as impedance from non-muscle tissue and *'cross-talk'* from EMG signals emanating from muscles other than the target muscle.

As surface EMG is an indirect measure of MUAPs, the tissue between the muscle fibre and the electrodes must be taken into account. Fat and skin tissue act as imperfect

electrical insulators, distorting the electrical activity generated by motor units and reducing the amplitude of the detectable signal at the skin's surface. Body tissue impedance also acts as a low-pass filter for the signal due to its tendency to attenuate higher frequency components of the signal while allowing lower frequencies to pass through (Cram & Kasman, 2010).

While the resistance of fat and skin tissue is an unavoidable limitation of surface EMG, its adverse effect on signal recording can be reduced by minimising the reactive impedance between electrode and skin. High electrode-skin impedance can result in reduced signal amplitude, distorted waveform recording, and increased power line interference (Clancy et al., 2002). The impedance can be reduced by preparing the skin prior to electrode application. This skin preparation involved cleaning the skin with alcohol to remove dirt and oil, then applying a conductive gel (NuPrep; Weaver and Co., USA) to gently abrade the skin's surface.

This impedance can also be reduced by using a signal amplifier with an input impedance at least 100 times greater than the maximum expected electrode-skin impedance (Cram & Kasman, 2010). In the case of the studies presented herein, the acceptable impedance threshold was set at $\leq 10k\Omega$; an electrode-skin impedance level greater than this threshold would result in reapplication of the electrode until this standard was met. Therefore, the required input impedance level of our signal amplifier was at least $10^3 k\Omega$. A target easily met by the Bagnoli system with its input impedance of $> 10^{12} k\Omega$.

The recorded EMG was further filtered using a notch-filter (Section 2.5) to remove any lingering $50Hz$ AC electrical noise, and low-frequency movement artefacts were visually identified and removed.

Once the recorded signal had been optimised, the same recording site was used for each participant, in each experimental condition to ensure consistent comparison. This removed the influence of the recording's signal-to-noise ratio on the statistical outcomes of each study.

2.3 Transcranial magnetic stimulation

When used to stimulate the primary motor cortex, TMS activates the corticospinal pathway by inducing an electrical current in the neural tissue, depolarising the neurons; and if the depolarisation reaches the firing threshold, generating action potentials

(Barker et al., 1985). Unlike electrical stimulation, it is able to do so without physical contact with the body.

The fundamental principle behind TMS function is electromagnetic induction, which is governed by Faraday's Law:

$$\nabla \times \mathbf{E} = -\frac{\partial \mathbf{B}}{\partial t} \tag{2.2}$$

Faraday's Law states that electrical field (**E**) is induced by the time-varying magnetic field (**B**), produced by the TMS coil. The induced electrical field drives an intracranial current: $\mathbf{J} = \sigma\mathbf{E}$, where σ represents the electrical conductivity of the brain, skull and scalp (Barker, 1991; Grandori & Ravazzani, 1991; Ilmoniemi et al., 1999; Ruohonen, 2003). The calculation for the total electromagnetic field induced in the brain can be easily performed by finding the sum of the primary field induced by Faraday's Law ($\mathbf{E_1}$, Figure 2.3) and the secondary field arising from surface changes in conductivity ($\mathbf{E_2}$). This secondary field varies greatly across participants due to the diversity of extra-cerebral features, such as skull thickness and skin hydration levels. As a result, the intensity of the primary electromagnetic field produced by the TMS coil must be altered on an individual basis.

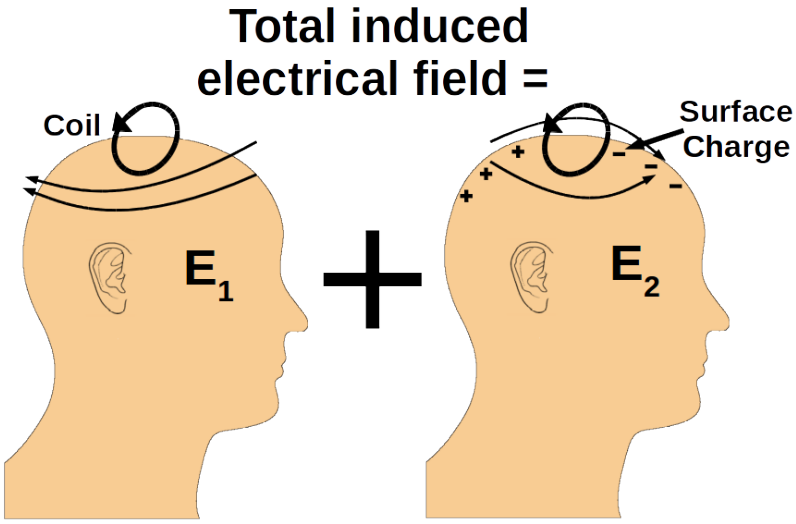

Figure 2.3: The total electrical field induced in the brain is the sum of the primary ($\mathbf{E_1}$) and the secondary ($\mathbf{E_2}$) fields. Adapted from Ruohonen (2003).

The TMS-induced electrical current flows in a parallel plane to the coil and the opposite direction to the original current within the coil (Hallett, 2000; Kobayashi & Pascual-Leone, 2003). In practical terms, this means that a TMS coil held tangentially to the scalp over the participant's M1 and orientated parallel to the interhemispheric fissure, will induce a current that flows in the posterior-anterior direction. Within the cortex, TMS preferentially

activates the pyramidal tract by indirectly recruiting excitatory interneurons (Burke et al., 1993; Klomjai et al., 2015; Rotenberg et al., 2014).

In general, subcortical structures cannot be stimulated by TMS. Firstly, the impedance of grey matter is significantly greater than white matter; therefore, higher amplitude currents are required to elicit activation in subcortical structures than in the more superficial layers of the cortex (Tofts, 1990). Secondly, TMS is generally only able to depolarise neurons at a depth of 1.5–2cm from the scalp. This is due to electromagnetic induction adhering to an inverse cube law: as the distance from the original current increases, there is an exponential decrease in the power of the induced magnetic field (Deng et al., 2013). Deeper structures can be reached by developing different coil types and shapes, however, by doing so, the current induced in neurons closer to the surface of the brain can become dangerously high.

TMS has been used to assess cortical excitability and plasticity, and the contribution of different brain regions to the control of human action (Chen et al., 1998; Leocani et al., 2000; Pascual-Leone et al., 2011; Sawaki et al., 2003; Siebner & Rothwell, 2003). While TMS can be used to modulate neural activity (Section 1.4.3), it was exclusively used in this thesis to functionally localise the participants' M1 and assess cortical excitability.

2.3.1 Motor-evoked potentials

When centred over the M1, a single, isolated pulse of TMS can directly stimulate corticospinal neurons, or the interneurons that synapse onto those corticospinal neurons (Burke et al., 1993; Fujiki et al., 1996; Macdonell et al., 1999). This stimulation has been shown to elicit a contralateral muscle response (R. Chen et al., 2008; Rothwell, 1997). This muscle twitch and the accompanying MUAPs can then be recorded using EMG as a motor-evoked potential (MEP).

Features of the resulting MEP, such as its latency and magnitude, can then be analysed. The onset latency of an MEP (Figure 2.4, A) is thought to provide information about the neural pathway between the stimulation site and the muscle of interest. A longer latency may infer a higher number of synapses or reduced myelination (Farzan, 2014).

To analyse MEP onset latency, a short MATLAB (2014b, Mathworks, Natick, MA) function was written that would first provide a measure of the baseline EMG, by averaging the trace over a 250ms period prior to the TMS pulse. Then a sliding-window approach was used to ascertain the first time window in which the averaged EMG increased or decreased

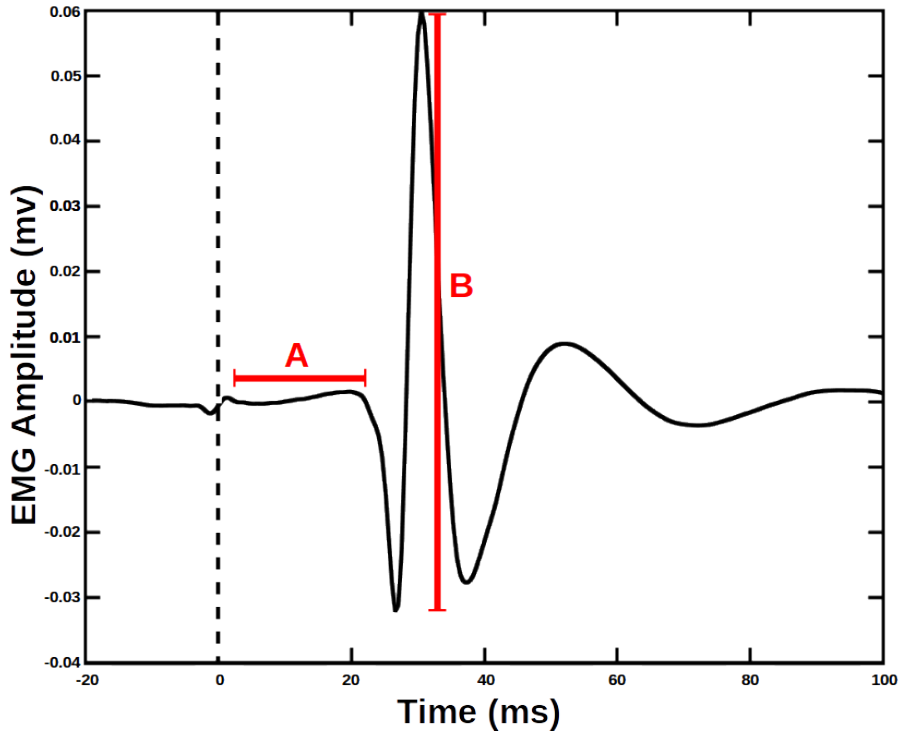

Figure 2.4: A typical motor-evoked potential, alongside its measurable components. ***A.*** MEP latency. ***B.*** Peak-to-peak amplitude of MEP.

to a level $\pm 2SD$ from the baseline. To ensure accuracy, this sliding-window approach was performed twice. The first time employed a window width of 5ms to capture the approximate onset of the MEP then a second window with a width of 1ms was used to ascertain the exact onset.

The magnitude of the elicited MEP is most commonly measured as the difference between the minimal trough and the maximal peak (the *'peak-to-peak amplitude'*) (Figure 2.4, B). MEP magnitude is thought to reflect the excitability of the motor cortex (R. Chen et al., 2008). The greater the magnitude, the greater the underlying corticomuscular excitability.

To analyse the peak-to-peak amplitude of the elicited MEP, a second MATLAB function was produced that defined an *'MEP-period'*, beginning at the previously defined onset of the MEP and lasting for 500ms. The duration of this MEP-period is far longer than the expected duration of any collected FDI MEP (Oliviero et al., 2006; Orth & Rothwell, 2004). This exaggerated duration was used to ensure that the MEP was not missed by the automated analysis, though a further visual check ensured that all MEP were captured correctly. The same function then performed a peak-analysis to find the minima ($\mathbf{MEP_{min}}$) and maxima ($\mathbf{MEP_{max}}$) of the EMG amplitude during the MEP-period. Peak-to-

peak amplitude ($\mathbf{MEP_{amp}}$) was then calculated as

$$\mathbf{MEP_{amp}} = \mathbf{MEP_{max}} - \mathbf{MEP_{min}} \tag{2.3}$$

2.3.2 Functional localisation of the primary motor cortex

In each of the upcoming studies, TMS was used to functionally localise the hand-area *'motor hotspot'*. The hotspot is the location on the participant's scalp that elicits the greatest amplitude MEP response in the FDI of the contralateral hand. Once found, the hotspot was designated as the primary hand area (M1h). The localisation procedure began with the identification and measurement of anatomical landmarks.

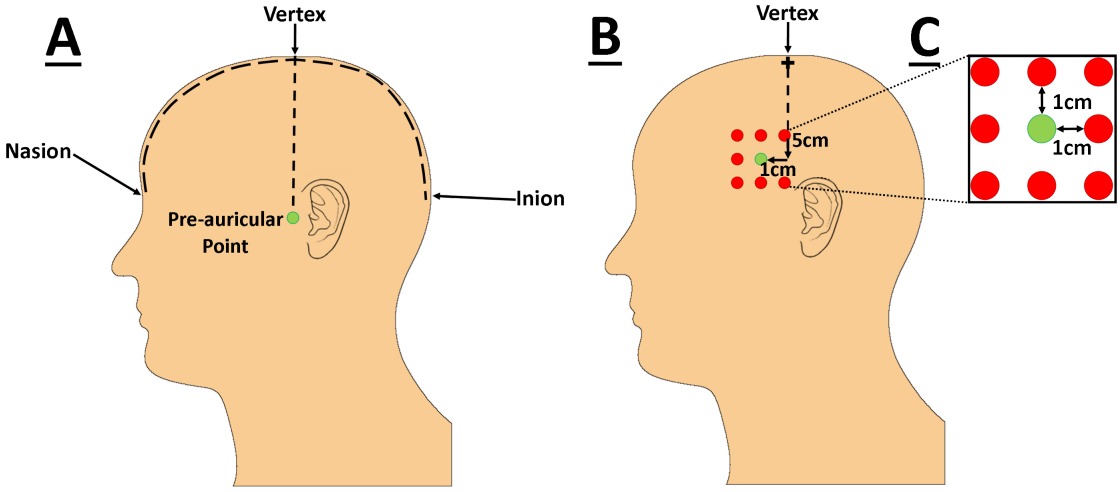

Figure 2.5: ***A.*** The vertex was located by finding the intersection of the midway point between the nasion and the inion, with the midway point between the left and right preauricular points. ***B.*** The initial estimate for the hand area of M1 (green dot) was 5cm inferior of the vertex and then 1cm anterior of that point. ***C.*** A 3x3 grid with 1cm spacing was then used to guide TMS coil placement for MEP induction.

The vertex was located by first measuring the distance from the nasion to the inion and marking the halfway point on the participant's scalp. Then the distance between the left and right preauricular points was also measured, and again the halfway point marked on the scalp. The vertex can then be located at the intersection of the two lines (Figure 2.5, A).

Once the vertex had been located, a dot was placed on the participant's scalp 5cm inferior to the vertex and 1cm anterior to that point. This was the initial anatomical estimate of M1h. A 9cm^2 grid was then placed on the scalp with the estimated M1h at its centre, and 1cm spacing between each dot in the grid. The grid was used to help systematically guide TMS stimulation to search for the location that consistently elicited the greatest

MEP amplitude (Figure 2.5, B).

To assess the appropriateness of a given scalp location, resting motor threshold (RMT) was calculated as the minimum stimulator intensity required to elicit an MEP with an $\mathbf{MEP_{amp}}$ greater than $50\mu V$ in 8 of 10 stimulations. To ensure consistency, and because the orientation of the coil is equally important as its position, the coil was always held tangentially to the scalp with the coil handle pointing backwards $45°$ laterally. This was to ensure that current flow was approximately perpendicular to the central sulcus and in a posterior-anterior direction (Opitz et al., 2013; Sakai et al., 1997).

A number of methods have been suggested to estimate RMT (Rossini et al., 2015). Of those suggested, a relative frequency method (Groppa et al., 2012) was selected, in part to ease the concerns of particularly nervous participants. This procedure involves starting stimulation at a subthreshold intensity of 30% of maximum stimulator output. No measurable MEP was elicited by stimulation at this intensity for any participants; however, it did allow them to feel the slight tapping sensation that TMS creates on the scalp. After this initial pulse, stimulator intensity was increased in steps of 5% until an MEP was consistently elicited. At this point, the stimulation intensity was then reduced by 1% until an $\mathbf{MEP_{amp}}$ greater than $50\mu V$ was no longer elicited from 8 of 10 stimulations. This stimulation intensity plus 1% was then defined as the RMT (Groppa et al., 2012; Rossini et al., 2015).

Table 2.1

Standard pulse generation parameters for the Magstim 200^2 Stimulator

Pulse intensity (%)*	Minimum inter-pulse interval (*s*)	Maximum number of sequential pulses
0–50	2	340
50–80	3	175
80–100	4	85

**Pulse intensity refers to the percentage of maximal stimulator output*

2.3.3 TMS stimulator and coil

Single-pulse TMS was generated using a Magstim 200^2 monophasic stimulator (Figure 2.6A) designed and built by Magstim (Whitland, UK). The stimulator had an intensity-dependent pulse generation rate: the higher the intensity, the longer the required interval between pulses to prevent overheating (Table 2.1). However, when necessary, this restriction could be overridden by digitally triggering pulse generation. This allowed for the generation of 1Hz pulses, but then limited the number of pulses that could be safely generated in a single train without the stimulator overheating (Table 2.2). This issue was of particular importance in the design of the studies found in Chapters 5 and 6, both of which occasionally required less than two-second intervals between pulses.

The stimulator was digitally triggered from an external source by delivering a 5V CMOS Logic Level via BNC. This feature allowed for the design of protocols that stimulated the participant in response to changes in their neural and muscular activity. A digital output also allowed the sending of markers to our EEG system and other recording hardware each time a pulse was generated. These digital markers could then be used to time-lock recordings to each stimulation event.

A standard 70mm figure-of-eight coil (Magstim, Whitland, UK) was used in all studies to allow for the focal application of the TMS pulse to the participant's scalp (Figure 2.6B).

Table 2.2

New safety parameters for the Magstim 200^2 Stimulator when digitally triggered

Pulse intensity (%)	Minimum inter-pulse interval (*s*)	Maximum number of sequential pulses
0–50	1	170
50–80	1	≈ 58
80–100	1	≈ 21

The coil in conjunction with the Magstim 200^2 had an average inductance of $15.5\mu H$ and was capable of generating a peak magnetic field of greater than 1.55T at a rate of 25×10^3 T/s.

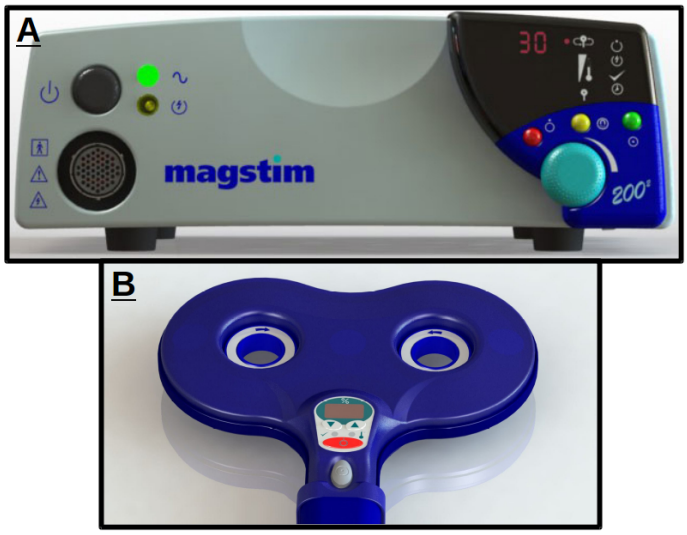

Figure 2.6: **A.** The Magstim 200^2 monophasic stimulator. **B.** The standard 70mm figure-of-eight coil used throughout the thesis.

2.3.4 TMS frame

Given the importance of maintaining coil position during stimulation, a TMS frame was specially designed and built. The frame was designed so that a participant could comfortably sit inside while placing their head in an ophthalmology chin rest. The TMS coil could then be held in place using a mechanical arm that could be locked in position. The frame itself was 80cm tall, 80cm wide and 80cm deep, was designed in AutoCAD (Autodesk, CA, USA) and built using a T-slot aluminium profile system (Figure 2.7).

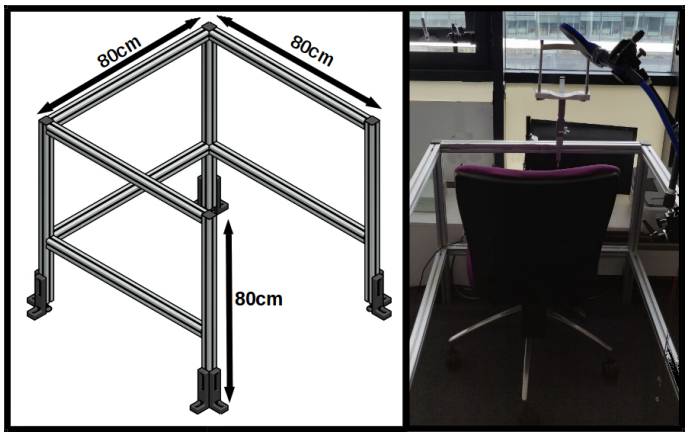

Figure 2.7: **Left Panel.** The original CAD design for the TMS frame. The dimensions of the frame were $80 \times 80 \times 80cm$. **Right Panel.** The constructed frame made from T-slot aluminium. The participant would sit with their head in the integrated chin rest. The TMS coil was then held in place using a lockable, mechanical arm.

2.4 Transcranial alternating current stimulation

2.4.1 Using tACS to entrain an individual's intrinsic neural oscillatory activity

One of the potential limitations of previous tACS studies is how the researchers determined their stimulation frequencies. In both studies mentioned above, they chose to use a typical frequency to represent a frequency band. Antal et al. (2008) used a frequency of $10Hz$ to represent alpha and $15Hz$ to represent beta band stimulation, while Pogosyan et al. (2009) used $20Hz$ to represent beta. This approach is perhaps a little too reductive, if not counter-productive given that there is inter-individual variation in the peak beta frequency (Brovelli et al., 2004; Davis et al., 2012; Neuper & Pfurtscheller, 2001b). Stimulating at a frequency other than an individual's intrinsic peak frequency may cause a desynchronisation of the underlying activity rather than entraining it to the stimulation frequency. This may explain why in the Pogosyan et al. (2009) study, they found that for two of fourteen participants, $20Hz$ stimulation actually had a facilitating effect on movement velocity (Pogosyan et al., 2009).

It has been posited that stimulation techniques such as tACS may be able to modulate neural oscillations (Sejnowski & Paulsen, 2006), but only when stimulating at a frequency similar to that of the ongoing activity. A simple model for how this may be achieved has been suggested by Thut and colleagues (Thut et al., 2011a). They argue that an oscillator with an intrinsic frequency; whether it be an individual neuron (Section 1.2.1), or a number of neural ensembles (Section 1.2.2), may be perturbed by an external, periodic force that oscillates at the same natural frequency.

This simplified model can be found in Figure 2.8 below. Both the model and the accompanying figure are best described by Thut and his colleagues:

"The dynamics of this model can be described conveniently as a vector rotating counter-clockwise along the unit circle in the complex plane (Figure 2.8A, left panel). In the absence of stimulation, the vector cycles with a constant rate around the circle depending on the frequency of the oscillation. The sinusoid (Figure 2.8A, right panel) describes the position of the oscillation with respect to the $360°$ *rotation of one full cycle, i.e., with respect to the phase (*$= \varphi$*,* $0° - 360°$*) over time* (Thut et al., 2011a, p.2)."

When the stimulation frequency is equal to that of the oscillating element, it can entrain the element, phase-locking it to the stimulation over time. In Figure 2.8 B, three oscillators (in this case neural ensembles: green, black and red) are sinusoidally active in the same frequency but out of phase with one another when stimulation is applied (blue vector). The

stimulation is already phase locked with oscillator 2 (black neural ensemble); therefore, elicits no change in the oscillator's phase. However, the stimulation is not phase-aligned with either oscillator 1 (red) or 3 (green neural ensemble). The model predicts that with each successive application of stimulation the phase of each oscillator advances slightly until, after the sixth stimulation they also become phase-locked to the stimulation. At the population level (Figure 2.8 C) this phase-locking of all three neural ensembles would result in an increase in the amplitude of the oscillation, measurable by EEG/MEG (Thut et al., 2011a).

Evidence that tACS may be able to entrain neural oscillations via a similar mechanism to the above model has come from investigations of occipital alpha activity. Zaehle and colleagues (2010) used EEG to find each participant's individual alpha frequency within their occipital cortex, then used tACS to stimulate the same region at its intrinsic frequency. Occipital alpha was increased after three minutes of alpha-tACS stimulation compared to sham (Zaehle et al., 2010). A further study replicated this finding, adding that the increase in occipital alpha lasts for up to thirty minutes after stimulation (Neuling et al., 2013). While, computational modelling has also shown that alpha oscillations are only elicited by tACS in a narrow band around the endogenous oscillatory frequency (Merlet et al., 2013).

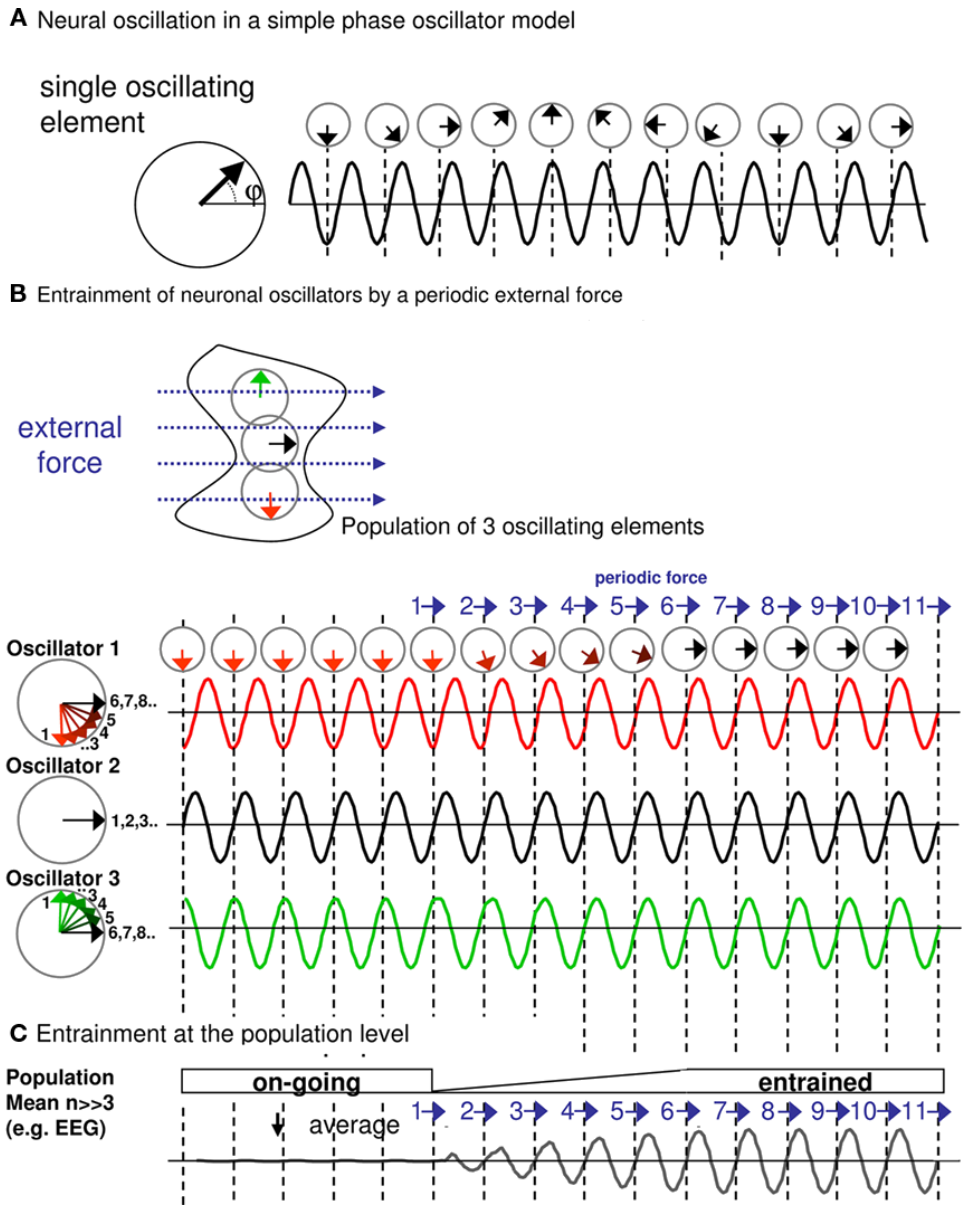

Figure 2.8: **A.** Model of a simple phase oscillator. *Left Panel.* The model can be described as a vector rotating counter-clockwise along the unit circle in the complex plane. In the absence of any stimulation the vector cycles at a constant rate, dependent on the frequency of the intrinsic oscillation. *Right panel.* The sinusoid reflects position of the oscillation in respect to the phase over time. **B.** The effects of periodic stimulation (blue vector) on three oscillators at different phases. The second oscillator (black) is already in phase with the stimulation and is immediately entrained. The other two oscillators are out of phase by $90°$, therefore, are not entrained until the phase of each advances to align with that of the stimulator. **C.** The summed entrainment of the three oscillators at the population level. By the sixth phase all three oscillators are entrained by the stimulation. Reproduced with permission from Thut et al. (2011a).

Studies that have investigated the ability of frequency-specific tACS to entrain neural oscillations are generally limited by the lack of concurrent EEG. Due to the substantial artefact generated by the stimulation itself, previous studies have tended to analyse the after-effects rather than the immediate effects of tACS on oscillatory activity. However, a study by Helfrich and colleagues (2014) used a novel form of artefact rejection to remove the stimulator noise from concurrent EEG. They demonstrated that tACS applied at the intrinsic frequency increases underlying parieto-occipital alpha (Helfrich et al., 2014).

Based on the model suggested by Thut et al. (2011a) and the previous success of other studies (Helfrich et al., 2014; Neuling et al., 2013; Zaehle et al., 2010), all tACS applied throughout this thesis was done so at the peak frequency of each individual.

2.4.2 Stimulator

All transcranial electrical stimulation (tES) was applied using a DC-STIMULATOR PLUS designed and built by neuroConn (neuroConn GmbH, Ilmenau, Germany). The DC-STIMULATOR PLUS is a single channel stimulator capable of both tDCS and tACS at frequencies up to 250Hz for a maximum of 30 minutes (Figure 2.9A). The stimulator is capable of a maximum output current of $4.5mA$ during tDCS and $3mA$ during tACS. More precisely, during tACS, the stimulator can output a sinusoidal waveform with a minimal value of $-1.5mA$ and a maximal value of $1.5mA$, therefore, a maximal peak-to-peak amplitude of $3mA$.

The stimulator has an internal sampling frequency of $2048Hz$, the same sampling rate as any concurrent EEG and EMG recordings. It can also be externally driven via BNC input and can provide a digital readout via BNC, compatible with the neuroPrax EEG system (Section 2.5) and the data acquisition interface (Section 2.6).

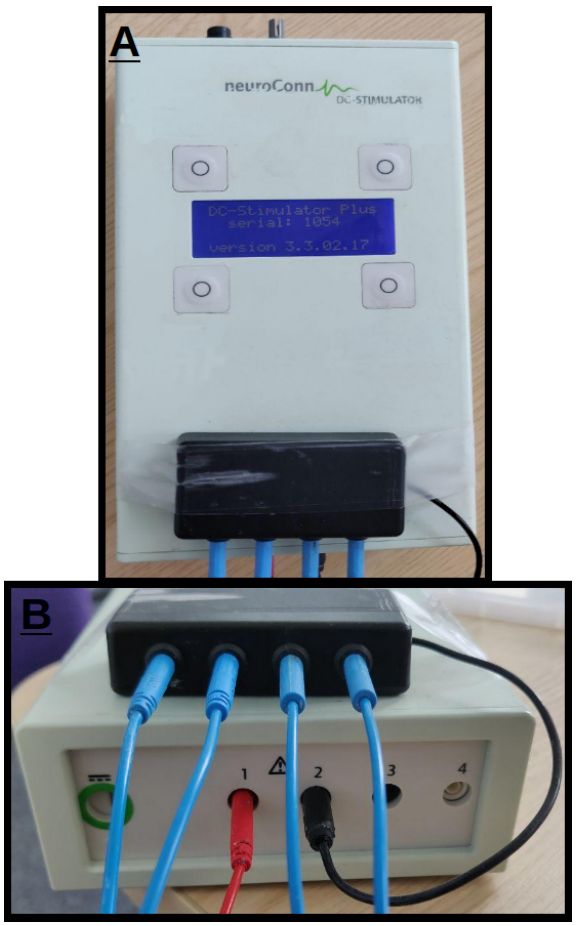

Figure 2.9: The DC-STIMULATOR PLUS tES stimulator used throughout this thesis. **A.** The tACS stimulator capable of outputting a sinusoidal waveform with a peak-to-peak amplitude of up to $3mA$. **B.** The four-to-one wire adapter used to allow the application of our HD-tACS electrode array.

2.4.3 Electrode array

Traditional tES, whether tDCS or tACS, involves applying two large (16-$35cm^2$) rectangular sponge electrodes to the scalp and passing a current between them (Nitsche et al., 2008). This type of stimulation appears to modulate cortical activity over a large area, and the greatest current density does not necessarily occur under the target electrode (Datta et al., 2009; Faria et al., 2011; Kuo et al., 2013; Lang et al., 2005).

This problem can be overcome by reducing the electrode size (Kuo et al., 2013; Nitsche et al., 2007) and by employing a different type of electrode montage. One such electrode montage that has been suggested and investigated is the 4×1 montage, also referred to as HD-tDCS/HD-tACS (Datta et al., 2009; Faria et al., 2011; Kuo et al., 2013). This type of montage involves placing an active electrode over the target area, then placing four return electrodes around the central electrode in a concentric circle (Figure 2.10, see also Datta et al., 2009). Modelling studies have suggested this type of montage restricts

the induced cortical current flow to the radius of the 4×1 circle, with the greatest current density centred over the target electrode (Datta et al., 2009, 2012; Edwards et al., 2013).

Comparisons have been made between conventional tDCS and HD-tDCS, finding that participants felt the more focal form of stimulation was just as tolerable as conventional tDCS when applied at up to $2mA$ (Borckardt et al., 2012; Villamar et al., 2013). Other studies have also demonstrated increased effects of tDCS when delivered using a 4×1 montage, for example, Kuo and colleagues (2013) demonstrated that changes in excitability lasted significantly longer after HD-tDCS than after conventional tDCS (Kuo et al., 2013).

In recent years, HD-tDCS has become more prevalent as the electrode montage of choice for stimulation paradigms. In the motor domain, it has been used to investigate cortical excitability (Cabibel et al., 2018; Caparelli-Daquer et al., 2012; Kuo et al., 2013), response inhibition (Hogeveen et al., 2016) and sensorimotor cortex involvement during finger tapping (Muthalib et al., 2016). The same cannot be said of HD-tACS, the use of which has, thus far, been very limited (Helfrich et al., 2014).

The potential of alternative montages, such as the 4×1 montage employed by HD-tDCS/tACS to deliver more focal stimulation, along with the lack of previous research into HD-tACS, led to my decision to use a similar montage to attempt to entrain motor oscillations. To that end, the central, active electrode was placed over the functionally localised M1h (Section 2.3.2), this was to ensure stimulation was tailored to target each individual's motor cortex, rather than more generalised and less precise 10-20 estimates. Four return electrodes were then placed in an approximation of a concentric circle around the centre (Figure 2.10).

The four return electrodes were each spaced 4cm away from the active electrode (ring centre to ring centre). Relative to those used in other studies (Caparelli-Daquer et al., 2012; Helfrich et al., 2014; Kuo et al., 2013), this montage is quite small. This choice was made for two reasons. Firstly, because previous modelling studies have suggested that the smaller the montage, the more focal the stimulation (Alam et al., 2016). Secondly, because I wanted to explore the treatment potential for HD-tACS, with a view to developing portable stimulators that could monitor and stimulate patients as required. For this to be a feasible form of treatment, the montage had to be relatively inconspicuous on the patient's scalp.

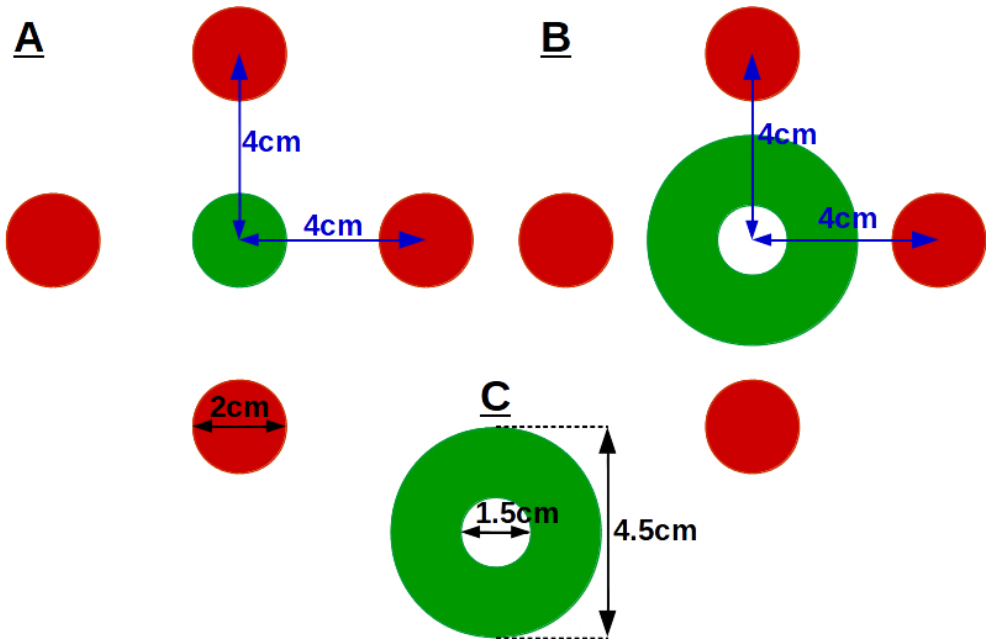

Figure 2.10: The two different 4×1 electrode montages used. ***A.*** The pure tACS montage with a central, active electrode (green) placed over M1h, and four return electrodes (red) arranged in a concentric circle around the centre. Each electrode had a diameter of 2cm and was spaced 4cm away from the centre of the active electrode. ***B.*** A second montage designed to be used with concurrent EEG. The central active *'doughnut'* electrode allowed for the placement of an EEG electrode in its centre. ***C.*** The total diameter of the *'doughnut'* electrode was 4.5cm with an inner diameter of 1.5cm.

Rubber circular electrodes were used for all tACS studies, with a diameter of $20mm$ and surface area of $3.14cm^2$ (neuroConn GmbH, Ilmenau, Germany). When tACS was used in conjunction with EEG the central electrode was replaced with a *'doughnut'* electrode (Figure 2.10, C). These electrodes were designed to allow the placement of an EEG electrode in their centre; therefore, they had a total diameter of $45mm$ and a hole in the centre with a diameter of $15mm$. This meant that these electrodes had a contact area of $14.13cm^2$. In both configurations, the four return electrodes were attached to the DC stimulator with a four-to-one wire adapter (Figure 2.9B).

As with EMG electrodes, the skin was prepared before applying the tACS electrodes. The scalp was cleaned with alcohol to remove oil and dirt then gently abraded with NuPrep conductive gel (Weaver and Co., USA). The electrodes were then affixed to the scalp using Ten20 conductive paste (Weaver and Co., USA). Impedance was measured by the DC stimulator and stimulation was not possible unless impedance was below $10k\Omega$.

2.5 Electroencephalography

Electroencephalography (EEG) is a measure of the summed electrical activity generated by the spontaneous firing of tens of thousands of anatomically-aligned neurons (Nunez

& Srinivasan, 2006). The most significant source of this scalp-recorded EEG is the post-synaptic potential, whether excitatory (EPSPs) or inhibitory (IPSPs) (Creutzfeldt & Houchin, 1974; Speckmann et al., 2011). Unlike other neuroimaging techniques, EEG and MEG are direct measures of neural activity. This feature provides EEG and MEG with excellent temporal resolution, in the order of tenths of a millisecond (Baillet et al., 2001).

EEG's high temporal resolution makes it ideally suited to the investigation of rapid and dynamic changes in neural activity. For many years following Grey Walter and colleagues discovery of the *'contingent negative variation'* (Grey Walter et al., 1964) the focus of EEG research has been on the event-related potential (ERP). An ERP is a time and phase-locked measure of the voltage change in neural activity in response to an external event and as such can provide a great deal of information about the temporal nature of neural processing. More recently, the literature has begun to point to the importance of neural oscillations in understanding brain function. Given that the ERP component may arise from changes in ongoing oscillations in multiple frequency bands (Başar et al., 1999; Buzsáki, 2006), the study of event-related oscillations has become one of major interest.

Throughout each of the experimental chapters described below, EEG is used to investigate changes in alpha and beta activity in the primary motor cortex during the preparation and execution of movement.

2.5.1 Amplifier

All EEG recordings were made using a DC-EEG feedback system, NEURO PRAX, designed and built by neuroConn (neuroConn GmbH, Ilmenau, Germany). This system allows for the recording of up to 128 channels at a sampling rate of 2048Hz. Each channel has a resolution of 24-bit, and the recorded signal is transferred from the DC amplifier to the monitor via optical fibre to ensure galvanic isolation. This system was specifically designed to be used in conjunction with both TMS and tES to provide biofeedback to the user. Therefore, it is capable of capturing concurrent electrophysiological recordings from the Bagnoli EMG system and receiving digital markers from both the Magstim 200^2 and the DC-STIMULATOR PLUS via 4 BNC inputs.

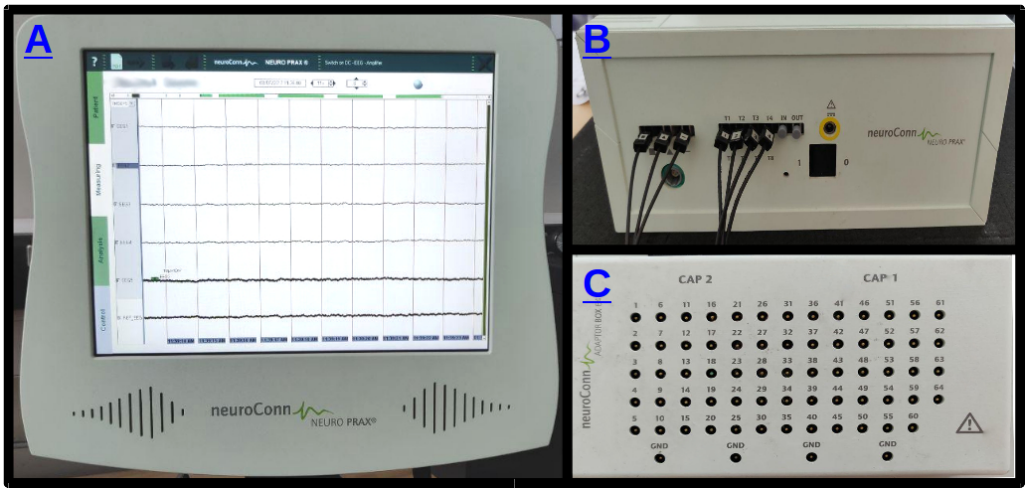

Figure 2.11: The NEURO PRAX DC-EEG feedback system. **A.** The EEG monitor, which allowed for online monitoring of the recorded signal. **B.** The EEG amplifier. Once the recorded signal is amplified it is sent to the monitor via optical fibre. **C.** The electrode adapter box which acts as an interface between the Ag/AgCl electrodes and the amplifier.

2.5.2 Electrode placement

A novel electrode montage was developed and used throughout this thesis, similar to those used in brain-computer interface (BCI) research (Edelman et al., 2016; Lotte et al., 2007; Wolpaw et al., 2000, 2002). These smaller, more focal, electrode montages are not a new concept as they have long been suggested to aid in scalp-current density (SCD) estimation (MacKay, 1983; Meckler et al., 2010; Perrin et al., 1987). A study presented by Takemi and colleagues (2013) used a similar montage to the one presented here to investigate beta ERD within the M1 (Takemi et al., 2013).

Throughout the presented work, source localisation was less of a priority due to our prior knowledge of the anatomy of the primary motor cortex. The functional localisation procedure described in Section 2.3.2 allowed localisation of the scalp coordinates corresponding with the activation of each individual's M1h. An EEG electrode montage was then placed on the scalp, centred at M1h, with a further six electrodes arranged in an elongated cross (Figure 2.12). This enables acquisition of data from comparable locations across participants while enabling confirmation of M1h as the largest source.

Each electrode was spaced 2cm apart from its neighbour (ring centre to ring centre) with one electrode (M1d) placed 2cm dorsal to M1h and a second (M1v) placed 2cm ventral. The four remaining electrodes were arranged along the anterior-posterior axis. Two were placed anterior to M1h, the first (M1a) 2cm anterior to M1h and the second (M1aa) 4cm anterior. The two posterior electrodes (M1p and M1pp) were placed in the same spatial

alignment as the anterior electrodes (Figure 2.12). These electrodes were placed as such to confirm optimal spatial positioning of the M1h electrode. Each of the seven active EEG electrodes was referenced online to an electrode placed over the right mastoid process.

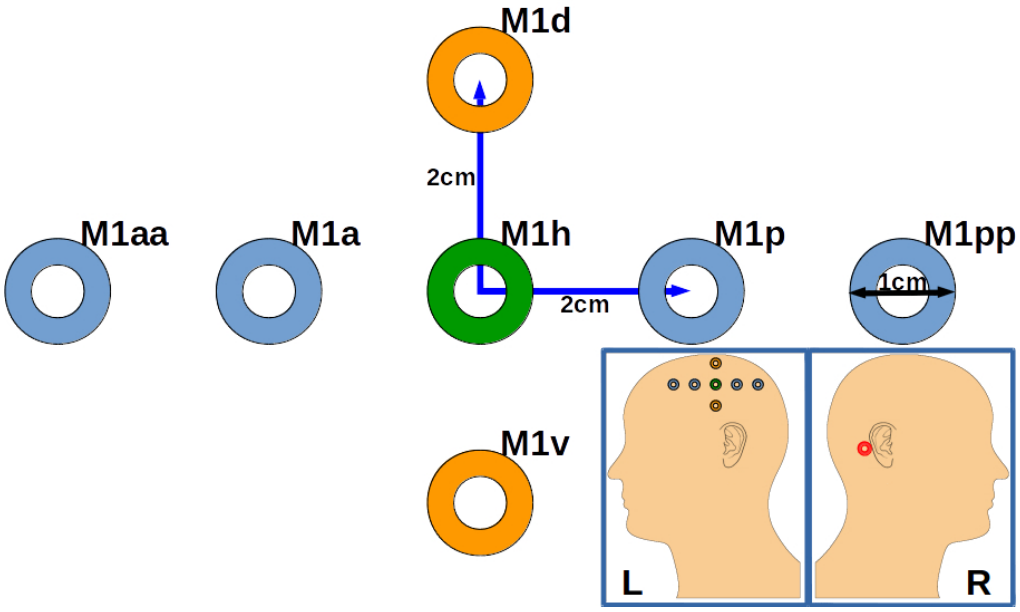

Figure 2.12: The novel EEG montage used throughout this thesis. The montage consisted of seven electrodes, arranged in an elongated cross, centred over the localised hand area (M1h) of the left hemisphere. Electrodes had a diameter of 1cm and were spaced 2cm apart. **Inset.** The montage was positioned over the left hemisphere and the reference electrode was placed over the right mastoid process.

Standard silver-silver chloride (Ag/AgCl) ring electrodes, with a diameter of 1cm, were used to record EEG signals from the scalp unless EEG was being recorded simultaneously with TMS stimulation. If this was the case, specially designed low-diameter conductive plastic electrodes coated in Ag/AgCl were employed. This was to prevent the overheating of electrodes due to eddy-current heating of electrodes caused by the magnetic field of TMS (Roth et al., 1992; Thut et al., 2005; Ilmoniemi & Kičić, 2010).

Prior to application, both the participant's scalp and the electrodes were prepared. The scalp was prepared using the same cleaning and abrasion procedure as was used for skin preparation prior to tACS (Section 2.4.3). The electrodes were coated with Ten20 conductive paste at least fifteen minutes before being affixed to the scalp. This was to ensure a stable polarisation potential of the electrodes and reduce the electrode-scalp impedance (Tallgren et al., 2005).

Due to the use of a novel montage a typical 10-20 electrode cap does not afford the required flexibility of positioning. Instead, the electrodes were attached to the scalp

using the Ten20 conductive paste before the inner diameter was filled with a chloride containing conductive EEG gel (Abralyt HiCl, Easycap GmbH, Germany). Prior to commencing recording, an online impedance check was made to ensure the electrode-scalp impedance of each electrode was below the threshold of $3k\Omega$.

2.5.3 Analysis

All recorded EEG data were exported and converted into ASCII text files. These were then imported into MATLAB (2014b, Mathworks, Natick, MA) so that they could be analysed offline. The data analysis was achieved through a combination of custom analysis scripts, in-built MATLAB functions, and functions provided by the FieldTrip open-source MATLAB toolbox (Oostenveld et al., 2011).

Baseline correction

Ultra-slow (0.1–$0.2Hz$) voltage changes in the recorded signal, mostly caused by changes in skin potential, can cause the signal to drift from a zero-mean baseline (Luck, 2014). This becomes an issue when wanting to compare the recorded EEG at two distinct time-points or when using an automated artefact removal based on a set voltage threshold.

Voltage drift is primarily prevented by careful preparation of the skin and electrodes; for example, using Ten20 conductive paste to stabilise the electrode polarisation, abrading the skin to ensure a low electrode-scalp impedance and securing electrodes with additional fixings to minimise (e.g. tape) to avoid movement. However, factors such as the temperature of the room and participant sweat concentration can also affect electrode-scalp impedance over time. Therefore, the referenced EEG signal from each of the active electrodes was baseline corrected by removal of linear trends in the complete EEG dataset based upon computing and subtracting the least-squares fit of a straight line to the trace.

Filtering

The referenced and baseline corrected EEG signal was filtered with a bandpass filter and notch-filter in the FieldTrip toolbox.

Specifically, a Hamming window-synced finite impulse response (FIR) filter was used to bandpass filter the EEG signal between 2 and $100Hz$ (Oppenheim & Schafer, 2013). An FIR filter is a non-recursive filter that is intrinsically stable and generally easier to implement than an infinite impulse response filter (Saramäki, 1993). FIR filters are the

primary filtering method in EEG research due to their high stability and accuracy (Oppenheim & Schafer, 2013). There are a number of different window types that can be used in a window-synced FIR filter; however, when applied to my data, the Hamming window produced the cleanest result.

The same Hamming window-synced FIR filter was then used as a notch-filter to remove the $50Hz$ electrical artefact from the EEG signal. The band-stop frequency was defined as 48.5–$51.5Hz$.

Artefact removal

Artefacts in the EEG were dealt with in three stages: avoidance, identification, and removal. Firstly, to pre-emptively avoid the occurrence of gross movement artefacts, participants were asked to seat themselves in a comfortable, relaxed position, relax their jaw and try to move only the limb of interest and only when instructed. They were also instructed not to speak unless absolutely necessary, to reduce the occurrence of jaw and tongue muscle artefacts. Ocular movements were limited through the use of a fixation cross in all studies. Rather than asking the participant to try to control their eye-blinks they were instructed just to blink as normal. This was done to prevent a consistent artefact time-locked to a trial event.

In general, artefacts as a result of ocular movements were limited by the relative placement of the recording and reference electrodes. Initial tests were performed using electrooculogram and a step-function (Luck, 2014) to investigate the occurrence of ocular artefact throughout the EEG montage. The results of these early tests indicated that the most anterior electrode (M1aa) had the highest incidence of ocular and facial muscle artefacts; while the more posterior electrodes, including the electrode over M1h, were relatively unaffected.

I wrote a custom MATLAB function that implemented a moving time-window with a width of 500ms to assess the peak-to-peak amplitude of the raw EEG signal. A threshold of two standard deviations from the mean peak-to-peak amplitude was used to define time-windows containing artefacts for rejection. This automated process would then plot the identified time-windows to allow artefacts to be visually assessed and marked for removal.

Time-frequency analysis

Time-frequency analysis was carried out using a Morlet wavelet transformation (Bertrand & Pantev, 1994; Tallon-Baudry & Bertrand, 1999). This transform was used to estimate the instantaneous power at each time-point by computing the sum of squares of the convolved data (Kiebel et al., 2005).

The main advantage of using a Morlet wavelet transform over other transforms, such as the short-term Fourier transform, is that the width of the Gaussian window used is coupled to the frequency under investigation. This means the width of the window during low frequencies is greater than at higher frequencies to ensure the same number of cycles across frequencies (Kiebel et al., 2005). The number of cycles used was fixed at ten cycles; this means that the window width at $40Hz$ was approximately $250ms$, while at $10Hz$ the window width would be $1000ms$. The analysed frequencies were between 0.5 and $100Hz$ in steps of $0.5Hz$. This allowed for the investigation of power changes in individual frequencies over time and in average frequency bands, such as alpha and beta.

Further analyses of time-frequency characteristics of the signal are described in each experimental chapter.

2.6 Data acquisition and event triggering

2.6.1 Power 1401-3

Figure 2.13: The Power 1401-3 data acquisition interface.

The data acquisition interface used to capture electromyographic and digital marker data was a Power 1401-3 (CED, Cambridge, UK). The Power 1401-3 is capable of recording from 16 waveform input channels and was used to digitise and store all recorded data at a sampling rate of $2048Hz$. Another feature of the Power 1401-3 is its ability to output waveforms from up to 4 different channels. This was particularly useful as a BNC output from the 1401 could be used to drive an equivalent waveform in the tACS stimulator. Alternatively, a 5V CMOS Logic Level could be outputted as a trigger for the TMS stimulator.

2.6.2 Signal

Signal (6.04, CED, Cambridge, UK) is a sweep-based data acquisition and analysis package, designed by CED to acquire data from their Power 1401-3. Due to its ability to continuously monitor a data channel, then record frames of data time-locked to an event, Signal was primarily used throughout this thesis to record MEPs.

When a TMS pulse was delivered by the Magstim 200^2 stimulator, a digital trigger was sent to the Power 1401-3. This trigger would then be interpreted by Signal as a recordable event at time-point zero. A frame of data would then be presented on screen for review beginning at -100ms and ending 100ms after the TMS. This allowed for the online assessment of the elicited MEP peak-to-peak amplitude during procedures like the functional localisation procedure (Section 2.3.2). Each recorded frame could then be digitised and exported into an ASCII text file for further offline analysis in MATLAB.

2.6.3 Spike2

Spike2 (7.18, CED, Cambridge, UK) is the second piece of software designed by CED. Like Signal, Spike2 acquires data from the Power 1401-3; however, rather than recording discrete data frames time-locked to an event, Spike2 is a continuous data acquisition package. This is particularly advantageous for using biological recordings as event triggers.

Spike2 is able to generate digital markers or trigger an event based on the recorded data from an input channel. Spike2 was used for the studies described in Chapters 5 and 6, to trigger TMS stimulation in response to a force threshold being surpassed when a finger was pressed on a force transducer. In Chapter 4, Spike2 was employed to send sinusoidal waveforms to the DC-STIMULATOR PLUS, to generate an equivalent tACS output.

2.6.4 Arduino Uno

Arduino (Arduino.cc) is an open-source electronics platform that produces easy-to-use hardware and software for commercial and personal use. One such piece of hardware is the Arduino Uno (Rev3) used throughout the body of work described in this thesis.

The Uno (Arduino.cc, 2017) is a microcontroller board based on the ATmega328P (Atmel, 2015). It has 14 digital input/output pins and can be controlled and powered via USB connector. The board can also be controlled wirelessly, via WiFi or Bluetooth, however, to

improve the trigger latency I only utilised the USB connector. The presence of the digital pins allowed me to solder female BNC connectors to the board. The rationale behind using BNC as my trigger outputs is simply that, as mentioned: the CED Power 1401-3 along with the EEG, TMS and tES systems all receive BNC inputs. To achieve some semblance of neatness, I only soldered four connectors to the board, but it is perfectly possible to attach a connector to each pin leaving you with 14 BNC connections to digitally trigger events.

A major advantage of using the Uno is that it is supported by MATLAB, with a number of official support packages made available. This allowed me to control the Uno board from within MATLAB-run experiments and to send millisecond long square pulses to each digital pin. This meant that at any point in an experimental trial a trigger could be sent to the EEG system to create a digital marker, or to the TMS stimulator to generate a time-locked TMS pulse, or to the tES stimulator to begin a train of tACS stimulation.

2.6.5 Chapter-specific methodology

A number of other apparatuses were used in each chapter; however, these were not used universally and will, therefore, be described in full in each experimental chapter.

Chapter 3

Transient alpha and beta synchrony underlies preparatory recruitment of directional motor networks.

The most exciting phrase to hear in science, the one that heralds the most discoveries, is not "Eureka!" but "That's funny. . ."

– Isaac Asimov (1920-1992)

3.1 Introduction

Modulations in motor cortical alpha and beta activity have been implicated in the preparation, execution and termination of voluntary movements. Abnormal forms of this modulation have been associated with neuropathologies that exhibit motor deficits, such as Parkinson's disease (PD; Brown, 2003; Brown et al., 2004; Hall et al., 2014; Kühn et al., 2006) and stroke (Hall et al., 2010b; Tecchio et al., 2006b). In this chapter, we used an established directional uncertainty paradigm to explore changes in alpha and beta activity during the preparation of movement.

3.1.1 Background

Neuronal populations have intrinsic oscillatory properties that allow the synchronous activation of multiple networks within the brain. The primary motor cortex exhibits oscillatory activity within beta and alpha frequency bands (Baker et al., 1997; Murthy & Fetz, 1992; Pfurtscheller & Aranibar, 1979). Motor-related beta activity is not constrained to the primary motor cortex (M1) and has been measured throughout the motor-related brain network (Klostermann et al., 2007). The cortical origins of the sensorimotor alpha (or mu) and beta rhythms have been proposed to originate from separate sources, with beta generated in M1 (Baker et al., 1997; Murthy & Fetz, 1992) and mu generated in the primary somatosensory cortex (Salmelin & Hari, 1994).

However, recent studies demonstrate that both alpha and beta rhythms are generated in multiple laminae of M1 (Rönnqvist et al., 2013; Yamawaki et al., 2008), with amplitude dependent on connectivity with S1 and other areas.

As early as two seconds before movement onset there is an event-related desynchronisation (ERD) of motor cortical alpha, reaching its peak at the point of movement (Crone, 1998a; Leocani et al., 1997; Pfurtscheller & Lopes Da Silva, 1999; Salmelin & Hari, 1994). This decrease in alpha power begins during the preparation of movement as a more general desynchronisation across bilateral somatosensory and motor cortices, then becomes more somatotopically focussed within the M1 at the point of movement execution (Crone, 1998a).

There is also some evidence to suggest that as the ERD peaks in the somatotopic area of the M1 responsible for the required motor output, there is a resynchronisation of alpha power in other motor regions that are not required for the movement execution (Fu et al., 2001; de Pesters et al., 2016; Pfurtscheller & Berghold, 1989; Pfurtscheller, 1992). This desynchronisation of task-relevant areas and concurrent synchronisation of task-irrelevant areas may be explained by the *'gating-by-inhibition'* hypothesis (Jensen & Mazaheri, 2010). If increased alpha activity is a correlate of cortical inhibition, then the synchronisation of motor areas that surround the ensemble required to make a movement may act as an inhibitory block, 'gating' the information flow toward the required ensemble.

Intrinsic beta activity is modulated during the preparation, execution, and termination of voluntary movements (Cheyne et al., 2008). During the preparation and execution of the movement, there is a beta ERD (Cheyne et al., 2006; Engel & Fries, 2010; Gaetz et al., 2010; Neuper & Pfurtscheller, 2001a; Pfurtscheller & Lopes Da Silva, 1999; Zhang et al., 2008). This beta desynchronisation usually occurs approximately one second before the movement onset and persists until movement cessation (Erbil & Ungan, 2007; Pfurtscheller & Lopes Da Silva, 1999; Stancák & Pfurtscheller, 1995).

The movement-related desynchronisation of beta activity can be divided into two phases: the preparatory-phase, the ERD that occurs prior to movement onset; and the response-phase, the ERD that occurs as the movement is executed. If the same effector is used to perform various types of movement, the amplitude of response-phase ERD varies very little (Pistohl et al., 2012; Salmelin et al., 1995a; Stancák & Pfurtscheller, 1995; Stancák

& Pfurtscheller, 1996a; Stančák et al., 1997). However, there is evidence to suggest that the more information a participant is given about the movement they are to perform, the greater the desynchronisation during the preparatory-phase ERD (Grent-'t Jong et al., 2014; Kaiser et al., 2001; Tzagarakis et al., 2010).

The functional role of beta oscillatory activity is, as yet, unclear. However, evidence from local field potential (LFP) measures of the basal ganglia of patients with PD suggests a link between exaggerated beta activity and impaired motor function (Brown & Williams, 2005; Kühn et al., 2005; Weinberger et al., 2006). Two theories have been suggested to explain the role of beta activity in motor function. The first, proposed by Pfurtscheller and colleagues (1996), suggests that beta activity is a correlate of idling motor activity (Pfurtscheller et al., 1996). More recently, a second theory has proposed that beta activity promotes postural and tonic activity at the expense of voluntary movements (Gilbertson et al., 2005; Pastötter et al., 2008). Slowing of voluntary movement during intrinsic elevations in cortical beta activity (Gilbertson et al., 2005) and during $20Hz$ entrainment using transcranial alternating current stimulation of motor cortex (Pogosyan et al., 2009) has been cited as further evidence for this theory (Jenkinson & Brown, 2011).

Recording from implanted deep brain stimulation electrodes enables measurement of LFPs and, therefore, oscillatory activity from the subthalamic nucleus (STN) of patients with PD who suffer from increased tonic activity (rigidity) and slowness of movement (bradykinesia). The observation of exaggerated beta power in the STN of these patients with PD further supports the theory that M1 beta promotes tonic activity (Hammond et al., 2007) at the expense of voluntary movement. Deep brain stimulation to the STN suppresses beta activity, and the degree of suppression correlates with the level of improvement in rigidity and bradykinesia (Bronte-Stewart et al., 2009; Kühn et al., 2008). This same correlation between the degree of reduced beta oscillatory activity and improvement in rigidity is observed following effective dopaminergic drug treatment (Kühn et al., 2006; Ray et al., 2008; Weinberger et al., 2006).

Further studies of both patient and neurotypical populations demonstrate beta suppression is a strong predictor of the efficacy of motor preparatory processes, with greater beta suppression reflected in shorter response times (Doyle et al., 2005; Williams et al., 2003). The latency of motor response is also well established to covary

with the degree of certainty in the movement direction (Bock & Arnold, 1992; Churchland et al., 2008; Dorris & Munoz, 1998; Pellizzer et al., 2006).

Therefore, in this chapter, we adopted an established motor-experimental paradigm for varying directional uncertainty (Pellizzer & Hedges, 2003; Pellizzer et al., 2006; Tzagarakis et al., 2010), to investigate changes in preparatory beta and alpha power. The task, developed by Pellizzer and Hedges (2003), was an instructed-delay reaching task that consisted of four key elements. First, the participant used a joystick to hold a crosshair within an outline of a circle in the centre of the screen for 2s. Following this wait period a spatial cue consisting of one, two or three circular targets was presented. After a jittered wait period of 1–1.5s, one of the targets was highlighted. Once a target was highlighted, the participant used the joystick to move the crosshair and hit the identified target. The participant's response time (RT) was defined as the time taken, following target identification, to move the crosshair out of the centre circle towards the identified target. A previous study by Tzagarakis and colleagues (2010) found by using this established paradigm that RTs are significantly lengthened and beta suppression significantly reduced as directional uncertainty increases (Tzagarakis et al., 2010).

3.1.2 Aims and research objectives

The aim of this study was to:

1. Identify the optimal location of the motor cortex hand area (M1h), controlling the first dorsal interosseous (FDI) (Section 2.3.2).
2. To confirm the findings of previous studies that as the degree of uncertainty about an upcoming movement increases, so do the resulting response times.
3. To characterise the time-frequency profile of oscillatory modulation at each phase of the movement for each individual.
4. To investigate the modulatory effect of directional uncertainty on the magnitude of alpha and beta ERD during both the preparatory and the response phase of movement.
5. To identify synchronous events that can reliably predict motor preparation and the speed of the behavioural response.

Based on the findings of previous research (Bock & Arnold, 1992; Churchland et al., 2008; Dorris & Munoz, 1998; Pellizzer et al., 2006; Tzagarakis et al., 2010), we predicted that as the number of spatial cues and, therefore, the degree of uncertainty about the direction of movement increases, there will be a significant increase in RT.

We suggest that, when at rest, beta synchrony is a correlate of postural and tonic activity being promoted above that of voluntary movement. Therefore, the desynchronisation of ongoing beta activity reflects a process of disengagement from the current motor set, to then allow the recruitment of the required functional assembly to perform an action. Based on this hypothesis, it was predicted that:

1. A greater disengagement and, therefore, greater ERD would occur when the participant was entirely certain about the required motor response.
2. The differentiation of beta ERD would occur at the earliest phase of the response, the preparatory phase.

Furthermore, based on the hypothesis that the recruitment of the required functional assembly occurs after disengagement from the current motor set, it was predicted that:

1. Following the initial preparatory ERD, there would be a synchronous event that would coincide with the recruitment of the correct functional assembly.

2. The creation of a specific functional assembly, accompanied by a synchronous event, can only occur when the function (direction) is known. Therefore, it will occur in the relevant interval when the required direction of movement is revealed.

3.2 Methodology

Eighty right-handed participants were recruited in total (19 male), with a mean age of 27 (range 18 – 71) years. Informed consent was obtained, and all studies were approved by the local ethics committee, in accordance with the ethical standards set by the 1964 Declaration of Helsinki. All participants passed a TMS safety screening, were free of medication and did not have any personal or family history of neurological or psychiatric illness. Subjects were excluded if over 20% of their trials were removed due to low EEG signal-to-noise or poor behavioural performance. As a result, six participants were excluded in total from the analysis.

3.2.1 Procedure

Surface electromyogram was recorded from the right first dorsal interosseous (FDI) using a Bagnoli 2-channel EMG-system (DelSys Inc., Boston, USA). EMG signals were amplified 10,000 times and sampled at a rate of $2048Hz$. Impedance was kept below $10k\Omega$, and all EMG signals were bandpass $(20–450Hz)$ and notch-filtered $(48.5–51.5Hz)$ using the same window-synced FIR filter applied to the EEG signal. EMG was recorded at the start of the experiment so that MEPs could be recorded during the functional localiser. Once complete, the electrodes were removed from the hand.

The left M1 was functionally localised using the TMS procedure outlined in Section 2.3.2. This allowed us to ascertain the participant's M1h and their resting motor threshold (RMT). RMT was defined as the lowest stimulator intensity required to consistently induce MEPs in the right FDI with a peak-to-peak amplitude greater than $50\mu V$ in 8 out of 10 trials. All induced MEPs in this study were collected at 100% of each individual's RMT. This scalp location was also used to guide EEG electrode placement.

All EEG data were recorded using the DC-EEG feedback system (Section 2.5.1). Ag/AgCl electrodes were arranged in our standard 7-electrode montage with the localised M1h at its centre (Section 2.5.2). EEG was referenced online to the ipsilateral mastoid and sampled at a rate of $2048Hz$ with impedance for all channels maintained below $3k\Omega$. EEG signals were bandpass filtered $(2–100Hz)$ and notch-filtered $(48.5–51.5Hz)$ to avoid power line contamination(Section 2.5.3).

Once the M1h had been localised and the EEG montage was in place, participants were seated at a desk and gripped a custom-made joystick with their right hand, resting their

forearm on the desk. The joystick was designed to be held between the thumb and index finger (Figure 3.1B) and was capable of full $360°$ rotation within the horizontal plane. The behavioural task was displayed on a 21-inch, high-definition monitor, placed at a comfortable height, 90cm in front of the participant. The task was controlled by a custom-made computer program (Microsoft Visual Basic), which recorded the coordinate position of the joystick at a sampling rate of $2048Hz$. Digital triggers were sent to the EEG system by an Arduino Uno (Section 2.6.4), these triggers marked the beginning of each trial, the cue onset, target identification and movement onset to aid in the time-locking of the EEG analyses.

3.2.2 Behavioural task and trial design

The task used was an instructed-delay reaching task based on the established paradigm (Pellizzer & Hedges, 2003; Pellizzer et al., 2006; Tzagarakis et al., 2010), as seen in Figure 3.1. The task consisted of 180 trials, presented in five blocks, comprised of 36 trials in each block. There was a two minute rest period between each block that the participant controlled. This was designed to allow the participant to skip the rest period if they felt they did not need it. Before beginning the task in full, the participant performed ten practice trials to ensure they understood the instructions. The data from these practice trials were checked to ensure the correct digital triggers had been marked and then discarded from further analysis.

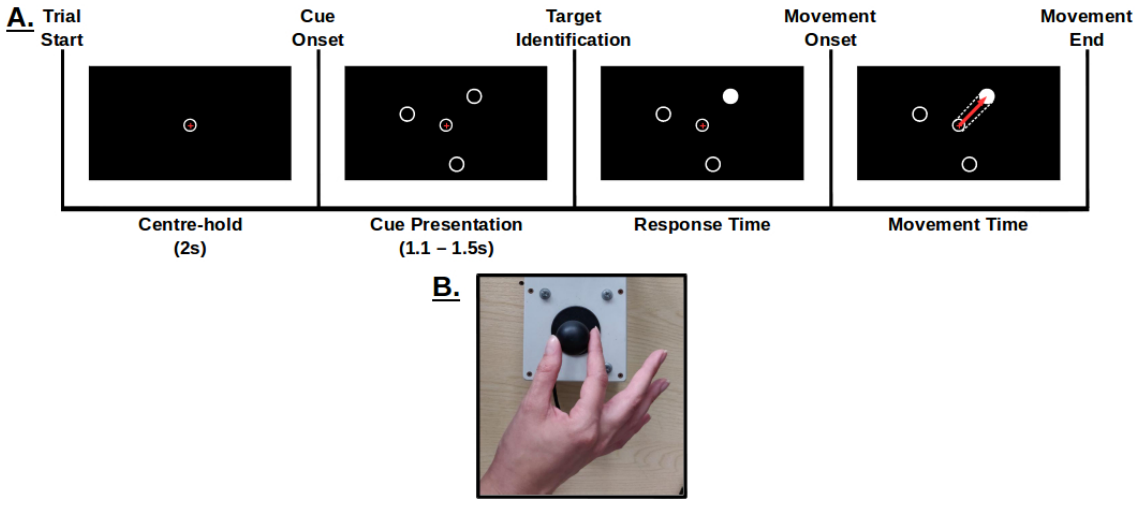

Figure 3.1: **A.** Diagram of the trial sequence for the instructed-delay task. Participants used the joystick to hold the crosshair in the centre of the screen for 2s. Then 1, 2 or 3 potential targets were presented on the screen for 1.1-1.5s. The figure depicts a '3-Target' trial in which the target at 45° was highlighted as the target the participant was to move the crosshair toward. RT was defined as the duration between target identification and movement onset. **B.** The custom-made joystick used throughout the study was designed to be held between the thumb and index finger.

Each trial comprised a 'centre-hold' period, a spatial cue presentation ('cue onset'), a target cue presentation ('target identification') and a participant response ('movement onset'). Each trial was initiated by the participant maintaining a joystick-controlled crosshair within an outline of a circle in the centre of the screen (radius, 0.6° of the visual angle (VA)) for 2s. Participants were instructed to fixate on the centre of the screen throughout the trial (Figure 3.1A).

Following the 'centre hold' period, a spatial cue was presented that varied randomly in duration between 1 and 1.5s. The spatial cue consisted of one, two or three possible targets, with the number and positions of targets pseudo-randomised for each trial. This resulted in three possible target presentations, each presented 20 times during the *one-target* condition and three possible combinations of targets, each presented 20 times, during the *two-target* condition. Sixty trials in total were presented for each target condition.

Each target consisted of an outline of a circle (radius, 0.75° VA) with a centre 4° VA away from the centre of the screen. Targets were presented at 45°, 165° and 285° relative to the centre of the screen. Following cue onset one of the targets was highlighted white (target identification). At this point, the participant used the joystick to move the crosshair from the centre of the screen towards the highlighted target circle as quickly and accurately as possible. Consequently, directional preparation was possible at cue onset in only the one-target condition, but not in the two-target or three-target conditions, where directional uncertainty continues until target identification.

Successful responses were defined as a trial in which the participant moved the crosshair from the centre of the screen to the target circle in a direct straight line (final panel, Figure 3.1A). Trials in which the participant deviated from this straight-line movement were removed from the analysis. The RT was defined as the period between target identification and movement onset.

For each of the three target conditions, RT outliers were removed from the dataset. The threshold used to detect outliers was the median $\pm$ 2* median absolute deviation (MAD), where MAD is calculated by finding the median of absolute deviations from the median (Huber & Ronchetti, 1981; Leys et al., 2013). This method of outlier detection is considered to be more appropriate and robust than using the mean $\pm$ SD (Hampel, 1971; Leys et al., 2013; Liu et al., 2004).

3.2.3 EEG analysis

Time-frequency analysis was performed using a Morlet wavelet transformation (Bertrand & Pantev, 1994; Tallon-Baudry & Bertrand, 1999). Spectral power in the alpha (8–$12Hz$) and beta (13–$30Hz$) bands were analysed based on the mean amplitude in each band. Analysis of resting beta power, during an initial two-minute recording, was used to confirm the central electrode as the optimal location for further analysis, which was used for all subsequent analysis. Epochs were defined using digital triggers produced by the Arduino-EEG interface for both cue onset and target identification for each trial. The preparation stage of movement was defined as the phase between cue onset and target identification for each trial (1000-1500ms).

Successful trials were defined as trials in which the participant identified the correct target and moved the crosshair to the centre of the target circle in a straight line. Unsuccessful trials were removed from analysis along with any trial in which the signal to noise ratio was too low. Subjects were removed from the analysis if over 20% of their trials were lost. As a result, the final analysis was carried out on 74 out of 80 participants.

3.2.4 Experimental design and statistical analyses

A fully counterbalanced repeated measures design was used. Differences in RTs, beta amplitude and alpha amplitude across the three directional uncertainty conditions were analysed using analyses of variance (ANOVAs) and paired t-tests.

The latency of oscillatory power change (ERD) was identified as the time point at which oscillatory power fell $2.5SD$ from the mean baseline power, following the method previously described (McAllister et al., 2013). Change in beta power was analysed with respect to a 1000ms baseline period beginning 1500ms before cue onset, for the initial change following cue onset and target identification. To further determine the relative change in oscillatory power between target identification and movement onset, data were normalised to the point of target identification.

To test the hypothesis that creation of a functional assembly requires and therefore coincides with transient synchrony, we analysed the change in synchronous power following the initial desynchronisation (uncoupling) from the beta. We used a sliding window approach (50ms) to compute the change in synchronous power between conditions (one, two, and three targets) from the minimum following cue onset to the

maximum in the interval up to target identification. We used the same approach to determine the difference in power between the 100ms pre-target identification and the interval up to movement onset. This approach was used to identify differences in synchronous power when direction was known in the post-cue onset (one-target) or post-target identification (three-target) conditions.

3.3 Results

3.3.1 Behaviour results

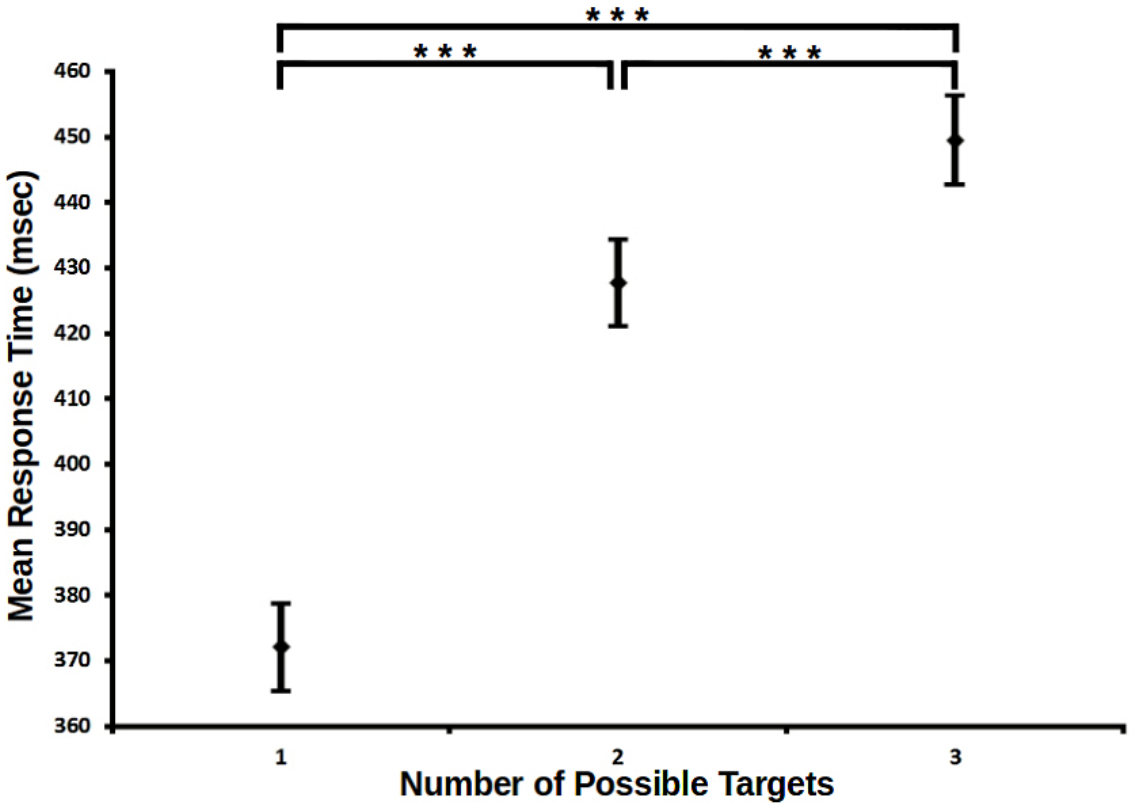

Figure 3.2: Mean RT for each target condition. The error bars represent standard error ($N = 74$ participants); one-target, $M = 372.16$ msec; two-targets, $M = 428.09$ msec; three-targets, $M = 449.78$ msec. ***, p<.001

Average RTs are plotted against number of targets in Figure 3.2. Results from a one-way ANOVA indicated that RT was significantly affected by number of targets, $F(2, 148) = 488.84,\ p < .001$, ANOVA, with planned contrasts indicating that RT during one-target presentation ($M = 372.1ms,\ SD = 56.2ms$) was significantly less than during two-target presentation ($M = 427.8ms,\ SD = 55.6ms$), $t(73) = -21.84,\ p < .001$, paired t test, and three-target presentation ($M = 449.5ms,\ SD = 57.5ms$), $t(73) = -30.3,\ p < .001$, paired t test. Average RT during two-target presentation was also significantly lower than during three-target presentations, $t(73) = -8.46,\ p < .001$, paired t test. These findings are in line with those of previous studies using a similar paradigm that found that as directional uncertainty increases, RTs lengthen (Tzagarakis et al., 2010).

3.3.2 Time series analysis of beta ERD

For each participant, beta-band power was normalised relative to a 1000ms baseline period, starting 1500ms before cue onset and averaged across all conditions. On a trial-by-trial basis, the power change from baseline to a 500ms period after cue onset was computed to determine the initial preparatory beta ERD. For each participant, power change was averaged for the number of targets presented (Figure 3.3).

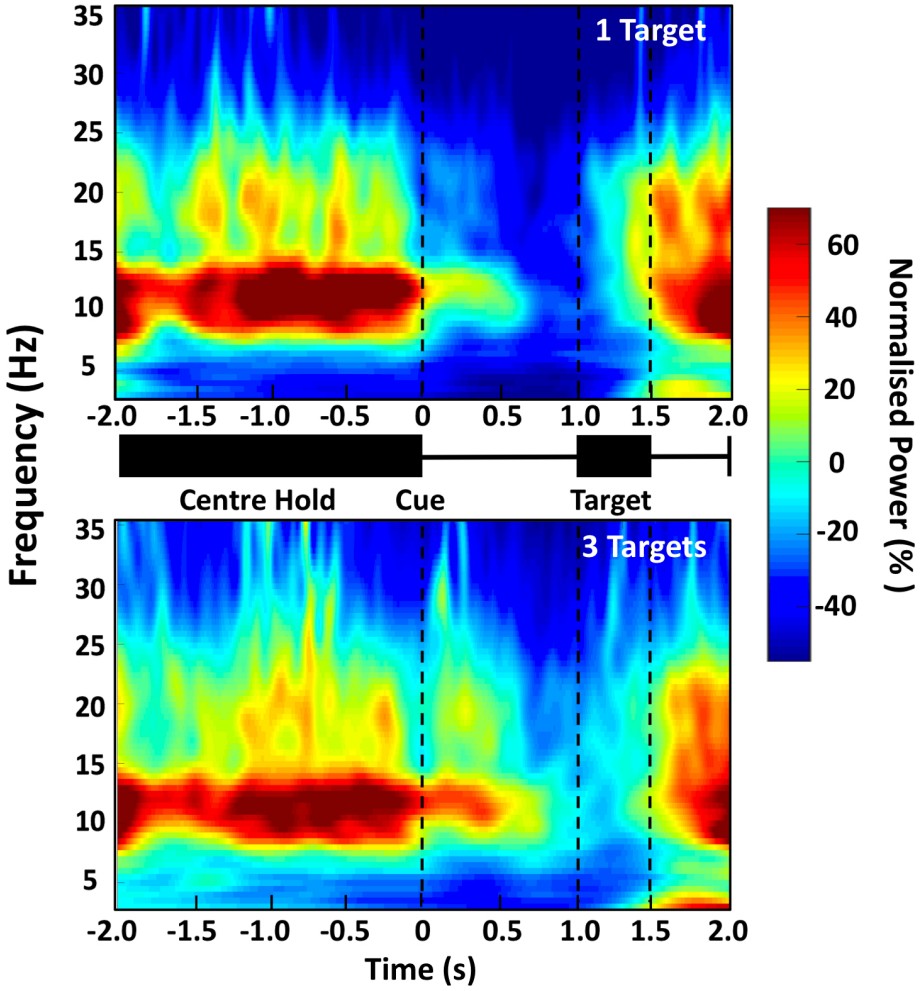

Figure 3.3: Averaged time-frequency power plots across participants for the 1 and 3-target conditions. The central schematic shows the 'centre hold' period (2 sec), the 'cue onset' and 'target' onset intervals. The time-frequency power plots show the profile of oscillatory power change (%) with respect to the pre-stimulus baseline period. A greater reduction in beta-band $(13–30Hz)$ power is associated with movement preparation afforded by directional certainty (1-target) compared with directional uncertainty (3-targets).

A decrease in beta-band power after cue onset was observed in all conditions (one, two and three-targets). The onset-latency of this beta desynchronisation occurred on average 173.8ms ($SD = 115.3ms$) after cue onset with no significant difference between target conditions ($F(2,148) = .689$, $p = 0.504$, ANOVA). The amplitude of initial preparatory beta desynchronisation was significantly different between conditions ($F(2,148) = 3.25$, $p = 0.041$), showing smaller reduction in power as the number of targets, and therefore the directional uncertainty, increased (Figure 3.4A). Specifically, during one-target trials, where subjects were certain of the direction of movement required, a significantly greater beta desynchronisation ($M = 20.25\%$, $SD = 20.47\%$) was observed than with three-target trials ($M = 12.53\%$, $SD = 18.92\%$), where required direction was unknown ($t(73) = -2.47$, $p = 0.014$, paired t-test, Figure 3.4B).

Following the initial preparatory desynchronisation, the one-target condition exhibited sustained beta suppression, whereas the two-target and three-target conditions showed a partial resynchronisation (i.e., an increase in beta power) until the point of target identification (Figure 3.4C).

Consequently, at the point of target identification, when directional uncertainty was resolved and subjects were cued to move, beta power was significantly greater in the three-target ($M = 83.14\%$, $SD = 18.97\%$) than the one-target ($M = 75.41\%$,$SD = 16.27\%$) condition ($t(73) = -2.84$, $p = 0.005$, paired t-test, Figure 3.4D).

Following target identification, average beta power reduced in all conditions, until the point of movement initiation, termed 'response-phase ERD' (Figure 3.5A). The onset latency of response-phase ERD showed no dependence upon the number of targets presented ($F(2,148) = 1.035$, $p = 0.358$, ANOVA). In contrast with a previous observation (Tzagarakis et al., 2010), we observed that the amplitude of the response phase ERD was not significantly different between the three different target conditions ($F(2,148) = .812$, $p = 0.445$, ANOVA, Figure 3.5B). This can be observed from the envelope of beta power when normalised to the 500ms prior to target identification (Figure 3.5C).

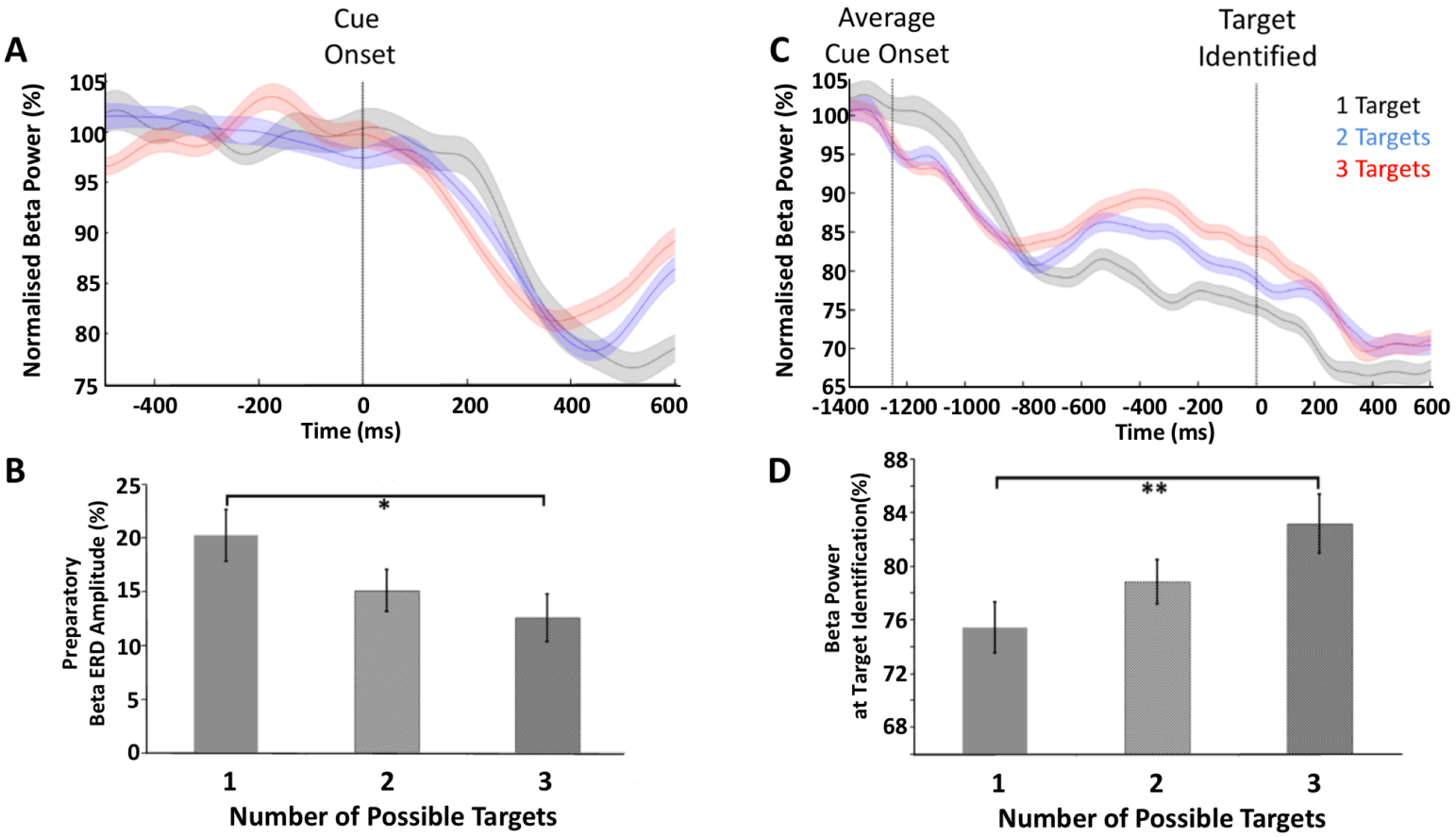

Figure 3.4: Power envelope plots of normalised preparatory beta power for each of the three target conditions (mean $\pm SEM$). **A.** Initial changes in preparatory beta power after cue onset. The onset latency of beta ERD ($< 2.5SD$ of baseline) does not vary across conditions. However, the absolute reduction in beta power is greater in the 1-target condition than 2 or 3-target conditions. **B.** Bar chart showing the amplitude of initial beta ERD (mean $\pm SD$). Beta desynchronisation is significantly greater in the 1 target than the 3-target condition (p=.014). **C.** Reduced Beta power is sustained up to the point of target identification the 1-target condition. The 2 and 3-target conditions show a partial resynchronisation in this interval. **D.** Beta power is significantly greater at the point of target identification during the 3-target, than in the 1-target conditions (p=.005).

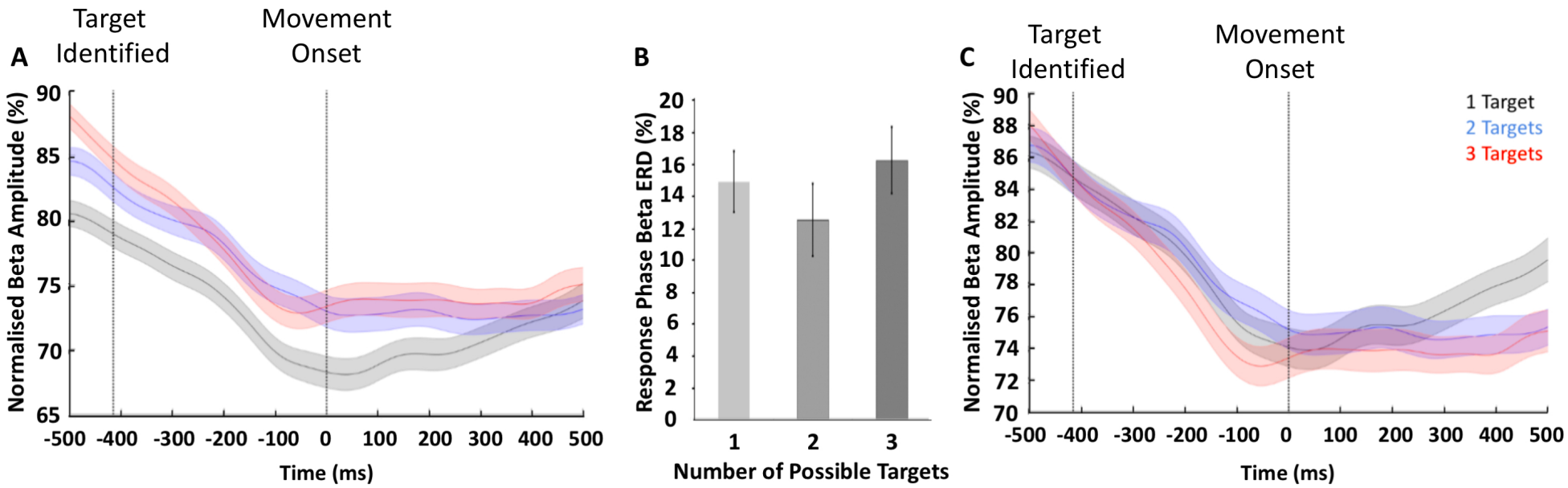

Figure 3.5: Power envelope plots of normalised beta power in the interval between target identification and movement onset for each of the three target conditions (mean $\pm SEM$). **A.** The onset latency of beta ERD does not vary across conditions, nor does the amplitude of beta ERD. **B.** Bar chart showing the amplitude (mean $\pm SD$) of response phase beta ERD, confirming no significant difference between conditions. **C.** Beta power normalised to the point of target identification, demonstrates that the amplitude of beta ERD is relative and not significantly different across the three target conditions.

3.3.3 Time series analysis of alpha ERD

Time-series analysis within the alpha frequency range (8–$12Hz$), revealed a decrease in power in all conditions following initial cue onset (Figure 3.6A). Alpha power showed significantly greater desynchronisation following one-target (high directional certainty) preparation ($M = 20.18\%/SD = 21.43\%$),than when compared to two-target ($M = 10.14\%/SD = 29.55\%$) preparation ($t(73) = -2.17,\ p = 0.031,$ paired t-test) and three-target ($M = 12.63\%/SD = 24.6\%$) preparation ($t(148) = -2.13,\ p = 0.034,$ paired t-test).

Following initial alpha preparatory-phase ERD, a transient increase in alpha synchrony was observed in the one-target condition ($M = 2.93\%,\ SD = 13.04\%,\ t(73) = 1.936,\ p = .057$, paired t-test), but not the two-target ($M = -2.33\%,\ SD = 14.58\%,\ t(73) = -1.373, p = .174$, paired t-test) or three-target ($M = -.73\%,\ SD = 14.93\%, t(73) = -.418, p = .677$, paired t-test) conditions (Figure 3.6B). Conversely, following target identification, a significant transient increase in alpha synchrony was observed in the two-target ($M = 6.32\%,\ SD = 17.34\%,\ t(73) = 3.134,\ p = .002$, paired t-test) and three-target ($M = 5.2\%,\ SD = 14.71\%,\ t(73) = 3.039,\ p = .003$, paired t-test) conditions, but not the one-target ($M = -.89\%,\ SD = 12.38\%,\ t(73) = -.617,\ p = .539$, paired t-test) condition (Figure 3.6D). This condition-dependent alpha synchrony is clearly visible in the envelope of alpha power (Figure 3.6A and C).

3.3.4 Response time and transient alpha synchrony

To further investigate the relationship between transient alpha synchrony and response time, we analysed the latency of peak alpha ERS following target identification in the two and three-target conditions. We found that peak alpha synchrony occurred significantly earlier in the two-target condition ($M = 203.4ms,\ SD = 75.56ms$) than in the three-target condition ($M = 242.7ms,\ SD = 72.44ms,\ F(2,148) = 5.525, p = 0.021,$ ANOVA), corresponding to the shorter reaction time in the two-target condition.

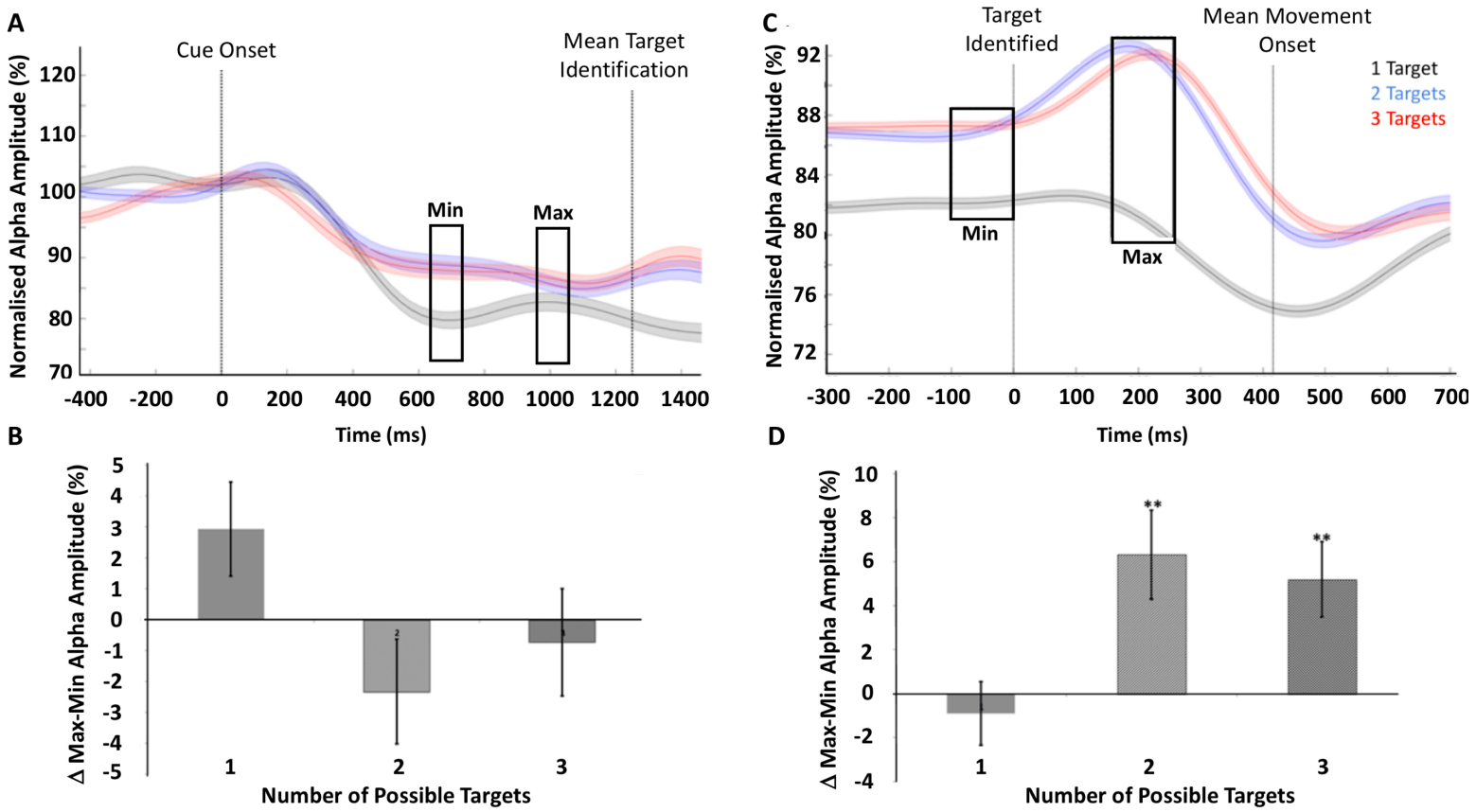

Figure 3.6: Power envelope plots of normalised alpha power for each of the three target conditions following cue onset and target identification (mean $\pm SEM$). **A.** Initial changes in preparatory alpha after cue onset. The onset latency ($< 2.5SD$ of baseline) of alpha ERD did not vary across the three conditions. However, the amplitude of alpha ERD is significantly greater in the 1-target than 2 or 3-target conditions. The black boxes indicate the mean interval of ERD minimum (min) and maximum (max) amplitude in the interval up to target identification. **B.** Bar chart showing the change in alpha synchrony (mean $\pm SD$) between the 100 msec min and max amplitudes. A non-significant increase in alpha was observed in the 1-target condition but not in the 2 or 3-target conditions, non-significance here is possibly due to the variance across trials as a result of the length of the interval. **C.** Following target identification, the difference in alpha was determined (as denoted by the black boxes) between the 100ms (min) and highest amplitude (max) in the interval between target identification and movement onset. **D.** Bar chart showing a significant increase in alpha synchrony (mean $\pm SD$) following target identification for 2 and 3-target conditions but not the 1-target condition.

3.3.5 Inter-trial variability in baseline beta power

During the statistical analysis for this chapter, I noticed a general trend in the data that was not initially hypothesised. From one trial to the next there was an increase in the baseline beta power. Given that this was not a factor I had intended to investigate prior to the study design, I performed an exploratory analysis to see if this increase in baseline power was statistically significant. In all 74 participants, there was an average increase in baseline beta power from one trial to the next, with this increase being statistically significant for 60 of the 74 participants ($\alpha = .05$). This meant that overall in each consecutive trial there was a significant increase in baseline beta power ($M = 28.51\%$, $SD = 27.27\%$; $t(73) = 9.996$, $p < .0001$, Figure 3.7B).

Further investigation revealed that this significant increase in baseline beta power from one trial to the next is likely due to the length of each trial in relation to the evoked changes in beta amplitude. The trials used throughout this study were seven seconds in length, with the 'GO cue' being the point at which a target was identified. This cue occurred in a jittered period 3.1–3.5 seconds after trial onset. Given the mean total movement time was 669.59ms($SD = 211.35ms$), the average movement was not completed until ~3.8–4.2 seconds after trial onset. As the termination of a movement is consistently followed by a post-movement beta rebound (PMBR) (Cassim et al., 2001; Gilbertson et al., 2005; Koelewijn et al., 2008; Pastötter et al., 2008; Pfurtscheller et al., 1996; Salmelin et al., 1995b), this meant that the start of the next trial began during a period of elevated beta power (Figure 3.7A). Because the second trial began during the preceding movement's corresponding PMBR, beta power did not return to a true *'resting'* baseline before cue onset.

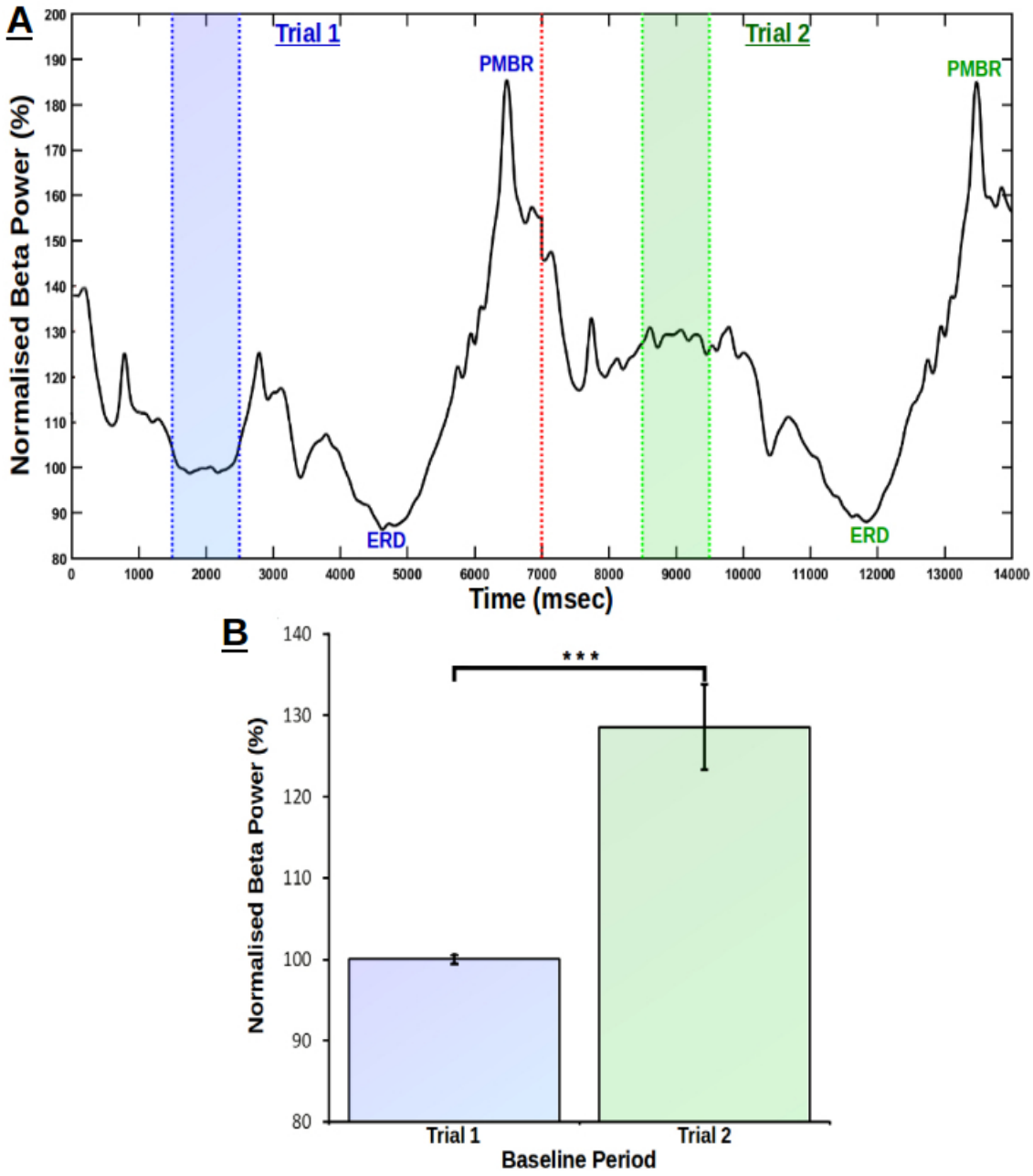

Figure 3.7: **A.** Power envelope plot of normalised beta power across two consecutive trials. During the baseline period of the second trial (green bar), average beta power was significantly greater than the corresponding baseline period of the preceding trial (blue bar). This increase is likely due to the onset of the second trial (red dashed line) beginning during the PMBR period of the first. **B.** Bar chart showing the amplitude (mean $\pm SD$) of baseline beta power during two consecutive trials. A significant increase was observed in baseline beta power between the first trial and the proceeding trial ($p < .001$).

Further analysis was carried out to investigate the extent to which the trial-by-trial increase in beta power altered baseline beta power throughout the course of the experiment. A grand average was calculated across all 74 participants for the first 25% and last 25% of trials for each block. The resulting plot can be found in Figure 3.8 below.

While there was a non-significant increase in baseline beta power between the first 25% and last 25% of trials in Block 1 ($t(73) = .506$, $p = .614$, $d = -.0425$), there were significant increases for each of the four remaining blocks (**Block 2**: $t(73) = 3.36$, $p = .0012$. $d = .26$; **Block 3**: $t(73) = 3.959$, $p < .001$, $d = .293$; **Block 4**: $t(73) = 3.438$, $p < .001$, $d = .521$; **Block 5**: $t(73) = 3.463$, $p < .001$, $d = .511$). As baseline beta power significantly increases over the course of each block the resultant beta power during the final nine trials of the experiment (25% of 36 trials in each block) is significantly greater than during the first nine trials of the experiment ($t(73) = 8.386$, $p < 1^{-11}$, $d = 1.318$).

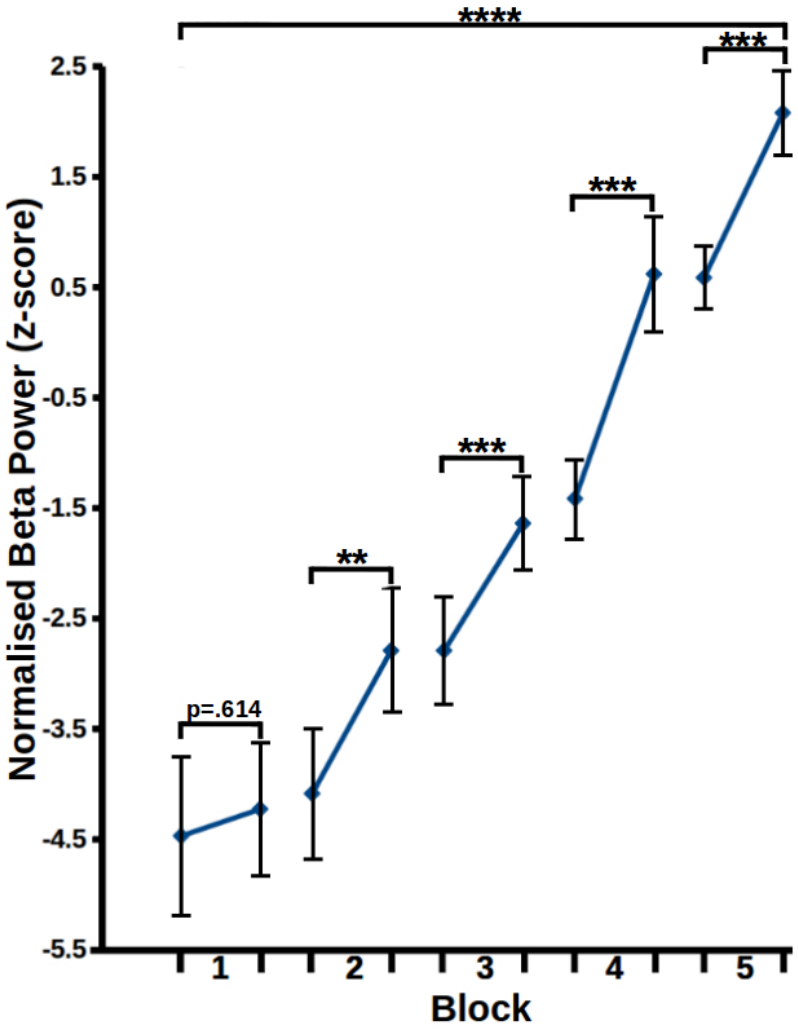

Figure 3.8: Changes in baseline beta power throughout the experiment. In all five blocks there was an average increase in baseline beta power between the first 25% and last 25% of trials within the block. This increase was significant in all but Block 1. Error bars reflect the SEM. ****, p<.0001, ***, p<.001, **, p<.01.

3.3.6 Summary of results

- An increase in directional uncertainty lead to a significant increase in RTs (Figure 3.2), with RT at each incremental level of uncertainty significantly slower than the previous level.
- With increased directional uncertainty the amplitude of preparatory-phase beta ERD was significantly reduced (Figure 3.4). When participants were entirely certain of the upcoming movement (one-target condition), preparatory beta suppression was significantly greater than when uncertainty was at its highest (three-target condition).
- This modulation of beta suppression was only true of the preparatory phase of the movement. During the response-phase, there was no significant effect of directional uncertainty on the amplitude of beta ERD (Figure 3.5).
- Preparatory alpha desynchronisation, like beta, was significantly greater when the participant was certain about the prepared movement than when directional uncertainty was high (Figure 3.6).
- Following the initial alpha desynchronisation, there was a transient increase in synchronous alpha power. This transient increase occurred immediately after the initial desynchronisation in the one-target condition. However, in the uncertain conditions, this transient increase was delayed until after the target was identified and the direction of movement was revealed (Figure 3.6).
- The transient increase in alpha activity following target identification occurred significantly later during the three-target condition than the two-target condition. This difference in peak latency was reflected in the longer RTs of the three-target condition (Figure 3.6).
- A further exploratory analysis revealed that, on a trial-by-trial basis, there is a significant increase in baseline beta power (Figure 3.7). This increase is likely due to the onset of each new trial beginning during the PMBR phase of the previous movement. This trial-by-trial increase led to a significant increase in baseline beta power throughout the course of the experiment (Figure 3.8).

3.4 Discussion

3.4.1 Summary

In this chapter, we demonstrate that both alpha and beta desynchronisation reflect a process of disengagement from existing networks, to enable the creation of functional assemblies. We also demonstrate a novel signature of transient alpha synchrony, which is predictive of reaction time and thus likely associated with the recruitment of a functional assembly required to generate the motor output.

3.4.2 Directional uncertainty lengthens response times

As expected, RT was directly dependent on the ability of participants to predict the direction of required movement, based upon the stimulus information. This finding is consistent with previous reports (Bock & Arnold, 1992; Churchland et al., 2008; Dorris & Munoz, 1998; Pellizzer et al., 2006; Tzagarakis et al., 2010) and confirms that participants engaged with the experiment as required. As suggested by Pellizzer & Hedges (2003), the use of discrete spatial cues in an instructed-delay reaching task is particularly effective as a measure of uncertainty on movement preparation.

3.4.3 Time-course of movement related changes in motor cortical alpha and beta activity

Consistent with general observations in a variety of experiments involving movement paradigms (Cheyne, 2013; Jurkiewicz et al., 2006; Pfurtscheller & Aranibar, 1979; Pfurtscheller & Lopes Da Silva, 1999; Pfurtscheller et al., 1996), a significant decrease in both alpha and beta synchronous power was observed following the presentation of the initial onset cue in all conditions. We propose that this desynchrony reflects a process of disengagement from ongoing network activity, to allow for the assignment of appropriate motor units to generate a required output.

Of note, the amplitude of both alpha and beta ERD is directly dependent upon the number of targets presented. This suggests that, where information is present that allows for the identification of the appropriate response, those neural populations are enabled to be disengaged in preparation for recruitment to an output assembly. Taken together, these observations of disengagement from an active network support the theory of beta, and indeed alpha, oscillations in the promotion of postural tone at the expense of voluntary movement (Gilbertson et al., 2005; Pastötter et al., 2008). However, the observation of

partial resynchronisation of the beta rhythm in the two and three target conditions is also consistent with an inhibition of movement in the absence of a motor plan.

Following initial ERD, we demonstrate that the ongoing profile of beta power is predictive of the participant's preparatory state. In the one-target condition, beta suppression is sustained up to the point of target identification, whereas the two-target and three-target conditions exhibit a partial resynchronisation of beta power until the required target direction is indicated. Given that temporary re-assignment to a postural network is unlikely, with the impending need to move, resynchronisation is likely to reflect the temporal realignment of potential units with the functional networks required to generate motor output after target identification. While speculative, this suggests that beta synchrony in motor cortex reflects and serves a dual purpose, including the maintenance of postural tone (Gilbertson et al., 2005; Pastötter et al., 2008) and providing a temporal pacemaker to maximise effective motor responses. The precise role of the beta rhythm notwithstanding, these data support the independence of the alpha and beta rhythms, which subserve separate functional processes (see van Wijk et al., 2012 for a review).

In contrast with previous observations (Tzagarakis et al., 2010), we observed no significant difference between conditions in either the latency or the amplitude of the response-phase ERD. Importantly, the differences in response-phase ERD amplitude can be accounted for directly by the oscillatory power at the point of target identification, which is predicted by the number of targets. Further change in synchronous power is removed by normalisation to that point. We propose that, while beta desynchronisation is an important process in the generation of movement, the critical distinction in this experiment lies in the preparatory, rather than response, phase.

3.4.4 Transient alpha synchrony coincides with the creation of a specific functional assembly

Importantly, we identify a novel oscillatory feature in this experiment that corresponds to the participants' ability to engage a specific motor network. Following the initial alpha and beta ERD, a transient 'burst' of alpha is observed in the one-target condition, but not in the two-target or three-target conditions. We propose that this signature reflects the recruitment of units to the functional assembly required to generate the motor output. This is supported by the observation that following target identification a transient burst of

alpha is observed in the two-target and three-target conditions, but not in the one-target condition.

These signatures are temporally consistent with the participants' ability to assign the appropriate network, based upon information about the required movement. This feature dependency is borne-out behaviourally, as the alpha burst occurs significantly earlier in the two-target than the three-target condition, corresponding to the significant difference in reaction time between those conditions.

This feature is consistent with electrophysiological recordings which have shown alpha oscillations reflect feedback inhibition in the cortex (Bastos et al., 2015; Michalareas et al., 2016), with feedback inhibition suggested to tune directional pyramidal cells in the motor cortex (Georgopoulos & Stefanis, 2007; Isomura et al., 2009; Merchant et al., 2008). We posit, given the occurrence of the transient alpha signal only when sufficient information is available to form a motor plan, that it reflects the recruitment in readiness of units required to execute the movement. This may include pyramidal tract neurons but is unlikely to be an independent generator given the relative minority of these cells (Keller, 1993).

The switching of beta and alpha here, given the relatively low spatial resolution of the EEG measurement, is consistent with the *'gating-by-inhibition'* hypothesis (Jensen & Mazaheri, 2010). In particular, when considered alongside the observation of increased alpha in M1, following removal of connectivity with S1 (Rönnqvist et al., 2013), it is possible that increased alpha reflects active inhibition of somatosensory input to facilitate formation of a motor plan based upon current information. Indeed, the inhibitory basis of these signals is supported by several studies that demonstrate the role of GABAergic modulation in generation of the beta (Hall et al., 2010a, 2011; Jensen et al., 2005; Muthukumaraswamy et al., 2013) and alpha (Rönnqvist et al., 2013) rhythms.

3.4.5 Inter-trial variability in baseline beta power

This study revealed a potential methodological confound that should be considered in the design of future studies. A baseline period of one second was selected at the beginning of each trial, starting 500ms after the beginning of the trial. On a trial-by-trial basis, the power change from this baseline was then averaged to reveal the relative decrease in preparatory beta power. This time series analysis used the same procedure as the majority of other studies of movement-related changes in oscillatory power (Cheyne et al., 2006; Engel & Fries, 2010; Gaetz et al., 2010; Neuper & Pfurtscheller,

2001a; Pfurtscheller & Lopes Da Silva, 1999; Zhang et al., 2008), and is necessary in order to ensure an appropriate signal-to-noise ratio.

However, we observed that beta power within this baseline period does not remain consistent. In fact, with each consecutive trial, there was a significant increase in baseline beta power. We propose that this increase is due to the onset of each trial beginning during the PMBR following the termination of the movement that occurred in the preceding trial. This resulted in the baseline period of each trial being recorded during a period of elevated beta power. While this may not necessarily affect measures of relative beta power change within a trial, other studies have already demonstrated the importance of absolute beta amplitude on motor behaviour, with higher power associated with a lengthening of RTs (Heinrichs-Graham & Wilson, 2016; Heinrichs-Graham et al., 2018; Rossiter et al., 2014).

However, we also found that, despite the increased baseline level of cortical beta power, there was no significant effect on RT. This may suggest that, though it appears that each consecutive trial begins during the tail-end of the previous trial's PMBR, the elevated beta power may be a consequence of motor learning. With each consecutive trial, the participant becomes more aware of the nature of the motor task. Realising that there are common components within each trial, despite variation in the number of possible targets to move toward and the direction of movement after the target has been identified. Regardless of target condition, each trial required the movement of the right arm, wrist, thumb and index finger. Therefore, increased beta power as the task progresses may be a result of the functional assemblies required to move those muscle groups remaining synchronised in preparation for recruitment.

If this trial-by-trial increase is due to an overlap with the previous PMBR, then this potential confound may be avoided by increasing the trial length during a motor task. By leaving a large enough interval between movement termination and the beginning of the next trial, underlying beta power may return to a more accurate, 'true' representation of the baseline level. This issue was explored further in Chapter 6.

3.4.6 Conclusion

In this chapter, I have demonstrated that, consistent with current proposals, alpha and beta desynchronisation reflects a process of disengagement from existing networks to enable the creation of functional assemblies. Also, that while preparatory alpha and

beta activity is significantly more suppressed when the participant is certain about the movement to be executed than uncertain, this alone is not enough to predict a decrease in RT.

Importantly, I have demonstrated that, following desynchronisation, a novel signature of transient alpha synchrony occurs. I propose that this neural signature underlies the recruitment of functional assemblies required for directional control. A proposal strengthened by the finding that this transient alpha synchrony only occurs once the participants have sufficient information to prepare their movement and that the latency of the synchrony shows a direct relationship with the resulting behavioural performance. A schematic of the proposed model can be found in Figure 3.9.

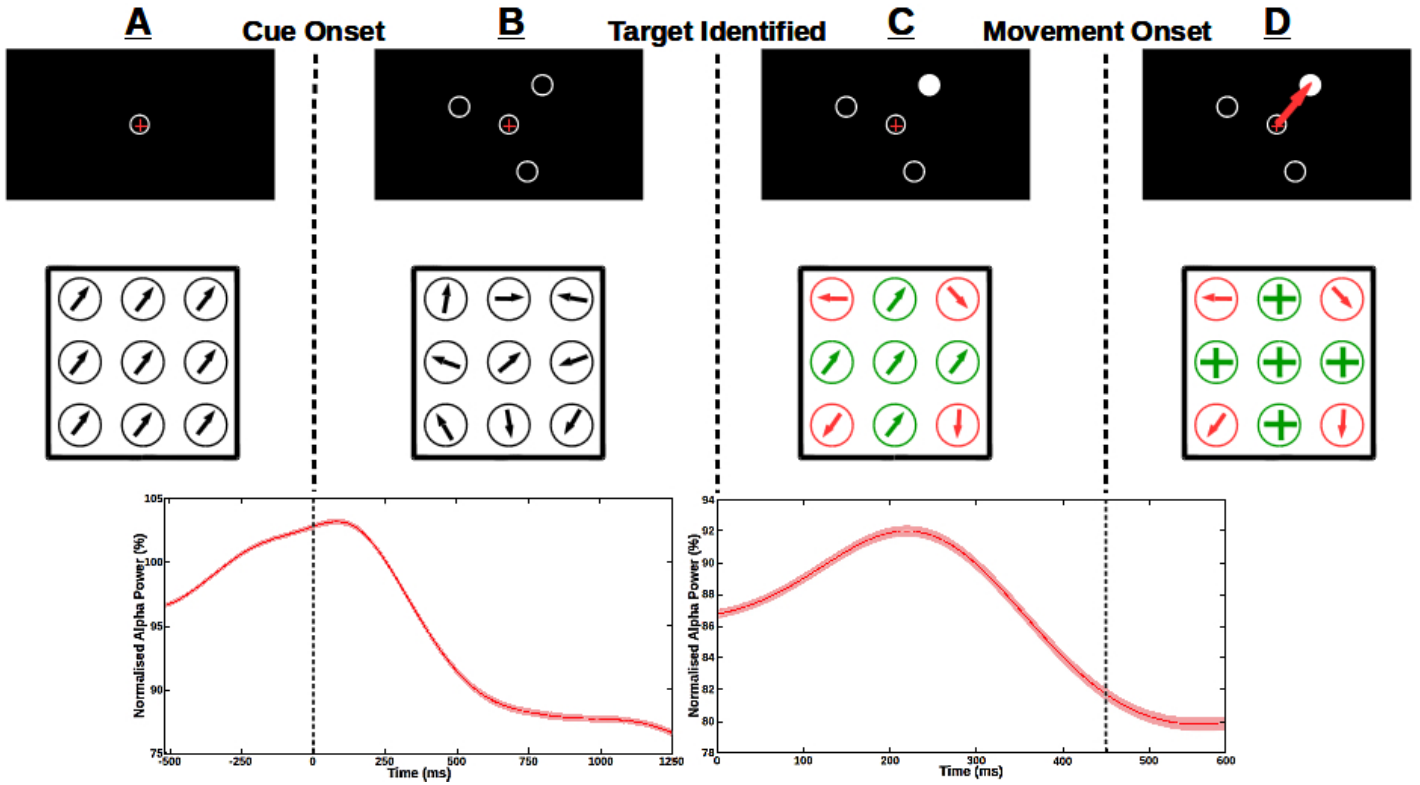

Figure 3.9: The proposed model to explain the relationship between alpha synchrony and the recruitment of the functional assemblies required for directional control. **Upper layer.** Diagram representing each stage of the instructed-delay reaching task. **Middle layer.** Simplified schematic of the M1, comprised of 9 neural ensembles. Arrows represent the phase of the underlying oscillation. **Lower layer.** Power envelope plots of alpha power during the instructed-delay reaching task. *Left panel* - The preparatory-ERD of alpha power following cue onset. *Right panel* - Transient increase in alpha power following target identification. **A.** During the initial centre-hold period, the motor cortex is at rest and synchrony among each ensemble is high. **B.** Following the onset of the spatial cues, each ensemble disengages from the ongoing oscillation, resulting in a desynchronisation of M1 alpha power. **C.** Once the target for movement has been identified, the directional uncertainty is resolved. The neural ensembles required to create the required functional assembly to move the hand in the target direction (green) then become synchronised. This simultaneous recruitment results in a transient increase in alpha power. **D.** The recruited ensembles then fire $(+)$ to generate the required motor output to move the joystick towards the target circle.

Chapter 4

Individually tailored, short-duration HD-tACS as a modulator of motor activity

For a moment, nothing happened. Then, after a second or so, nothing continued to happen.

– Douglas Adams (1952-2001)

4.1 Introduction

In Chapter 3, we found that during the preparation of voluntary movement there is an event-related desynchronisation (ERD) of both ongoing alpha and beta activity within the primary motor cortex (M1). We suggested that this ERD reflects a process of disengagement from existing networks, to enable the creation of the required functional assemblies to make a movement. To further investigate the potential functional role of alpha and beta ERD, a follow-up study was designed to apply transcranial alternating current (tACS) to M1 in an attempt to entrain ongoing alpha and beta activity and reduce the magnitude of the preparatory ERD.

4.1.1 Background

Alpha and beta band oscillations have been consistently linked with the human motor system (Baker et al., 1997; Murthy & Fetz, 1992; Pfurtscheller & Aranibar, 1979). In particular, as early as two-seconds before movement onset there is an ERD of ongoing motor cortical alpha and beta activity (Crone, 1998a; Cheyne et al., 2006; Gaetz et al., 2010; Leocani et al., 1997; Pfurtscheller & Lopes Da Silva, 1999; Salmelin & Hari, 1994). The findings of our previous study and others, suggest that the magnitude of this preparatory desynchronisation is modulated by the level of information the participant receives prior to making their movement. The more certain they can be about their movement the greater the desynchronisation (Grent-'t Jong et al., 2014; Kaiser et al.,

2001; Tzagarakis et al., 2010; Rhodes et al., 2018). We argue that this modulation is due to efficient recruitment of the functional assembly required to create the motor output. When certainty is high, disengagement of the relevant neural network from the postural or idling rhythm (desynchronisation), is a prerequisite to recruitment (transient synchronisation) of the current functional ensemble (Rhodes et al., 2018).

High resting beta power and reduced beta ERD during movement execution have been suggested to result in poor motor performance in both healthy and patient populations. Work by Heinrichs-Graham and colleagues has demonstrated that, controlling for age, high resting beta power and reduced ERD magnitude, resulted in a lengthening of response times (Heinrichs-Graham & Wilson, 2016; Heinrichs-Graham et al., 2018). Studies of patients with Parkinson's disease (PD) have linked exaggerated beta activity with motor impairment (Brown & Williams, 2005; Kühn et al., 2005; Weinberger et al., 2006). PD patients have also been shown to have reduced beta ERD during movement preparation (Heinrichs-Graham et al., 2014b). This may be indicative that a combination of abnormally high cortical synchrony, along with an inability to disengage the correct functional assembly from the synchronised network, contributes to the motor deficits suffered by PD patients.

Deep brain stimulation (DBS), an invasive form of electrical stimulation, involves delivering high-frequency stimulation ($\sim 130Hz$) via electrodes implanted into the STN of PD patients. This treatment has been found to improve motor function, leading to a reduction of tremor and bradykinesia (Deuschl et al., 2006), and coincides with a reduction in the amplitude of exaggerated beta activity, not only in the STN (Bronte-Stewart et al., 2009) but also in cortical motor regions (Li et al., 2012; Swann et al., 2011). The exact mechanism for how DBS achieves this reduction in beta power is still under some debate; however, one possibility is that high-frequency stimulation of the STN modifies the firing rate of its corticofugal projections, destroying the beta dominance in the M1 and restoring motor control (Li et al., 2012).

DBS is highly invasive and is not suitable for all patients, however, it represents an opportunity to investigate how electrical stimulation can improve motor function. tACS may be a viable alternative to DBS as it is significantly less invasive and can be delivered directly to M1. This kind of transcranial stimulation is relatively cheap, simple to apply, and can be tested with minimal risk on both healthy and patient populations.

The potential of tACS to temporarily increase neural synchrony within a given frequency could provide vital information about disorders, such as PD, that have abnormally high levels of oscillatory power.

tACS has been suggested to be able to entrain neural firing to the stimulation frequency by alternating between excitation and inhibition of the subthreshold membrane potential of neurons (Guerra et al., 2016; Thut et al., 2011a; Weinrich et al., 2017). This entrainment is most effective when the stimulation frequency falls within a narrow band around the intrinsic oscillatory frequency of the target network, with stimulation at 'flanker' frequencies, outside that narrow band, thought to be ineffective (Thut et al., 2011a; Zaehle et al., 2010).

The potential of tACS to selectively entrain specific frequencies makes it a promising tool to functionally investigate neural processes that are strongly correlated with changes in oscillatory activity. For example, Pogosyan and colleagues (2009), showed that applying tACS to the M1 at $20Hz$ during a simple motor tracking task, resulted in a slowing of voluntary movement (Pogosyan et al., 2009). The authors concluded that this slowing of movement was due to entrainment of intrinsic beta activity, as evidenced by increased corticomuscular coherence within the beta band. They also found that this increased coherence occurred only $1.12 \pm 0.23s$ after stimulation onset (Pogosyan et al., 2009).

A further study that applied $20Hz$ tACS to the M1 found that the stimulation altered the phase relationship that exists between M1 and secondary motor areas of the brain (Weinrich et al., 2017). tACS entrainment of the M1 caused the underlying neurons to shift from optimal phase alignment with the rest of the motor network, effectively acting as a source of noise within the network. The 'communication-through-coherence' hypothesis (Fries, 2005) would suggest that phase alignment is necessary for optimal communication between neurons and that, by artificially driving M1 neurons out of phase with other motor network nodes, this communication is disrupted.

In the present study, we explored the functional significance of preparatory alpha and beta ERD to motor performance by applying tACS to M1 at individual peak frequencies. This was to investigate whether entrainment of M1 to the resting rhythm results in a disruption of the process of disengagement from the ongoing rhythm that is required for recruitment of the functional assembly that generates motor output. Furthermore, the present study investigated the frequency specificity of tACS, as posited by Thut et al. (2011a), along

with its potential to disrupt specific function through altered network synchrony.

4.1.2 Aims and research objectives

The aim of this study was to:

1. Characterise the individual frequency specificity of oscillatory change in M1 of each during motor preparation.
2. Determine the effect of brief ($< 1.5s$), frequency specific M1 stimulation during motor preparation on motor functional performance.
3. Determine the effect of cortically delivered high-frequency tACS stimulation (consistent with DBS parameters) on M1 activity and motor functional performance.

To address these questions, we applied the same directional uncertainty paradigm described in Chapter 3. The task, developed by Pellizzer and Hedges (2003), was an instructed-delay reaching task that consisted of four key elements. First, the participant used a joystick to hold a crosshair within an outline of a circle in the centre of the screen for 2s. Following this wait period a spatial cue consisting of one, two or three circular targets was presented. After a jittered wait period of 1–1.5s, one of the targets was highlighted. Once a target was highlighted, the participant used the joystick to move the crosshair and hit the identified target. The participant's response time (RT) was defined as the time taken, following target identification, to move the crosshair out of the centre circle towards the identified target.

As previously described (Grent-'t Jong et al., 2014; Kaiser et al., 2001; Rhodes et al., 2018; Tzagarakis et al., 2010), we predicted that within each stimulation condition there would be a significant effect of directional uncertainty on RT. With responses made following the one-target presentation, when certainty is high, being significantly faster than following the two or three-target presentation, when the participant can no longer be certain of the required movement direction.

Based on the finding of Pogosyan et al. (2009) that tACS is able to entrain M1 activity in as little as 1.12s, we applied individually specific tACS during the preparation phase between cue onset and target identification, to entrain M1 activity.

We predicted that:

1. tACS delivered at the individual peak alpha frequency, would result in a change in the optimal phase alignment of underlying neurons and cause a lengthening of the resulting RT.

2. tACS delivered at the peak beta frequency during motor preparation would result in sub-optimal motor preparation and lengthen RTs.

3. So-called non-peak 'flanker' frequencies would be unable to entrain the underlying oscillation (Thut et al., 2011a). We predicted that flanker frequencies would have no effect on RT.

4. Stimulation at $130Hz$, like DBS in the STN, would disrupt ongoing beta activity and shorten RT.

4.2 Methodology

Participants who had taken part in the study described in Chapter 3 were invited to take part in a follow-up stimulation study. To avoid any adverse effect of fatigue, the stimulation session was scheduled at a later date (2–7 days post-EEG study). We believed that, despite the EEG recording being on a different day to the stimulation session, there would be no significant variation in underlying oscillatory power between the two days. This assumption was based on the finding of a previous study, that there is high intra-individual reliability in movement-related beta oscillations even over the course of several weeks (Espenhahn et al., 2017). To ensure there were no effects of circadian rhythm or simply time of day on oscillatory activity (Toth et al., 2007; Wilson et al., 2014a), the stimulation session was scheduled to begin at the same time as the previous EEG study.

One confound that was not considered, but should be in future experiments, is the potential link between hormone changes that occur during the menstrual cycle and GABA concentrations within the brain. Previous magnetic resonance spectroscopy work by Epperson and colleagues found that in healthy, menstruating women cortical GABA concentration significantly decreases from the follicular to the midluteal phase (Epperson et al., 2002, 2005). These spectroscopy studies come with a caveat, both studies have relatively low subject numbers and suffer from a multiple comparisons problem. However, animal studies have also demonstrated that allopregnanolone, a neuroactive metabolite of progesterone, influences changes in GABA-A receptor expression (Lovick et al., 2005; Maguire et al., 2005; Turkmen et al., 2010).

Given the extensive body of work that has linked increased cortical GABA concentration with oscillatory beta power (Gaetz et al., 2011; Hall et al., 2010a, 2011; Jensen et al., 2005; Muthukumaraswamy et al., 2013), the potential link between changes in gonadal hormone levels and cortical beta power should be considered in future work. Previous EEG studies have demonstrated a relative decrease in cortical beta power during the luteal phase (Feshchenko et al., 1997; van Lier et al., 2004), these findings are in line with those of Epperson and colleagues who found a decrease in GABA concentration during the mid and late-luteal phase. The link between the menstrual cycle to cortical GABA concentration, and subsequently to GABA driven neural oscillations, is yet to be convincingly made. However, the research currently available is enough to suggest that the menstrual cycle should be taken into consideration during the design of longitudinal

studies of neural oscillations.

Of the 74 participants who took part in the study described in Chapter 3, 32 were able to attend the follow-up stimulation session. Of the 32 recruited, all were right-handed (25 female), with a mean age of 26 (range 18–70). Informed consent was obtained, and all studies were approved by the local ethics committee, in accordance with the ethical standards set by the 1964 Declaration of Helsinki. All participants passed a TMS safety screening, were free of medication and did not have any personal or family history of neurological or psychiatric illness.

Subjects were excluded if over 20% of their trials were removed due to poor behavioural performance. As a result, one participant was removed from the overall analysis.

4.2.1 Procedure

As mentioned above, the study comprised of two separate sessions on different days. The EEG session, described in Chapter 3, allowed for the analysis of each individual's neural response during an instructed-delay reaching task. Changes in alpha and beta power during the preparation of movement were calculated to determine the frequencies that underwent the greatest desynchronisation prior to making a response. Then, during the stimulation session, tACS was applied at those peak frequencies during the preparation phase of the same instructed-delay reaching task to determine if tACS entrainment could alter participant responses.

4.2.2 Spectral analysis and selection of individual stimulation frequencies

All stimulation was tailored towards the individual. Therefore, prior to attending the stimulation session, time-frequency analyses were performed on the averaged EEG data for each individual's performance of the one-target condition. Peak alpha and beta frequency for each individual were determined as the frequencies that decreased in power most during the preparatory phase of movement.

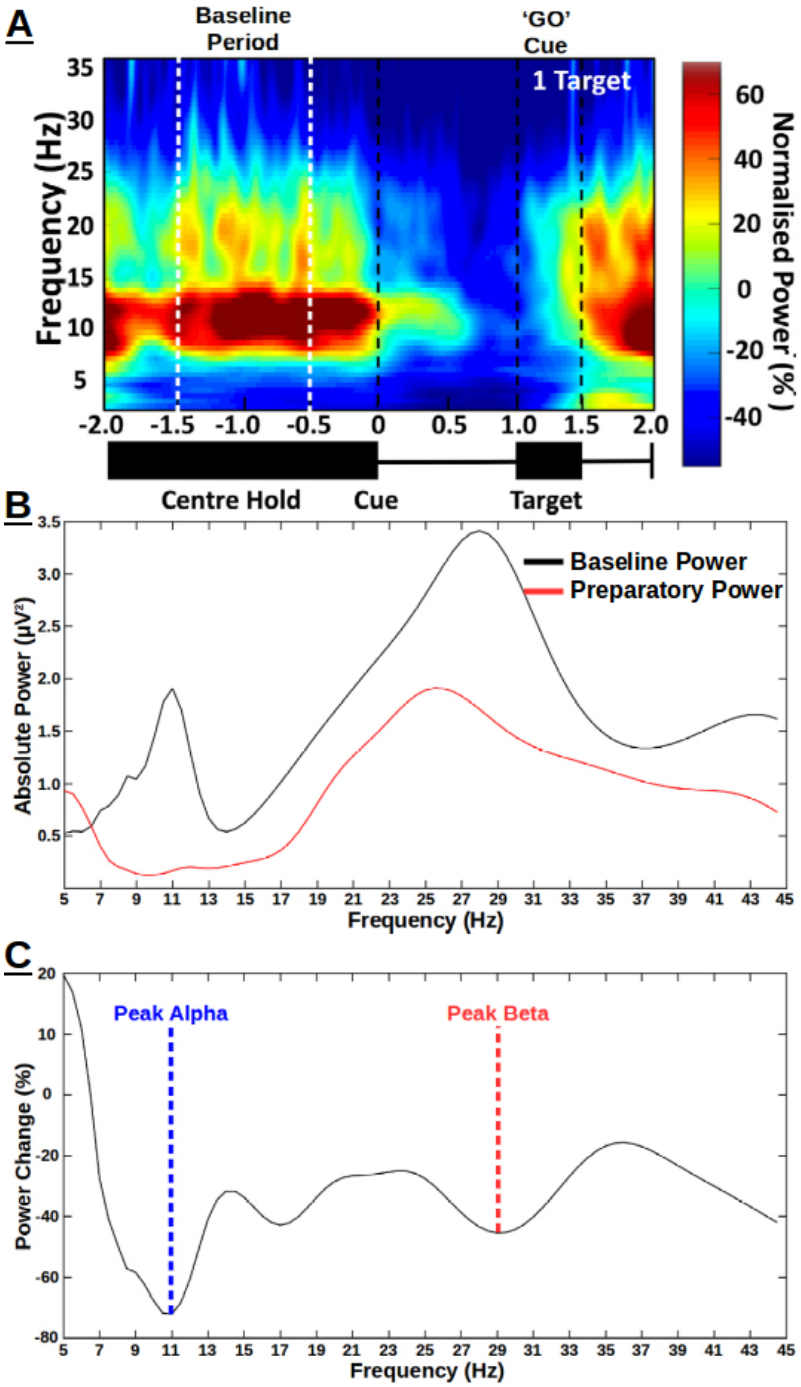

Figure 4.1: **A.** Averaged time-frequency power plot across participants for the one-target condition. The central schematic shows the 'centre hold' period (2 sec), the 'cue onset' and 'target' onset intervals. The time-frequency power plots show the profile of oscillatory power change (%) with respect to the pre-stimulus baseline period. **B.** Averaged power spectral density plot for a typical participant showing the absolute power in the alpha and beta bands during the baseline period (black line) and after motor preparation (red line). **C.** Power spectral density plot of the percentage change in alpha and beta power between baseline and motor preparation for the same participant. The peak decrease in alpha power occurred at $11Hz$, while peak beta decrease occurred at $29Hz$.

Change in alpha and beta power was analysed with respect to a 1000ms baseline period beginning 1500ms before cue onset (Figure 4.1A). On a trial-by-trial basis, the power change from baseline to a 500ms period, beginning 250ms before target identification, was computed to determine preparatory change in power.

There were five EEG-determined stimulation conditions. These were:

1. Peak alpha - The frequency within the alpha range (8–$12Hz$) that underwent the greatest decrease in power during the preparatory phase of the one-target response. The mean peak alpha frequency was $9.82Hz$ ($SD = 1.3Hz$).

2. Peak beta - The frequency within the beta range (13–$30Hz$) that underwent the greatest decrease in power during the preparatory phase of the one-target response. The mean peak beta frequency was $21.62Hz$ ($SD = 3.51Hz$).

3. Low beta - This frequency was used as a 'flanker stimulation frequency' and was defined as $2.5Hz$ lower than the previously defined peak beta frequency.

4. High beta - This frequency was used as a 'flanker stimulation frequency' and was defined as $2.5Hz$ higher than the previously defined peak beta frequency.

5. $130Hz$ - This frequency was used to investigate whether stimulating the M1 at a frequency that is commonly used during DBS would have a similar effect on motor performance as DBS to the STN.

4.2.3 HD-tACS parameters

This study was designed with a view towards future applications of tACS. Therefore, we wanted to investigate the potential for tACS to be used as a form of wearable treatment that could, in future, be combined with an EEG based BCI that would function in a similar manner to the adaptive, closed-loop DBS currently in use (Little & Brown, 2012; Little et al., 2013). As such the stimulation parameters in the present study were designed to be entirely non-invasive. A low-profile HD-tACS electrode montage was used and stimulation intensity was kept below a sensation threshold so that the participant was unaware of the stimulation.

The stimulation session began with the functional localisation of the left M1 using the TMS procedure outlined in Section 2.3.2. This allowed us to ascertain the location of each participant's M1h. This scalp location was then used to guide tACS electrode placement.

Following M1h localisation, the HD-tACS electrode array (Section 2.4.3) was placed on the participant's scalp, with the active electrode placed directly over M1h and the four return electrodes surrounding it in a concentric circle (Datta et al., 2009; Faria et al., 2011; Kuo et al., 2013). Each return electrode was spaced 4cm away from the active electrode (ring centre to ring centre). Impedance was measured by the DC stimulator and stimulation was not possible unless impedance was below $10k\Omega$.

For each individual, intensity of the sinusoidal current was adjusted to ensure that the participant was unaware of the stimulation. To obtain this sensation threshold, a similar procedure to that described in Neuling et al. (2013) was used. Stimulation was initially applied at an intensity of $500\mu A$ (peak-to-peak). If the participant reported no skin sensation or phosphene perception during this initial stimulation then the intensity was increased in steps of $100\mu A$. Once the participant reported any skin sensation or phosphene perception, the intensity was then decreased by $100\mu A$. Each intensity step was applied three times for a duration of 10s without any fade in/out. This sub-sensation intensity was then used as the stimulation intensity.

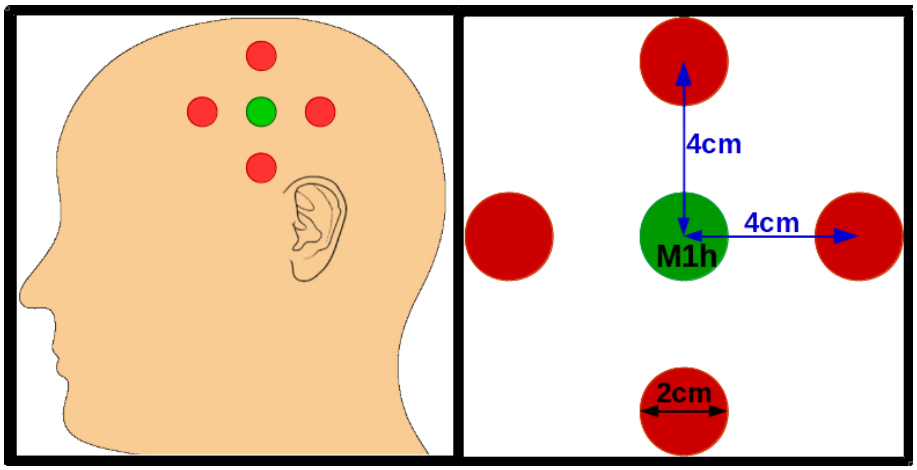

Figure 4.2: The HD-tACS electrode array. A 4×1 electrode array was placed over the localised M1h. The active electrode (green) was placed directly over the left M1h, with four return electrodes (red) arranged in a concentric circle around the centre. Each electrode had a diameter of 2cm and was spaced 4cm away from the active electrode.

Maintaining stimulation below a sensation threshold allowed for the study of tACS as a non-invasive form of treatment, but it is also important for the ensuring that any measured effect of stimulation is due to stimulation alone. If the stimulation itself is perceptible, then this may engage an attentional process that orientates the participant to the point of target identification, allowing the participant to pre-empt their response, reducing RT.

Each of the five EEG-determined stimulation frequencies was generated using a

sinusoidal waveform with a duration of 1.1–1.5s to match the duration of the preparatory phase of the response. The sham condition consisted of 1.5s of random noise (tRNS). A random level of current was generated for every sample (sampling rate 1280 samples/s). Statistically, the random numbers are normally distributed over time, and the probability density follows a Gaussian bell curve. This 'white noise' stimulation contains all frequencies up to and including $640Hz$. For each participant, sham stimulation was only applied twice, once during the first trial of the experimental block and a second time during the final trial.

4.2.4 Behavioural task and trial design

The same instructed-delay reaching task was used for the stimulation session as was used in the previous EEG study (Chapter 3). The task, based on an established paradigm (Pellizzer & Hedges, 2003; Pellizzer et al., 2006; Tzagarakis et al., 2010), can be seen in Figure 4.3. There were six blocks in total, one for each of the stimulation frequencies, comprised of 36 trials. This meant that there were 216 trials overall. The order of stimulation was pseudo-randomised for each participant to ensure that there were no effects of time of stimulation on response times. There was a two minute rest period between each block that the participant controlled. This was designed to allow the participant to skip the rest period if they felt they did not need it.

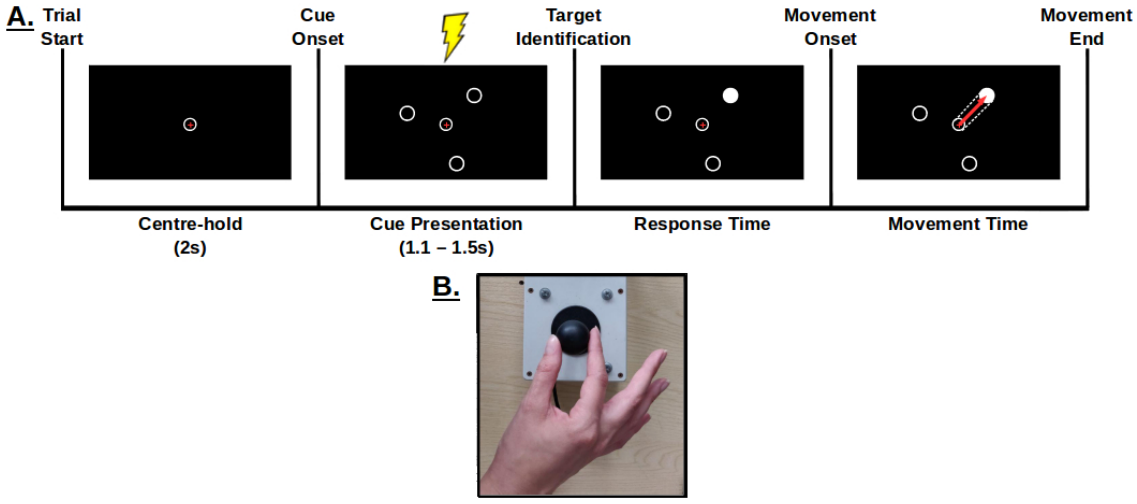

Figure 4.3: **A.** Diagram of the trial sequence for the instructed-delay task. Participants used the joystick to hold the crosshair in the centre of the screen for 2s. Then 1, 2 or 3 potential targets were presented on the screen for 1.1-1.5s. It was during this preparatory phase that stimulation was applied. The figure depicts a '3-Target' trial in which the target at $45°$ was highlighted as the target the participant was to move the crosshair toward. RT was defined as the duration between target identification and movement onset. **B.** The custom-made joystick used throughout the study was designed to be held between the thumb and index finger.

Each trial comprised a 'centre-hold' period, a spatial cue presentation ('cue onset'), a target cue presentation ('target identification') and a participant response ('movement onset'). Each trial was initiated by the participant maintaining a joystick-controlled crosshair within an outline of a circle in the centre of the screen (radius, 0.6° of the VA) for 2s. Participants were instructed to fixate on the centre of the screen throughout the trial (Figure 4.3A).

Following the 'centre hold' period, a spatial cue was presented that varied randomly in duration between 1 and 1.5s. The spatial cue consisted of one, two or three possible targets, with the number and positions of targets pseudo-randomised for each trial. This resulted in three possible target presentations, each presented 20 times during the *one-target* condition and three possible combinations of targets, each presented 20 times, during the *two-target* condition. Seventy-two trials were presented in total for each target condition. It was during the presentation of this spatial cue that stimulation was applied.

Each target consisted of an outline of a circle (radius, 0.75° VA) with a centre 4° VA away from the centre of the screen. Targets were presented at 45°, 165° and 285° relative to the centre of the screen. Following cue onset one of the targets was highlighted white (target identification). At this point, the participant used the joystick to move the crosshair from the centre of the screen towards the highlighted target circle as quickly and accurately as possible. Consequently, directional preparation was possible at cue onset in only the one-target condition, but not in the two-target or three-target conditions, where directional uncertainty continues until target identification.

Successful responses were defined as a trial in which the participant moved the crosshair from the centre of the screen to the target circle in a direct straight line (final panel, Figure 3.1A). Trials in which the participant deviated from this straight-line movement were removed from the analysis. The RT was defined as the period between target identification and movement onset.

For each of the three target conditions, RT outliers were removed from the dataset. The threshold used to detect outliers was the median $\pm$ 2* MAD, where MAD is calculated by finding the median of absolute deviations from the median (Huber & Ronchetti, 1981; Leys et al., 2013). This method of outlier detection is considered to be more appropriate and robust than using the mean $\pm$ SD (Hampel, 1971; Leys et al., 2013; Liu et al., 2004).

4.2.5 Experimental design and statistical analyses

A repeated measures ANOVA was performed to analyse the change in RT. The number of targets presented was one factor and the second factor was the stimulation frequency (peak beta, low beta, high beta, peak alpha, $130Hz$ & sham). Fifteen further planned contrasts were performed to compare each of the five stimulation frequencies to sham, across the three target conditions.

4.3 Results

4.3.1 Overall response times

Average RTs are plotted against number of targets in Figure 4.4. As predicted, RT was significantly affected by number of targets, $F(2,90) = 16.816$, $p < .0001$, ANOVA, with planned contrasts indicating that RT during one-target presentation ($M = 346.31ms$, $SD = 56.3ms$) was significantly less than during two-target presentation ($M = 404.45ms$, $SD = 56.15ms$; $t(30) = -10.148$, $p < .0001$, paired t test), and three-target presentation ($M = 429.4ms$, $SD = 60.92ms$; $t(30) = -11.427$, $p < .0001$, paired t test). Average RT during two-target presentation was also significantly lower than during three-target presentations ($t(30) = -10.169$, $p < .0001$, paired t test). These findings are in line with those of our previous study (Section 3.3.1) and of previous studies using a similar paradigm that found as directional uncertainty increases, RTs lengthen (Tzagarakis et al., 2010).

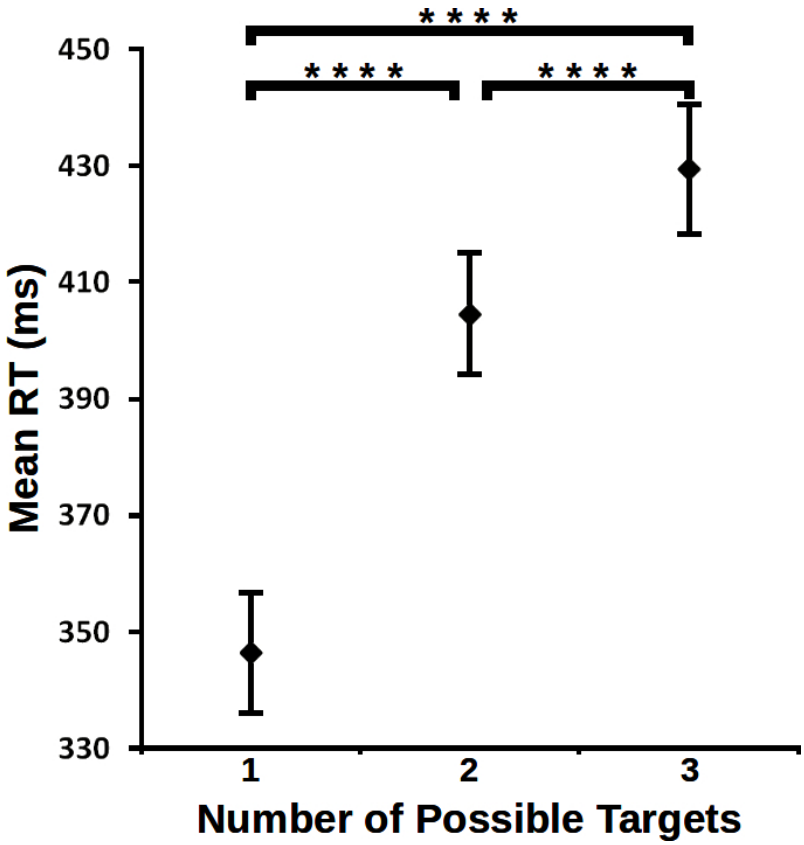

Figure 4.4: Mean RT for each target condition, regardless of stimulation. The error bars represent standard error ($N = 31$ participants); one-target, $M = 346.38ms$; two-targets, $M = 404.45ms$; three-targets, $M = 429.4ms$. ****, p<.0001

4.3.2 Efficacy of sham stimulation as a control condition

Results from a one-way ANOVA indicated that there was no significant effect of sham stimulation on RTs during the stimulation session compared to the RTs recorded during the earlier EEG session ($F(1,184) = 1.259$, $p = .263$, ANOVA). Despite there being a slight trend towards faster RTs during sham stimulation, there was no significant difference in RTs in the one-target condition for sham ($M = 354.76ms$, $SD = 65.08ms$) vs no stimulation ($M = 358.37ms$, $SD = 60.02ms$; $t(30) = .374$, $p = .711$, paired t-test). Nor was there any significant difference in the two-target condition for sham ($M = 400.23ms$, $SD = 52.9ms$) vs no stimulation ($M = 418.66ms$, $SD = 60.71ms$; $t(30) = 1.422$, $p = .165$, paired t-test); or in the three-target condition for sham ($M = 424.85ms$, $SD = 56.8ms$) vs no stimulation ($M = 435.97ms$, $SD = 63.1ms$; $t(30) = 1.267$, $p = .215$, paired t-test).

This lack of significant difference between RTs recorded during the sham stimulation and RTs recorded during the EEG session earlier in the week (Figure 4.5) led us to conclude that the sham condition was a valid control condition for comparing the effects of stimulation frequency on RT.

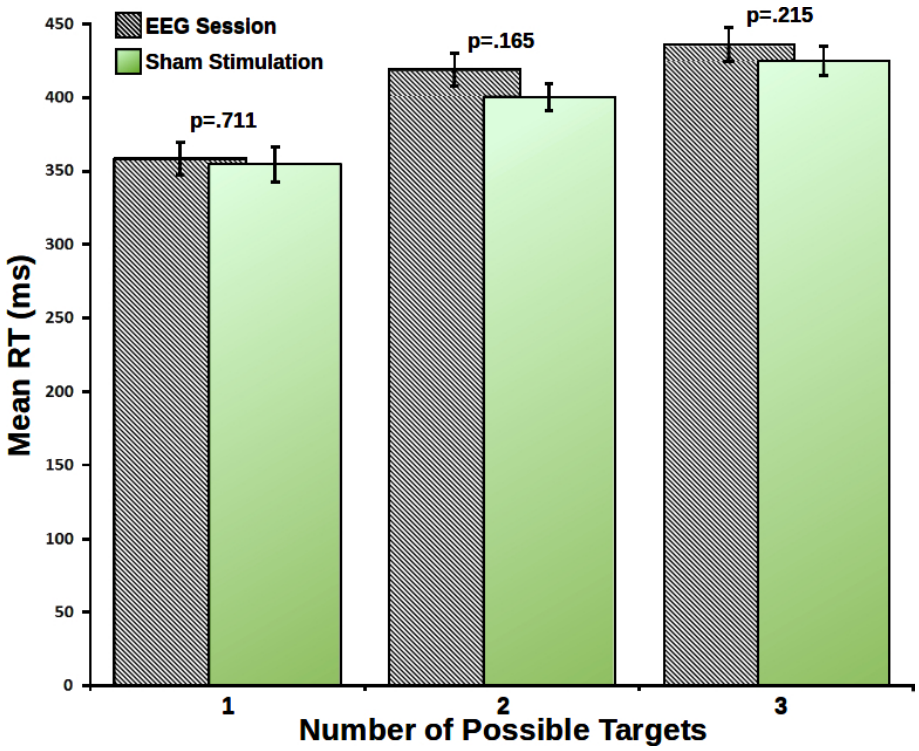

Figure 4.5: Mean RT for each target condition during the initial EEG session (black and white hatched bars) and the sham stimulation condition (green bars). Error bars represent SEM. There was no significant difference in RT between the sham stimulation condition and the previous EEG session for any of the three target presentations.

4.3.3 Frequency-specific effects of HD-tACS on motor performance

Overall, there was no significant effect of stimulation on RTs ($F(5, 185) = .051$, $p = .998$, ANOVA). Further comparisons were carried out using paired t-tests to investigate effects of each EEG-determined stimulation frequency on RT across the three different target presentations in relation to sham stimulation. The result of each of these comparisons can be found in Table 4.1.

Interestingly, during the one-target condition, when the participant is certain of their action, there was an overall trend towards stimulation of any kind having a facilitatory effect on response time. The opposite was true during the two uncertain conditions, as response times during both the two-target and three-target conditions appear to be lengthened slightly by any form of stimulation (Figure 4.6). However, no effect of stimulation on response time was found to be significant, therefore, no conclusion can be made from this apparent trend.

Table 4.1

Statistical comparison of mean RT for each stimulation frequency in contrast to the sham condition

Targets Presented	Stimulation Frequency*	Mean Difference in RT (ms)	Standard Error (ms)	Paired T-Test Result
One-Target	Peak Beta	-5.95	7.81	$t(30) = -.762,\ p = .452$
	Low Beta	-1.1	7.12	$t(30) = -.154,\ p = .879$
	High Beta	-13.05	7.09	$t(30) = -1.841,\ p = .076$
	Peak Alpha	-6.82	8.01	$t(30) = -.851,\ p = .401$
	$130Hz$	-8.85	8.21	$t(30) = -1.079,\ p = .289$
Two-Targets	Peak Beta	5.52	5.43	$t(30) = 1.017,\ p = .317$
	Low Beta	4.87	7.17	$t(30) = .68,\ p = .502$
	High Beta	8.39	5.27	$t(30) = 1.593,\ p = .122$
	Peak Alpha	3.29	7.24	$t(30) = .454,\ p = .653$
	$130Hz$	6.24	6.89	$t(30) = .906,\ p = .372$
Three-Targets	Peak Beta	13.11	6.6	$t(30) = 1.986,\ p = .056$
	Low Beta	7.76	7.38	$t(30) = 1.051,\ p = .302$
	High Beta	4.71	6.78	$t(30) = .695,\ p = .493$
	Peak Alpha	.89	7.69	$t(30) = .115,\ p = .909$
	$130Hz$	12.65	7.23	$t(30) = 1.749,\ p = .09$

**Peak, low and high beta, along with peak alpha, frequencies were calculated for each individual using data from a previous EEG session.*

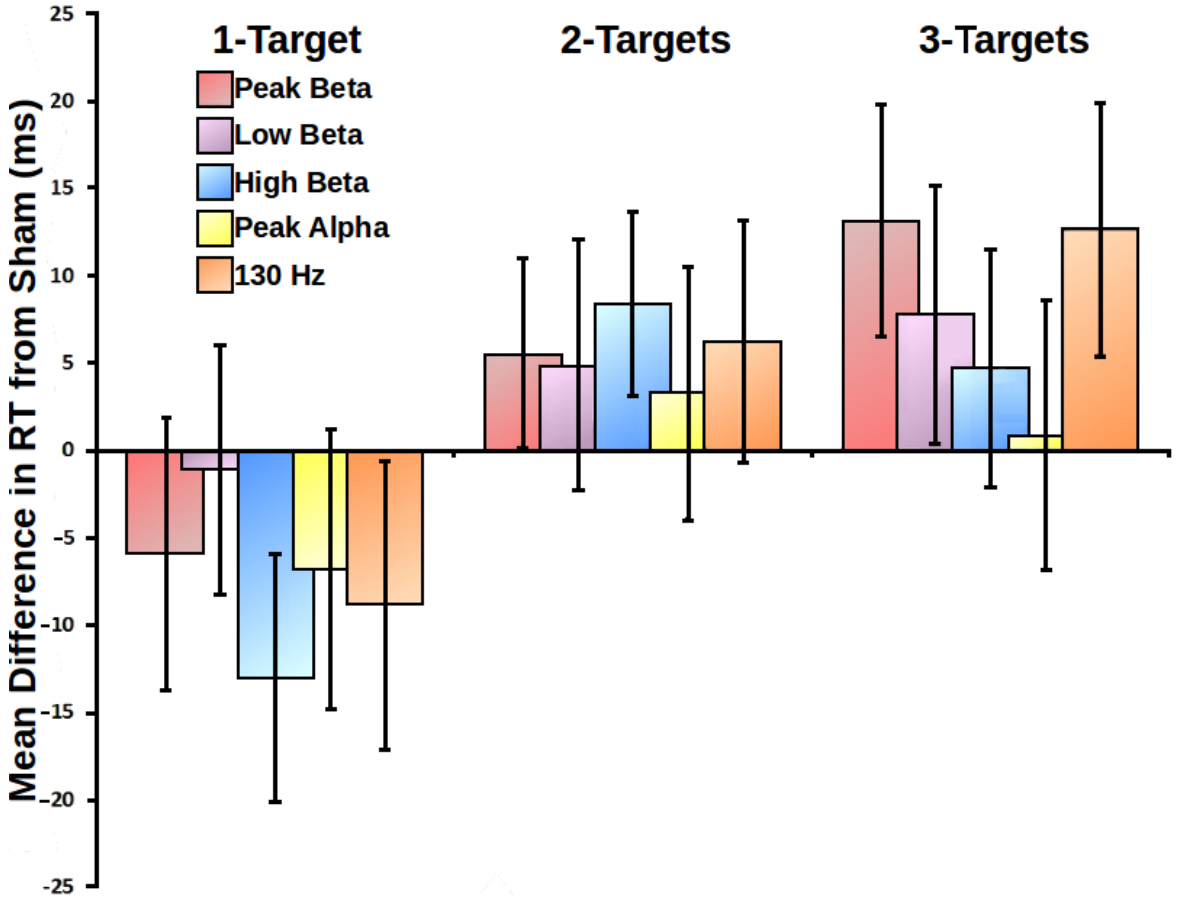

Figure 4.6: Modulation of RT following application of HD-tACS stimulation at individual peak frequencies. Across the three target presentations, there were no significant improvements or slowing of motor RTs.

4.3.4 Summary of results

- The predicted effect of directional uncertainty on average RT was found, regardless of stimulation condition. When the participant was certain of their movement, during the one-target condition, average RT was significantly faster than when they were uncertain (two and three-target conditions).
- There was no significant difference in RT during the sham stimulation and the earlier EEG session in which no stimulation was applied.
- Neither peak alpha nor peak beta tACS significantly lengthened RT.
- Unlike DBS to the STN, stimulation of the motor cortex at $130Hz$ had no facilitatory effect on motor performance.
- There was no significant effect of stimulation of any kind on RT. Though, there was an interesting trend towards a general facilitatory effect of tACS on RT during the one-target condition. During the two and three-target conditions this effect was reversed, resulting in a non-significant lengthening of RT.

4.4 Discussion

4.4.1 Summary

In this chapter, we attempted to modulate motor performance by using HD-tACS to entrain alpha and beta oscillations during the preparation of movement. Overall, there was no significant evidence that stimulation had any effect on motor performance. However, this finding is somewhat inconsistent with previous work within the field and is likely due to methodological limitations in the current study.

4.4.2 Directional uncertainty consistently lengthens RT regardless of stimulation

As predicted, RT was directly dependent on the ability of participants to predict the direction of the required movement, based upon the stimulus information. As the number of presented targets and, therefore, the level of uncertainty about the required movement direction increased, there was a significant increase in RT. This finding agrees with that of our previous study (Section 3.4.2) and is consistent with previous reports (Bock & Arnold, 1992; Churchland et al., 2008; Dorris & Munoz, 1998; Pellizzer et al., 2006; Tzagarakis et al., 2010).

The ability of discrete spatial cues in this kind of instructed-delay reaching task to robustly modulate directional uncertainty during motor preparation was evidenced by the same significant effect on RT being observed regardless of the type of stimulation being delivered.

4.4.3 Sham stimulation is a valid control condition

To ensure that there was no confounding effect of the participant being in some way aware of the stimulation onset and, therefore, being able to pre-empt and predict the 'GO' cue, RT was compared between the sham condition and the earlier EEG session. There was no significant difference in RT between the sham condition and the EEG session, which indicates that participants were not using any perceptible feature of stimulation to orientate their attention and aid in movement preparation.

There was a slight, non-significant improvement in motor performance during sham stimulation compared to the previous EEG session. However, this improvement is more likely to be a result of the participants having prior knowledge of the instructed-delay task.

4.4.4 Low-amplitude, short duration HD-tACS has no significant effect on motor performance

We found that, in contrast to our predictions, the application of HD-tACS over M1 during the preparatory phase of movement had no significant effect on the resulting RT.

Based on our previous findings, we predicted that stimulation of the M1 at peak alpha and beta frequencies would result in an entrainment of the ongoing oscillation. This entrainment would then interfere with the efficient recruitment of the functional ensemble required to make the upcoming movement, lengthening RTs. While uncertainty was high, there was a general trend towards peak alpha and beta stimulation increasing RT; however, this increase was non-significant and wasn't restricted to peak frequencies. In fact, any form of HD-tACS to the M1 seemed to lengthen RTs during the two and three-target presentations.

This lack of an effect of any type of tACS is likely due to our choice of stimulation parameters. This study was specifically designed to investigate the efficacy of HD-tACS as a potential, non-invasive treatment for patients who suffer from neurological disorders, such as PD. Therefore, our stimulation parameters were particularly restrictive.

To begin, the 4×1 electrode montage used throughout this study had particularly low spacing between each electrode at only 4cm centre-to-centre. The rationale behind this choice was that we had a very specific stimulation target in the left M1h and, therefore, we could use an electrode montage with a smaller, more focal radius. However, this increased focality comes with a caveat of reduced stimulation intensity within the target brain region (Dmochowski et al., 2011). We attempted to negate this reduced stimulation intensity within the M1 by using small-diameter electrodes (2cm), as reduced electrode size has been found to improve the overall current density of stimulation (Nitsche et al., 2007; Stagg & Nitsche, 2011). However, without modelling the stimulation to discover its current density and the intensity at M1 it is difficult to know if any stimulation occurred.

Another limitation of our stimulation design was that we only stimulated for a maximum duration of $1.5s$. The onset of stimulation aligned with the spatial cue onset of the instructed-delay task and ended when the target was identified. This encompassed the response-phase, during which our previous study had demonstrated significant desynchronisation of alpha and beta frequencies. The finding of Pogosyan et al. (2009)

that entrainment appears to begin as early as $1.12s$ after stimulation onset provided us with a precedent to suggest that this short stimulation duration could entrain preparatory oscillatory activity. However, the duration of each stimulation period that Pogosyan and colleagues used to find a significant slowing of movement was $10s$ long with a total stimulation time of $300s$ per frequency condition (Pogosyan et al., 2009), while the previously cited, Weinrich et al. (2017) study, used four stimulation periods of $80s$ for a total duration of $360s$. The stimulation periods used in both of these studies were significantly longer than those of the present study, which had a total stimulation time per frequency of only $45s$.

In the light of the Thut and colleagues' model of neural entrainment (Thut et al., 2011a), described in Section 2.4.1, it is perfectly possible that the short duration of each stimulation period used did not apply enough external force to entrain the intrinsic oscillation of M1.

4.5 Conclusion

In this chapter, we attempted to interfere with motor preparation using non-invasive tACS. Despite some interesting data trends, there were no significant effects of stimulation at any frequency on RT. This lack of significance is likely due to limitations of the stimulation parameters used and should not be taken as evidence of HD-tACS being an inefficient modulator of cortical oscillations.

In future, a similar study design could be used that, rather than attempt to entrain underlying activity only during the preparatory-phase of movement, applies stimulation for a more typical period of 10–20mins before beginning the task (Stagg, 2014; Stagg & Nitsche, 2011). The hypothesis being that an extended period of stimulation at peak beta frequency would lead to an increase in spontaneous beta power within the M1, leading to a lengthening in RT during an instructed-delay reaching task due to impaired coherence within the motor network.

Chapter 5

Post-movement beta rebound inhibits cortical excitability

Existence of an excited state is not a prerequisite for the production of inhibition; inhibition can exist apart from excitation no less than, when called forth against an excitation already in progress, it can suppress or moderate it.

– Charles Scott Sherrington (1857 - 1952)

5.1 Introduction

Voluntary movement in humans has been associated with well-established patterns of neural oscillatory activity throughout the motor system. During the preparation for and the execution of a movement, there is a strong event-related desynchronisation (ERD) in both the beta and alpha frequency bands. Following the cessation of movement, there is resynchronisation of the beta band, the post-movement beta rebound (PMBR). An inverse relationship has been suggested between beta and cortical excitability with the beta ERD generally thought to reflect excitation of motor networks and the PMBR considered to represent cortical inhibition. The current chapter aims to employ motor-evoked potentials (MEPs), an established measure of cortical excitability, to investigate to what extent PMBR inhibits the primary motor cortex following movement termination.

5.1.1 Background

PMBR was first described by Pfurtscheller and colleagues (1996) as an event-related synchronisation of a ∼20Hz rhythm following both self-paced finger extension and flexion, and externally paced wrist movements. Just as ERD in the alpha and beta bands are robust correlates of motor preparation and execution (Formaggio et al., 2010; Leocani et al., 1997; Miller et al., 2010; Pfurtscheller & Berghold, 1989; Pfurtscheller & Lopes

Da Silva, 1999), PMBR is a consistent oscillatory feature following movement termination (Cassim et al., 2001; Cheyne et al., 2006; Pfurtscheller et al., 1996; Salmelin et al., 1995b; Stancák & Pfurtscheller, 1995). PMBR reaches its maximal amplitude 500-1000ms after movement termination and continues for a further 1000ms before returning to a baseline level (Cheyne et al., 2006; Gaetz et al., 2010; Jurkiewicz et al., 2006).

Beta ERD and PMBR appear to originate in spatially distinct regions of the motor system, with ERD involving the more supplementary motor areas: contralateral S1, PPC, SMA and the cerebellum. PMBR, on the other hand, has been reported in the contralateral M1, PMC, SMA and the frontal association cortex (Cheyne et al., 2006; Gaetz et al., 2010; Heinrichs-Graham et al., 2014b; Jurkiewicz et al., 2006; Ohara et al., 2000; Wilson et al., 2010). ERD is also more generalised and widespread than the PMBR, the peak of which is centred over the somatotopic representation of the effector being moved (Stancák & Pfurtscheller, 1995). It is, therefore, possible that the beta ERD and PMBR are neural correlates of two different motor processes.

The functional significance of PMBR is still unclear, although a number of possible explanations have been posited. Pfurtscheller and colleagues originally suggested that underlying beta activity represents an 'idling' cortex. They hypothesised that ERD reflects cortical excitation and the recruitment of motor networks required to execute a movement, while PMBR represents a return to an idling cortex once the movement is complete (Pfurtscheller, 1992; Pfurtscheller et al., 1996, 1997). A second and perhaps more prominent theory is that underlying beta activity promotes tonic and postural control over voluntary movement. Several studies have shown that when beta power is high, the existing motor state and postural set is favoured and reinforced while the initiation of new movement is impaired (Gilbertson et al., 2005; Pastötter et al., 2008; Van Wijk et al., 2008).

As previously mentioned, the PMBR has a more focal spatial distribution than beta ERD; being localised over the area of the M1 responsible for the movement being generated (Stancák & Pfurtscheller, 1995). PMBR also differs from ERD as it appears to be modulated by movement parameters (Fry et al., 2016; Parkes et al., 2006; Stančák et al., 1997), for example, a resisted finger extension elicits a greater PMBR than the same movement without any resistance (Stančák et al., 1997). In opposition to the two theories mentioned above, a third theory has been suggested that takes into account the

dependence of PMBR on the type of movement performed. This theory states that the PMBR reflects a process of sensory reafference, providing feedback about the completed movement (Alegre et al., 2002; Cassim et al., 2001). This feedback allows the motor system to compare the original motor plan with the executed movement, and adjust accordingly. During this sensory reafference, the motor cortex may be actively inhibited to prevent further movement error. This may explain why a greater PMBR has been observed following motor errors (Koelewijn et al., 2008).

Regardless of the theory one chooses to subscribe to, it is generally accepted that PMBR reflects active inhibition of the motor system following the cessation of both motor execution and motor imagery (Cassim et al., 2001; Gilbertson et al., 2005; Koelewijn et al., 2008; Pastötter et al., 2008; Pfurtscheller et al., 1996; Salmelin et al., 1995b). This is further evidenced by studies that have shown: (1) That PMBR is attenuated during periods of cortical activation (Pfurtscheller et al., 2002; Schnitzler et al., 1997); (2) That the expected PMBR period correlates with reduced excitability of M1 neurons (Chen et al., 1998; Leocani et al., 2000); and (3) that tACS induced beta activity within the M1 inhibits motor performance (Pogosyan et al., 2009). Enhanced PMBR has been observed during a 'Go/NoGo' paradigm following the 'NoGo' cue, a finding which was interpreted as an indication that PMBR functions as a physiological marker of movement inhibition (Alegre et al., 2004b). An MEP study also found that corticomotor excitability was greatly reduced following a 'NoGo' cue compared to a 'Go' cue (Coxon et al., 2006).

Further evidence that PMBR may reflect an inhibitory process comes from studies of the cellular mechanisms that generate motor network beta. GABAergic interneurons within the deeper cortical layers (L5/L6) of M1 form an inhibitory network. Previous studies have demonstrated that motor beta oscillations are driven by GABAergic modulation (Hall et al., 2010a, 2011; Yamawaki et al., 2008), with a significant positive relationship between GABA concentration and underlying beta power during PMBR (Gaetz et al., 2011). Magnetic resonance spectroscopy studies have also demonstrated that changes in cortical excitability, as measured by TMS, correlate with changes in underlying glutamate and GABA concentrations (Stagg, Bestmann, et al., 2011); and that there is an inverse relationship between resting connectivity of the motor network and GABA concentrations (Stagg et al., 2014).

As briefly touched upon above and in Section 2.3.1, TMS-induced MEPs have become

the method of choice for investigating cortico-spinal excitability in the motor domain (Hallett, 2000). The onset latency and amplitude of an MEP are modulated by the level of ongoing muscle excitability, with higher levels of muscle excitability resulting in a shorter onset latency and a greater MEP amplitude (Rossini et al., 1988; Rossini & Rossi, 1998; Tomberg & Caramia, 1991). This finding is not restricted to increased muscle excitability during the execution of the movement but has also been observed during motor imagery (Facchini et al., 2002; Fadiga et al., 1995; Fourkas et al., 2008; Sakamoto et al., 2009).

Therefore, following a simple muscle response, one would expect the underlying muscle contraction to decrease over time. The time-course of this decrease would coincide with a lengthening of the onset latency and reduction in MEP amplitude back to baseline levels. However, if the amplitude of an MEP reflects underlying cortical excitability, then a period of active inhibition, such as PMBR, should coincide with a reduction of MEP amplitude below that of the baseline. A number of previous studies have supported this theory by providing evidence that, following the termination of a movement, there is a decrease in induced MEP amplitude (Chen et al., 1998; Coxon et al., 2006; Leocani et al., 2000).

Several studies have attempted to investigate the relationship between spontaneous oscillatory activity and cortical excitability changes, using TMS and MEP paradigms. It is difficult, however, to draw any definite conclusion from their results. Sauseng et al. (2009) and Zarkowski et al. (2006) both found a negative correlation between Rolandic alpha and MEP amplitude and no correlation between beta and MEP amplitude. Lepage et al. (2008) and Mäki & Ilmoniemi (2010), however, found a negative correlation between Rolandic beta and MEP amplitude, though it was not quite significant in the latter case (Mäki & Ilmoniemi, 2010). McAllister and colleagues (2013) provided further evidence of the link between elevated beta and cortical inhibition, through the use of continuous theta burst stimulation and concurrent MEG. They found that, consistent with earlier findings (Di Lazzaro et al., 2005; Huang et al., 2005), theta burst stimulation induced strong cortical inhibition which coincided with increased spontaneous beta power (McAllister et al., 2013).

As mentioned, beta ERD is thought to reflect excitability within the motor cortex, and MEP evidence seems to support this. A study of motor imagery found that MEP amplitude was significantly greater during periods of beta ERD than during rest and that there was

a significant positive correlation between the extent of beta ERD and MEP amplitude (Takemi et al., 2013).

The Takemi et al. (2013) study is, to the best of my knowledge, the only study that directly correlates movement-related changes in beta amplitude with cortical excitability. Other studies either correlate MEP measures of excitability with transient changes in beta power, or use an estimated time-period prior to and following a movement to suggest changes in beta power may correlate with changes in cortical excitability (Chen et al., 1998; Coxon et al., 2006; Leocani et al., 2000). These latter studies make indirect inferences about movement-related changes in beta power without directly measuring neural activity with EEG or MEG.

There has been little research into changes in the onset latency of induced MEPs during a motor task, with most studies only reporting changes in MEP amplitude (Chen et al., 1998; Coxon et al., 2006; Leocani et al., 2000). Similarly to amplitude, some facilitation of onset latency has been observed during the execution of a movement (Nomura et al., 2001; Starr et al., 1988), but it is unclear whether this is due to an increase in cortical excitability or to an increase in the underlying muscle activity.

5.1.2 Aims and research objectives

The aim of this study was to:

1. Identify the optimal location of the motor cortex hand area (M1h), controlling the first dorsal interosseous (FDI) (Section 2.3.2).
2. Use EEG to characterise the time-frequency profile of oscillatory modulation at an individual level.
3. Apply the time-course of the averaged beta ERD and PMBR trace for each individual to guide the temporal delivery of the TMS stimuli for MEP collection

To the best of our knowledge, this is the first study to use individuals' beta power profile to determine movement-related changes in cortical excitability using MEP measurement. This provides a considerable advantage over previous studies that have relied on an approximation of when PMBR would occur (Chen et al., 1998; Coxon et al., 2006; Leocani et al., 2000).

I hypothesised that:

- There will be an inverse relationship between motor cortical beta power and MEP amplitude. More precisely:

    1. MEPs that are induced immediately after the cessation of movement, and therefore during a period of beta ERD prior to PMBR onset, will be significantly greater in amplitude than MEPs collected at rest.
    2. The amplitude of an MEP induced during the peak PMBR period will be significantly less than that of an MEP induced during a rest period.

- I further hypothesised that there will be a relationship between MEP onset latency, the phase of movement and coincident beta power and muscle activity. Specifically, I predicted that MEPs collected immediately after the response termination would occur significantly earlier than those collected at rest. However, given the limited previous research into changes in the onset latency of MEPs collected after a movement has been terminated I was unable to make a clear prediction. Instead, I theorised that in all likelihood one of two outcomes would occur, either:

    1. The onset latency will follow a similar pattern to that of the predicted amplitude change. Shortening during the ERD period, then lengthening beyond baseline during a PMBR period.
    2. MEP onset latency will be related to the underlying muscle activity, shortest during the high EMG activity associated with a muscle response and longer, then lengthening over time as muscle activity returns to baseline.

5.2 Methodology

Twenty-five right-handed participants were recruited in total (17 male), with a mean age of 24 (range 18 – 69) years. Informed consent was obtained, and all studies were approved by the local ethics committee, in accordance with the ethical standards set by the 1964 Declaration of Helsinki. All participants passed a TMS safety screening, were free of medication and did not have any personal or family history of neurological or psychiatric illness. Two participants were excluded in total from the analysis due to a hardware fault that led to the recorded EMG being sampled incorrectly.

5.2.1 Data acquisition

The left M1 was functionally localised using the TMS procedure outlined in Section 2.3.2. This allowed us to ascertain the participant's primary hand area (M1h) and their resting motor threshold (RMT). RMT was defined as the lowest stimulator intensity required to consistently induce MEPs in the right FDI with a peak-to-peak amplitude greater than $50\mu V$ in 8 out of 10 trials. All induced MEPs in this study were collected at 100% of each individual's RMT. This scalp location was also used to guide EEG electrode placement.

All EEG data were recorded using the DC-EEG feedback system (Section 2.5.1). Ag/AgCl electrodes were arranged in our standard 7-electrode montage with the localised M1h at its centre (Section 2.5.2). EEG was referenced online to the ipsilateral mastoid and sampled at a rate of $2048Hz$ with impedance for all channels maintained below $3k\Omega$. EEG signals were bandpass filtered (2–$100Hz$) and notch-filtered (48.5–$51.5Hz$) to avoid power line contamination (Section 2.5.3).

Surface electromyogram was recorded from both the left and right first dorsal interossei (FDI) using the Bagnoli 2-channel EMG-system (DelSys Inc., Boston, USA). EMG signals were amplified 10,000 times and sampled at a rate of $2048Hz$ to align with sampled EEG data. Impedance was kept below $10k\Omega$, and all EMG signals were bandpass (20–$450Hz$) and notch-filtered (48.5–$51.5Hz$) using the same window-synced FIR filter applied to the EEG signal.

EMG was recorded during the EEG stage of the experiment to aid in movement detection. Each time the participant pressed down with their index finger, there was a significant increase in the FDI muscle response, as recorded by EMG. The onset and offset of this increased muscle activity was calculated to accurately assess the latency of the

accompanying beta ERD and PMBR. During the MEP stage of the experiment, EMG was again used to calculate the offset of the index finger movement to time-lock TMS stimulation. EMG was, of course, used as well during this stage to measure the peak-to-peak amplitude of the induced MEPs.

Single-pulse TMS was delivered using the Magstim 200^2 (Magstim, Whitland, UK) equipped with a standard 70mm, figure-of-eight coil. The optimal coil position and orientation for inducing MEPs in the right FDI was marked in pen on the participant's scalp to ensure exact coil placement throughout the study. Given the length of the study and the importance of maintaining coil position to ensure consistency, a TMS frame was specially designed and built (Section 2.3.4). This frame allowed the participant to position themselves comfortably while placing their head in an ophthalmology chin rest. The TMS coil was held in position against the participant's head using a mechanical arm. I then stood beside the participant throughout the study to ensure neither they nor the TMS coil changed position.

The Power 1401-3 USB data acquisition interface along with the Spike2 data acquisition package (Cambridge Electronic Design, UK) was used to store EMG and force sensor output and to trigger single-pulse TMS. The beginning and end of each trial were recorded via a digital marker generated by MATLAB sent through the Arduino Uno BNC interface.

5.2.2 Study design and procedure

The study design was a two-part, within-subjects design that was performed in two stages, an EEG stage and an MEP stage (Figure 5.1). The first half of the study was an EEG experiment, during which the participant repeatedly performed a cued simple isometric finger contraction while EEG was recorded from the contralateral M1. Each participant's neural response was then averaged offline to create time-frequency plots of the individual's typical PMBR. The latency of the peak of the PMBR was calculated and used to trigger timed TMS pulses during the second part of the study (Figure 5.3). Both the EEG and MEP stages were performed on the same day.

Once the left M1 was functionally localised and the participant's motor threshold was ascertained, EEG electrodes were placed on the scalp and the participant was asked to sit in front of a computer screen. They then performed the simple response time task as described below. There were 170 EEG trials in total, each with a duration of ten seconds. The first ten trials were used as practice to ensure the participant knew how to respond

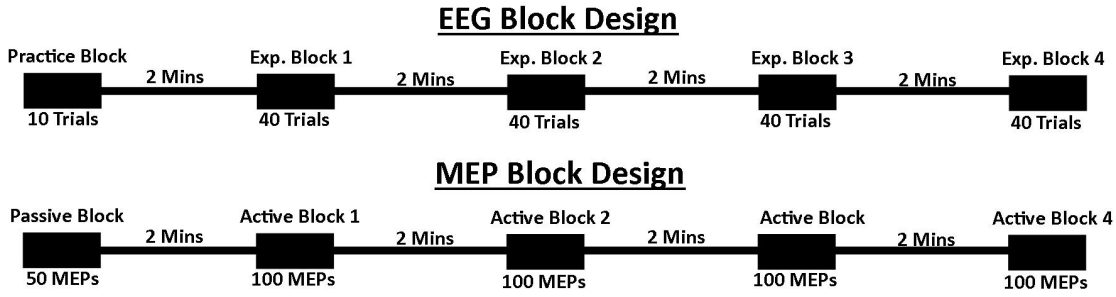

Figure 5.1: The EEG stage consisted of 170 response trials in total, beginning with a practice block of 10 trials followed by four experimental blocks each consisting of 40 trials. The participant rested for two minutes between each block. The MEP stage began with 50 induced MEPs while the participant was completely passive. Following this there were four active blocks consisting of 50 response trials, during each of which two MEPs were induced at different time points. 400 active MEPs were recorded in total.

correctly and that all the recording hardware was functioning as expected. Following the practice, there were a further four blocks of 40 trials. Once all four blocks were completed the EEG electrodes were removed from the scalp and the participant was asked to wait while the EEG analysis was performed.

5.2.3 Task design

The same simple reaction time task was used for both EEG and MEP data acquisition (Figure 5.2). Participants were instructed to fixate on the centre of the screen at all times while resting their right index finger on a Mini S-Beam force sensor (Applied Measurements Ltd., UK). They were also instructed to keep both hands flat and that their right index finger should never lift off the force sensor during a trial.

Each trial presented was 10s in duration. For the first 1-1.5s, a red circle was presented in the centre of the screen. This period was randomised on a trial-by-trial basis to reduce the possibility of participants anticipating the 'GO cue' and responding too early. After this initial wait period, the circle in the centre of the screen changed from red to blue. Subjects were instructed that this was the 'GO cue', their cue to respond, and that they should do so as quickly as possible. They responded by pressing down on the force sensor as swiftly and as sharply as possible. This isometric finger flexion was practised before the main task so that participants learned to simply press down and then relax their finger, as opposed to pressing down and then lifting their finger from the sensor.

Once their response had been made participants were told to wait until the centre circle returned to red and await the next 'GO cue'. Given that time between the 'GO cue' and the termination of the response was expected to take up to 1000ms, this long 10s trial design

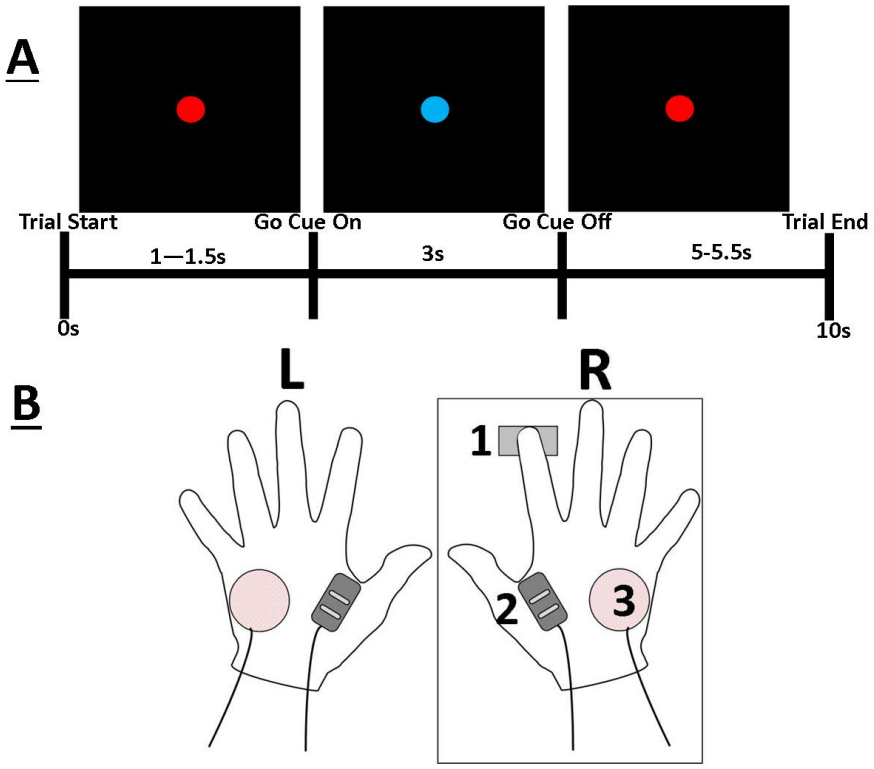

Figure 5.2: Motor task and recording apparatus. **A.** The 10s trial layout used for both the EEG stage and MEP stage. Subjects fixated on a red circle in the true centre of the screen. After a delay randomised between 1 and 1.5s the circle turned blue. This was the participant's cue to respond. **B.** When cued the participant responded by rapidly pressing the force sensor with their right index finger (**1**). EMG recordings were recorded using single differential surface electrodes over both left and right FDI muscles (**2**), referenced to the back of each hand (**3**).

meant that responses should terminate within the first 2–2.5s of a trial, leaving 7.5–8s to measure the PMBR produced by the response. We predicted based on previous research that PMBR should reach its maximal amplitude 500-1000ms after response termination and return to baseline levels after a further 1000ms (Cheyne et al., 2006; Gaetz et al., 2010; Jurkiewicz et al., 2006). Therefore, to avoid any possible overlap between the PMBR of the previous trial and the start of the next trial our trials needed to be at least five seconds long. Therefore, a 10-second interval was used to avoid this issue.

5.2.4 Time-locking MEPs to response termination and PMBR

All EEG data were analysed offline using MATLAB and FieldTrip (Oostenveld et al., 2011). The filtered EEG data for each trial was time-locked to the onset of the 'GO cue' before a Morlet-wavelet time-frequency analysis (Section 2.5.3) was performed to ascertain average beta band power over time. Rather than average across the entire beta band, an initial analysis was performed to find the peak PMBR frequency for each individual. A narrower band with a width of $5Hz$ around the peak PMBR frequency was

then averaged and used for further analysis. This narrower band was used due to the findings of previous studies that the frequency of PMBR varies between individual participants and is dependent on the movement effector (Gaetz et al., 2011; Neuper & Pfurtscheller, 2001b).

Force sensor and EMG data were used to determine when a response occurred and when the response was terminated. The maximal peak of the force produced during the response was defined as its latency and was therefore used to calculate response time (RT). This is because the active part of the response is the downwards press of the index finger. The decrease in force after the maximum reflects the passive relaxation of the finger. This is also reflected in the EMG activity recorded from the right FDI muscle, with an increase in activity up until the peak of the force response followed by a sharp return to baseline levels (Figure 5.3 B. and C.). The mean point at which EMG activity returned to baseline was defined as the termination of the response.

Trials in which no response occurred were removed from the analysis as were any trials in which the RT fell outside the acceptable range (median RT $\pm$ 2*MAD). Finally, trials with a poor EEG signal-to-noise ratio were also excluded from the analysis. A threshold was defined, where any participant that lost over 20% of their trials was removed from the analysis. No participant exceeded this threshold.

5.2.5 MEP collection

MEPs were collected while the participant was passively at rest and while they were actively performing the task described above. There were five *'active'* MEP conditions to be collected at different time-points during each trial; four coincided with changes in beta power while the other was taken when the participant returned to a resting state. These were defined as follows:

1. **Response termination** – A time-point immediately after the response has been terminated. This was defined as the average point at which right FDI EMG returns to baseline after the response has been made. For all participants, this period was during ERD of motor beta activity. Our hypothesis predicts that the amplitude of MEPs collected at this time-point would be significantly greater than the baseline (active rest).

2. **Early PMBR** – This time-point was defined as the earliest time that the averaged

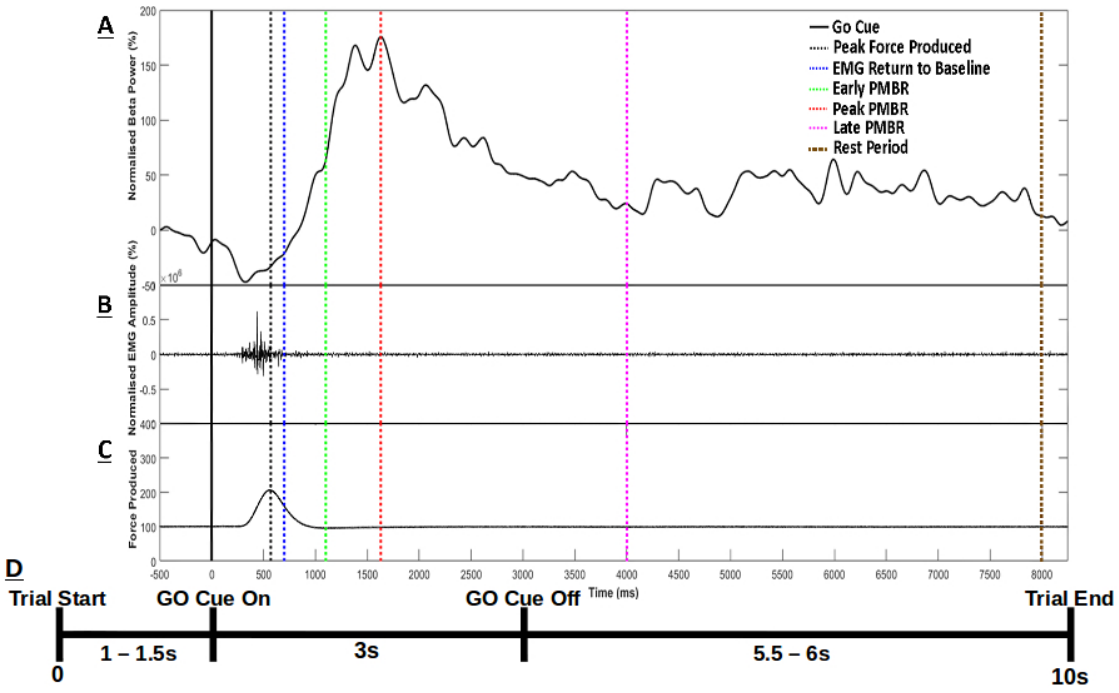

Figure 5.3: Averaged beta power (**A.**), right FDI EMG activity (**B.**), and force transducer amplitude (**C.**) across 170 trials for a typical participant. Solid black line: Cue to move; Dashed black line: Peak of response; Dashed blue line: End of EMG activity; Dashed green line: Early PMBR period; Dashed red line: Peak PMBR period; Dashed magenta line: Late PMBR period; Brown dashed line: Active rest period. **D.** Timeline of trial events

beta power for an individual reaches half the maximal amplitude of the PMBR.

3. **Peak PMBR** – This time-point is defined as the time at which averaged beta power reaches its maximal amplitude after response termination. We predicted that the amplitude of MEPs collected during this time-point would be significantly lower than the baseline (active rest).

4. **Late PMBR** – This time-point was guided by visual analysis of the averaged time-frequency plot of an individuals beta power. It was defined as the time at which beta stops steadily decreasing after PMBR.

5. **Active rest period** – The active rest period was defined as 500ms prior to the end of each trial. We predicted that beta should have returned to a baseline by this point in time; therefore, it should be a good measure of the difference between passive rest, when not expecting to move in the near future, and a more active, preparatory rest period.

The rationale for choosing three different time-points based on the peak of the PMBR was to determine whether changes in MEP amplitude are merely related to muscle

excitation. If we look at our participant's data from Figure 5.3 we can see that they make their response $\approx 550ms$ after the 'GO' cue and that their EMG activity returns to within one SD of the baseline at $\approx 700ms$. An MEP collected at this point may have a larger amplitude than one collected at the peak PMBR time-point ($\approx 1650ms$) purely due to a slight decrease in FDI muscle excitation over time. If only these two time-points were used, it would not be possible to distinguish between muscle excitation and cortical beta power as the correlate for the induced MEP amplitude.

To address this, we used three time-points to characterise the PMBR event:

1. The early time-point occurs when beta power reaches half the maxima of the peak PMBR.
2. The peak of the PMBR was defined as the average time-point at which an individual's cortical beta power reached its maximal amplitude after response termination.
3. The late time-point occurs when beta power first stops steadily decreasing after PMBR.

If muscle excitation was modulating MEP amplitude, then the induced MEPs would simply decrease in amplitude over time following the response termination. If, however, as predicted, MEP amplitude depends on underlying beta power then MEPs collected at the late time-point would be closest in amplitude to the baseline, while those collected during the early period would have reduced amplitude and those collected at the peak of PMBR would have an even greater reduction in amplitude.

Once the latency of each time-point was calculated for the individual (Figure 5.3) they were asked to return to their seat in front of the computer screen and to place their right index finger on the force sensor (Figure 5.2). At this point, 50 MEPs were induced at 100% of RMT with an inter-stimulus-interval of 5s, while the participant was instructed to remain entirely passive. Once complete the participant was informed that the MEP stage was about to begin and that they were to perform the same response time task as they had during the EEG stage.

There were 200 trials in total during this MEP stage, divided into four blocks of 50. During each trial, the participant was stimulated twice using single-pulse TMS to induce MEPs, the first pulse was received at one of the four beta time-points described above and the

second was received during the rest period at the end of each trial. This resulted in 50 MEPs being induced for each of the four beta time-points and 200 MEPs being induced for the active rest period. Due to there being one condition, the active rest condition, that had a significantly larger sample size than the other conditions, a random sample of 25 MEPs per condition was selected for the analysis.

5.2.6 MEP analysis

The peak-to-peak amplitude and the latency of each MEP were calculated using the methods described in Section 2.3.1. Trials in which no MEP was induced were excluded from the analysis, as were any trials that contained outliers (median amplitude $\pm$ 2*MAD). For each participant, the mean peak-to-peak amplitude and the mean latency of MEPs that were induced during the active rest period were used as the baseline for normalisation. An amplitude larger than this baseline would reflect a relative increase in cortical excitability, while a reduced amplitude would reflect cortical inhibition.

The effects of time of stimulation on MEP amplitude and onset latency were analysed by analysis of variance (ANOVA) with repeated measures. Time-point was used as the repeated measure and the amplitude and onset latency of the induced MEPs were the dependent variables. A Bonferroni correction was applied to account for multiple comparisons.

Significant effects were further analysed using post-hoc unpaired t-tests, to test for a significant difference from the baseline (active rest period) between each of the four beta-related time-points. Further t-tests were then used to carry out planned contrasts between each of the four beta-related time-points to investigate changes in MEP amplitude and onset latency. Finally, MEP amplitudes were compared between the passive rest period and the active rest period to investigate whether there was an overall effect of being involved in a motor task on cortical excitability.

5.3 Results

5.3.1 Beta-related changes in peak-to-peak amplitude

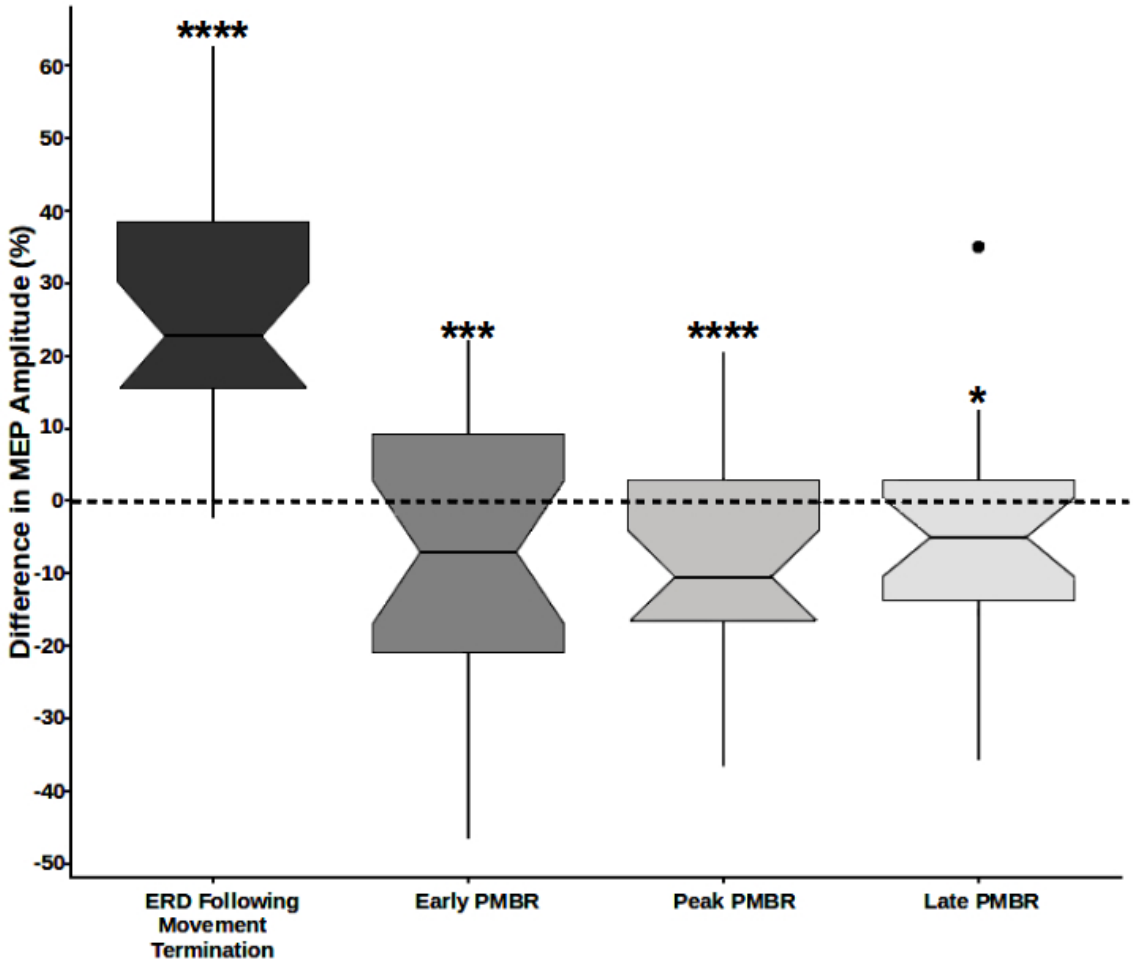

Figure 5.4: Difference in peak-to-peak amplitude of MEPs induced during the four different time-points and the active rest period. Zero on the y-axis represents the mean amplitude of MEPs collected during the active rest period. Amplitudes of MEPs were all normalised as a percentage of this baseline. ****, p<.0001, ***, p<.001, *, p<.05.

Figure 5.4 shows the normalised group-average MEP peak-to-peak amplitude induced from the right FDI. Zero on the y-axis represents the mean amplitude of MEPs collected during the active rest period; therefore a positive value reflects an MEP with a greater peak-to-peak amplitude than an MEP that was collected at rest. There was a significant main effect of time-point on collected MEP amplitude ($F(4) = 52.403$, $p < .0001$, $\eta_p^2 = .084$).

MEPs induced during the relative ERD period immediately following response termination were significantly greater in amplitude than at rest (mean difference (MD)$= +24.16\%$, $SD = 52.43$, $t(574) = 11.671$, $p < .0001$, $d = .487$). In contrast, MEPs induced during the early ($MD = -7.07\%$, $SD = 43.78$, $t(574) = -3.87$, $p < .001$, $d = -.166$), peak ($MD = -7.93\%$, $SD = 44.87$, $t(574) = -4.239$, $p < .0001$, $d = -.184$) and

late ($MD = -4.98\%,\ SD = 47.14,\ t(574) = -2.53,\ p = .012,\ d = -.112$) PMBR periods were significantly reduced in amplitude compared to rest.

Planned contrasts between each of the four beta-related time-points found that, as predicted, MEPs induced during the relative ERD period immediately following response termination were significantly greater in amplitude than any MEP induced during the three PMBR periods. ERD vs early PMBR ($t(574) = 11.409,\ p < .0001,\ d = .675$), ERD vs peak PMBR ($t(574) = 11.486,\ p < .0001,\ d = .685$), and ERD vs late PMBR ($t(574) = 10.616,\ p < .0001,\ d = .612$). There was no significant difference in the elicited MEP amplitude between any of the three PMBR periods; early vs peak PMBR ($t(574) = 0.33,\ p = .741,\ d = .02$), early vs late PMBR ($t(574) = -0.769,\ p = .442,\ d = -.046$) and peak vs late PMBR ($t(574) = -1.121,\ p = .263,\ d = -.43$).

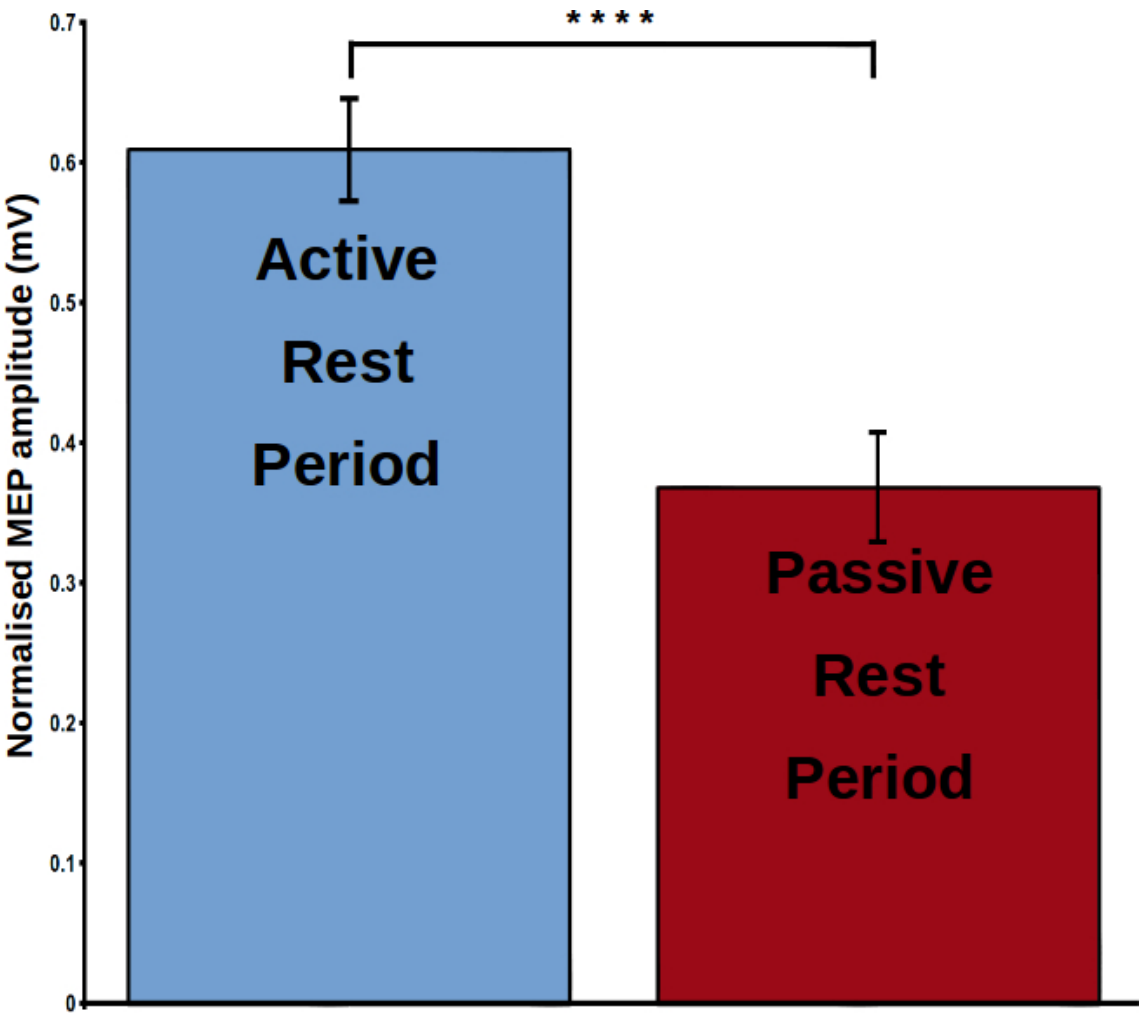

Figure 5.5: Group averaged normalised MEP amplitudes for MEPs induced during the passive and active rest periods. MEPs induced during the active rest period were significantly greater in amplitude than those induced during the passive rest period (p<.0001).

Figure 5.5 shows the group average normalised MEP amplitude for the two different rest periods. The active rest period, when participants were at rest between trials; and the passive rest period, collected before the task began when participants were instructed to relax completely. MEPs induced during the active rest period ($M = 0.609mV$, $SD = 0.873mV$) were significantly greater in amplitude than those induced during the passive rest period ($M = 0.369mV$, $SD = 0.936mV$, $t(574) = 13.8135$, $p < .0001$, $d = .834$).

5.3.2 Time-course or beta-related changes in MEP latency

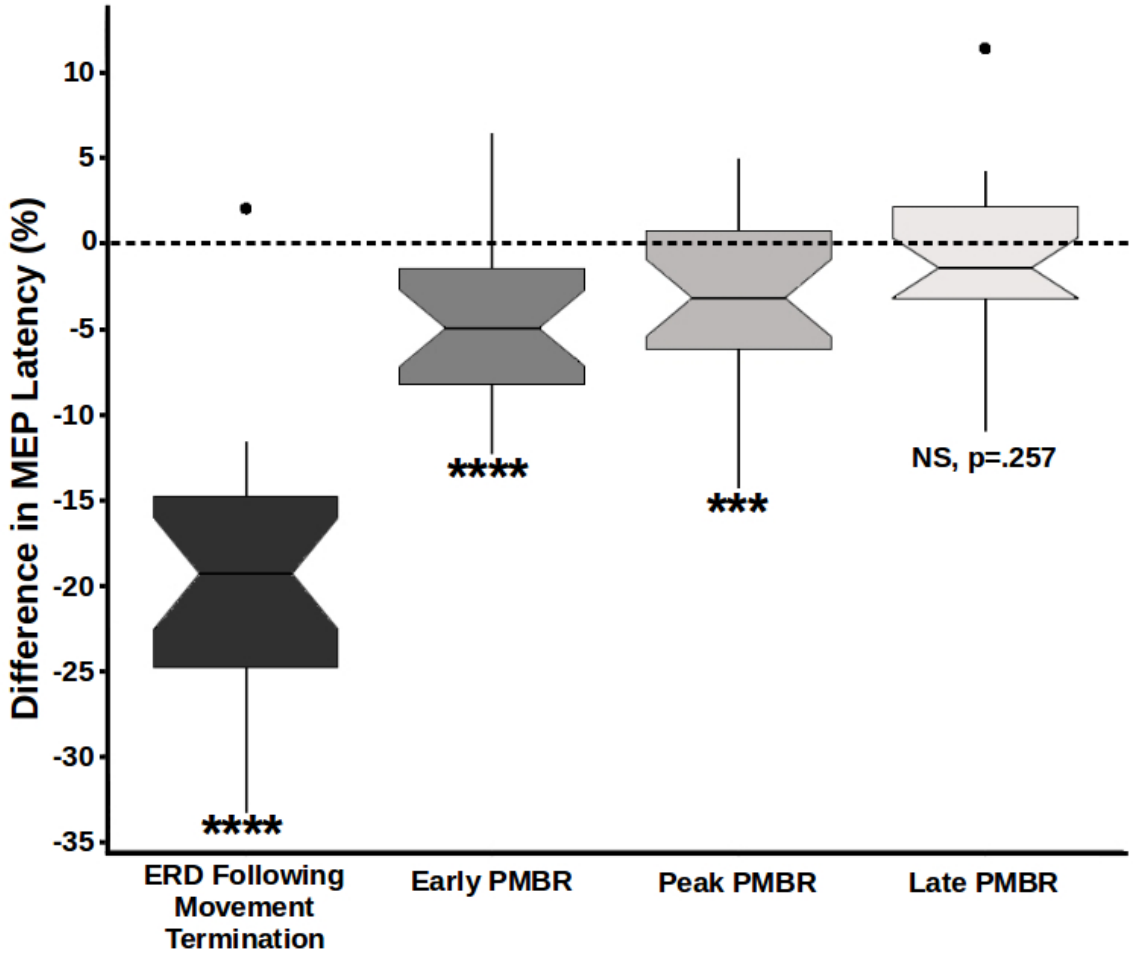

Figure 5.6: Difference in the latency of MEPs induced during the 4 different time-points and the active rest period. Zero on the y-axis represents the mean latency of MEPs collected during the active rest period. The latency of MEPs were normalised as a percentage of this baseline. ****, p<.0001, ***, p<.001.

Figure 5.6 shows the normalised group average of the onset latency of MEPs induced during the four beta time-points. Zero on the y-axis represents the mean latency of MEPs collected during the active rest period; therefore a negative value reflects an earlier MEP than at rest. There was a significant main effect of time-point on the onset latency of the collected MEPs ($F(4) = 64.518$, $p < .0001$, $\eta_p^2 = .101$).

The mean onset latency of MEPs collected during the ERD period ($MD = -18.01$, $SD = 36.89$) was significantly shorter than the latency of MEPs collected at rest ($t(574) = -12.278$, $p < .0001$, $d = -.674$). The same is true of MEPs collected during the early ($MD = -3.51$, $SD = 20.18$; $t(574) = -5.222$, $p < .0001$, $d = -.25$) and the peak PMBR periods ($MD = -2.25$, $SD = 20.2$; $t(574) = -3.727$, $p < .001$, $d = -.179$). In contrast, MEPs collected during the late PMBR period ($MD = +0.14$, $SD = 15.73$) actually had a longer mean latency than those collected at rest, though the difference

was not significant ($t(574) = -1.135$, $p = .257$, $d = .049$).

The onset latency of MEPs collected during the ERD period occurred significantly early than MEPs induced during any of the three PMBR time-points: ERD vs early PMBR ($t(574) = -8.258$, $p < .0001$, $d = -.488$), ERD vs peak PMBR ($t(574) = -8.875$, $p < .0001$, $d = -.53$), ERD vs late PMBR ($t(574) = -11.068$, $p < .0001$, $d = -.64$).

Contrasts between the three PMBR time-points found that MEPs collected during both the early ($t(574) = -3.34$, $p < .001$, $d = -.202$) and the peak PMBR ($t(574) = -2.2001$, $p = 0.028$, $d = -.132$) time-points had significantly shorter onset latencies than those collected during the later PMBR period. There was however, no significant difference in the onset latencies of MEPs collected during early and peak PMBR time periods ($t(574) = -1.026$, $p = .305$, $d = -.062$).

Overall, there was no significant relationship between the onset latency and the amplitude of an MEP collected ($r = -.02$, $N = 2875$, $p = .915$).

5.3.3 Summary of results

- An inverse relationship between motor cortical beta power and MEP amplitude was found. Induced MEP amplitude underwent significant facilitation during a period of beta suppression (ERD) while being significantly inhibited during the PMBR compared to rest (Figure 5.4).

- There was no significant difference in MEP amplitude between the three PMBR periods (early, peak and late), though the pattern of amplitude change matched that of the underlying beta modulation (Figure **??**). When beta power was at its highest (peak PMBR), MEP amplitude was at its lowest, lower than when beta power was at half its maximal amplitude(early PMBR) and when beta power had almost returned to baseline (late PMBR).

- The onset latencies of MEPs collected during the ERD phase of the movement as well as the early and peak PMBR phases were significantly shorter than those collected at rest (Figure 5.6). The onset latency of MEPs collected during the late PMBR period did not vary from rest. This pattern appears to be related to the underlying muscle activity rather than the coinciding change in cortical beta power. During a period of high EMG activity, MEP onset was short, then lengthened over time as the muscle activity returned to baseline.

- The amplitude of MEPs that were induced during the active rest period between trials was significantly greater than those induced during a period of totally passive rest, in which the participant was explicitly instructed to be as still as possible (Figure 5.5).

5.4 Discussion

5.4.1 Summary

In this chapter, we used TMS induced MEPs to investigate the relationship between motor cortical beta activity and cortical excitation. A simple isometric finger contraction task consistently led to a desynchronisation of the underlying beta power during the execution of the movement followed by a PMBR after the cessation of the movement.

As predicted, MEPs collected during the ERD period were significantly larger in amplitude than those collected at rest, while, MEPs collected during the PMBR period showed a significant reduction in amplitude. These findings suggest that there is an inverse relationship between motor cortical beta power and cortical excitability and that PMBR does reflect a period of cortical inhibition. Interestingly, there was also a significant effect of time-point on MEP onset latency, with the latency shortest immediately following the movement, then lengthening over time until returning to baseline. There also seems to be a contextual effect during the passive rest period that alters motor cortical excitability, or alternatively, increases cortical excitability during the motor task.

5.4.2 Beta-related changes in cortical excitability

Prior to the work described in this chapter, previous research has mostly relied upon indirect measures to infer the relationship between motor-related changes in cortical beta power and cortical excitability. These studies have either correlated MEP amplitudes to ongoing spontaneous beta power in the absence of any movement (Lepage et al., 2008; Mäki & Ilmoniemi, 2010), or investigated the time-course of MEP amplitudes following the cessation of a movement without concurrent EEG to measure changes in the underlying beta power (Chen et al., 1998; Coxon et al., 2006; Leocani et al., 2000). However, the above studies all concluded that there is appears to be an inverse relationship between motor cortical beta power and MEP amplitude.

To investigate this inverse relationship, we used EEG to first determine the latency of each individual's peak ERD and PMBR, before then using TMS to collect MEPs at each time-point. We found that there was a significant effect of time-point on MEP amplitude and that, as predicted, MEP amplitude was significantly increased during a period of beta ERD. This finding is supported by the work of Takemi et al. (2013) who demonstrated that

MEPs collected during a beta ERD induced by a motor imagery task, were significantly greater in amplitude than at baseline. We also found that the amplitude of MEPs collected during each of the three PMBR periods was significantly smaller than the baseline. This finding agrees with previous studies of spontaneous beta power (Lepage et al., 2008; Mäki & Ilmoniemi, 2010) and suggests that PMBR does indeed reflect an inhibition of the motor system (Cassim et al., 2001; Gilbertson et al., 2005; Koelewijn et al., 2008; Pastötter et al., 2008; Pfurtscheller et al., 1996; Salmelin et al., 1995b).

By selecting three different time-points based on the peak of the PMBR (early, peak and late) we hoped to show that the relationship between beta power and MEP amplitude persists throughout the time-course of the PMBR. That is to say, the amplitude of MEPs collected during the peak of the PMBR would be smaller than those collected at the half-maxima of the peak (early PMBR). Also, that the amplitude of MEPs collected during the late PMBR period would be closest to the baseline amplitude and therefore greater in amplitude than either peak or early PMBR induced MEPs. We found that this did indeed occur but the difference between each PMBR period was non-significant.

This non-significant result is likely due to inter-trial variability in the PMBR. This is a difficult factor to control for as the amplitude and latency of the peak PMBR can vary with movement properties (Stančák et al., 1997). Therefore, it is likely that this slight variation exists between each trial. This may, however, potentially be avoided in the future by using a BCI-design EEG or MEG study (Takemi et al., 2013) that can analyse the PMBR online and trigger the TMS to stimulate once a predefined peak is met. The NeuroPrax amplifier we use does not allow for online analysis; therefore, the entire study had to be performed in two stages with EEG data collected first so that it could then be analysed offline to trigger TMS. However, the poor signal-to-noise ratio of a single EEG or MEG trial may require many trials being recorded before a BCI system could recognise the onset and offset of PMBR. The ideal study, therefore, would employ a BCI with ECoG measures of cortical beta.

PMBR and cortical beta power, in general, is thought to be driven by GABAergic interneurons (Gaetz et al., 2011; Hall et al., 2011; Jensen et al., 2005). Pharmacological interventions have consistently shown that the enhancement of GABAergic function can result in a reduction in MEP amplitude (Boroojerdi et al., 2001; Heidegger et al., 2010; Kimiskidis et al., 2006; Di Lazzaro et al., 2000; Schönle et al., 1989; Ziemann et al.,

2015). Therefore, our finding of significantly reduced MEP amplitude during the PMBR supports the theory that PMBR reflects an increase in GABAergic inhibition.

5.4.3 Time-course or beta-related changes in MEP latency

There was a significant effect of beta time-point on the onset latency of an MEP. As predicted, the onset latency of an MEP, collected during a period of beta ERD, was significantly shorter than baseline. This finding is in line with previous studies that have suggested onset latency is shortest when closer in time to the execution of a movement (Nomura et al., 2001; Starr et al., 1988). The same was also true during early and peak periods of the PMBR, though both were significantly longer than the onset latency of MEPs collected during the ERD. The only time-point at which the onset latency of MEPs did not differ from baseline was the late PMBR period. This may be indicative that the change in onset latency is due to the length of time between movement offset and MEP collection.

There was no relationship between MEP amplitude and onset latency which may also be indicative that the change in onset latency is not due to underlying beta power but to the time between response and stimulation. If both MEP amplitude and onset latency are to be thought of as measures of cortical excitability, there should be a relationship between the two measures. During high cortical excitability, MEP amplitude should be high, and onset latency should be short; while during a period of cortical inhibition, there should be a lengthening of the onset latency and a reduction in MEP amplitude compared to baseline levels. We observed this pattern in the amplitude of the induced MEPs, but there was no such pattern in the onset latencies. Instead, onset latency seemed to lengthen linearly with time.

The onset latency of an MEP reflects the conduction time between the stimulation site and the muscle of interest. This conduction time is affected by a number of factors including the conduction velocity of corticospinal projections, the temporal summation of descending volleys to the spinal motoneuron, and the conduction time along alpha neurons (Bestmann & Krakauer, 2015; Farzan, 2014). These factors can be used to subdivide MEP onset latency into central (cortex to spine) and peripheral (spinal nerves to muscle) motor conduction time (Kobayashi & Pascual-Leone, 2003; Rossini et al., 2015). During and immediately following the voluntary contraction of a muscle, spinal motoneurons are closer to their firing threshold, and discharge can be generated by an

earlier descending volley (Rossini et al., 2015). As it takes time for spinal motoneurons to return to their baseline level of activity, this may explain why there is a linear increase in the onset latency of MEPs following movement termination.

5.4.4 Context-dependent change in cortical excitability

The finding that there was a significant increase in MEP amplitude between the passive rest period and the active rest period may be indicative of a general increase in baseline activity within the motor cortex. As the participant becomes aware that they are part of a motor task, they realise they are expected to make a finger movement during each trial. This contextual knowledge may cause a preparatory increase in motor cortical excitability resulting in a negative shift in the baseline beta level during the inter-trial (*'active'*) rest period compared to during the passive rest period before the task.

However, I would argue that there is a different type of contextual effect causing this difference. Each participant was explicitly instructed before the passive rest condition that the stimulation session would last longer than four minutes (250 seconds) and that they were required to be as still as possible for the duration of the session. This information may have been enough to exert top-down control of motor cortical excitation, actively inhibiting the motor cortex to prevent any movement.

In future studies, the distinction between these two theories should be investigated, as the vast majority of EEG and MEG studies that investigate motor-related changes in cortical beta power use some form of trial-by-trial baseline. If the mere context of being involved in a motor task is enough to alter this baseline from a true resting level, then researchers must take this into account when designing their studies.

The theory behind using a RMT to investigate changes in cortical excitability should also be scrutinised. Often researchers instruct their participants to remain as still as possible while their RMT is ascertained. If this instruction is enough to cause an inhibition of the motor cortex then the RMT is no longer a measure of the motor threshold at rest, rather it is a measure of an inhibited motor system. This again changes our interpretation of baseline motor activity.

I investigate the potential effect of contextual knowledge on underlying beta power further in Chapter 6.

5.4.5 Conclusion

I have demonstrated, for the first time in this chapter, that beta activity within the motor cortex has an inverse relationship with cortical excitability. During periods of beta desynchronisation, cortical excitability increases, and the amplitudes of generated MEPs are significantly greater than at baseline. While, during PMBR the motor cortex undergoes a process of cortical inhibition, as evidenced by the significant reduction in induced MEP amplitudes. The use of a BCI system that can measure motor cortical beta power and trigger stimulation at the peak of a PMBR may allow for a more precise and direct measure of this phenomenon.

While MEP amplitude is modulated by movement-related changes in cortical beta power, the onset latency appears to reflect a different neural process. I concluded that after the cessation of a muscle response there is a brief period of enhanced spinal motoneuron excitability. During this period the onset latency of an MEP is significantly shorter than at baseline.

Changes in cortical excitability are not limited to the movement trial period, as there appears to be a significant decrease in cortical excitability when a participant is instructed to remain as still as possible. This finding underlines the importance of investigating the effect of contextual knowledge on cortical excitability and changes in motor cortical beta power.

Chapter 6

Experimental context modulates resting beta oscillatory activity

To know an object is to lead to it through a context which the world provides.

– William James (1842-1910)

6.1 Introduction

The original concept behind the work described in this chapter was born of two findings from previous chapters:

1. The baseline, used to investigate changes in beta activity throughout the time-course of a trial, varies between trials (Section 3.4.5).
2. The MEPs collected during a passive rest period were significantly lower in amplitude than those collected in the inter-trial rest period between movement trials (Section 5.4.4).

Both findings suggest that there is a significant difference in the absolute level of spontaneous beta activity during a motor task when compared to the non-trial rest period. It is possible that the inter-trial variance in beta power is a consequence of trial duration. Specifically, a short period may result in the onset of each new trial occurring during a period of elevated beta power, at the tail-end of the PMBR that forms part of the motor response of the previous trial. This raises important questions when considering the relationship between PMBR and cortical inhibition (Chapter 5). Specifically, while each trial begins during a period of incrementally increased 'absolute' beta power, participants were still able to perform the motor task, which suggests that relative beta power change may be more important than absolute beta power in the control of human movement.

The second finding, that cortical excitability is higher during a motor task than when passively at rest, is not unexpected given the evidence that beta is suppressed during motor performance (Formaggio et al., 2010; Leocani et al., 1997; Miller et al., 2010; Pfurtscheller & Berghold, 1989; Pfurtscheller & Lopes Da Silva, 1999) and that there is an inverse relationship between beta power and cortical excitability (Chen et al., 1998; Lepage et al., 2008; Mäki & Ilmoniemi, 2010; McAllister et al., 2013; Takemi et al., 2013). However, it is interesting to note that, while PMBR appears to reflect relative cortical inhibition following a motor response, the mean amplitude of MEPs collected during this period was still significantly greater than when the participant was completely passive. This finding suggests that the context of being in the middle of a motor task increases cortical excitability in the anticipation of an upcoming motor requirement (Section 5.4.4).

To investigate the role motor anticipation plays in the modulation of cortical beta activity, we designed a study that, through the use of on-screen prompts and researcher intervention, would alter the participant's anticipation of an upcoming motor requirement.

6.1.1 Background

Beta-band oscillations have been consistently linked with the resting and functional state of the motor cortex (Cheyne et al., 2006; Crone, 1998a; Engel & Fries, 2010; Gaetz et al., 2010; Heinrichs-Graham et al., 2018; Neuper & Pfurtscheller, 2001a; Pfurtscheller & Lopes Da Silva, 1999; Rossiter et al., 2014; Zhang et al., 2008). Absolute beta power of the resting cortex has been shown to vary with a person's age (Heinrichs-Graham & Wilson, 2016; Heinrichs-Graham et al., 2018; Rossiter et al., 2014), the time of day recordings were made (Cacot et al., 1995; Wilson et al., 2014a; Toth et al., 2007), and between healthy and disordered brain states (Brown, 2007; Jenkinson & Brown, 2011; Pollok et al., 2012). While the relative change in beta power during motor paradigms has been consistently linked with the recruitment and inhibition of motor networks.

Prior to and during the execution of a movement, there is an event-related desynchronisation (ERD) of motor cortical beta power (Cheyne et al., 2006; Engel & Fries, 2010; Gaetz et al., 2010; Neuper & Pfurtscheller, 2001a; Pfurtscheller & Lopes Da Silva, 1999; Zhang et al., 2008). This beta desynchronisation usually occurs approximately one second before the movement onset and persists until movement cessation (Erbil & Ungan, 2007; Pfurtscheller & Lopes Da Silva, 1999; Stancák & Pfurtscheller, 1995). This beta ERD not only coincides with movement preparation and

execution, it has also been observed during motor observation (Avanzini et al., 2012; Babiloni et al., 2002; Duann & Chiou, 2016; Press et al., 2011) and imagery (Duann & Chiou, 2016; McFarland, 2000; Miller et al., 2010; Pfurtscheller & Neuper, 1997; Yuan et al., 2010).

Previous studies have demonstrated that spontaneous beta power and beta ERD are linearly related. Rossiter and colleagues (2014) demonstrated that not only does absolute resting beta power increase from early to late adulthood, the relative magnitude of beta ERD does so as well (Rossiter et al., 2014). This finding was later corroborated by further MEG studies that found the motor cortices of elder adults exhibited much larger absolute beta power, as well as a significantly stronger ERD, than in younger adults (Heinrichs-Graham & Wilson, 2016; Heinrichs-Graham et al., 2018).

The same relationship between spontaneous beta power and the magnitude of beta ERD has been demonstrated by Wilson and colleagues (2014a), who investigated changes in beta amplitude in relation to circadian rhythm. They found that absolute beta power significantly increased from 8am to 8pm. They demonstrated that at times when absolute beta power was high, the relative suppression of beta power during movement-related ERD was significantly increased (Wilson et al., 2014a).

The magnitude of PMBR has also, indirectly, been shown to vary with the absolute power of spontaneous beta activity. Gaetz and colleagues (2010) demonstrated that absolute beta power linearly decreases with age, from young children to adulthood. In the same MEG study, they also found that the relative PMBR increases linearly with age (Gaetz et al., 2010). Further studies have demonstrated a similar negative relationship between resting beta power and relative PMBR magnitude between young and older adults. As resting beta power begins to increase with age the magnitude of PMBR drastically decreases from early to late-adulthood (Heinrichs-Graham et al., 2018; Labyt et al., 2003; Liu et al., 2017; Rossiter et al., 2014).

There have been several studies that have investigated movement-related changes in oscillatory activity; modulating movement factors, such as the degree of certainty about the upcoming movement or contrasting timed-responses with self-initiated responses. There have also been a number of studies now, that have investigated changes in absolute resting power with age or throughout the day and linking absolute power with these movement-related changes in oscillatory activity. However, to the best of my

knowledge, no study to date has reported on the change in beta power between the intra and extra experimental rest periods. In summary, determining the effect of being involved in a motor study on resting, spontaneous beta power.

As we previously demonstrated in Chapter 3, the amount of information the participant receives prior to the 'GO' cue modulates the magnitude of beta desynchronisation. The more salient the information the participant is given, the greater their certainty about the upcoming movement requirement and, subsequently, the greater the preparatory-phase beta ERD. This finding, supported by those of previous studies (Grent-'t Jong et al., 2014; Kaiser et al., 2001; Tzagarakis et al., 2010), suggests that the anticipation of an upcoming movement modulates motor cortical beta activity.

Imagining yourself performing a movement is also enough to cause a desynchronisation of ongoing motor cortical beta activity (Duann & Chiou, 2016; McFarland, 2000; Miller et al., 2010; Pfurtscheller & Neuper, 1997; Yuan et al., 2010). Therefore, it would appear that, when a participant is given enough information about an upcoming motor requirement for them to imagine or prepare the necessary action, there is a decrease in ongoing spontaneous beta activity.

This may explain why in our previous study Section 5.4.4 there was a significant increase in cortical excitability during a motor task, even during periods of relative inhibition, compared to when the participant was passively at rest. If motor cortical beta power is a correlate of cortical inhibition, then beta power would be modulated as a consequence of the participant's awareness of the motoric nature of the study.

While a relatively simple premise, the implications of this subject are far reaching. The majority of the literature on motor oscillatory modulation to date assumes that the inter-trial rest period is a true reflection of 'resting state'. Therefore, all comparisons, interpretations and conclusions are drawn from this assumption. Moreover, there is good reason to suggest that these findings are not limited to the oscillatory state of the motor system, but would also apply to many (if not all) neuronal network observations across the brain.

Here, to test the influence of experimental context on a participant's motor oscillatory state, we developed a study in which the expectation of the experimental tasks was manipulated out the outset. Participants commenced the experiment expecting that they would perform either a visual task, with no motor component, or a purely motor task.

Following an initial visual 'distractor' task, the purely motoric nature of the main experiment was revealed.

6.1.2 Aims and research objectives

The aim of this study was to:

1. Determine the effect of contextual cues on the time-frequency profile of beta activity.
2. Investigate the relationship between motor anticipation and absolute beta power.
3. Investigate the relationship between the absolute power of spontaneous beta activity and the relative change in power during movement-related modulation.

We hypothesised that the information the participant receives throughout the experiment will alter their anticipation of an upcoming motor requirement and that this change in motor anticipation would be reflected in resting beta power recorded from M1.

Based on our previous finding that the more certain a participant is during motor preparation, the greater the suppression of M1 beta activity; we predicted that an increase in motor anticipation would result in a reduction in M1 beta power. More precisely:

1. During rest periods when expected motor anticipation is high, resting M1 beta power will be low.
2. During rest periods when expected motor anticipation is low, resting M1 beta power will be high.

Furthermore, based on the findings of previous studies that there is a relationship between spontaneous beta power and motor-related changes in beta power (Gaetz et al., 2010; Heinrichs-Graham et al., 2016; Rossiter et al., 2014; Wilson et al., 2014a), I further hypothesised that:

1. The relative magnitude of beta ERD will be significantly greater during motor trials with high spontaneous beta power at rest compared to trials with low resting beta power.
2. In contrast, the relative magnitude of the PMBR following movement termination will be significantly reduced when absolute beta power is high at trial onset compared to when absolute beta power is low.

6.2 Methodology

Fifty-five right-handed participants were recruited in total (31 male), with a mean age of 23 (range 18 – 69) years. Informed consent was obtained, and all studies were approved by the local ethics committee, in accordance with the ethical standards set by the 1964 Declaration of Helsinki. All participants passed a TMS safety screening, were free of medication and did not have any personal or family history of neurological or psychiatric illness. Seven participants were excluded from complete analysis, due to rejection of $> 20\%$ of trials due to signal-to-noise or incomplete behavioural performance.

6.2.1 Data acquisition

The left M1 was functionally localised using the TMS procedure outlined in Section 2.3.2. This allowed us to ascertain the participant's primary motor cortex hand area (M1h) and their resting motor threshold (RMT). RMT was defined as the lowest stimulator intensity required to consistently induce MEPs in the right FDI with a peak-to-peak amplitude greater than $50\mu V$ in 8 out of 10 trials. This scalp location was also used to guide EEG electrode placement.

Single-pulse TMS was delivered using the Magstim 200[2] (Magstim, Whitland, UK), equipped with a standard 70mm, figure-of-eight coil. The optimal coil position and orientation for inducing MEPs in the right FDI was marked in pen on the participant's scalp to ensure exact coil placement throughout the study.

All EEG data were recorded using the DC-EEG feedback system (Section 2.5.1). Ag/AgCl electrodes were arranged in our standard 7-electrode montage with the localised M1h at its centre (Section 2.5.2). EEG was referenced online to the ipsilateral mastoid and sampled at a rate of $2048Hz$ with impedance for all channels maintained below $3k\Omega$. EEG signals were bandpass filtered (2–$100Hz$) and notch-filtered (48.5–$51.5Hz$) to avoid power line contamination (Section 2.5.3).

Surface electromyogram was recorded from both the left and right FDI muscles using the Bagnoli 2-channel EMG-system (DelSys Inc., Boston, USA). EMG signals were amplified 10,000 times and sampled at a rate of $2048Hz$ to align with sampled EEG data. Impedance was kept below $10k\Omega$, and all EMG signals were bandpass (20–$450Hz$) and notch-filtered (48.5–$51.5Hz$) using the same window-synced FIR filter applied to the EEG signal.

EMG was recorded and used to determine the time-point of movement onset/offset. Each index finger movement was accompanied by an increase in EMG activity recorded from the FDI muscle. The onset and offset of this increased muscle activity was calculated to accurately assess the latency of the accompanying beta ERD and PMBR.

The Power 1401-3 USB data acquisition interface along with the Spike2 data acquisition package (Cambridge Electronic Design, UK) was used to store EMG and force sensor output. The beginning and end of each trial were recorded via digital markers generated by MATLAB sent through the Arduino Uno BNC interface.

6.2.2 Study design and procedure

Participant instructions

Participants were informed that they had been randomly allocated to either a visual or motor task group and that, after the TMS localiser procedure had been performed, they would complete either a visual or motor task lasting ~ 55 minutes, while EEG was recorded. Participants were informed that the researcher did not know which experimental group they had been assigned and that both they and the researcher would discover the assignment on commencement of the first task.

Resting state protocol

Following M1h localisation, the EEG montage and EMG electrodes were put in place and the participant was seated 90cm in front of a 21-inch, high-definition monitor. The initial TMS stimulation of M1h and the coincident muscle twitch represented a potential cue for the participant's involvement in the motor task group. Participants were instructed to relax while an initial two-minute resting EEG recording was performed (Figure 6.1B).

Following this initial rest measure, the participant was informed that they were a member of the visual task group. Participants then performed a five-minute visual distractor 'practice' task, described in detail below. A second two-minute resting EEG was recorded to determine resting state oscillatory activity in the absence of an expected motor task (Figure 6.1B).

At this point, participants were informed of the true nature of the experimental task, as participation in a motor study (Section 6.2.4), which was then explained to the participant, and the force sensor was placed beneath their right index finger. Following ten practice trials of the motor task, a third recording of resting EEG was completed. This measure

was used to further determine the impact of task awareness on motor cortical oscillations (Figure 6.1B).

Behavioural Protocol

All participants then went on to perform a further four blocks of the behavioural task. Each block contained 40 trials, lasting 6m 40s. After each experimental block, a two-minute resting EEG recording was made (Figure 6.1B). These rest periods were applied to determine oscillatory fluctuation following each experimental block.

Following the last experimental block and a subsequent two-minute resting oscillatory measure, a five-minute visual distractor task, identical to the 'practice' visual task described above (and in Section 6.2.3) was completed. A final two-minute resting EEG measure was obtained for comparison with earlier resting state measures.

6.2.3 Visual distractor task

Dots were either blue (90%), or red (10%). Participants were instructed to silently/non-verbally count the number of red dot during the task, then report the total at the end of the experiment.

In total, 600 dots were presented over the course of a five-minute block (540 blue, 60 red). Dots had a diameter of $.5°$ visual angle (VA) and appeared on screen for 500ms (Figure 6.1A).

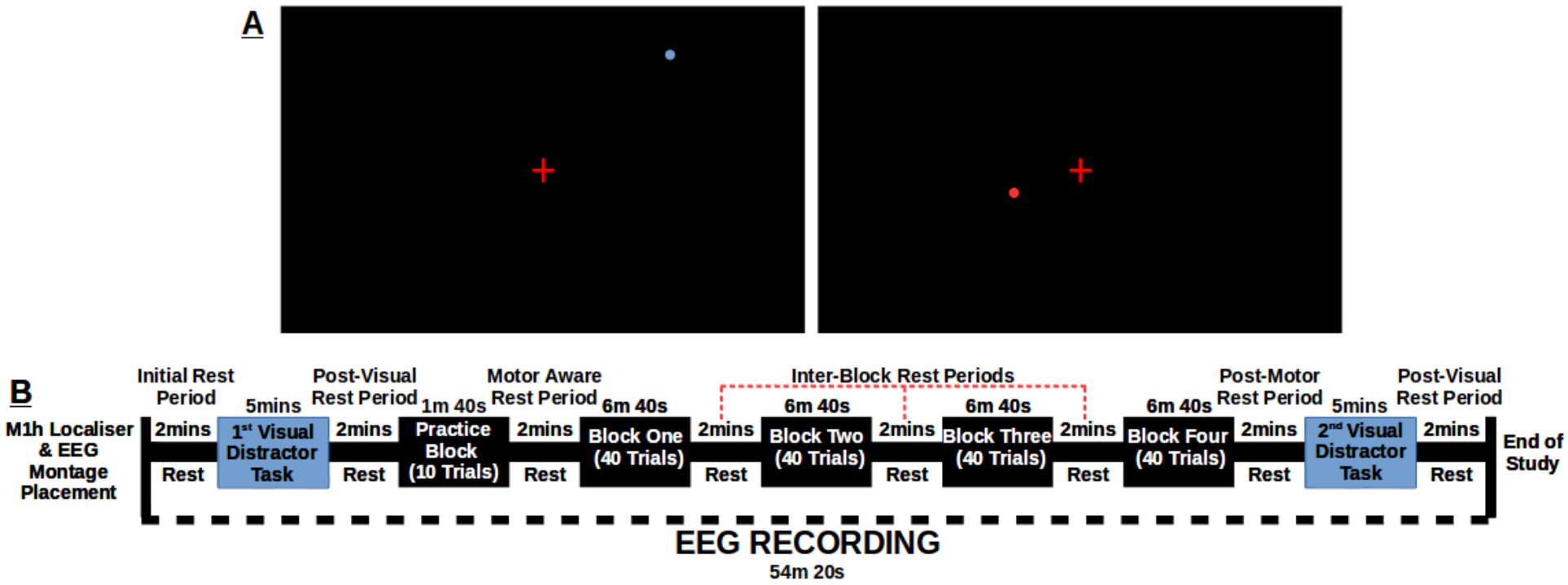

Figure 6.1: Visual distractor task and study design. **A.** The visual distractor task. Participants fixated on the centre of the screen while 600 dots were pseudo-randomly presented on screen. Of the 600 dots, 540 were blue and were to be ignored by the participant, the other 60 were red and were to be silently counted. Each dot had a diameter of $.5°$ VA and appeared on screen for 500ms. **B.** A schematic of the study design. Following the M1h localiser and EEG setup, there was a 2-min resting EEG recording. The first 5-min visual distractor task was then performed before a second 2-min resting EEG recording. The participant was then informed they were to be involved in a motor task and practised that task for ten trials. Another resting recording was made. Following this, the participant performed four more blocks of the motor task, each consisted 40 trials and had a duration of 6m 40s. After each experimental block, a further 2-min resting EEG recording was made. Finally, the second visual distractor task was performed, followed by a final resting EEG recording.

6.2.4 Motor task design

This study replicated the previous simple reaction time task found in Chapter 5. Participants were instructed to maintain central fixation, while resting their right index finger on a Mini S-Beam force sensor (Applied Measurements Ltd., UK). They were also instructed to keep both hands flat and maintain contact with the force sensor throughout (Figure 6.2).

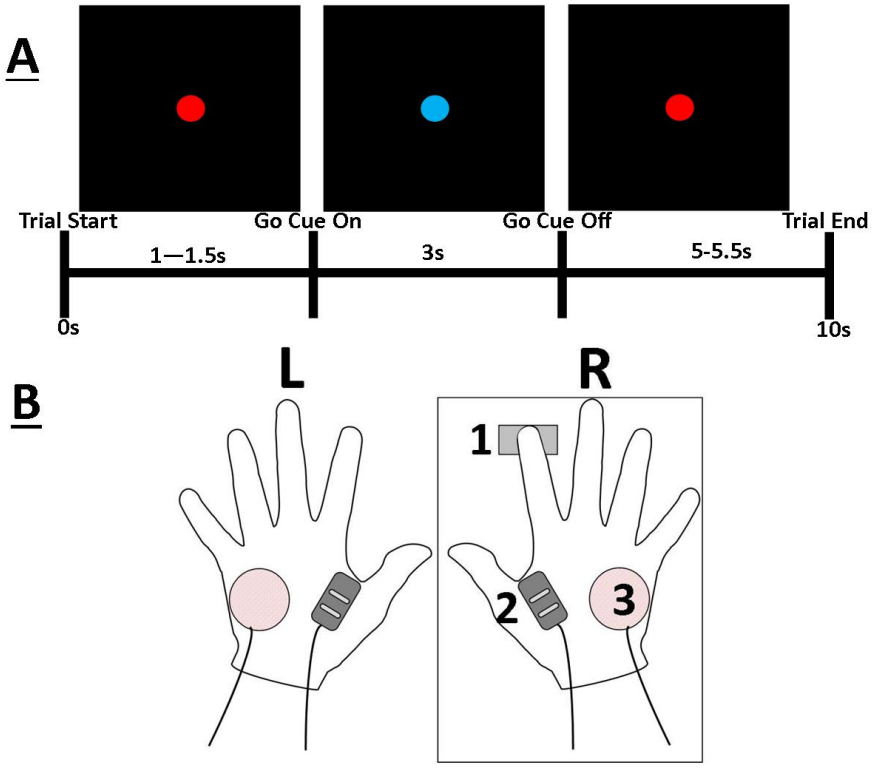

Figure 6.2: Motor task and recording apparatus. **A.** The 10s trial layout used throughout the motor response task. Subjects fixated on a red circle in the true centre of the screen. After a delay randomised between 1 and 1.5s the circle turned blue. This was the participant's cue to respond. **B.** When cued the participant responded by rapidly pressing the force sensor with their right index finger (**1**). EMG recordings were recorded using single differential surface electrodes over both left and right FDI muscles (**2**), referenced to the back of each hand (**3**).

Each trial was 10s in duration. A red circle was presented in the centre of the screen for 1-1.5s, randomised to remove anticipation of the 'GO cue' and early responses. After this initial wait period, the central fixation circle changed from red to blue. Subjects were instructed that this was the 'GO cue', to which they should press the force sensor as quickly and as sharply as possible. This isometric finger flexion was practised before the main task so that participants learned to simply press down and then relax their finger, as opposed to pressing down and then lifting their finger from the sensor.

Following the response, participants were required to wait for the central fixation circle to

return to red and await the next 'GO cue'. The typical interval between the 'GO cue' and the termination of the response was 1000ms, allowing 7-5–8s to measure the PMBR and for the return to baseline. This provided the minimum six-second post-movement interval indicated as a requirement in our previous study (Section 3.4.5).

Consistent with Chapter 5, force sensor and EMG data were used to determine the time-point of response onset and completion. The maximal force interval was defined as the response, used to calculate response time (RT), consistent with the maximal accumulation of force in the 'active' downwards press period. The decrease in force reflect the passive relaxation of the finger. These periods are reflected in the increase and decrease in EMG activity. The point at which EMG returned to baseline was defined as the termination of the response.

Trials where no response occurred, where RT fell outside the acceptable range (median RT $\pm$ 2*MAD) or with poor EEG signal-to-noise ratio were excluded from the analysis. Any participant, where more than 20% of trials were removed would be excluded from the analysis. No participant exceed this threshold.

6.2.5 EEG analysis

Time-frequency analysis was performed using a Morlet wavelet transformation (Bertrand & Pantev, 1994; Tallon-Baudry & Bertrand, 1999). Spectral power in the beta (13–$30Hz$) band was analysed, based on the mean amplitude of the band. Analysis of resting beta power, during an initial two-minute recording, was used to confirm the central electrode as the optimal location for further analysis, which was used for all subsequent analyses.

Epochs for analysis were defined using digital triggers, produced by the Arduino-EEG interface. For the analysis of changes in absolute beta power, triggers were sent at the onset and end of each of the eight two-minute rest periods. Relative beta power was defined as the change in beta power within a trial, therefore triggers were sent at trial onset and at the 'GO' cue onset for each trial.

For analysis of the larger, two-minute epochs a sliding-window approach was used averaging beta power in 500ms windows. Windows in which beta power exceeded a threshold of mean $\pm$ 2*SD were removed from the overall average. This approach was taken to ensure that particularly noisy events, such as the participant moving their head during a rest period, were removed from the spectral analysis.

6.2.6 Experimental design and statistical analyses

Differences in RTs, beta ERD magnitude and PMBR magnitude between trials with high absolute beta power and trials with low absolute power were analysed using analyses of variance (ANOVAs) and paired t-tests. Seven participants were removed from the analysis due to poor signal-to-noise in the EEG recording or as a result of hardware failure. This meant that the analyses were performed on 48 participants in total.

To investigate the effect of contextual cues on changes in the absolute beta power, two-minute baseline measures of beta power were taken at eight different times throughout the course of the experiment for each participant. These eight resting periods (Figure 6.1B) were:

- 1. **Initial Rest Period** - The initial two-minute baseline period recorded after the localisation of M1h, which we predicted would potentially cue the participant to believe they were to be involved in the motor task group.
- 2. **First Post-Visual Rest Period** The two-minute period immediately after the visual distractor task. During which, we predicted that the participant would believe that they were part of the visual cohort and would no longer be expecting a motor task.
- 3. **Motor Aware Rest Period** - The baseline period after the participant had been informed they were to be performing a motor task and had executed the ten practice trials. At this point, the participant is fully aware of the motor task they are to perform and the number of blocks and trials they are yet to complete.
- 4–6. **Inter-Block Rest Periods** - The three two-minute rest periods between each of the four motor response blocks.
- 7. **The Post-Motor Rest Period** The two-minute rest period recorded after the fourth and final block of the motor task. At this point, the participant was told that the motor study was over and there would be no more motor-response trials.
- 8. **Second Post-Visual Rest Period** The final resting period was recorded after the second visual distractor task. This rest measure allowed a direct comparison to be made with the 1st post-visual rest period.

During the motor task, the dynamic interplay between spontaneous beta power and the movement-related modulation of beta power that occurs during beta ERD and PMBR was investigated. The resting beta power from a 500ms baseline period at trial onset was calculated for each trial to provide a measure of the absolute beta power within that trial. The percentage change in beta power that then occurred during beta ERD and PMBR was calculated to assess the relative change in beta power that occurred in each trial. This relative change in beta power was compared between trials with high absolute beta power at onset and trials with lower absolute beta power at trial onset.

6.3 Results

6.3.1 Behavioural results

Overall, there was no significant difference in response times when absolute beta power was high at trial onset ($M = 518.85ms$, $SD = 120.89ms$) than when absolute beta power was low at trial onset ($M = 512.44ms$, $SD = 107.5ms$; $t(48) = -.917$, $p = .364$). There was also no significant effects of sex (31 male, 24 female; $t(46) = .564$, $p = .576$) or age ($M = 23$ years, $Range = 18 - 69$ years; $r = .062$, $N = 48$, $p = .664$) of participants on response times, nor was there any effect of the time of day (morning or afternoon) the participant performed the task ($t(46) = .74$, $p = .463$) on response times.

There was also no significant correlation between the magnitude of the relative beta ERD that preceded the response with response times ($r = -.122$, $N = 48$, $p = .407$). No significant relationship existed between the speed of the response and the resulting PMBR either ($r = -.183$, $N = 48$, $p = .213$).

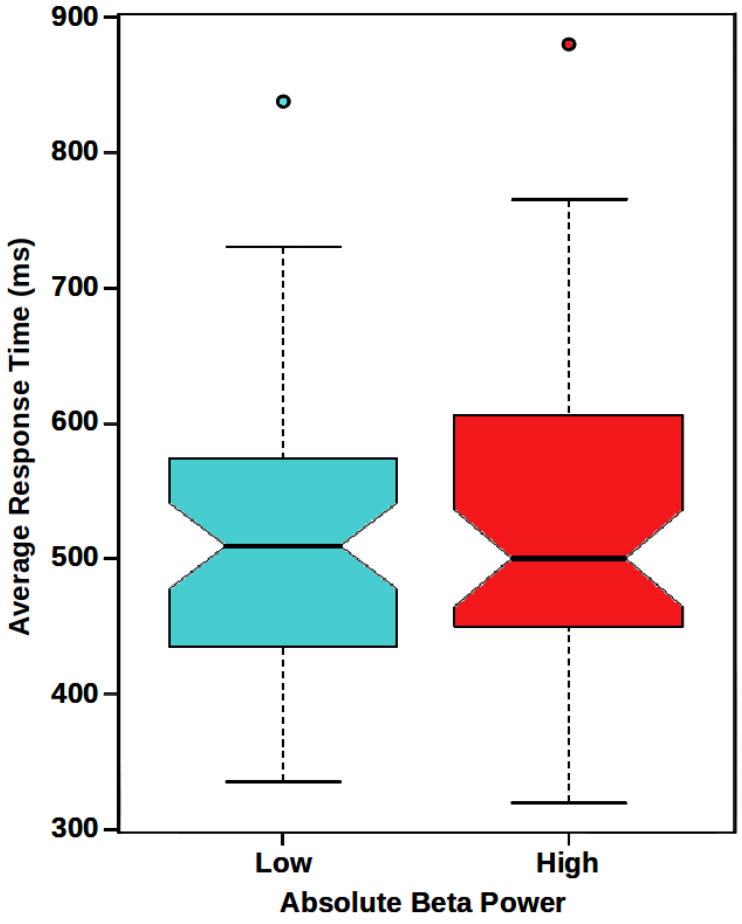

Figure 6.3: Box plot of the average response time across the four motor task blocks during high and low absolute beta power. There was no significant difference in response time between trials with high absolute beta power at onset and trials with low absolute beta power at onset ($p = .364$).

6.3.2 Contextual effects on the anticipation of motor involvement and resting beta power

Resting beta power was significantly reduced after the first visual distractor task ($M = .159\mu V^2$, $SD = .191\mu V^2$) compared to during the initial rest period ($M = .295\mu V^2$, $SD = .256\mu V^2$; $t(47) = 2.919$, $p = .005$).

Following the first visual distractor task, participants were informed of the motoric nature of the study. After a ten trial practice session resting beta power was significantly increased ($M = .319\mu V^2$, $SD = .233\mu V^2$; $t(47) = -3.528$, $p = .0009$) compared to the post-visual rest period, while there was no significant difference when compared with the initial rest period ($t(47) = -.518$, $p = .607$).

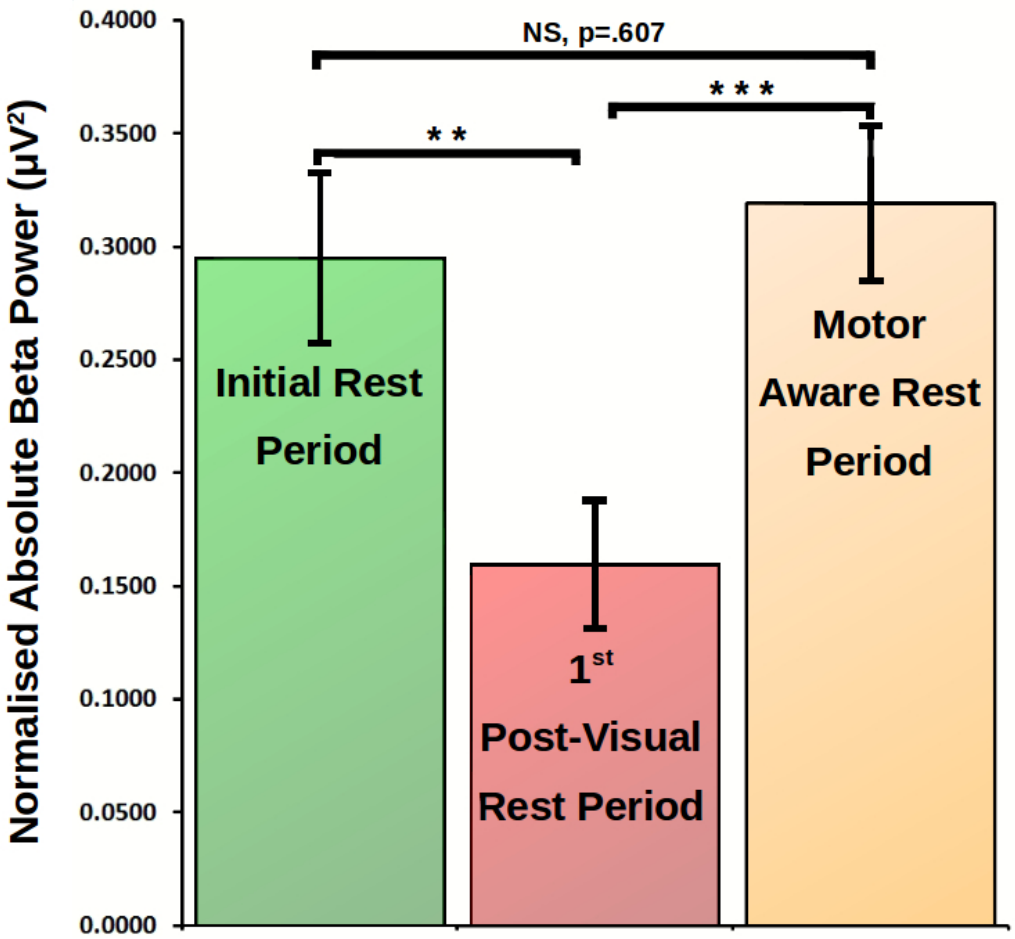

Figure 6.4: Resting beta power changes with motor awareness. The change in resting beta power from the initial rest period compared to the 1st post-visual rest period and the motor aware rest period. Error bars reflect SEM. ***, p<.001; **, p<.01.

During the motor task, there was no significant difference in resting beta power between blocks. Specifically, the first inter-block rest period ($M = .269\mu V^2$, $SD = .253\mu V^2$) did not differ significantly from the second inter-block rest period ($M = .217\mu V^2$, $SD = .183\mu V^2$; $t(47) = 1.365$, $p = .179$) or the third inter-block rest period ($M = .272\mu V^2$, $SD = .219\mu V^2$; $t(47) = -.078$, $p = .938$). and there was no significant difference in resting beta power between the second and third inter-block rest periods ($t(47) = -1.698$, $p = .096$).

Following completion of the motor task, resting beta power ($M = .074\mu V^2$, $SD = .168\mu V^2$) significantly decreased compared to any of the three inter-block rest periods (Figure 6.5). This significant decrease was observed when comparing absolute beta power between the post-motor rest period and the first inter-block rest period ($t(47) = 4.027$, $p = .0002$), the second inter-block rest period ($t(47) = 3.516$, $p = .001$) and the third inter-block rest period ($t(47) = 5.031$, $p =< .0001$).

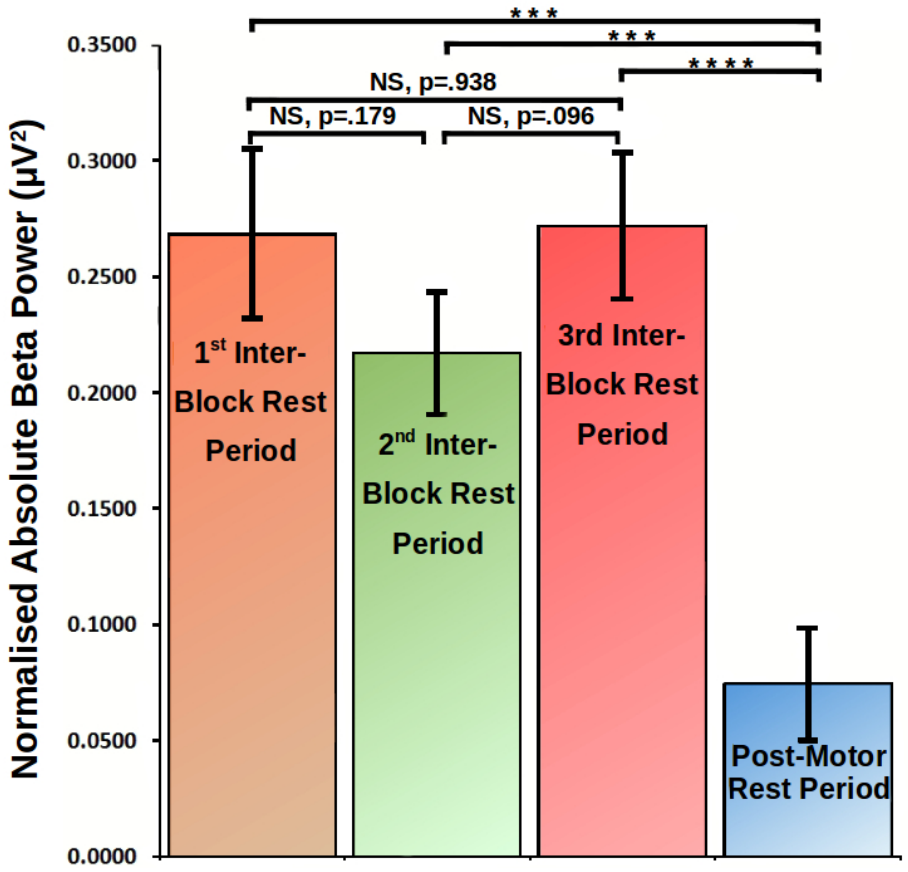

Figure 6.5: Resting beta power between blocks and following the motor task. There was no significant difference in resting beta power during any of the three inter-block rest periods. However, once the task was complete there was a significant decrease in beta power. Error bars reflect SEM. ****, p<.0001; ***, p<.001.

There was no significant difference in resting beta power during the first post-visual rest period ($M = .159\mu V^2$, $SD = .191\mu V^2$) and during the second post-visual rest period ($M = .17\mu V^2$, $SD = .157\mu V^2$; $t(47) = -.333$, $p = .741$). This lack of difference is likely due to the participant being in a similar anticipatory state after each distractor task (Figure 6.6).

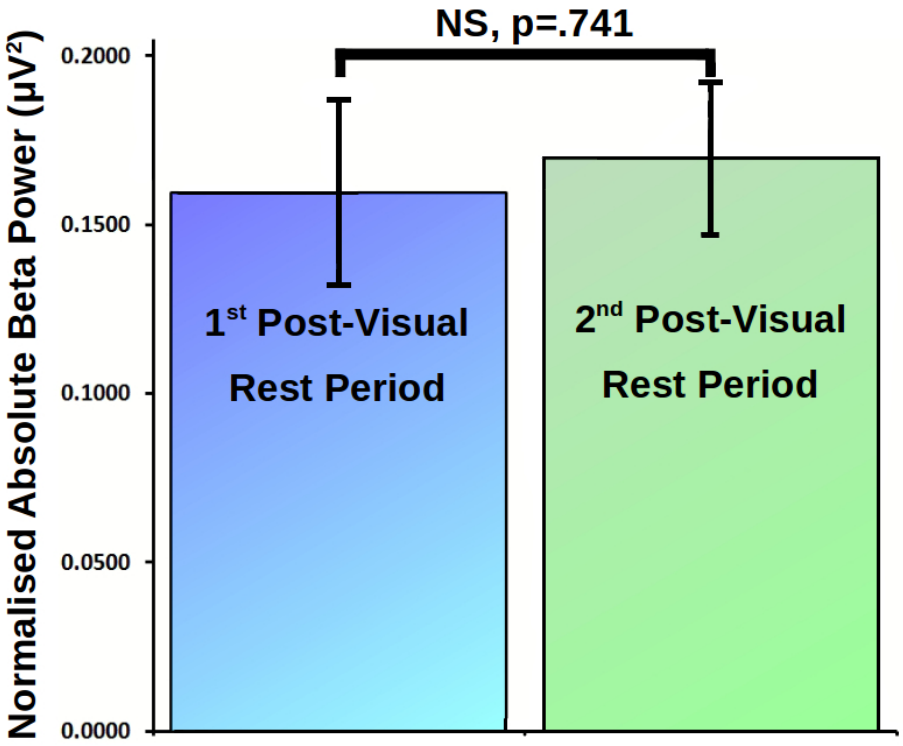

Figure 6.6: Resting beta power following the first and second visual distractor task. There was no significant difference in absolute beta power following either of the two visual distractor tasks.

Overall there was a significant effect of the time at which baselines were recorded and the mean resting beta power ($F(3,188) = 15.085,\ p < .0001$). Further analysis revealed that during a period of high motor anticipation, such as during the initial rest period ($M = .294\mu V^2,\ SD = .256\mu V^2$), resting beta power was significantly higher than during periods of low motor anticipation (Figure 6.7), such as, during the post-visual rest periods ($M = .165\mu V^2,\ SD = .14\mu V^2;\ t(47) = 3.118,\ p = .003$), or the post-motor rest period ($M = .074\mu V^2, SD = .168\mu V^2; t(47) = 4.873,\ p < .0001$).

There was no significant difference between the two periods of high motor anticipation, the initial rest period and the three inter-block rest periods during the motor task ($M = .269\mu V^2, SD = .131\mu V^2; t(47) = .578,\ p = .566$). However, like the initial rest period, beta power during the motor task was significantly greater than during both post-visual rest periods ($t(47) = 3.73,\ p = .0005$), and the post-motor rest period ($t(47) = 5.954,\ p < .0001$). Finally, there was also a significant reduction in resting beta power during the post-motor rest period compared to the two post-visual rest periods ($t(47) = -3.061,\ p = .004$).

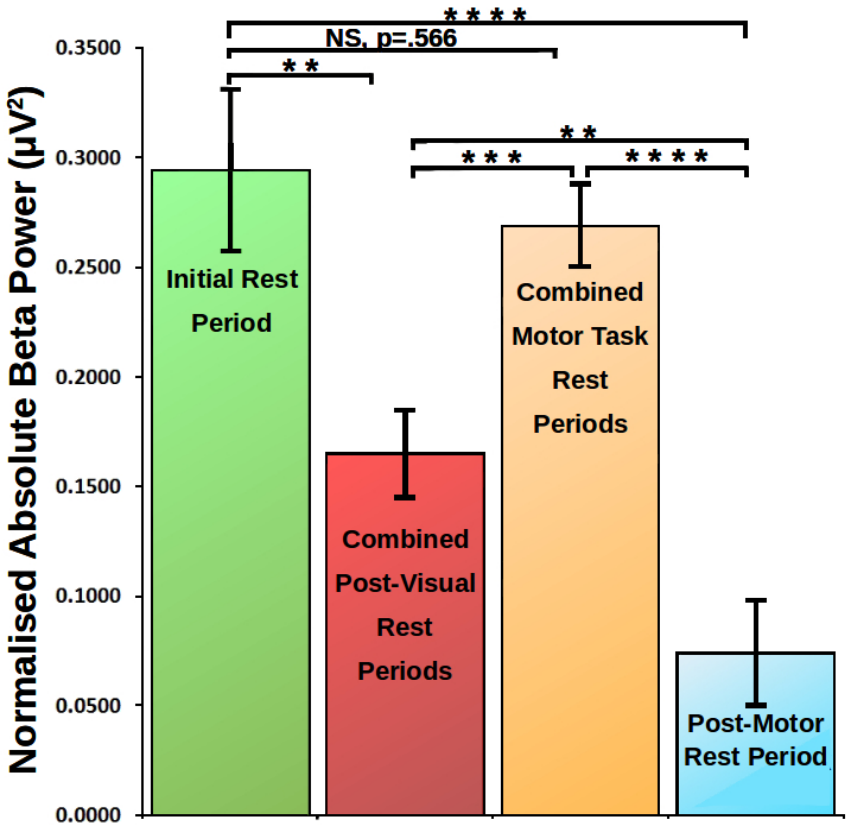

Figure 6.7: Change in resting beta power throughout the time-course of the study. During periods of high motor anticipation, such as, during the initial rest period and during the motor task, resting beta power was high. Whereas, during periods of low motor anticipation, such as, after each visual distractor task or once the motor task was complete, resting beta power was significantly lower. Error bars reflect the SEM. ****, p<.0001; ***, p<.001; **, p<.01.

6.3.3 Effect of absolute beta power on movement-related beta modulation

For each participant, beta-band power was computed relative to a 500ms baseline period, starting at trial onset. Due to the jitter in the trial design, this baseline period ended 600–1000ms prior to the 'GO' cue. For each trial, the beta ERD period was defined as a 500ms window, beginning 250ms before the motor response was made. The PMBR period was defined as a 500ms window beginning 1000ms after movement termination.

To investigate the dynamic interplay between the spontaneous beta power during the baseline period of each trial and the subsequent movement-related change in beta power, trials were divided into high and low absolute beta power groups for each individual. Trials were sorted on the basis of beta power amplitude during the 500ms baseline period, the high absolute beta power group was defined as the top 25% of trials and the low absolute beta power group was defined as the bottom 25% of trials.

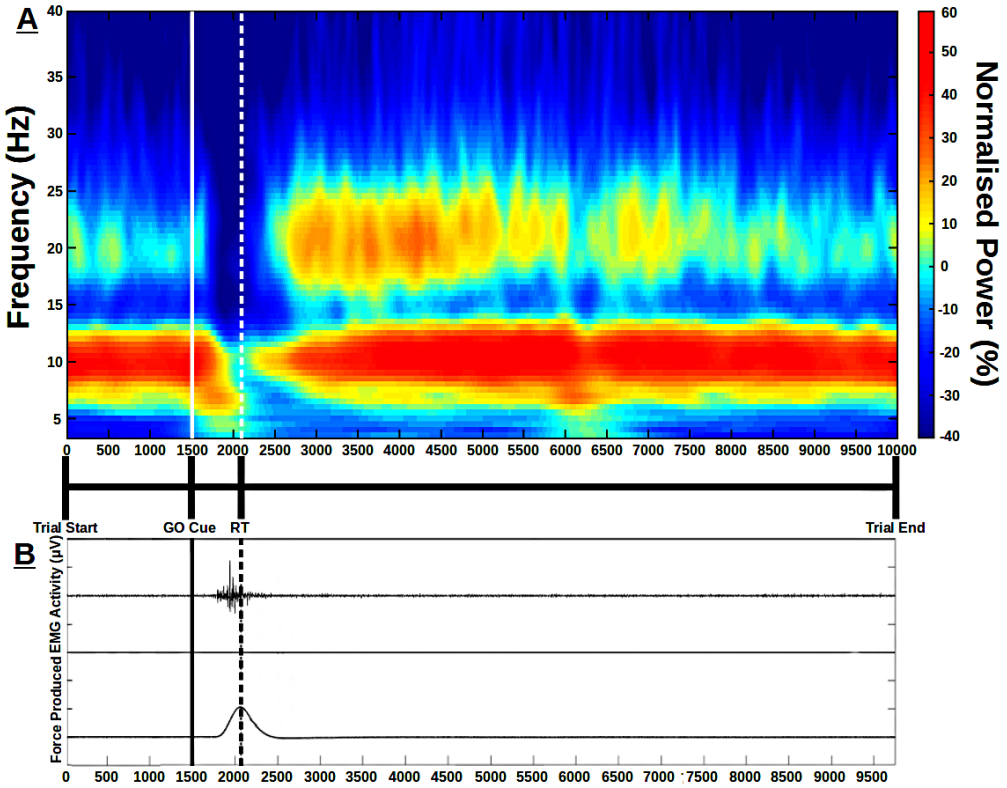

Figure 6.8: **A.** Averaged time-frequency power plot of relative oscillatory power change during a response trial. The central schematic shows the initial jittered wait period until the 'GO' cue at 1500ms. Following the 'GO' cue the mean response time was 509ms. An ERD of the underlying beta power began after the go cue and lasted until approx 500ms after the response was made. Following this, there was a significant, extended period of PMBR. **B.** Averaged force produced and EMG activity recorded from the right FDI during the motor response.

There was a strong correlation between the absolute beta power at trial onset and the absolute power at the peak of the ERD ($r = .803$, $N = 96$, $p < .0001$, two-tailed) and at the peak of PMBR ($r = .898$, $N = 96$, $p < .0001$, two-tailed). There was no significant difference in absolute power at the peak of beta ERD when trial onset power was high ($M = .736\mu V^2$, $SD = .612\mu V^2$) than when power at trial onset was low ($M = .708\mu V^2$, $SD = .62\mu V^2$; $t(47) = -1.124$, $p = .267$). There was also no significant difference in absolute PMBR power between trials with high beta power at onset ($M = 5.259\mu V^2$, $SD = 9.348\mu V^2$) and trials with low beta power at onset ($M = 4.914\mu V^2$, $SD = 8.534\mu V^2$; $t(47) = -1.748$, $p = .087$).

There was, however, an effect of absolute beta power at trial onset on the relative power change of the beta-band during movement-related modulation (Figure 6.9). The percentage change in beta amplitude during ERD was significantly greater when absolute beta power was high at trial onset ($M = -58.82\%$, $SD = 11.4\%$) than when absolute beta power was low at trial onset ($M = -38.34\%$, $SD = 13.4\%$; $t(47) = 14.847$, $p < .0001$). In contrast, the percentage change in beta amplitude during PMBR was significantly reduced when absolute beta power was high at trial onset ($M = 89.4\%$, $SD = 49.82\%$) than when absolute beta power was low at trial onset ($M = 207.2\%$, $SD = 148.41\%$; $t(47) = -7.221$, $p < .0001$).

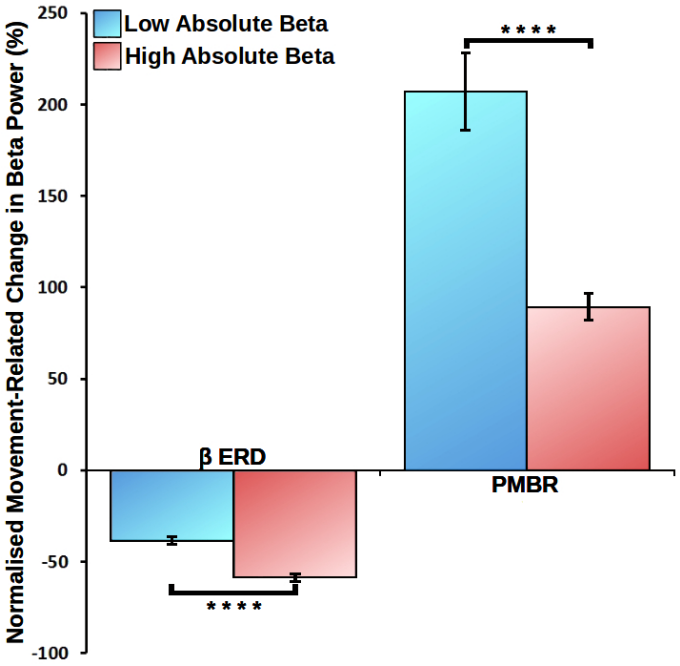

Figure 6.9: Comparison of relative changes in beta amplitude during high and low absolute beta power. Percentage change in beta ERD was significantly greater when absolute power was high at trial onset. In contrast, percentage change during PMBR was greater when absolute beta power was low at trial onset. Error bars reflect SEM. ****, p<.0001.

6.3.4 Inter-trial variability in baseline beta power

In contrast to our previous finding (Section 3.3.5), there was no significant change in the absolute beta power from one trial to the next (Figure 6.10B). A paired t-test comparison of averaged consecutive trial pairs found that the baseline beta power did not significantly vary between the first of the pair and the second ($MD = -.182\%$, $SD = 5.739\%$; $t(53) = -.233$, $p = .817$).

This lack of change in baseline beta power is likely due to the use of longer trial durations in the present study. A trial length of ten-seconds appears to be long enough to allow cortical beta power to reset to a resting level before the onset of the next trial (Figure 6.10A).

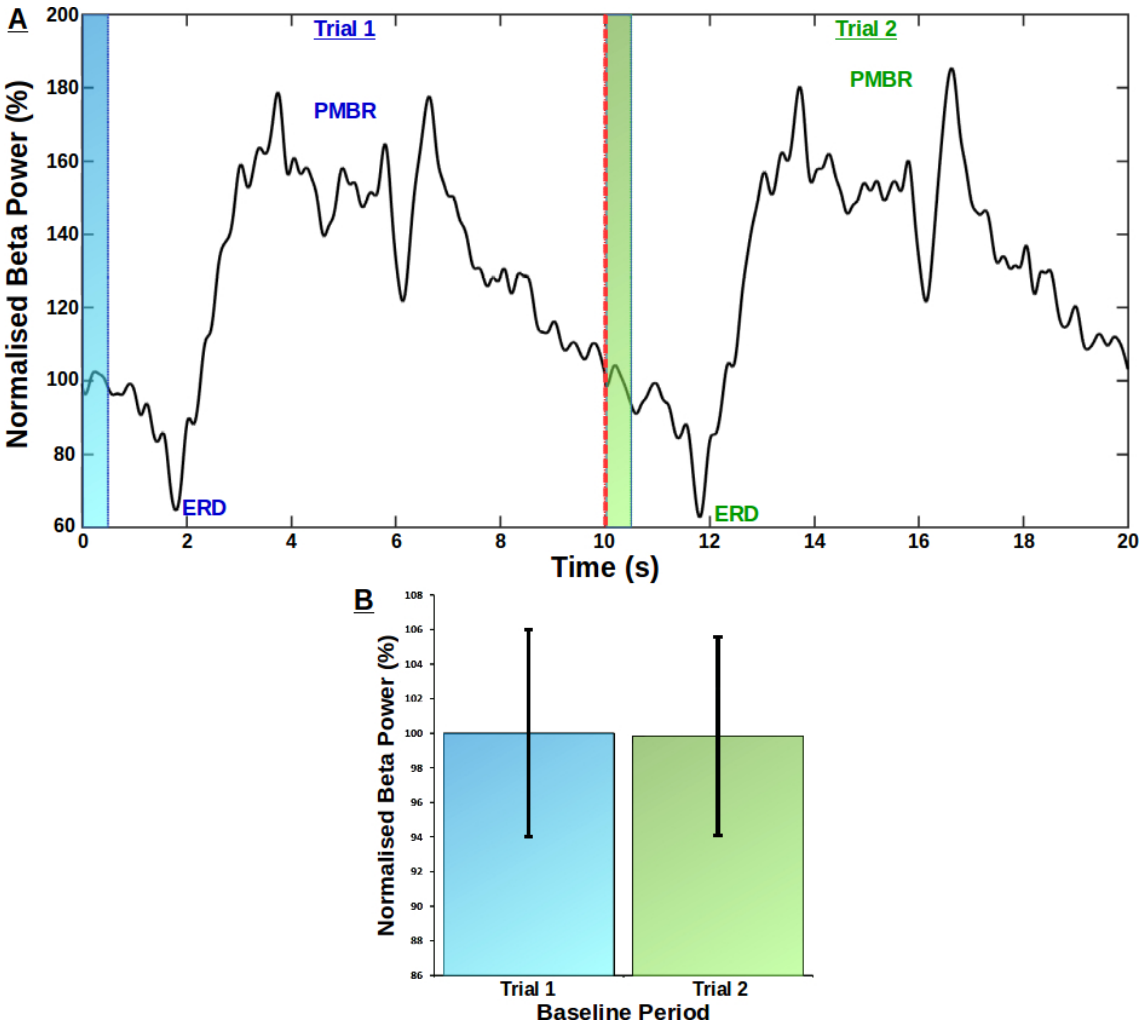

Figure 6.10: **A.** Power envelope plot of normalised beta power across two consecutive trials. There was no significant change in beta power during the baseline period of the second trial (green bar), from the corresponding baseline period of the preceding trial (blue bar). It appears that a trial length of 10s is more appropriate for the study of motor-related changes in beta power as the onset of the second trial (red dashed line) does not overlap with the PMBR period of the first. **B.** Bar chart showing the amplitude (mean $\pm SD$) of baseline beta power during two consecutive trials. There was no significant change in baseline beta power between the first trial and the proceeding trial ($p = .817$).

6.3.5 Summary of results

- The information participants received throughout the course of the experiment was designed to alter their anticipation of an upcoming motor requirement. In contrast to our prediction, resting beta power was significantly greater when motor anticipation was high than when anticipation was low.
- The effect of motor anticipation on absolute beta power significantly higher when comparing beta power during the motor task to the post-motor rest period. There was no significant difference between the three inter-block rest periods. However, following completion of the final motor task, there was a significant reduction in resting beta power.
- There was a significantly greater relative beta ERD during motor trials with a higher resting beta power than trials with lower resting beta power at trial onset.
- Conversely, the relative increase in beta amplitude during PMBR was significantly reduced in trials with high resting beta power compared to those with low resting beta power at onset.
- There was no significant effect of absolute beta power at trial onset on the resulting response time.
- While resting beta power varied within each trial, this variation was not significant between two consecutive trials.

6.4 Discussion

6.4.1 Summary

In this chapter, we attempted to investigate the change in resting beta power throughout the course of a motor study. By providing the participant with conflicting information about the nature of the task they were to perform, we hoped to modulate their anticipation of a motor requirement.

As predicted, there was a significant effect of motor anticipation on the power of ongoing motor cortical beta at rest. However, this significant effect was in the opposite direction to the one initially predicted. As the participant began to anticipate an upcoming movement there was a significant increase in resting beta power, then as the likelihood of future motor involvement decreased there was a concurrent significant decrease in resting beta power.

The relationship between absolute beta power and movement-related modulation of cortical beta was as we predicted. The relative decrease in power during beta ERD was significantly greater during trials with a high level of absolute beta power than trials with lower absolute beta power. Furthermore, there was a significant reduction in the relative PMBR following the termination of movement in trials with higher absolute beta power compared to those with low. However, this change in relative beta modulation did not significantly affect participant response times.

6.4.2 Contextual cues modulate motor anticipation and resting beta power

To the best of our knowledge, the present study was the first of its kind to investigate changes in resting, spontaneous beta power throughout the course of a motor experiment. This design allowed us to investigate the effect of a participant's motor anticipation and contextual awareness on their cortical beta power, from being unaware of any upcoming motor requirement to being fully cognisant of the exact nature and length of the motor task.

Throughout the time-course of the presented study, several resting baselines were collected. These baselines were collected after the participant had been provided some form of contextual cue about the upcoming task. The initial baseline measure was taken after the functional localisation of each participant's M1h. At this point, surface EMG had been applied to the participants' hands, a tangible twitch had been produced in their

right and left FDI, and they were instructed that the following task would either be purely visual, with no motor components, or a purely motor task. We expected with this contextual information that the participant, being more aware of their hands, yet unsure of being involved in a motor study, would have a moderate level of anticipation about an upcoming motor requirement.

Following this initial two-minute baseline period, the participant performed a visual distractor task, which was employed to convince the participant that they were not part of the motor cohort and would be performing a series of visual tasks. Therefore, at this point, motor anticipation was expected to be low. Following the visual distractor task, the participant was informed that they were, in fact, part of the motor cohort and would be required to perform a series of motor tasks. They then performed ten practice trials and were instructed that there would be a further four blocks of 40 trials to perform. We expected, at this point, motor anticipation would be at its highest, as the participant was fully aware of the extent of the motor requirement. Following the fourth block of the motor task, the participant was informed the study was over and that they could relax. At this point, we expected motor anticipation to be at its lowest.

In contrast to our prediction of an inverse relationship between resting beta power and motor anticipation, there was a significant increase in resting beta power during periods of high motor anticipation. Beta power during the initial rest period after functional localisation of the M1h, when we believed the participant would be expecting a motor task, was significantly greater than beta power during post-visual rest period, when we believed participants would have lower motor anticipation (Figure 6.4). This same relationship between resting beta power and motor anticipation was then observed when participants became aware they were involved in a motor study, as there was a significant increase in resting beta power that coincided with this contextual revelation.

The most significant change in resting beta power came following completion of the motor task, once the participant had been informed that there would be no further motor response trials. At this point, average resting beta power significantly decreased to an amplitude lower than that of any other resting baseline recording throughout the course of the experiment.

6.4.3 Resting beta power reflects motor network coherence

Once the exact nature of the motor task was divulged to the participant there was a significant increase in resting beta power. We argue that the increase in cortical beta power measured over the M1h is due to an increase in functional connectivity of the motor network. As previously touched upon (Section 1.2.2), the *'communication-through-coherence'* hypothesis (Fries, 2005) argues that a neural ensemble is more easily recruited when the input signal is received in phase with the ongoing oscillation. Our finding of increased motor cortical synchrony may reflect entrainment of the entire motor cortex to more readily allow the reception of a synchronous input signal by the appropriate ensemble.

Increased beta coherence has previously been suggested to reflect the anticipatory recruitment of motor networks (Babiloni et al., 2006; Pollok et al., 2008). Task-related desynchronisation of the beta rhythm coincides with an increase in intra-cortical coherence of motor regions within the beta band (Brovelli et al., 2004; Leocani et al., 1997; Manganotti et al., 1998; Pfurtscheller & Andrew, 1999). There is also a strong corticomuscular coherence within the beta band that has been shown to increase during PMBR and may reflect a process of motor recalibration (Baker, 2007; Baker et al., 1997). Riddle & Baker (2006) demonstrated that this corticomuscular coherence was greatest following a large movement than following a small movement, suggesting the greater the displacement from the current postural set, the greater the network synchrony (Riddle & Baker, 2006).

We argue that the increased resting beta synchrony reflects a similar neural process to that of the PMBR. In anticipation of an upcoming movement, there is a *'recalibration'* of the sensorimotor network. A sensory check to establish the current motor state, in anticipation of an upcoming perturbation from that state. This would also suggest a form of top-down control of motor attention/readiness when the participant is provided with enough contextual information about an upcoming motor requirement.

The design of most studies of task-related modulation of oscillatory activity does not incorporate a baseline measure of ongoing activity prior to beginning a motor experiment. An EEG pilot study found that absolute beta during a continuous tracking task was greater than during the rest period prior to task onset and a second rest period after the task was complete (Yang et al., 2017). Given that the sample size of this pilot study was one,

this evidence is hardly decisive; however, it does add weight to our current finding in the absence of any further similar studies.

6.4.4 Relationship between spontaneous beta power and beta ERD and PMBR

We have demonstrated that increased resting beta power results in a significantly greater relative beta ERD during the motor task. This finding corroborates those of previous studies, that have demonstrated the same positive relationship between ERD magnitude and increased spontaneous beta power, whether it be due to age (Heinrichs-Graham & Wilson, 2016; Heinrichs-Graham et al., 2018; Rossiter et al., 2014) or the time of day (Wilson et al., 2014a).

Interestingly, there was no significant effect of absolute beta power on the RTs of our participants, nor was there any correlation between the relative change in power during either ERD or PMBR, and the RTs. Previous studies of age-related changes in absolute and relative beta power have demonstrated that increased beta ERD correlates negatively with movement and reaction time, even when controlling for age (Heinrichs-Graham & Wilson, 2016; Heinrichs-Graham et al., 2018). However, the motor paradigm used in these studies was significantly more complex than the one presented here, involving the movement of several digits over a longer period of time. Given the relative similarity between the paradigm used here and that used by Wilson et al. (2014a), who also reported no correlations between RT and beta measures, we can conclude that, in such simple motor tasks, neither increased resting beta nor the proportional change in movement-related beta significantly slows the motor response.

The exact mechanism that underlies this increase in relative ERD magnitude, concurrent with an increase in baseline beta power is as yet unknown. However, we posit that high spontaneous beta power reflects an increase in the degree of coherence between primary motor cortical neurons and potentially with other neurons in secondary motor areas such as the PMC, SMA, PPC, the cerebellum and the thalamus. An overall increase in neural synchrony would mean that when a subset of those neurons was recruited to form a motor output the overall level of desynchronisation would also be increased when compared to when the same ensemble is recruited from a poorly synchronised network.

Wilson et al. (2014a) posited an alternative hypothesis that rather than the level of synchrony within the motor network increasing, the number of neurons that make up the network increases. If PMBR does reflect a process of sensory reafference and the

entrainment of further sensorimotor regions to the ongoing beta oscillation, this would explain why the relative amplitude of PMBR is reduced. If a greater number of primary and secondary motor neurons are synchronised at rest, then the proportional increase to the larger network that occurs during PMBR will be reduced. However, this hypothesis does not explain the greater magnitude of beta ERD during periods of high spontaneous beta power. If beta desynchronisation coincides with the required ensemble for motor output uncoupling from the ongoing network activity, then the same ensemble uncoupling from a large network will result in a proportionally smaller desynchronisation than if it had uncoupled from a smaller network. Our theory of increased synchrony within the same network is a better fit for the relationship between ongoing beta power and the relative change in beta ERD and PMBR.

6.4.5 Inter-trial variability in baseline beta power is negated by increasing trial duration

A different, longer behavioural task was used for this chapter than in the previous chapter (Chapter 3). As a result, there was no significant change in baseline beta power from one trial to the next. This lack of change in the baseline power between two consecutive trials appears to be due to the longer trial duration of the behavioural task used in this study. In the previous chapter (Figure 3.7), a shorter trial duration of seven-seconds was used. This shorter trial duration meant that each trial began during a period of elevated beta power that followed the termination of the previous movement.

This elevated beta power between trials may simply be due to the second trial beginning during the PMBR of the first trial. However, given our present finding that the anticipation of an upcoming movement in the near, but not immediate, future leads to an increase in beta synchrony, the elevated beta power may be due to motor adaptation. This theory is given additional weight by our finding that PMBR reflects cortical inhibition (Chapter 5), yet response times were not significantly longer in each consecutive trial of our shorter duration motor task (Section 3.4.5).

We, therefore, posit that increased beta power during the inter-trial baseline is a result of motor preparation. As the participant becomes aware of the motor requirements of the task, such as the range of muscles required to respond, the functional assemblies that generate motor output to those muscle groups remain synchronised and do not disengage from the ongoing motor set. In the case of our directional uncertainty

paradigm from Chapter 3, even though the direction of the response is unknown, the muscle groups required to make the response are consistent; therefore, motor assemblies required to control those muscle groups remain synchronised for a time in preparation for the next trial.

This increase in baseline beta power may then reflect the recalibration of the motor system during the task, updating the postural set in preparation of a likely movement. This would also explain why when the trial duration is increased, absolute beta power returns to a similar baseline at the onset of each trial. The functional assemblies required for the upcoming movement are briefly synchronised in preparation, however, as no 'GO' cue is received the M1 is gradually recalibrated to a resting level. This brief maintenance of motor memory has been observed previously to facilitate the next movement in a motor task (Howard et al., 2012).

6.5 Conclusion

The work I have presented in this chapter demonstrates, for the first time, that there is a significant increase in absolute resting beta power when the participant anticipates an upcoming motor requirement. This finding was the inverse of my initial prediction that, as is the case with motor preparation and imagery, the anticipation of a motor task would result in a desynchronisation of the ongoing beta rhythm.

We posit a model for this beta synchrony that closely matches that of the suggested role of PMBR in sensory recalibration (Baker et al., 1997; Sanes & Donoghue, 1993; Spinks et al., 2008). The anticipation of an upcoming motor task results in increased beta synchrony alongside an increase in cortico-cortico and corticomuscular coherence. This increased coherence is a reflection of the sensory recalibration of the central motor system with the periphery. The increased neural synchrony also allows for the more efficient recruitment of the correct neural ensemble when required for motor output.

Chapter 7

General discussion and further work

I don't pretend we have all the answers. But the questions are certainly worth thinking about.

– Arthur Charles Clarke (1917-2018)

THE overarching aim of this thesis was to use neuroimaging and neuromodulation techniques to further understand the relationship between changes in oscillatory power and the preparation, execution and termination of voluntary movement. This chapter contains a description of some key findings from this work and suggestions for methodological considerations in future work.

7.1 Key findings

7.1.1 Preparatory desynchronisation of alpha and beta activity is a prerequisite for the recruitment of the functional assemblies required for motor output

In Chapter 3, the desynchronisation of M1 alpha and beta activity was investigated during the preparation and response-phase of movement to ascertain the earliest point at which the modulatory effect of directional uncertainty alters motor cortical oscillatory activity.

I demonstrated that the magnitude of both beta and alpha preparatory-phase ERD is significantly attenuated when uncertainty about the required movement is high. Furthermore, that the ongoing profile of beta power is predictive of the participant's preparatory state. When the participant is certain of the direction of movement, beta suppression is sustained up to the point of target identification, whereas when the participant is uncertain, there is a partial resynchronisation of beta power until the required target direction is indicated.

I posit that the initial decrease in alpha and beta power reflects a process of disengagement from the ongoing network to allow the recruitment of the functional assemblies required to produce motor output. However, when the participant is

uncertain of the direction of movement, the partial resynchronisation of beta activity coincides with the realignment of potential directional units to the functional assembly until the uncertainty is resolved and the correct units can be recruited.

7.1.2 A novel signature of transient alpha synchrony reflects the recruitment of the required functional assembly

Following the preparatory desynchronisation, a novel signature of transient alpha synchrony occurs. I propose that this neural signature underlies the recruitment of functional assemblies required for directional control. A proposal strengthened by the finding that this transient alpha synchrony only occurs once the participant has sufficient information to prepare their movement and that the latency of the synchrony shows a direct relationship with the resulting behavioural performance.

7.1.3 There is an inverse relationship between M1 beta power and cortical excitability

In Chapter 5, I used single-pulse TMS to collect MEP measures of cortical excitability during beta ERD and PMBR. Prior to this study, a number of others had relied on indirect measures to infer the relationship between motor-related changes in cortical beta power and cortical excitability. These studies either correlated MEP amplitudes to ongoing spontaneous beta power in the absence of any movement (Lepage et al., 2008; Mäki & Ilmoniemi, 2010), or investigated the time-course of MEP amplitudes following the cessation of a movement without concurrent EEG to measure changes in the underlying beta power (Chen et al., 1998; Coxon et al., 2006; Leocani et al., 2000). The study I presented used EEG to first determine the latency of each individual's peak ERD and PMBR, before then using TMS to collect MEPs at each time-point.

I demonstrate that the peak-to-peak amplitude of MEPs collected during a period of beta ERD was significantly greater than a resting baseline. Conversely, there was a significant reduction in MEP amplitude during a period of PMBR. This suggests that there is an inverse relationship between M1 beta power and cortical excitability.

7.1.4 Contextual awareness modulates M1 beta synchrony

An interesting additional finding from Chapter 5 was that MEP amplitudes were significantly greater during the inter-trial rest period than during a 'passive' rest period recorded before the motor task. Both measures are purportedly measures of a resting

M1, yet they differ significantly. It is possible then that the context of being part of a motor study results in an anticipatory increase in motor cortical excitability.

To further investigate the effect of experimental context on M1 beta activity the study described in Chapter 6 was designed. This study was, to the best of my knowledge, the first to modulate the participant's anticipation of a motor requirement by providing them with conflicting information about the nature of the task they were to perform.

As the participant began to anticipate an upcoming movement there was a significant increase in resting beta power, then as the likelihood of future motor involvement decreased there was a concurrent significant decrease in resting beta power. I argue that the increase in cortical beta power measured over M1 is due to an increase in functional connectivity of the motor network.

This theory is largely based on the *'communication-through-coherence'* hypothesis (Fries, 2005), which states that a neural ensemble is more easily recruited when the input signal is received in phase with the ongoing oscillation. The anticipation of a future motor requirement results in entrainment of the entire motor cortex to more readily allow the reception of a synchronous input signal to disengage and recruit the required functional assemblies.

It has been suggested the PMBR reflects a process of sensory reafference or *'recalibration'* (Baker, 2007; Baker et al., 1997; Riddle & Baker, 2006). I argue that the increase in resting beta power reflects a similar process, a sensory check to establish the current motor state, in anticipation of an upcoming perturbation from that state. This would also suggest a form of top-down control of motor attention/readiness when the participant is provided with enough contextual information about an upcoming motor requirement.

This theory can also be applied to the partial resynchronisation of beta power observed during the preparation of uncertain movements described in Chapter 3. In the absence of information about the exact direction of the upcoming movement, there is a transient increase in beta synchrony as the potential units required for movement are synchronised to allow for their recruitment when the exact direction is known. These two processes may be the same but on different scales.

7.1.5 Resting beta power at trial onset alters measures of the relative movement-related change in beta power

The study in Chapter 6 also allowed me to investigate whether changes in resting beta power have an effect on the relative change in beta power that occurs during movement. The findings of our study confirmed those of previous studies that had suggested that high resting beta power before the execution of movement would result in a proportionally greater desynchronisation during movement execution (Heinrichs-Graham & Wilson, 2016; Heinrichs-Graham et al., 2018; Rossiter et al., 2014; Wilson et al., 2014a). Conversely, the relative increase in beta power during PMBR was significantly reduced when resting beta power was high.

I posit that the relationship I found between resting beta power and beta ERD is a result of network coherence. Increased resting beta power reflects an increase in network coherence, therefore, when a subset of neurons is recruited from the network to form a motor output, the overall level of desynchronisation is increased compared to when the same ensemble is recruited from a poorly synchronised network.

I suggest that PMBR reflects a process of sensory integration, briefly synchronising the larger sensorimotor network to integrate sensory information about the motor output with the initial motor plan to better execute the next movement. During periods of high resting beta power, coherence within the larger sensorimotor network is high; therefore, the brief entrainment of the network that occurs during PMBR will be proportionally reduced compared to a period when resting beta power and, therefore, overall network entrainment is low.

7.2 Methodological considerations and future directions

7.2.1 The importance of defining a 'resting' baseline

One of the primary methodological considerations that came from the work described in this thesis is the variation in the baseline measure used to compute movement-related changes in beta power. The vast majority of EEG/MEG studies that investigate the neural correlates of motor control use an inter-trial measure of resting oscillatory power, then compare oscillatory changes that occur within that trial with the resting baseline (Cheyne et al., 2006; Engel & Fries, 2010; Gaetz et al., 2010; Neuper & Pfurtscheller, 2001a; Pfurtscheller & Lopes Da Silva, 1999; Zhang et al., 2008). This procedure assumes that

the baseline used to compare oscillatory change does not vary between trials.

The work presented here clearly demonstrates that not only does resting beta power during this inter-trial baseline significantly increase between trials when the trial duration is too short (Section 3.4.5), the mere context of being involved in a motor study significantly increases resting beta power (Chapter 6). Further studies are required to investigate the relationship between resting beta power and the relative movement-related change in power, to allow for better, more accurate conclusions to be drawn about the potential functional role of the beta rhythm in motor function.

The study described in Chapter 6 was the first of its kind to investigate the effect of experimental context on resting beta power. Further studies need to be performed to confirm our finding of increased resting beta power during periods of high motor anticipation. In particular, the finding of increased resting beta power during high motor anticipation is difficult to reconcile with our finding that there is an inverse relationship between cortical excitability and M1 beta power (Chapter 5). Without a measure of concurrent EEG during the 'passive' rest period it is difficult to know why, during a period where we would expect motor anticipation and therefore beta synchrony to be low, there is an overall inhibition of cortical excitability. A replication of the study in Chapter 5 using a combination of EEG and TMS throughout the entire study is required to help further our understanding of the relationship between resting beta power, PMBR and cortical excitability.

7.2.2 Frequency-specific tACS to entrain motor oscillations

In my opinion, the design of the study described in Chapter 4 was too ambitious. There were too many untested stimulation parameters used to attempt to investigate the ability of tACS to entrain and disrupt M1 motor activity. However, the concept behind the use of tACS as a potential modulator of motor oscillations is based on solid scientific research (Pogosyan et al., 2009; Thut et al., 2011a; Weinrich et al., 2017).

The theory put forward by Thut et al. (2011a) that the oscillation frequency of an external force must equal that of the intrinsic neural oscillation is an important theory to keep in mind when designing tACS experiments. Previous studies within the visual domain have already demonstrated the importance of delivering tACS within a narrow frequency band around the individual peak frequency (Merlet et al., 2013; Neuling et al., 2013; Zaehle et al., 2010). While, a later study by Thut and colleagues (2011b) demonstrated the

importance of delivering rTMS at peak alpha frequency to ensure neural entrainment (Thut et al., 2011b).

The study in Chapter 4 was specifically designed to investigate the efficacy of HD-tACS as a potential, non-invasive treatment for patients who suffer from neurological disorders, such as PD. Therefore, the stimulation parameters were particularly restrictive.

One such restriction was that the 4×1 electrode montage used had very low spacing between each electrode at 4cm centre-to-centre compared to a more typical 7cm (Dmochowski et al., 2011; Nitsche et al., 2007; Stagg & Nitsche, 2011). A future study may have more success if an electrode montage that has been previously found to entrain oscillatory activity was used.

Secondly, the maximum duration of stimulation at $1.5s$ was extremely short compared to previous studies (Pogosyan et al., 2009; Weinrich et al., 2017). While this duration was chosen based on the previous finding of (Pogosyan et al., 2009) that entrainment appears to begin as early as $1.12s$ after stimulation onset, this duration is still extremely short, especially considering the low amplitude of stimulation used. A future study may employ a more traditional approach by stimulating for 10–20mins before the task (Stagg, 2014; Stagg & Nitsche, 2011), then monitoring oscillatory change and behavioural performance during the same direction uncertainty paradigm. The hypothesis being that an extended period of stimulation at peak beta frequency would lead to an increase in spontaneous beta power within the M1, leading to a lengthening in RT during an instructed-delay reaching task due to impaired coherence within the motor network.

7.3 Concluding remarks

The work presented in this thesis has further demonstrated the oscillatory correlates of motor control, with a particular focus on movement-related changes in alpha and beta activity. Importantly, I have highlighted that the relative movement-related change in beta power is dependent on the power of the ongoing rhythm and suggested that the relationship between M1 beta activity, network coherence, cortical excitability and motor performance is significantly more complex than current research suggests. The finding that experimental context has an effect on M1 beta power has far reaching implication not just for motor network research, but also for purely behavioural research and studies of other oscillatory features within the brain.

List of references

Achuthan, S., & Canavier, C. C. (2009). Phase-resetting curves determine synchronization, phase locking, and clustering in networks of neural oscillators. *Journal of Neuroscience*, *29*(16), 5218–5233. doi: 10.1523/jneurosci.0426-09.2009

Adrian, E. D., & Yamagiwa, K. (1934). The origin of the Berger rhythm. *Brain*, *58*, 323–351. doi: 10.1093/brain/58.3.323

Afifi, A. K., & Bergman, R. A. (2005). *Functional neuroanatomy: Text and atlas* (A. K. Afifi & R. A. Bergman, Eds.). New York: Lange Medical Books.

Akkal, D., Dum, R. P., & Strick, P. L. (2007). Supplementary motor area and presupplementary motor area: targets of basal ganglia and cerebellar output. *Journal of Neuroscience*, *27*(40), 10659–10673. doi: 10.1523/jneurosci.3134-07.2007

Alam, M., Truong, D. Q., Khadka, N., & Bikson, M. (2016). Spatial and polarity precision of concentric high-definition transcranial direct current stimulation (HD-tDCS). *Physics in Medicine and Biology*, *61*(12), 4506–4521. doi: 10.1088/0031-9155/61/12/4506

Albert, R., & Barabási, A.-L. (2002). Statistical mechanics of complex networks. *Reviews of Modern Physics*, *74*(1), 47–97. doi: 10.1103/revmodphys.74.47

Aldini, G. (1804). *Essai theorique et experimental sur le galvanisme*. Paris: De l'imprimerie de Fournier Fils.

Alegre, M., Alonso-Frech, F., Rodríguez-Oroz, M. C., Guridi, J., Zamarbide, I., Valencia, M., ... Artieda, J. (2005). Movement-related changes in oscillatory activity in the human subthalamic nucleus: ipsilateral vs. contralateral movements. *European Journal of Neuroscience*, *22*(9), 2315–2324. doi: 10.1111/j.1460-9568.2005.04409.x

Alegre, M., Alvarez-Gerriko, I., Valencia, M., Iriarte, J., & Artieda, J. (2008). Oscillatory changes related to the forced termination of a movement. *Clinical Neurophysiology*, *119*(2), 290–300. doi: 10.1016/j.clinph.2007.10.017

Alegre, M., de Gurtubay, I. G., Labarga, A., Iriarte, J., Malanda, A., & Artieda, J. (2004a). Alpha and beta oscillatory activity during a sequence of two movements. *Clinical Neurophysiology*, *115*(1), 124–130. doi: 10.1016/s1388-2457(03)00311-0

Alegre, M., de Gurtubay, I. G., Labarga, A., Iriarte, J., Valencia, M., & Artieda, J. (2004b). Frontal and central oscillatory changes related to different aspects of the motor process: a study in go/no-go paradigms. *Experimental Brain Research*, *159*(1), 14–22. doi: 10.1007/s00221-004-1928-8

Alegre, M., Labarga, A., de Gurtubay, I., Iriarte, J., Malanda, A., & Artieda, J. (2003). Movement-related changes in cortical oscillatory activity in ballistic, sustained and negative movements. *Experimental Brain Research*, *148*(1), 17–25. doi: 10.1007/s00221-002-1255-x

Alegre, M., Labarga, A., de Gurtubay, I. G., Iriarte, J., Malanda, A., & Artieda, J. (2002). Beta electroencephalograph changes during passive movements: sensory afferences contribute to beta event-related desynchronization in humans. *Neuroscience Letters*, *331*(1), 29–32. doi: 10.1016/s0304-3940(02)00825-x

Amiez, C., & Petrides, M. (2012). Neuroimaging evidence of the anatomo-functional organization of the human cingulate motor areas. *Cerebral Cortex*, *24*(3), 563–578. doi: 10.1093/cercor/bhs329

Amunts, K., Schleicher, A., Bürgel, U., Mohlberg, H., Uylings, H., & Zilles, K. (1999). Broca's region revisited: cytoarchitecture and intersubject variability. *Journal of Comparative Neurology*, *412*(2), 319–341. doi: 10.1002/(sici)1096-9861(19990920)412:2<319::aid-cne10>3.0.co;2-7

Amunts, K., Schleicher, A., Ditterich, A., & Zilles, K. (2003). Broca's region: cytoarchitectonic asymmetry and developmental changes. *Journal of Comparative Neurology*, *465*(1), 72–89. doi: 10.1002/cne.10829

Andersen, R. A., & Buneo, C. A. (2002). Intentional maps in posterior parietal cortex. *Annual Review of Neuroscience*, *25*(1), 189–220. doi: 10.1146/annurev.neuro.25.112701.142922

Andersen, R. A., Essick, G. K., & Siegel, R. M. (1985). Encoding of spatial location by posterior parietal neurons. *Science*, *230*(4724), 456–458. doi: 10.1126/science.4048942

Andrew, C., & Pfurtscheller, G. (1999). Lack of bilateral coherence of post-movement central beta oscillations in the human electroencephalogram. *Neuroscience Letters*, *273*(2), 89–92. doi: 10.1016/s0304-3940(99)00632-1

Antal, A., Boros, K., Poreisz, C., Chaieb, L., Terney, D., & Paulus, W. (2008). Comparatively weak after-effects of transcranial alternating current stimulation (tACS) on cortical excitability in humans. *Brain Stimulation*, *1*(2), 97–105. doi: 10.1016/j.brs.2007.10.001

Antonenko, D., Schubert, F., Bohm, F., Ittermann, B., Aydin, S., Hayek, D., ... Flöel, A. (2017). tDCS-induced modulation of GABA levels and resting-state functional connectivity in older adults. *The Journal of Neuroscience*, *37*(15), 4065–4073. doi: 10.1523/jneurosci.0079-17.2017

Arai, N., Okabe, S., Furubayashi, T., Mochizuki, H., Iwata, N. K., Hanajima, R., ... Ugawa, Y. (2007). Differences in after-effect between monophasic and biphasic high-frequency rTMS of the human motor cortex. *Clinical Neurophysiology*, *118*(10), 2227–2233. doi: 10.1016/j.clinph.2007.07.006

Arduino.cc. (2017). *Arduino: Arduino Uno Rev 3.* Retrieved from https://www.arduino.cc/en/uploads/Main/Arduino_Uno_Rev3-schematic.pdf

Arroyo, S., Lesser, R. P., Gordon, B., Uematsu, S., Jackson, D., & Webber, R. (1993). Functional significance of the mu rhythm of human cortex: an electrophysiologic

study with subdural electrodes. *Electroencephalography and Clinical Neurophysiology*, *87*(3), 76–87. doi: 10.1016/0013-4694(93)90114-b

Astafiev, S. V., Shulman, G. L., Stanley, C. M., Snyder, A. Z., Van Essen, D. C., & Corbetta, M. (2003). Functional organization of human intraparietal and frontal cortex for attending, looking, and pointing. *Journal of Neuroscience*, *23*(11), 4689–4699. doi: 10.1523/jneurosci.23-11-04689.2003

Athanasiou, A., Klados, M. A., Styliadis, C., Foroglou, N., Polyzoidis, K., & Bamidis, P. D. (2018). Investigating the role of alpha and beta rhythms in functional motor networks. *Neuroscience*, *378*, 54–70. doi: 10.1016/j.neuroscience.2016.05.044

Atmel. (2015). *ATmega328P Datasheet.* Retrieved from http://www.atmel.com/images/Atmel-8271-8-bit-AVR-Microcontroller-ATmega48A-48PA-88A-88PA-168A-168PA-328-328P_datasheet_Complete.pdf

Avanzini, P., Fabbri-Destro, M., Volta, R. D., Daprati, E., Rizzolatti, G., & Cantalupo, G. (2012). The dynamics of sensorimotor cortical oscillations during the observation of hand movements: an EEG study. *PLoS ONE*, *7*(5), 37534. doi: 10.1371/journal.pone.0037534

Averbeck, B. B., Chafee, M. V., Crowe, D. A., & Georgopoulos, A. P. (2003). Neural activity in prefrontal cortex during copying geometrical shapes. *Experimental Brain Research*, *150*(2), 127–141. doi: 10.1007/s00221-003-1416-6

Averbeck, B. B., Jeong-Woo, S., & Lee, D. (2006). Activity in prefrontal cortex during dynamic selection of action sequences. *Nature Neuroscience*, *9*(2), 276. doi: 10.1038/nn1634

Averbeck, B. B., & Lee, D. (2007). Prefrontal neural correlates of memory for sequences. *Journal of Neuroscience*, *27*(9), 2204–2211. doi: 10.1523/jneurosci.4483-06.2007

Babiloni, C., Babiloni, F., Carducci, F., Cincotti, F., Cocozza, G., Percio, C. D., ... Rossini, P. M. (2002). Human cortical electroencephalography (EEG) rhythms during the observation of simple aimless movements: a high-resolution EEG study. *NeuroImage*, *17*(2), 559–572. doi: 10.1006/nimg.2002.1192

Babiloni, C., Branucci, A., Vecchio, F., Arendt-Nielsen, L., Chen, A. C. N., & Rossini, P. M. (2006). Anticipation of somatosensory and motor events increases centro-parietal functional coupling: an EEG coherence study. *Clinical Neurophysiology*, *117*(5), 1000–1008. doi: 10.1016/j.clinph.2005.12.028

Babiloni, C., Percio, C. D., Vecchio, F., Sebastiano, F., Gennaro, G. D., Quarato, P. P., ... Mirabella, G. (2016). Alpha, beta and gamma electrocorticographic rhythms in somatosensory, motor, premotor and prefrontal cortical areas differ in movement execution and observation in humans. *Clinical Neurophysiology*, *127*(1), 641–654. doi: 10.1016/j.clinph.2015.04.068

Bachtiar, V., Near, J., Johansen-Berg, H., & Stagg, C. J. (2015). Modulation of GABA and resting state functional connectivity by transcranial direct current stimulation. *eLife*, *4*. doi: 10.7554/elife.08789

Badre, D., & D'Esposito, M. (2007). Functional magnetic resonance imaging evidence for a hierarchical organization of the prefrontal cortex. *Journal of Cognitive Neuroscience*, *19*(12), 2082–2099. doi: 10.1162/jocn.2007.91201

Baillet, S., Mosher, J. C., & Leahy, R. M. (2001). Electromagnetic brain mapping. *IEEE Signal Processing Magazine*, *18*(6), 14–30. doi: 10.1109/79.962275

Baker, M. R., & Baker, S. N. (2003). The effect of diazepam on motor cortical oscillations and corticomuscular coherence studied in man. *The Journal of Physiology*, *546*(3), 931–942. doi: 10.1113/jphysiol.2002.029553

Baker, S. N. (2007). Oscillatory interactions between sensorimotor cortex and the periphery. *Current Opinion in Neurobiology*, *17*(6), 649–655. doi: 10.1016/j.conb.2008.01.007

Baker, S. N., Kilner, J. M., Pinches, E. M., & Lemon, R. N. (1999). The role of synchrony and oscillations in the motor output. *Experimental Brain Research*, *128*(1-2), 109–117. doi: 10.1007/s002210050825

Baker, S. N., Olivier, E., & Lemon, R. N. (1997). Coherent oscillations in monkey motor cortex and hand muscle EMG show task-dependent modulation. *The Journal of Physiology*, *501*(1), 225–241. doi: 10.1111/j.1469-7793.1997.225bo.x

Barbas, H., & Pandya, D. N. (1987). Architecture and frontal cortical connections of the premotor cortex (area 6) in the rhesus monkey. *Journal of Comparative Neurology*, *256*(2), 211–228. doi: 10.1002/cne.902560203

Barbas, H., & Rempel-Clower, N. (1997, oct). Cortical structure predicts the pattern of corticocortical connections. *Cerebral Cortex*, *7*(7), 635–646. doi: 10.1093/cercor/7.7.635

Barker, A. T. (1991). An introduction to the basic principles of magnetic nerve stimulation. *Journal of clinical neurophysiology: official publication of the American Electroencephalographic Society*, *8*(1), 26–37. doi: 10.1097/00004691-199101000-00005

Barker, A. T., Jalinous, R., & Freeston, I. L. (1985). Non-invasime magnetic stimulation of human motor cortex. *The Lancet*, *325*(8437), 1106–1107. doi: 10.1016/s0140-6736(85)92413-4

Bartos, M., Vida, I., Frotscher, M., Meyer, A., Monyer, H., Geiger, J. R. P., & Jonas, P. (2002). Fast synaptic inhibition promotes synchronized gamma oscillations in hippocampal interneuron networks. *Proceedings of the National Academy of Sciences*, *99*(20), 13222–13227. doi: 10.1073/pnas.192233099

Bartos, M., Vida, I., & Jonas, P. (2007). Synaptic mechanisms of synchronized gamma oscillations in inhibitory interneuron networks. *Nature Reviews Neuroscience*, *8*(1), 45–56. doi: 10.1038/nrn2044

Başar, E., Başar-Eroğlu, C., Karakaş, S., & Schürmann, M. (1999). Are cognitive processes manifested in event-related gamma, alpha, theta and delta oscillations in the EEG? *Neuroscience Letters*, *259*(3), 165–168. doi: 10.1016/s0304-3940(98)00934-3

Bastos, A. M., Vezoli, J., Bosman, C. A., Schoffelen, J.-M., Oostenveld, R., Dowdall, J. R., ... Fries, P. (2015). Visual areas exert feedforward and feedback influences through distinct frequency channels. *Neuron*, *85*(2), 390–401. doi: 10.1016/j.neuron.2014.12.018

Bathellier, B., Carleton, A., & Gerstner, W. (2008). Gamma oscillations in a nonlinear regime: a minimal model approach using heterogeneous integrate-and-fire networks. *Neural Computation*, *20*(12), 2973–3002. doi: 10.1162/neco.2008.11-07-636

Beckmann, M., Johansen-Berg, H., & Rushworth, M. F. S. (2009). Connectivity-based parcellation of human cingulate cortex and its relation to functional specialization. *Journal of Neuroscience*, *29*(4), 1175–1190. doi: 10.1523/jneurosci.3328-08.2009

Benali, A., Weiler, E., Benali, Y., Dinse, H. R., & Eysel, U. T. (2008). Excitation and inhibition jointly regulate cortical reorganization in adult rats. *Journal of Neuroscience*, *28*(47), 12284–12293. doi: 10.1523/jneurosci.1952-08.2008

Berger, B., Gaspar, P., & Verney, C. (1991). Dopaminergic innervation of the cerebral cortex: unexpected differences between rodents and primates. *Trends in Neurosciences*, *14*(1), 21–27. doi: 10.1016/0166-2236(91)90179-x

Berger, H. (1929). Über das elektrenkephalogramm des menschen. *European Archives of Psychiatry and Clinical Neuroscience*, *87*(1), 527–570. doi: 10.1007/bf01797193

Bergmann, T. O., Groppa, S., Seeger, M., Mölle, M., Marshall, L., & Siebner, H. R. (2009). Acute changes in motor cortical excitability during slow oscillatory and constant anodal transcranial direct current stimulation. *Journal of Neurophysiology*, *102*(4), 2303–2311. doi: 10.1152/jn.00437.2009

Bertrand, O., & Pantev, C. (1994). Stimulus frequency dependence of the transient oscillatory auditory evoked responses (40 Hz) studied by electric and magnetic recordings in human. In *Oscillatory event-related brain dynamics* (pp. 231–242). Springer. doi: 10.1007/978-1-4899-1307-4_17

Bestmann, S., & Krakauer, J. W. (2015). The uses and interpretations of the motor-evoked potential for understanding behaviour. *Experimental Brain Research*, *233*(3), 679–689. doi: 10.1007/s00221-014-4183-7

Betz, W. (1874). Anatomischer nachweis zweier gehirncentra. *Zentralbl Med Wiss*, *12*(578).

Binkofski, F., Dohle, C., Posse, S., Stephan, K. M., Hefter, H., Seitz, R. J., & Freund, H.-J. (1998). Human anterior intraparietal area subserves prehension: A combined lesion and functional MRI activation study. *Neurology*, *50*(5), 1253–1259. doi: 10.1212/WNL.50.5.1253

Binzegger, T., Douglas, R. J., & Martin, K. A. C. (2004, sep). A quantitative map of the circuit of cat primary visual cortex. *Journal of Neuroscience*, *24*(39), 8441–8453. doi: 10.1523/jneurosci.1400-04.2004

Blankenburg, S., Wu, W., Lindner, B., & Schreiber, S. (2015). Information filtering in resonant neurons. *Journal of Computational Neuroscience*, *39*(3), 349–370. doi: 10.1007/s10827-015-0580-6

Bock, O., & Arnold, K. (1992). Motor control prior to movement onset: preparatory mechanisms for pointing at visual targets. *Experimental Brain Research*, *90*(1), 209–216. doi: 10.1007/BF00229273

Bollimunta, A., Chen, Y., Schroeder, C. E., & Ding, M. (2008, oct). Neuronal mechanisms of cortical alpha oscillations in awake-behaving macaques. *Journal of Neuroscience*, *28*(40), 9976–9988. doi: 10.1523/jneurosci.2699-08.2008

Bonifazi, P., Goldin, M., Picardo, M. A., Jorquera, I., Cattani, A., Bianconi, G., ... Cossart, R. (2009). GABAergic hub neurons orchestrate synchrony in developing hippocampal networks. *Science*, *326*(5958), 1419–1424. doi: 10.1126/science.1175509

Borckardt, J. J., Bikson, M., Frohman, H., Reeves, S. T., Datta, A., Bansal, V., ... George, M. S. (2012). A pilot study of the tolerability and effects of high-definition transcranial direct current stimulation (HD-tDCS) on pain perception. *The Journal of Pain*, *13*(2), 112–120. doi: 10.1016/j.jpain.2011.07.001

Börgers, C., Epstein, S., & Kopell, N. J. (2005). Background gamma rhythmicity and attention in cortical local circuits: a computational study. *Proceedings of the National Academy of Sciences of the United States of America*, *102*(19), 7002–7007. doi: 10.1073/pnas.0502366102

Börgers, C., & Kopell, N. (2003). Synchronization in networks of excitatory and inhibitory neurons with sparse, random connectivity. *Neural Computation*, *15*(3), 509–538. doi: 10.1162/089976603321192059

Bornschlegl, M., & Asanuma, H. (1987). Importance of the projection from the sensory to the motor cortex for recovery of motor function following partial thalamic lesion in the monkey. *Brain Research*, *437*(1), 121–130. doi: 10.1016/0006-8993(87)91533-2

Boroojerdi, B., Battaglia, F., Muellbacher, W., & Cohen, L. G. (2001). Mechanisms influencing stimulus-response properties of the human corticospinal system. *Clinical Neurophysiology*, *112*(5), 931–937. doi: 10.1016/s1388-2457(01)00523-5

Bosch-Bouju, C., Hyland, B. I., & Parr-Brownlie, L. C. (2013). Motor thalamus integration of cortical, cerebellar and basal ganglia information: implications for normal

and parkinsonian conditions. *Frontiers in Computational Neuroscience*, *7*. doi: 10.3389/fncom.2013.00163

Brittain, J.-S., & Brown, P. (2014). Oscillations and the basal ganglia: motor control and beyond. *NeuroImage*, *85*, 637–647. doi: 10.1016/j.neuroimage.2013.05.084

Britton, T. C., Thompson, P. D., Day, B. L., Rothwell, J. C., Findley, L. J., & Marsden, C. D. (1993). Modulation of postural wrist tremors by magnetic stimulation of the motor cortex in patients with Parkinson's disease or essential tremor and in normal subjects mimicking tremor. *Annals of Neurology*, *33*(5), 473–479. doi: 10.1002/ana.410330510

Brodmann, K. (1907). *Beiträge zur histologischen lokalisation der grosshirnrinde: Die cortexgliederung des menschen. VI*. Verlag von Johann Ambrosius Barth.

Bronte-Stewart, H., Barberini, C., Koop, M. M., Hill, B. C., Henderson, J. M., & Wingeier, B. (2009). The STN beta-band profile in Parkinson's disease is stationary and shows prolonged attenuation after deep brain stimulation. *Experimental Neurology*, *215*(1), 20–28. doi: 10.1016/j.expneurol.2008.09.008

Brovelli, A., Ding, M., Ledberg, A., Chen, Y., Nakamura, R., & Bressler, S. L. (2004). Beta oscillations in a large-scale sensorimotor cortical network: directional influences revealed by Granger causality. *Proceedings of the National Academy of Sciences of the United States of America*, *101*(26), 9849–9854. doi: 10.1073/pnas.0308538101

Brown, P. (2000). Cortical drives to human muscle: the Piper and related rhythms. *Progress in Neurobiology*, *60*(1), 97–108. doi: 10.1016/s0301-0082(99)00029-5

Brown, P. (2003). Oscillatory nature of human basal ganglia activity: relationship to the pathophysiology of Parkinson's disease. *Movement Disorders*, *18*(4), 357–363. doi: 10.1002/mds.10358

Brown, P. (2007). Abnormal oscillatory synchronisation in the motor system leads to impaired movement. *Current Opinion in Neurobiology*, *17*(6), 656–664. doi: 10.1016/j.conb.2007.12.001

Brown, P., Mazzone, P., Oliviero, A., Altibrandi, M. G., Pilato, F., Tonali, P. A., & Di Lazzaro, V. (2004). Effects of stimulation of the subthalamic area on oscillatory pallidal activity in Parkinson's disease. *Experimental Neurology*, *188*(2), 480–490. doi: 10.1016/j.expneurol.2004.05.009

Brown, P., Oliviero, A., Mazzone, P., Insola, A., Tonali, P., & Di Lazzaro, V. (2001). Dopamine dependency of oscillations between subthalamic nucleus and pallidum in Parkinson's disease. *The Journal of Neuroscience*, *21*(3), 1033–1038. doi: 10.1523/jneurosci.21-03-01033.2001

Brown, P., & Williams, D. (2005). Basal ganglia local field potential activity: character and functional significance in the human. *Clinical Neurophysiology*, *116*(11), 2510–2519. doi: 10.1016/j.clinph.2005.05.009

Bruce, C. J., & Goldberg, M. E. (1985). Primate frontal eye fields. I. Single neurons discharging before saccades. *Journal of Neurophysiology*, *53*(3), 603–635. doi: 10.1152/jn.1985.53.3.603

Bruno, R. M., & Sakmann, B. (2006). Cortex is driven by weak but synchronously active thalamocortical synapses. *Science*, *312*(5780), 1622–1627. doi: 10.1126/science.1124593

Buffalo, E. A., Fries, P., Landman, R., Buschman, T. J., & Desimone, R. (2011, jun). Laminar differences in gamma and alpha coherence in the ventral stream. *Proceedings of the National Academy of Sciences*, *108*(27), 11262–11267. doi: 10.1073/pnas.1011284108

Buhl, E. H., Tamás, G., & Fisahn, A. (1998, nov). Cholinergic activation and tonic excitation induce persistent gamma oscillations in mouse somatosensory cortexin vitro. *The Journal of Physiology*, *513*(1), 117–126. doi: 10.1111/j.1469-7793.1998.117by.x

Buneo, C. A., Jarvis, M. R., Batista, A. P., & Andersen, R. A. (2002). Direct visuomotor transformations for reaching. *Nature*, *416*(6881), 632–636. doi: 10.1038/416632a

Burke, D., Hicks, R., Gandevia, S. C., Stephen, J., Woodforth, I., & Crawford, M. (1993). Direct comparison of corticospinal volleys in human subjects to transcranial magnetic and electrical stimulation. *The Journal of Physiology*, *470*(1), 383–393. doi: 10.1113/jphysiol.1993.sp019864

Buzsáki, G. (2006). *Rhythms of the brain*. Oxford University Press. doi: 10.1093/acprof:oso/9780195301069.001.0001

Buzsáki, G., & Draguhn, A. (2004). Neuronal oscillations in cortical networks. *Science*, *304*(5679), 1926–1929. doi: 10.1126/science.1099745

Buzsáki, G., Geisler, C., Henze, D. A., & Wang, X.-J. (2004). Interneuron diversity series: circuit complexity and axon wiring economy of cortical interneurons. *Trends in Neurosciences*, *27*(4), 186–193. doi: 10.1016/j.tins.2004.02.007

Buzsáki, G., & Wang, X.-J. (2012). Mechanisms of gamma oscillations. *Annual Review of Neuroscience*, *35*(1), 203–225. doi: 10.1146/annurev-neuro-062111-150444

Cabibel, V., Muthalib, M., Teo, W.-P., & Perrey, S. (2018). High-definition transcranial direct-current stimulation of the right M1 further facilitates left M1 excitability during crossed facilitation. *Journal of Neurophysiology*, *119*(4), 1266–1272. doi: 10.1152/jn.00861.2017

Cacot, P., Tesolin, B., & Sebban, C. (1995). Diurnal variations of EEG power in healthy adults. *Electroencephalography and Clinical Neurophysiology*, *94*(5), 305–312. doi: 10.1016/0013-4694(94)00298-y

Calabrese, R. L. (1998). Cellular, synaptic, network, and modulatory mechanisms involved in rhythm generation. *Current Opinion in Neurobiology*, *8*(6), 710–717. doi: 10.1016/S0959-4388(98)80112-8

Campbell, A. W. (1905). *Histological studies on the localisation of cerebral function*. Cambridge University Press: Cambridge. doi: 10.1192/bjp.50.211.651

Canavan, A. G. M., Nixon, P. D., & Passingham, R. E. (1989). Motor learning in monkeys (Macaca fascicularis) with lesions in motor thalamus. *Experimental Brain Research*, *77*(1), 113–126. doi: 10.1007/BF00250573

Caparelli-Daquer, E. M., Zimmermann, T. J., Mooshagian, E., Parra, L. C., Rice, J. K., Datta, A., ... Wassermann, E. M. (2012). A pilot study on effects of 4x1 high-definition tDCS on motor cortex excitability. In *2012 annual international conference of the IEEE engineering in medicine and biology society.* IEEE. doi: 10.1109/embc.2012.6346036

Cardin, J. A., Carlén, M., Meletis, K., Knoblich, U., Zhang, F., Deisseroth, K., ... Moore, C. I. (2009). Driving fast-spiking cells induces gamma rhythm and controls sensory responses. *Nature*, *459*(7247), 663. doi: 10.1038/nature08002

Cassim, F., Monaca, C., Szurhaj, W., Bourriez, J.-L., Defebvre, L., Derambure, P., & Guieu, J.-D. (2001). Does post-movement beta synchronization reflect an idling motor cortex? *Neuroreport*, *12*(17), 3859–3863. doi: 10.1097/00001756-200112040-00051

Cauller, L. (1995). Layer I of primary sensory neocortex: where top-down converges upon bottom-up. *Behavioural Brain Research*, *71*(1), 163–170. doi: 10.1016/0166-4328(95)00032-1

Cerletti, U. (1940). L'elettroshock. *Riv Sper Freniat Med leg Alienment*, *64*, 209–310.

Chen, R., Cros, D., Curra, A., Lazzaro, V. D., Lefaucheur, J.-P., Magistris, M. R., ... Ziemann, U. (2008). The clinical diagnostic utility of transcranial magnetic stimulation: report of an IFCN committee. *Clinical Neurophysiology*, *119*(3), 504–532. doi: 10.1016/j.clinph.2007.10.014

Chen, R., Yaseen, Z., Cohen, L. G., & Hallett, M. (1998). Time course of corticospinal excitability in reaction time and self-paced movements. *Annals of Neurology*, *44*(3), 317–325. doi: 10.1002/ana.410440306

Chen, Y.-Y., Sy, H.-N., & Wu, S.-L. (2008). Zolpidem improves akinesia, dystonia and dyskinesia in advanced Parkinson's disease. *Journal of Clinical Neuroscience*, *15*(8), 955–956. doi: 10.1016/j.jocn.2007.07.082

Cheyne, D., Bakhtazad, L., & Gaetz, W. (2006). Spatiotemporal mapping of cortical activity accompanying voluntary movements using an event-related beamforming approach. *Human Brain Mapping*, *27*(3), 213–229. doi: 10.1002/hbm.20178

Cheyne, D., Bells, S., Ferrari, P., Gaetz, W., & Bostan, A. C. (2008). Self-paced movements induce high-frequency gamma oscillations in primary motor cortex. *NeuroImage*, *42*(1), 332–342. doi: 10.1016/j.neuroimage.2008.04.178

Cheyne, D., Gaetz, W., Garnero, L., Lachaux, J.-P., Ducorps, A., Schwartz, D., & Varela, F. J. (2003). Neuromagnetic imaging of cortical oscillations accompanying tactile stimulation. *Cognitive Brain Research*, *17*(3), 599–611. doi: 10.1016/s0926-6410(03)00173-3

Cheyne, D. O. (2013). MEG studies of sensorimotor rhythms: a review. *Experimental Neurology*, *245*, 27–39. doi: 10.1016/j.expneurol.2012.08.030

Cho, R.-H., Segawa, S., Mizuno, A., & Kaneko, T. (2004). Intracellularly labeled pyramidal neurons in the cortical areas projecting to the spinal cord: I. Electrophysiological properties of pyramidal neurons. *Neuroscience Research*, *50*(4), 381–394. doi: 10.1016/j.neures.2004.08.007

Choi, S., Yu, E., Kim, D., Urbano, F. J., Makarenko, V., Shin, H.-S., & Llinás, R. R. (2010). Subthreshold membrane potential oscillations in inferior olive neurons are dynamically regulated by P/Q-and T-type calcium channels: a study in mutant mice. *The Journal of Physiology*, *588*(16), 3031–3043. doi: 10.1113/jphysiol.2009.184705

Chouinard, P. A., & Paus, T. (2006, apr). The primary motor and premotor areas of the human cerebral cortex. *The Neuroscientist*, *12*(2), 143–152. doi: 10.1177/1073858405284255

Chouinard, P. A., Van Der Werf, Y. D., Leonard, G., & Paus, T. (2003). Modulating neural networks with transcranial magnetic stimulation applied over the dorsal premotor and primary motor cortices. *Journal of Neurophysiology*, *90*(2), 1071–1083. doi: 10.1152/jn.01105.2002

Chu, Z., Galarreta, M., & Hestrin, S. (2003). Synaptic interactions of late-spiking neocortical neurons in layer 1. *Journal of Neuroscience*, *23*(1), 96–102. doi: 10.1523/jneurosci.23-01-00096.2003

Churchland, A. K., Kiani, R., & Shadlen, M. N. (2008). Decision-making with multiple alternatives. *Nature Neuroscience*, *11*(6), 693–702. doi: 10.1038/nn.2123

Churchland, P., & Sejnowski, T. (1999). *The computational brain*. Boston, MA: MIT Press. doi: 10.1016/0893-6080(94)90015-9

Clancy, E. A., Morin, E. L., & Merletti, R. (2002). Sampling, noise-reduction and amplitude estimation issues in surface electromyography. *Journal of Electromyography and Kinesiology*, *12*(1), 1–16. doi: 10.1016/s1050-6411(01)00033-5

Cohen, Y. E., & Andersen, R. A. (2002). A common reference frame for movement plans in the posterior parietal cortex. *Nature Reviews Neuroscience*, *3*(7), 553. doi: 10.1038/nrn873

Colby, C. L. (1998). Action-oriented spatial reference frames in cortex. *Neuron*, *20*(1), 15–24. doi: 10.1016/S0896-6273(00)80429-8

Connolly, J. D., Andersen, R. A., & Goodale, M. A. (2003). fMRI evidence for a parietal reach region in the human brain. *Experimental Brain Research*, *153*(2), 140–145. doi: 10.1007/s00221-003-1587-1

Costa, L., & Bauer, L. (1997). Quantitative electroencephalographic differences associated with alcohol, cocaine, heroin and dual-substance dependence. *Drug and Alcohol Dependence*, *46*(1-2), 87–93. doi: 10.1016/s0376-8716(97)00058-6

Courtemanche, R., Fujii, N., & Graybiel, A. M. (2003). Synchronous, focally modulated β-band oscillations characterize local field potential activity in the striatum of awake behaving monkeys. *The Journal of Neuroscience*, *23*(37), 11741–11752. doi: 10.1523/jneurosci.23-37-11741.2003

Courtine, G., Bunge, M. B., Fawcett, J. W., Grossman, R. G., Kaas, J. H., Lemon, R., ... Edgerton, V. R. (2007, may). Can experiments in nonhuman primates expedite the translation of treatments for spinal cord injury in humans? *Nature Medicine*, *13*(5), 561–566. doi: 10.1038/nm1595

Coutin-Churchman, P., Moreno, R., Añez, Y., & Vergara, F. (2006). Clinical correlates of quantitative EEG alterations in alcoholic patients. *Clinical Neurophysiology*, *117*(4), 740–751. doi: 10.1016/j.clinph.2005.12.021

Coxon, J. P., Stinear, C. M., & Byblow, W. D. (2006). Intracortical inhibition during volitional inhibition of prepared action. *Journal of Neurophysiology*, *95*(6), 3371–3383. doi: 10.1152/jn.01334.2005

Cram, J. R., & Kasman, G. S. (2010). The basics of surface electromyography. In E. Criswell (Ed.), *Cram's introduction to surface electromyography* (Second ed., pp. 3–64). Sudbury, MA: Jones & Bartlett Learning.

Cram, J. R., Kasman, G. S., & Holtz, J. (2010). Electrode placements. In E. Criswell (Ed.), *Cram's introduction to surface electromyography* (Second ed., p. 335). Sudbury, MA: Jones & Bartlett Learning.

Creem-Regehr, S. H., & Lee, J. N. (2005). Neural representations of graspable objects: are tools special? *Cognitive Brain Research*, *22*(3), 457–469. doi: 10.1016/j.cogbrainres.2004.10.006

Creutzfeldt, O., & Houchin, J. (1974). Neuronal basis of EEG waves. In A. Remond (Ed.), *Handbook of electroencephalography and clinical neurophysiology* (Vol. 2, pp. 5–55). Amsterdam: Elsevier.

Crone, N. (1998a). Functional mapping of human sensorimotor cortex with electrocorticographic spectral analysis. I. Alpha and beta event- related desynchronization. *Brain*, *121*(12), 2271–2299. doi: 10.1093/brain/121.12.2271

Crone, N. (1998b). Functional mapping of human sensorimotor cortex with electrocorticographic spectral analysis. II. Event-related synchronization in the gamma band. *Brain*, *121*(12), 2301–2315. doi: 10.1093/brain/121.12.2301

Culham, J. C., Cavina-Pratesi, C., & Singhal, A. (2006). The role of parietal cortex in visuomotor control: What have we learned from neuroimaging? *Neuropsychologia*, *44*(13), 2668–2684. doi: 10.1016/j.neuropsychologia.2005.11.003

Culham, J. C., Danckert, S. L., De Souza, J. F. X., Gati, J. S., Menon, R. S., & Goodale, M. A. (2003). Visually guided grasping produces fMRI activation in dorsal but not ventral stream brain areas. *Experimental Brain Research*, *153*(2), 180–189. doi: 10.1007/s00221-003-1591-5

Cunningham, D. A., Machado, A., Yue, G. H., Carey, J. R., & Plow, E. B. (2013). Functional somatotopy revealed across multiple cortical regions using a model of complex motor task. *Brain research*, *1531*, 25–36. doi: 10.1016/j.brainres.2013.07.050

Cunnington, R., Windischberger, C., Deecke, L., & Moser, E. (2002). The preparation and execution of self-initiated and externally-triggered movement: a study of event-related fMRI. *NeuroImage*, *15*(2), 373–385. doi: 10.1006/nimg.2001.0976

Damasio, H. (2005). *Human brain anatomy in computerized images* (Second ed.). Oxford University Press. doi: 10.1093/acprof:oso/9780195165616.001.0001

Daniele, A., Albanese, A., Gainotti, G., Gregori, B., & Bartolomeo, P. (1997). Zolpidem in Parkinson's disease. *The Lancet*, *349*(9060), 1222–1223. doi: 10.1016/s0140-6736(05)62416-6

Datta, A., Bansal, V., Diaz, J., Patel, J., Reato, D., & Bikson, M. (2009). Gyri-precise head model of transcranial direct current stimulation: improved spatial focality using a ring electrode versus conventional rectangular pad. *Brain Stimulation*, *2*(4), 201–207. doi: 10.1016/j.brs.2009.03.005

Datta, A., Truong, D., Minhas, P., Parra, L. C., & Bikson, M. (2012). Inter-individual variation during transcranial direct current stimulation and normalization of dose using MRI-derived computational models. *Frontiers in Psychiatry*, *3*. doi: 10.3389/fpsyt.2012.00091

Davare, M., Rothwell, J. C., & Lemon, R. N. (2010). Causal connectivity between the human anterior intraparietal area and premotor cortex during grasp. *Current Biology*, *20*(2), 176–181. doi: 10.1016/j.cub.2009.11.063

Davis, N. J., Tomlinson, S. P., & Morgan, H. M. (2012). The role of beta-frequency neural oscillations in motor control. *Journal of Neuroscience*, *32*(2), 403–404. doi: 10.1523/jneurosci.5106-11.2012

Dechent, P., & Frahm, J. (2003). Functional somatotopy of finger representations in human primary motor cortex. *Human Brain Mapping*, *18*(4), 272–283. doi: 10.1002/hbm.10084

Deecke, L., & Kornhuber, H. H. (1978). An electrical sign of participation of the mesial supplementary motor cortex in human voluntary finger movement. *Brain Research*, *159*(2), 473–476. doi: 10.1016/0006-8993(78)90561-9

Deiber, M.-P., Honda, M., Ibañez, V., Sadato, N., & Hallett, M. (1999). Mesial motor areas in self-initiated versus externally triggered movements examined with fMRI: effect of movement type and rate. *Journal of Neurophysiology*, *81*(6), 3065–3077. doi: 10.1152/jn.1999.81.6.3065

DelSys. (2017). *Bagnoli 2-channel handheld EMG system: User's guide*. Boston, MA: DelSys Inc.

Deng, Z.-D., Lisanby, S. H., & Peterchev, A. V. (2013). Electric field depth–focality tradeoff in transcranial magnetic stimulation: Simulation comparison of 50 coil designs. *Brain Stimulation*, *6*(1), 1–13. doi: 10.1016/j.brs.2012.02.005

de Pesters, A., Coon, W. G., Brunner, P., Gunduz, A., Ritaccio, A. L., Brunet, N. M., ... Schalk, G. (2016). Alpha power indexes task-related networks on large and small scales: a multimodal ECoG study in humans and a non-human primate. *NeuroImage*, *134*, 122–131. doi: 10.1016/j.neuroimage.2016.03.074

Descarries, L., Lemay, B., Doucet, G., & Berger, B. (1987). Regional and laminar density of the dopamine innervation in adult rat cerebral cortex. *Neuroscience*, *21*(3), 807–824. doi: 10.1016/0306-4522(87)90038-8

Deuschl, G., Schade-Brittinger, C., Krack, P., Volkmann, J., Schäfer, H., Bötzel, K., ... Voges, J. (2006). A randomized trial of deep-brain stimulation for Parkinson's disease. *New England Journal of Medicine*, *355*(9), 896–908. doi: 10.1056/nejmoa060281

De Zeeuw, C. I., Hoogenraad, C. C., Koekkoek, S. K. E., Ruigrok, T. J. H., Galjart, N., & Simpson, J. I. (1998). Microcircuitry and function of the inferior olive. *Trends in Neurosciences*, *21*(9), 391–400. doi: 10.1016/S0166-2236(98)01310-1

Di Lazzaro, V., Oliviero, A., Meglio, M., Cioni, B., Tamburrini, G., Tonali, P., & Rothwell, J. C. (2000). Direct demonstration of the effect of lorazepam on the excitability of the human motor cortex. *Clinical Neurophysiology*, *111*(5), 794–799. doi: 10.1016/s1388-2457(99)00314-4

Di Lazzaro, V., Pilato, F., Saturno, E., Oliviero, A., Dileone, M., Mazzone, P., ... Rothwell, J. C. (2005). Theta-burst repetitive transcranial magnetic stimulation suppresses specific excitatory circuits in the human motor cortex. *The Journal of Physiology*, *565*(3), 945–950. doi: 10.1113/jphysiol.2005.087288

Dmochowski, J. P., Datta, A., Bikson, M., Su, Y., & Parra, L. C. (2011, jun). Optimized multi-electrode stimulation increases focality and intensity at target. *Journal of Neural Engineering*, *8*(4), 046011. doi: 10.1088/1741-2560/8/4/046011

Donoghue, J. P., Leibovic, S., & Sanes, J. N. (1992). Organization of the forelimb area in squirrel monkey motor cortex: representation of digit, wrist, and elbow muscles. *Experimental Brain Research*, *89*(1), 1–19. doi: 10.1007/BF00228996

Dorris, M. C., & Munoz, D. P. (1998). Saccadic probability influences motor preparation signals and time to saccadic initiation. *Journal of Neuroscience*, *18*(17), 7015–7026. doi: 10.1523/jneurosci.18-17-07015.1998

Douglas, R. J., & Martin, K. A. C. (2004). Neuronal circuits of the neocortex. *Annual Reviews Neuroscience*, *27*, 419–451. doi: 10.1146/annurev.neuro.27.070203.144152

Doyle, L. M. F., Yarrow, K., & Brown, P. (2005). Lateralization of event-related beta desynchronization in the EEG during pre-cued reaction time tasks. *Clinical Neurophysiology*, *116*(8), 1879–1888. doi: 10.1016/j.clinph.2005.03.017

Duann, J.-R., & Chiou, J.-C. (2016). A comparison of independent event-related desynchronization responses in motor-related brain areas to movement execution, movement imagery, and movement observation. *PLOS ONE*, *11*(9), 0162546. doi: 10.1371/journal.pone.0162546

Dudman, J. T., & Gerfen, C. R. (2015). The basal ganglia. In G. Paxinos (Ed.), *The rat nervous system.* Elsevier. doi: 10.1016/B978-0-12-374245-2.00017-6

Duhamel, J.-R., Colby, C. L., & Goldberg, M. E. (1992). The updating of the representation of visual space in parietal cortex by intended eye movements. *Science*, *255*(5040), 90. doi: 10.1126/science.1553535

Dum, R. P., & Strick, P. L. (1991). The origin of corticospinal projections from the premotor areas in the frontal lobe. *Journal of Neuroscience*, *11*(3), 667–689. doi: 10.1523/jneurosci.11-03-00667.1991

Dum, R. P., & Strick, P. L. (1993). Cingulate motor areas. In B. A. Vogt & M. Gabriel (Eds.), *Neurobiology of cingulate cortex and limbic thalamus* (pp. 415–441). Springer. doi: 10.1007/978-1-4899-6704-6_15

Dum, R. P., & Strick, P. L. (1996). Spinal cord terminations of the medial wall motor areas in macaque monkeys. *Journal of Neuroscience*, *16*(20), 6513–6525. doi: 10.1002/bdm

Dum, R. P., & Strick, P. L. (2004). Motor areas in the frontal lobe: The anatomical substrate for the central control of movement. In A. Riehle & E. Vaadia (Eds.), *Motor cortex in voluntary movements: A distributed system for distributed functions.* CRC Press. doi: 10.1201/9780203503584.sec1

Eccles, J. C., & Sherrington, C. S. (1930). Numbers and contraction-values of individual motor-units examined in some muscles of the limb. *Proceedings of the Royal Society B: Biological Sciences*, *106*(745), 326–357. doi: 10.1098/rspb.1930.0032

Edelman, B. J., Baxter, B., & He, B. (2016). EEG source imaging enhances the decoding of complex right-hand motor imagery tasks. *IEEE Transactions on Biomedical Engineering*, *63*(1), 4–14. doi: 10.1109/tbme.2015.2467312

Edwards, D., Cortes, M., Datta, A., Minhas, P., Wassermann, E. M., & Bikson, M. (2013). Physiological and modeling evidence for focal transcranial electrical brain stimulation in humans: a basis for high-definition tDCS. *NeuroImage*, *74*, 266–275. doi: 10.1016/j.neuroimage.2013.01.042

Engel, A. K., & Fries, P. (2010). Beta-band oscillations—signalling the status quo? *Current Opinion in Neurobiology*, *20*(2), 156–165. doi: 10.1016/j.conb.2010.02.015

Epperson, C. N., Haga, K., Mason, G. F., Sellers, E., Gueorguieva, R., Zhang, W., ... Krystal, J. H. (2002, sep). Cortical γ-Aminobutyric Acid levels across the menstrual cycle in healthy women and those with premenstrual dysphoric disorder. *Archives of General Psychiatry*, *59*(9), 851. doi: 10.1001/archpsyc.59.9.851

Epperson, C. N., O'Malley, S., Czarkowski, K. A., Gueorguieva, R., Jatlow, P., Sanacora, G., ... Mason, G. F. (2005, jan). Sex, GABA, and nicotine: The impact of smoking on cortical GABA levels across the menstrual cycle as measured with proton magnetic resonance spectroscopy. *Biological Psychiatry*, *57*(1), 44–48. doi: 10.1016/j.biopsych.2004.09.021

Erbil, N., & Ungan, P. (2007). Changes in the alpha and beta amplitudes of the central EEG during the onset, continuation, and offset of long-duration repetitive hand movements. *Brain Research*, *1169*, 44–56. doi: 10.1016/j.brainres.2007.07.014

Espenhahn, S., de Berker, A. O., van Wijk, B. C. M., Rossiter, H. E., & Ward, N. S. (2017). Movement-related beta oscillations show high intra-individual reliability. *NeuroImage*, *147*, 175–185. doi: 10.1016/j.neuroimage.2016.12.025

Facchini, S., Muellbacher, W., Battaglia, F., Boroojerdi, B., & Hallett, M. (2002). Focal enhancement of motor cortex excitability during motor imagery: a transcranial magnetic stimulation study. *Acta Neurologica Scandinavica*, *105*(3), 146–151. doi: 10.1034/j.1600-0404.2002.1o004.x

Fadiga, L., Fogassi, L., Pavesi, G., & Rizzolatti, G. (1995). Motor facilitation during action observation: a magnetic stimulation study. *Journal of Neurophysiology*, *73*(6), 2608–2611. doi: 10.1152/jn.1995.73.6.2608

Fang, P.-C., Stepniewska, I., & Kaas, J. H. (2006). The thalamic connections of motor, premotor, and prefrontal areas of cortex in a prosimian primate (Otolemur garnetti). *Neuroscience*, *143*(4), 987–1020. doi: 10.1016/j.neuroscience.2006.08.053

Faria, P., Hallett, M., & Miranda, P. C. (2011). A finite element analysis of the effect of electrode area and inter-electrode distance on the spatial distribution of the current density in tDCS. *Journal of Neural Engineering*, *8*(6), 066017. doi: 10.1088/1741-2560/8/6/066017

Farzan, F. (2014). Single-pulse transcranial magnetic stimulation (TMS) protocols and outcome measures. In A. Rotenberg, J. Horvath, & A. Pascual-Leone (Eds.), *Transcranial magnetic stimulation* (Vol. 89, pp. 69–115). New York: Springer. doi: 10.1007/978-1-4939-0879-0_5

Fattori, P., Gamberini, M., Kutz, D. F., & Galletti, C. (2001). Arm-reaching neurons in the parietal area V6A of the macaque monkey. *European Journal of Neuroscience*, *13*(12), 2309–2313. doi: 10.1046/j.0953-816X.2001.01618.x

Ferrier, D. (1873). The localization of function in the brain. *Proceedings of the Royal Society of London*, *22*(148-155), 228–232. doi: 10.1098/rspl.1873.0032

Ferrier, D. (1876). *The functions of the brain*. Smith, Elder & Company. doi: 10.1037/12860-000

Feshchenko, V. A., Veselis, R. A., & Reinsel, R. A. (1997). Comparison of the EEG effects of midazolam, thiopental, and propofol: the role of underlying oscillatory systems. *Neuropsychobiology*, *35*(4), 211–220. doi: 10.1159/000119347

Flint, A. C., & Connors, B. W. (1996, feb). Two types of network oscillations in neocortex mediated by distinct glutamate receptor subtypes and neuronal populations. *Journal of Neurophysiology*, *75*(2), 951–957. doi: 10.1152/jn.1996.75.2.951

Fogelson, N., Williams, D., Tijssen, M., van Bruggen, G., Speelman, H., & Brown, P. (2005). Different functional loops between cerebral cortex and the subthalmic area in Parkinson's disease. *Cerebral Cortex*, *16*(1), 64–75. doi: 10.1093/cercor/bhi084

Formaggio, E., Storti, S. F., Cerini, R., Fiaschi, A., & Manganotti, P. (2010). Brain oscillatory activity during motor imagery in EEG-fMRI coregistration. *Magnetic Resonance Imaging*, *28*(10), 1403–1412. doi: 10.1016/j.mri.2010.06.030

Förster, E., Zhao, S., & Frotscher, M. (2006). Laminating the hippocampus. *Nature Reviews Neuroscience*, *7*(4), 259–268. doi: 10.1038/nrn1882

Fourkas, A. D., Bonavolonta, V., Avenanti, A., & Aglioti, S. M. (2008). Kinesthetic imagery and tool-specific modulation of corticospinal representations in expert tennis players. *Cerebral Cortex*, *18*(10), 2382–2390. doi: 10.1093/cercor/bhn005

Freund, H.-J. (2011). Abnormalities of motor behavior after cortical lesions in humans. In D. M. Pollock (Ed.), *Comprehensive physiology* (pp. 763–810). John Wiley & Sons, Inc. doi: 10.1002/cphy.cp010519

Frey, S. H., Vinton, D., Norlund, R., & Grafton, S. T. (2005). Cortical topography of human anterior intraparietal cortex active during visually guided grasping. *Cognitive Brain Research*, *23*(2), 397–405. doi: 10.1016/j.cogbrainres.2004.11.010

Fried, I., Katz, A., McCarthy, G., Sass, K. J., Williamson, P., Spencer, S. S., & Spencer, D. D. (1991). Functional organization of human supplementary motor cortex studied by electrical stimulation. *Journal of Neuroscience*, *11*(11), 3656–3666. doi: 10.1523/jneurosci.11-11-03656.1991

Friedman-Hill, S., Maldonado, P. E., & Gray, C. M. (2000). Dynamics of striate cortical activity in the alert macaque: I. Incidence and stimulus-dependence of gamma-band neuronal oscillations. *Cerebral Cortex*, *10*(11), 1105–1116. doi: 10.1093/cercor/10.11.1105

Fries, P. (2005). A mechanism for cognitive dynamics: neuronal communication through neuronal coherence. *Trends in Cognitive Sciences*, *9*(10), 474–480. doi: 10.1016/j.tics.2005.08.011

Fries, P., Nikolić, D., & Singer, W. (2007). The gamma cycle. *Trends in Neurosciences*, *30*(7), 309–316. doi: 10.1016/j.tins.2007.05.005

Fries, P., Schröder, J.-H., Roelfsema, P. R., Singer, W., & Engel, A. K. (2002). Oscillatory neuronal synchronization in primary visual cortex as a correlate of stimulus selection. *Journal of Neuroscience*, *22*(9), 3739–3754. doi: 10.1523/jneurosci.22-09-03739.2002

Fritsch, G., & Hitzig, E. (1870). Uber die elektrische Erregbartkeit des Grosshirns. *Archiv fur Anatomie und Physiologie*, 300–332. doi: 10.1016/j.yebeh.2009.03.001

Fröhlich, F. (2016). Parkinson's disease. In *Network neuroscience* (pp. 291–296). Elsevier. doi: 10.1016/b978-0-12-801560-5.00023-9

Fry, A., Mullinger, K. J., O'Neill, G. C., Barratt, E. L., Morris, P. G., Bauer, M., ... Brookes, M. J. (2016). Modulation of post-movement beta rebound by contraction force and rate of force development. *Human Brain Mapping*, *37*(7), 2493–2511. doi: 10.1002/hbm.23189

Fu, K.-M. G., Foxe, J. J., Murray, M. M., Higgins, B. A., Javitt, D. C., & Schroeder, C. E. (2001). Attention-dependent suppression of distracter visual input can be cross-modally cued as indexed by anticipatory parieto–occipital alpha-band oscillations. *Cognitive Brain Research*, *12*(1), 145–152. doi: 10.1016/s0926-6410(01)00034-9

Fuggetta, G., Fiaschi, A., & Manganotti, P. (2005). Modulation of cortical oscillatory activities induced by varying single-pulse transcranial magnetic stimulation intensity over the left primary motor area: a combined EEG and TMS study. *NeuroImage*, *27*(4), 896–908. doi: 10.1016/j.neuroimage.2005.05.013

Fujiki, M., Isono, M., Hori, S., & Ueno, S. (1996). Corticospinal direct response to transcranial magnetic stimulation in humans. *Electroencephalography and Clinical Neurophysiology/Electromyography and Motor Control*, *101*(1), 48–57. doi: 10.1016/0013-4694(95)00122-0

Fulton, J. F. (1935). A note on the definition of the ”motor” and ”premotor” areas. *Brain*, *58*(2), 311–316. doi: 10.1093/brain/58.2.311

Fuster, J. M. (2015). *The prefrontal cortex* (Fifth ed.). Academic Press. doi: 10.1016/B978-0-12-407815-4.00009-X

Gabbott, P. L. A., & Somogyi, P. (1986). Quantitative distribution of GABA-immunoreactive neurons in the visual cortex (area 17) of the cat. *Experimental Brain Research*, *61*(2), 323–331. doi: 10.1007/BF00239522

Gaetz, W., Edgar, J. C., & Roberts, D. J. W. T. P. L. (2011). Relating MEG measured motor cortical oscillations to resting γ-Aminobutyric acid (GABA) concentration. *NeuroImage*, *55*(2), 616–621. doi: 10.1016/j.neuroimage.2010.12.077

Gaetz, W., Macdonald, M., Cheyne, D., & Snead, O. C. (2010). Neuromagnetic imaging of movement-related cortical oscillations in children and adults: age predicts post-movement beta rebound. *NeuroImage*, *51*(2), 792–807. doi: 10.1016/j.neuroimage.2010.01.077

Gallese, V., Murata, A., Kaseda, M., Niki, N., & Sakata, H. (1994). Deficit of hand preshaping after muscimol injection in monkey parietal cortex. *Neuroreport*, *5*(12), 1525–1529. doi: 10.1097/00001756-199407000-00029

Gardner, E. P., Debowy, D. J., Ro, J. Y., Ghosh, S., & Babu, K. S. (2002). Sensory monitoring of prehension in the parietal lobe: a study using digital video. *Behavioural Brain Research*, *135*(1), 213–224. doi: 10.1016/S0166-4328(02)00167-5

Gastaut, H. (1952). Etude électrocorticographique de la réactivité des rythmes rolandiques. *Rev Neurol (Paris)*, *87*, 176–182.

Gastaut, H., Terzian, H., & Gastaut, Y. (1952). Etude d'une activité électroencéphalographique méconnue: "Le rythme rolandique en arceau". *Marseille Méd.*, *89*, 296–310.

Gatev, P., Darbin, O., & Wichmann, T. (2006). Oscillations in the basal ganglia under normal conditions and in movement disorders. *Movement Disorders*, *21*(10), 1566–1577. doi: 10.1002/mds.21033

Georgopoulos, A. P., & Stefanis, C. N. (2007). Local shaping of function in the motor cortex: motor contrast, directional tuning. *Brain Research Reviews*, *55*(2), 383–389. doi: 10.1016/j.brainresrev.2007.05.001

Ghez, C., & Thatch, W. T. (2000). The cerebellum. In E. Kandel, J. Schwartz, & T. Jessel (Eds.), *Principles of neural science* (Fourth ed., pp. 832–852). New York: McGraw-Hill. doi: 10.1007/978-1-4020-6359-6_581

Gilbertson, T., Lalo, E., Doyle, L., Di Lazzaro, V., Cioni, B., & Brown, P. (2005). Existing motor state is favored at the expense of new movement during 13-35 Hz oscillatory synchrony in the human corticospinal system. *Journal of Neuroscience*, *25*(34), 7771–7779. doi: 10.1523/JNEUROSCI.1762-05.2005

Goldberg, J. H., & Fee, M. S. (2011). Vocal babbling in songbirds requires the basal ganglia-recipient motor thalamus but not the basal ganglia. *Journal of Neurophysiology*, *105*(6), 2729–2739. doi: 10.1152/jn.00823.2010

Golomb, D., & Hansel, D. (2000). The number of synaptic inputs and the synchrony of large, sparse neuronal networks. *Neural Computation*, *12*(5), 1095–1139. doi: 10.1162/089976600300015529

Golomb, D., & Rinzel, J. (1994). Clustering in globally coupled inhibitory neurons. *Physica D: Nonlinear Phenomena*, *72*(3), 259–282. doi: 10.1016/0167-2789(94)90214-3

Gonzalez-Rosa, J. J., Natali, F., Tettamanti, A., Cursi, M., Velikova, S., Comi, G., ... Leocani, L. (2015). Action observation and motor imagery in performance of complex movements: Evidence from EEG and kinematics analysis. *Behavioural Brain Research*, *281*, 290–300. doi: 10.1016/j.bbr.2014.12.016

Grandori, F., & Ravazzani, P. (1991). Magnetic stimulation of the motor cortex-theoretical considerations. *IEEE Transactions on Biomedical Engineering*, *38*(2), 180–191. doi: 10.1109/10.76385

Graziano, M. S. A., Taylor, C. S. R., & Moore, T. (2002). Complex movements evoked by microstimulation of precentral cortex. *Neuron*, *34*(5), 841–851. doi: 10.1016/S0896-6273(02)00698-0

Grefkes, C., & Fink, G. R. (2005). The functional organization of the intraparietal sulcus in humans and monkeys. *Journal of Anatomy*, *207*(1), 3–17. doi: 10.1111/j.1469-7580.2005.00426.x

Grefkes, C., Ritzl, A., Zilles, K., & Fink, G. R. (2004). Human medial intraparietal cortex subserves visuomotor coordinate transformation. *NeuroImage*, *23*(4), 1494–1506. doi: 10.1016/j.neuroimage.2004.08.031

Grent-'t Jong, T., Oostenveld, R., Jensen, O., Medendorp, W. P., & Praamstra, P. (2014). Competitive interactions in sensorimotor cortex: oscillations express separation between alternative movement targets. *Journal of Neurophysiology*, *112*(2), 224–232. doi: 10.1152/jn.00127.2014

Grey Walter, W., Cooper, R., Aldrige, V. J., McCallum, W. C., & Winter, A. L. (1964). Contingent negative variation : an electric sign of sensori-motor association and expectancy in the human brain. *Nature*, *203*(4943), 380–384. doi: 10.1038/203380a0

Groppa, S., Oliviero, A., Eisen, A., Quartarone, A., Cohen, L. G., Mall, V., ... Siebner, H. R. (2012). A practical guide to diagnostic transcranial magnetic stimulation: Report of an IFCN committee. *Clinical Neurophysiology*, *123*(5), 858–882. doi: 10.1016/j.clinph.2012.01.010

Gross, J., Pollok, B., Dirks, M., Timmermann, L., Butz, M., & Schnitzler, A. (2005). Task-dependent oscillations during unimanual and bimanual movements in the human primary motor cortex and SMA studied with magnetoencephalography. *NeuroImage*, *26*(1), 91–98. doi: 10.1016/j.neuroimage.2005.01.025

Grunbaum, A. S. F., & Sherrington, C. S. (1901). Observations on the physiology of the cerebral cortex of some of the higher apes.(Preliminary communication.). *Proceedings of the Royal Society of London*, *69*(451-458), 206–209. doi: 10.1098/rspl.1903.0033

Guerra, A., Pogosyan, A., Nowak, M., Tan, H., Ferreri, F., Lazzaro, V. D., & Brown, P. (2016). Phase dependency of the human primary motor cortex and cholinergic inhibition cancelation during beta tACS. *Cerebral Cortex*, *26*(10), 3977–3990. doi: 10.1093/cercor/bhw245

Haber, S. N., & Calzavara, R. (2009). The cortico-basal ganglia integrative network: the role of the thalamus. *Brain Research Bulletin*, *78*(2), 69–74. doi: 10.1016/j.brainresbull.2008.09.013

Hall, S. D., Barnes, G. R., Furlong, P. L., Seri, S., & Hillebrand, A. (2010a). Neuronal network pharmacodynamics of GABAergic modulation in the human cortex determined using pharmaco-magnetoencephalography. *Human Brain Mapping*, *31*(4), 581–594. doi: 10.1002/hbm.20889

Hall, S. D., Prokic, E. J., McAllister, C. J., Ronnqvist, K. C., Williams, A. C., Yamawaki, N., ... Stanford, I. M. (2014). GABA-mediated changes in inter-hemispheric beta frequency activity in early-stage Parkinson's disease. *Neuroscience*, *281*, 68–76. doi: 10.1016/j.neuroscience.2014.09.037

Hall, S. D., Stanford, I. M., Yamawaki, N., McAllister, C. J., Rönnqvist, K. C., Woodhall, G. L., & Furlong, P. L. (2011). The role of GABAergic modulation in motor function related neuronal network activity. *NeuroImage*, *56*(3), 1506–1510. doi: 10.1016/j.neuroimage.2011.02.025

Hall, S. D., Yamawaki, N., Fisher, A. E., Clauss, R. P., Woodhall, G. L., & Stanford, I. M. (2010b). GABA(A) alpha-1 subunit mediated desynchronization of elevated low frequency oscillations alleviates specific dysfunction in stroke – A case report. *Clinical Neurophysiology*, *121*(4), 549–555. doi: 10.1016/j.clinph.2009.11.084

Hallett, M. (2000). Transcranial magnetic stimulation and the human brain. *Nature*, *406*(6792), 147–150. doi: 10.1038/35018000

Hammond, C., Bergman, H., & Brown, P. (2007). Pathological synchronization in Parkinson's disease: networks, models and treatments. *Trends in Neurosciences*, *30*(7), 357–364. doi: 10.1016/j.tins.2007.05.004

Hampel, F. R. (1971). A general qualitative definition of robustness. *The Annals of Mathematical Statistics*, *42*(6), 1887–1896. doi: 10.1214/aoms/1177693054

Hansel, D., & Mato, G. (2001). Existence and stability of persistent states in large neuronal networks. *Physical Review Letters*, *86*(18), 4175–4178. doi: 10.1103/physrevlett.86.4175

Hansel, D., & Mato, G. (2003). Asynchronous states and the emergence of synchrony in large networks of interacting excitatory and inhibitory neurons. *Neural Computation*, *15*(1), 1–56. doi: 10.1162/089976603321043685

Hari, R., & Salenius, S. (1999). Rhythmical corticomotor communication. *Neuroreport*, *10*(2), 1–10.

Hari, R., Salmelin, R., Mäkelä, J. P., Salenius, S., & Helle, M. (1997). Magnetoencephalographic cortical rhythms. *International Journal of Psychophysiology*, *26*(1-3), 51–62. doi: 10.1016/s0167-8760(97)00755-1

Hasenstaub, A., Shu, Y., Haider, B., Kraushaar, U., Duque, A., & McCormick, D. A. (2005). Inhibitory postsynaptic potentials carry synchronized frequency information in active cortical networks. *Neuron*, *47*(3), 423–435. doi: 10.1016/j.neuron.2005.06.016

He, S.-Q., Dum, R. P., & Strick, P. L. (1993). Topographic organization of corticospinal projections from the frontal lobe: motor areas on the lateral surface of the hemisphere. *Journal of Neuroscience*, *13*(3), 952–980. doi: 10.1523/jneurosci.13-03-00952.1993

Heidegger, T., Krakow, K., & Ziemann, U. (2010, aug). Effects of antiepileptic drugs on associative LTP-like plasticity in human motor cortex. *European Journal of Neuroscience*, *32*(7), 1215–1222. doi: 10.1111/j.1460-9568.2010.07375.x

Heimer, G., Rivlin-Etzion, M., Bar-Gad, I., Goldberg, J. A., Haber, S. N., & Bergman, H. (2006). Dopamine replacement therapy does not restore the full spectrum of normal pallidal activity in the 1-methyl-4-phenyl-1,2,3,6-tetra-hydropyridine primate model of Parkinsonism. *Journal of Neuroscience*, *26*(31), 8101–8114. doi: 10.1523/jneurosci.5140-05.2006

Heinrichs-Graham, E., Arpin, D. J., & Wilson, T. W. (2016). Cue-related temporal factors modulate movement-related beta oscillatory activity in the human motor circuit. *Journal of Cognitive Neuroscience*, *28*(7), 1039–1051. doi: 10.1162/jocn_a_00948

Heinrichs-Graham, E., Kurz, M. J., Becker, K. M., Santamaria, P. M., Gendelman, H. E., & Wilson, T. W. (2014a). Hypersynchrony despite pathologically reduced beta oscillations in patients with Parkinson's disease: a pharmaco-magnetoencephalography study. *Journal of Neurophysiology*, *112*(7), 1739–1747. doi: 10.1152/jn.00383.2014

Heinrichs-Graham, E., Kurz, M. J., Gehringer, J. E., & Wilson, T. W. (2017). The functional role of post-movement beta oscillations in motor termination. *Brain Structure and Function*, *222*(7), 3075–3086. doi: 10.1007/s00429-017-1387-1

Heinrichs-Graham, E., McDermott, T. J., Mills, M. S., Wiesman, A. I., Wang, Y.-P., Stephen, J. M., ... Wilson, T. W. (2018). The lifespan trajectory of neural oscillatory activity in the motor system. *Developmental Cognitive Neuroscience*, *30*, 159–168. doi: 10.1016/j.dcn.2018.02.013

Heinrichs-Graham, E., & Wilson, T. W. (2015). Coding complexity in the human motor circuit. *Human Brain Mapping*, *36*(12), 5155–5167. doi: 10.1002/hbm.23000

Heinrichs-Graham, E., & Wilson, T. W. (2016). Is an absolute level of cortical beta suppression required for proper movement? Magnetoencephalographic evidence from healthy aging. *NeuroImage*, *134*, 514–521. doi: 10.1016/j.neuroimage.2016.04.032

Heinrichs-Graham, E., Wilson, T. W., Santamaria, P. M., Heithoff, S. K., Torres-Russotto, D., Hutter-Saunders, J. A. L., ... Gendelman, H. E. (2014b). Neuromagnetic evidence of abnormal movement-related beta desynchronization in Parkinson's disease. *Cerebral Cortex*, *24*(10), 2669–2678. doi: 10.1093/cercor/bht121

Helfrich, R. F., Schneider, T. R., Rach, S., Trautmann-Lengsfeld, S. A., Engel, A. K., & Herrmann, C. S. (2014). Entrainment of brain oscillations by transcranial alternating current stimulation. *Current Biology*, *24*(3), 333–339. doi: 10.1016/j.cub.2013.12.041

Hensch, T. K. (2005). Critical period plasticity in local cortical circuits. *Nature Reviews Neuroscience*, *6*(11), 877–888. doi: 10.1038/nrn1787

Hines, M. (1929). On cerebral localization. *Physiological Reviews*, *9*(3), 462–574. doi: 10.1113/jphysiol.1882.sp000107

Hluštík, P., Solodkin, A., Gullapalli, R. P., Noll, D. C., & Small, S. L. (2001). Somatotopy in human primary motor and somatosensory hand representations revisited. *Cerebral Cortex*, *11*(4), 312–321. doi: 10.1093/cercor/11.4.312

Hodgkin, A. L., & Huxley, A. F. (1952). A quantitative description of membrane current and its application to conductance and excitation in nerve. *Journal of Physiology*, *117*, 500. doi: 10.1113/jphysiol.1952.sp004764

Hogeveen, J., Grafman, J., Aboseria, M., David, A., Bikson, M., & Hauner, K. K. (2016). Effects of high-definition and conventional tDCS on response inhibition. *Brain Stimulation*, *9*(5), 720–729. doi: 10.1016/j.brs.2016.04.015

Hommelsen, M., Schneiders, M., Schuld, C., Keyl, P., & Rupp, R. (2017). Sensory feedback interferes with mu rhythm based detection of motor commands from

electroencephalographic signals. *Frontiers in Human Neuroscience*, *11*. doi: 10.3389/fnhum.2017.00523

Hooks, B. M., Mao, T., Gutnisky, D. A., Yamawaki, N., Svoboda, K., & Shepherd, G. M. G. (2013). Organization of cortical and thalamic input to pyramidal neurons in mouse motor cortex. *Journal of Neuroscience*, *33*(2), 748–760. doi: 10.1523/JNEUROSCI.4338-12.2013

Howard, I. S., Ingram, J. N., Franklin, D. W., & Wolpert, D. M. (2012). Gone in 0.6 seconds: the encoding of motor memories depends on recent sensorimotor states. *Journal of Neuroscience*, *32*(37), 12756–12768. doi: 10.1523/jneurosci.5909-11.2012

Huang, Y.-Z., Edwards, M. J., Rounis, E., Bhatia, K. P., & Rothwell, J. C. (2005). Theta burst stimulation of the human motor cortex. *Neuron*, *45*(2), 201–206. doi: 10.1016/j.neuron.2004.12.033

Huber, P. J., & Ronchetti, E. M. (1981). *Robust statistics*. New York: John Wiley. doi: 10.1002/0471725250

Huesler, E. J., Hepp-Reymond, M. C., & Dietz, V. (1998). Task dependence of muscle synchronization in human hand muscles. *Neuroreport*, *9*(10), 2167–2170. doi: 10.1097/00001756-199807130-00003

Hutcheon, B., & Yarom, Y. (2000). Resonance, oscillation and the intrinsic frequency preferences of neurons. *Trends in Neurosciences*, *23*(5), 216–222. doi: 10.1016/S0166-2236(00)01547-2

Hutchins, K. D., Martino, A. M., & Strick, P. L. (1988). Corticospinal projections from the medial wall of the hemisphere. *Experimental Brain Research*, *71*(3), 667–672. doi: 10.1007/BF00248761

Hutchison, W. D., Dostrovsky, J. O., Walters, J. R., Courtemanche, R., Boraud, T., Goldberg, J., & Brown, P. (2004). Neuronal oscillations in the basal ganglia and movement disorders: evidence from whole animal and human recordings. *Journal of Neuroscience*, *24*(42), 9240–9243. doi: 10.1523/jneurosci.3366-04.2004

Ilmoniemi, F. J., Ruohonen, J., & Karhu, J. (1999). Transcranial magnetic stimulation–A new tool for functional imaging. *Critical Reviews in Biomedical Engineering*, *27*(3-5), 241–284.

Ilmoniemi, R. J., & Kičić, D. (2010, January). Methodology for Combined TMS and EEG. *Brain Topography*, *22*(4), 233–248. doi: 10.1007/s10548-009-0123-4

Inase, M., Tokuno, H., Nambu, A., Akazawa, T., & Takada, M. (1999). Corticostriatal and corticosubthalamic input zones from the presupplementary motor area in the macaque monkey: comparison with the input zones from the supplementary motor area. *Brain Research*, *833*(2), 191–201. doi: 10.1016/S0006-8993(99)01531-0

Indovina, I., & Sanes, J. N. (2001). On somatotopic representation centers for finger movements in human primary motor cortex and supplementary motor area. *NeuroImage*, *13*(6), 1027–1034. doi: 10.1006/nimg.2001.0776

Innocenti, G. M., Lehmann, P., & Houzel, J.-C. (1994). Computational structure of visual callosal axons. *European Journal of Neuroscience*, *6*(6), 918–935. doi: 10.1111/j.1460-9568.1994.tb00586.x

Isomura, Y., Harukuni, R., Takekawa, T., Aizawa, H., & Fukai, T. (2009). Microcircuitry coordination of cortical motor information in self-initiation of voluntary movements. *Nature Neuroscience*, *12*(12), 1586–1593. doi: 10.1038/nn.2431

Ito, M. (1984). *The cerebellum and neural control*. New York: Raven. doi: 10.1126/science.229.4713.547

Jasper, H., & Penfield, W. (1949). Electrocorticograms in man: Effect of voluntary movement upon the electrical activity of the precentral gyrus. *Archiv für Psychiatrie und Nervenkrankheiten*, *183*(1-2), 163–174. doi: 10.1007/bf01062488

Jasper, H. H., & Andrews, H. L. (1938). Brain potentials and voluntary muscle activity in man. *Journal of Neurophysiology*, *1*(2), 87–100. doi: 10.1152/jn.1938.1.2.87

Jeljeli, M., Strazielle, C., Caston, J., & Lalonde, R. (2003). Effects of ventrolateral-ventromedial thalamic lesions on motor coordination and spatial orientation in rats. *Neuroscience Research*, *47*(3), 309–316. doi: 10.1016/S0168-0102(03)00224-4

Jenkins, I. H., Jahanshahi, M., Jueptner, M., Passingham, R. E., & Brooks, D. J. (2000). Self-initiated versus externally triggered movements: II. The effect of movement predictability on regional cerebral blood flow. *Brain*, *123*(6), 1216–1228. doi: 10.1093/brain/123.6.1216

Jenkinson, N., & Brown, P. (2011). New insights into the relationship between dopamine, beta oscillations and motor function. *Trends in Neurosciences*, *34*(12), 611–618. doi: 10.1016/j.tins.2011.09.003

Jensen, O., Goel, P., Kopell, N., Pohja, M., Hari, R., & Ermentrout, B. (2005). On the human sensorimotor-cortex beta rhythm: Sources and modeling. *NeuroImage*, *26*(2), 347–355. doi: 10.1016/j.neuroimage.2005.02.008

Jensen, O., Kaiser, J., & Lachaux, J.-P. (2007). Human gamma-frequency oscillations associated with attention and memory. *Trends in Neurosciences*, *30*(7), 317–324. doi: 10.1016/j.tins.2007.05.001

Jensen, O., & Mazaheri, A. (2010). Shaping functional architecture by oscillatory alpha activity: Gating by inhibition. *Frontiers in Human Neuroscience*, *4*. doi: 10.3389/fnhum.2010.00186

Johnson, P. B., Ferraina, S., Bianchi, L., & Caminiti, R. (1996). Cortical networks for visual reaching: physiological and anatomical organization of frontal and parietal lobe arm regions. *Cerebral Cortex*, *6*(2), 102–119. doi: 10.1093/cercor/6.2.102

Joundi, R. A., Brittain, J.-S., Green, A. L., Aziz, T. Z., Brown, P., & Jenkinson, N. (2012). Oscillatory activity in the subthalamic nucleus during arm reaching in Parkinson's disease. *Experimental Neurology*, *236*(2), 319–326. doi: 10.1016/j.expneurol.2012.05.013

Jurkiewicz, M. T., Gaetz, W. C., Bostan, A. C., & Cheyne, D. (2006). Post-movement beta rebound is generated in motor cortex: evidence from neuromagnetic recordings. *NeuroImage*, *32*(3), 1281–1289. doi: 10.1016/j.neuroimage.2006.06.005

Kaas, J. H. (2004). Evolution of somatosensory and motor cortex in primates. *The Anatomical Record*, *281A*(1), 1148–1156. doi: 10.1002/ar.a.20120

Kaas, J. H., & Stephniewska, I. (2002). Motor cortex. In V. S. Ramachandran (Ed.), *Encyclopedia of the human brain* (pp. 159–169). Elsevier Science. doi: 10.1016/B0-12-227210-2/00217-X

Kaiser, J., Birbaumer, N., & Lutzenberger, W. (2001). Event-related beta desynchronization indicates timing of response selection in a delayed-response paradigm in humans. *Neuroscience Letters*, *312*(3), 149–152. doi: 10.1016/s0304-3940(01)02217-0

Kaneko, T., Cho, R.-H., Li, Y.-Q., Nomura, S., & Mizuno, N. (2000). Predominant information transfer from layer III pyramidal neurons to corticospinal neurons. *Journal of Comparative Neurology*, *423*(1), 52–65. doi: 10.1002/1096-9861(20000717)423:1<52::AID-CNE5>3.0.CO;2-F

Karayannis, T., Huerta-Ocampo, I., & Capogna, M. (2006). GABAergic and pyramidal neurons of deep cortical layers directly receive and differently integrate callosal input. *Cerebral Cortex*, *17*(5), 1213–1226. doi: 10.1093/cercor/bhl035

Karnath, H.-O., & Perenin, M.-T. (2005). Cortical control of visually guided reaching: evidence from patients with optic ataxia. *Cerebral Cortex*, *15*(10), 1561–1569. doi: 10.1093/cercor/bhi034

Kawaguchi, Y., & Kubota, Y. (1997). GABAergic cell subtypes and their synaptic connections in rat frontal cortex. *Cerebral Cortex*, *7*(6), 476–486. doi: 10.1093/cercor/7.6.476

Kawaguchi, Y., & Kubota, Y. (1998). Neurochemical features and synaptic connections of large physiologically-identified GABAergic cells in the rat frontal cortex. *Neuroscience*, *85*(3), 677–701. doi: 10.1016/S0306-4522(97)00685-4

Keller, A. (1993). Intrinsic synaptic organization of the motor cortex. *Cerebral Cortex*, *3*(5), 430–441. doi: 10.1093/cercor/3.5.430

Kiebel, S. J., Tallon-Baudry, C., & Friston, K. J. (2005). Parametric analysis of oscillatory activity as measured with EEG/MEG. *Human Brain Mapping*, *26*(3), 170–177. doi: 10.1002/hbm.20153

Kilner, J. M., Vargas, C., Duval, S., Blakemore, S.-J., & Sirigu, A. (2004). Motor activation prior to observation of a predicted movement. *Nature Neuroscience*, *7*(12), 1299–1301. doi: 10.1038/nn1355

Kim, S., Stephenson, M. C., Morris, P. G., & Jackson, S. R. (2014). tDCS-induced alterations in GABA concentration within primary motor cortex predict motor learning and motor memory: a 7T magnetic resonance spectroscopy study. *NeuroImage*, *99*, 237–243. doi: 10.1016/j.neuroimage.2014.05.070

Kimiskidis, V. K., Papagiannopoulos, S., Kazis, D. A., Sotirakoglou, K., Vasiliadis, G., Zara, F., ... Mills, K. R. (2006). Lorazepam-induced effects on silent period and corticomotor excitability. *Experimental Brain Research*, *173*(4), 603–611. doi: 10.1007/s00221-006-0402-1

Kitano, K., & Fukai, T. (2007). Variability v.s. synchronicity of neuronal activity in local cortical network models with different wiring topologies. *Journal of Computational Neuroscience*, *23*(2), 237–250. doi: 10.1007/s10827-007-0030-1

Klein, P.-A., Duque, J., Labruna, L., & Ivry, R. B. (2016). Comparison of the two cerebral hemispheres in inhibitory processes operative during movement preparation. *NeuroImage*, *125*, 220–232. doi: 10.1016/j.neuroimage.2015.10.007

Klockgether, T., Schwarz, M., Turski, L., & Sontag, K.-H. (1986). The rat ventromedial thalamic nucleus and motor control: role of N-methyl-D-aspartate-mediated excitation, GABAergic inhibition, and muscarinic transmission. *Journal of Neuroscience*, *6*(6), 1702–1711. doi: 10.1523/jneurosci.06-06-01702.1986

Klomjai, W., Katz, R., & Lackmy-Vallée, A. (2015). Basic principles of transcranial magnetic stimulation (TMS) and repetitive TMS (rTMS). *Annals of Physical and Rehabilitation Medicine*, *58*(4), 208–213. doi: 10.1016/j.rehab.2015.05.005

Klostermann, F., Nikulin, V. V., Kühn, A. A., Marzinzik, F., Wahl, M., Pogosyan, A., ... Curio, G. (2007). Task-related differential dynamics of EEG alpha-and beta-band synchronization in cortico-basal motor structures. *European Journal of Neuroscience*, *25*(5), 1604–1615. doi: 10.1111/j.1460-9568.2007.05417.x

Kobayashi, M., & Pascual-Leone, A. (2003). Transcranial magnetic stimulation in neurology. *The Lancet Neurology*, *2*(3), 145–156. doi: 10.1016/s1474-4422(03)00321-1

Koechlin, E., Ody, C., & Kouneiher, F. (2003). The architecture of cognitive control in the human prefrontal cortex. *Science*, *302*(5648), 1181–1185. doi: 10.1126/science.1088545

Koechlin, E., & Summerfield, C. (2007). An information theoretical approach to prefrontal executive function. *Trends in Cognitive Sciences*, *11*(6), 229–235. doi: 10.1016/j.tics.2007.04.005

Koelewijn, T., van Schie, H. T., Bekkering, H., Oostenveld, R., & Jensen, O. (2008). Motor-cortical beta oscillations are modulated by correctness of observed action. *NeuroImage*, *40*(2), 767–775. doi: 10.1016/j.neuroimage.2007.12.018

Kopell, N., Ermentrout, G. B., Whittington, M. A., & Traub, R. D. (2000). Gamma rhythms and beta rhythms have different synchronization properties. *Proceedings of the National Academy of Sciences*, *97*(4), 1867–1872. doi: 10.1073/pnas.97.4.1867

Koyama, M., Hasegawa, I., Osada, T., Adachi, Y., Nakahara, K., & Miyashita, Y. (2004). Functional magnetic resonance imaging of macaque monkeys performing visually guided saccade tasks. *Neuron*, *41*(5), 795–807. doi: 10.1016/S0896-6273(04)00047-9

Kravitz, A. V., Freeze, B. S., Parker, P. R. L., Kay, K., Thwin, M. T., Deisseroth, K., & Kreitzer, A. C. (2010). Regulation of parkinsonian motor behaviors by optogenetic control of basal ganglia circuitry. *Nature*, *466*(7306), 622. doi: 10.1038/nature09159.Regulation

Krubitzer, L., & Huffman, K. J. (2000). Arealization of the neocortex in mammals: genetic and epigenetic contributions to the phenotype. *Brain, Behavior and Evolution*, *55*(6), 322–335. doi: 10.1159/000006667

Kühn, A. A., Kempf, F., Brücke, C., Doyle, L. G., Martinez-Torres, I., Pogosyan, A., ... others (2008). High-frequency stimulation of the subthalamic nucleus suppresses oscillatory β activity in patients with Parkinson's disease in parallel with improvement in motor performance. *Journal of Neuroscience*, *28*(24), 6165–6173. doi: 10.1523/JNEUROSCI.0282-08.2008

Kühn, A. A., Kupsch, A., Schneider, G.-H., & Brown, P. (2006). Reduction in subthalamic 8–35 Hz oscillatory activity correlates with clinical improvement in Parkinson's disease. *European Journal of Neuroscience*, *23*(7), 1956–1960. doi: 10.1111/j.1460-9568.2006.04717.x

Kühn, A. A., Trottenberg, T., Kivi, A., Kupsch, A., Schneider, G.-H., & Brown, P. (2005). The relationship between local field potential and neuronal discharge in the subthalamic nucleus of patients with Parkinson's disease. *Experimental Neurology*, *194*(1), 212–220. doi: 10.1016/j.expneurol.2005.02.010

Kühn, A. A., Tsui, A., Aziz, T., Ray, N., Brücke, C., Kupsch, A., ... Brown, P. (2009). Pathological synchronisation in the subthalamic nucleus of patients with Parkinson's disease relates to both bradykinesia and rigidity. *Experimental Neurology*, *215*(2), 380–387. doi: 10.1016/j.expneurol.2008.11.008

Kühn, A. A., Williams, D., Kupsch, A., Limousin, P., Hariz, M., Schneider, G.-H., ... Brown, P. (2004). Event-related beta desynchronization in human subthalamic nucleus correlates with motor performance. *Brain*, *127*(4), 735–746. doi: 10.1093/brain/awh106

Kuo, H.-I., Bikson, M., Datta, A., Minhas, P., Paulus, W., Kuo, M.-F., & Nitsche, M. A. (2013). Comparing cortical plasticity induced by conventional and high-definition 4x1 ring tDCS: a neurophysiological study. *Brain Stimulation*, *6*(4), 644–648. doi: 10.1016/j.brs.2012.09.010

Laaksonen, K., Helle, L., Parkkonen, L., Kirveskari, E., Mäkelä, J. P., Mustanoja, S., ... Forss, N. (2013). Alterations in spontaneous brain oscillations during stroke recovery. *PLoS ONE*, *8*(4), 61146. doi: 10.1371/journal.pone.0061146

Labyt, E., Szurhaj, W., Bourriez, J.-L., Cassim, F., Defebvre, L., Destée, A., ... Derambure, P. (2003). Changes in oscillatory cortical activity related to a visuomotor task in young and elderly healthy subjects. *Clinical Neurophysiology*, *114*(6), 1153–1166. doi: 10.1016/s1388-2457(03)00058-0

Lachaux, J.-P., George, N., Tallon-Baudry, C., Martinerie, J., Hugueville, L., Minotti, L., ... Renault, B. (2005). The many faces of the gamma band response to complex visual stimuli. *NeuroImage*, *25*(2), 491–501. doi: 10.1016/j.neuroimage.2004.11.052

Lago-Fernández, L. F., Huerta, R., Corbacho, F., & Sigüenza, J. A. (2000). Fast response and temporal coherent oscillations in small-world networks. *Physical Review Letters*, *84*(12), 2758–2761. doi: 10.1103/physrevlett.84.2758

Lampl, I., & Yarom, Y. (1993). Subthreshold oscillations of the membrane potential: a functional synchronizing and timing device. *Journal of Neurophysiology*, *70*(5), 2181–2186. doi: 10.1152/jn.1993.70.5.2181

Lang, N., Siebner, H. R., Ward, N. S., Lee, L., Nitsche, M. A., Paulus, W., ... Frackowiak, R. S. (2005). How does transcranial DC stimulation of the primary motor cortex alter regional neuronal activity in the human brain? *European Journal of Neuroscience*, *22*(2), 495–504. doi: 10.1111/j.1460-9568.2005.04233.x

Larimer, P., & Strowbridge, B. W. (2008). Nonrandom local circuits in the dentate gyrus. *Journal of Neuroscience*, *28*(47), 12212–12223. doi: 10.1523/jneurosci.3612-08.2008

Larsell, O. (1970). *Comparative anatomy and histology of the cerebellum*. Minneapolis: University of Minnesota Press.

Lefort, S., Tomm, C., Sarria, J.-C. F., & Petersen, C. C. H. (2009). The excitatory neuronal network of the c2 barrel column in mouse primary somatosensory cortex. *Neuron*, *61*(2), 301–316. doi: 10.1016/j.neuron.2008.12.020

Leocani, L., Cohen, L. G., Wassermann, E. M., Ikoma, K., & Hallett, M. (2000). Human corticospinal excitability evaluated with transcranial magnetic stimulation during different reaction time paradigms. *Brain*, *123*(6), 1161–1173. doi: 10.1093/brain/123.6.1161

Leocani, L., Toro, C., Manganotti, P., Zhuang, P., & Hallett, M. (1997). Event-related coherence and event-related desynchronization/synchronization in the 10 Hz

and 20 Hz EEG during self-paced movements. *Electroencephalography and Clinical Neurophysiology/Evoked Potentials Section*, *104*(3), 199–206. doi: 10.1016/S0168-5597(96)96051-7

Lepage, J.-F., Saint-Amour, D., & Théoret, H. (2008). EEG and neuronavigated single-pulse TMS in the study of the observation/execution matching system: are both techniques measuring the same process? *Journal of Neuroscience Methods*, *175*(1), 17–24. doi: 10.1016/j.jneumeth.2008.07.021

Levy, R., Hutchison, W. D., Lozano, A. M., & Dostrovsky, J. O. (2000). High-frequency synchronization of neuronal activity in the subthalamic nucleus of parkinsonian patients with limb tremor. *The Journal of Neuroscience*, *20*(20), 7766–7775. doi: 10.1523/jneurosci.20-20-07766.2000

Levy, R., Hutchison, W. D., Lozano, A. M., & Dostrovsky, J. O. (2002). Synchronized neuronal discharge in the basal ganglia of parkinsonian patients is limited to oscillatory activity. *The Journal of Neuroscience*, *22*(7), 2855–2861. doi: 10.1523/jneurosci.22-07-02855.2002

Leys, C., Ley, C., Klein, O., Bernard, P., & Licata, L. (2013). Detecting outliers: do not use standard deviation around the mean, use absolute deviation around the median. *Journal of Experimental Social Psychology*, *49*(4), 764–766. doi: 10.1016/j.jesp.2013.03.013

Leyton, A. S. F., & Sherrington, C. S. (1917). Observations on the excitable cortex of the chimpanzee, orang-utan and gorilla. *Quarterly Journal of Experimental Physiology*, *11*(2), 135–222. doi: 10.1113/expphysiol.1917.sp000240

Li, Q., Ke, Y., Chan, D. C. W., Qian, Z.-M., Yung, K. K. L., Ko, H., ... Yung, W.-H. (2012). Therapeutic deep brain stimulation in parkinsonian rats directly influences motor cortex. *Neuron*, *76*(5), 1030–1041. doi: 10.1016/j.neuron.2012.09.032

Little, S., & Brown, P. (2012). What brain signals are suitable for feedback control of deep brain stimulation in Parkinson's disease? *Annals of the New York Academy of Sciences*, *1265*(1), 9–24. doi: 10.1111/j.1749-6632.2012.06650.x

Little, S., Pogosyan, A., Neal, S., Zavala, B., Zrinzo, L., Hariz, M., ... Brown, P. (2013). Adaptive deep brain stimulation in advanced Parkinson disease. *Annals of Neurology*, *74*(3), 449–457. doi: 10.1002/ana.23951

Litvak, V., Eusebio, A., Jha, A., Oostenveld, R., Barnes, G., Foltynie, T., ... Brown, P. (2012). Movement-related changes in local and long-range synchronization in parkinson's disease revealed by simultaneous magnetoencephalography and intracranial recordings. *Journal of Neuroscience*, *32*(31), 10541–10553. doi: 10.1523/jneurosci.0767-12.2012

Liu, H., Shah, S., & Jiang, W. (2004). On-line outlier detection and data cleaning. *Computers & Chemical Engineering*, *28*(9), 1635–1647. doi: 10.1016/j.compchemeng.2004.01.009

Liu, L., Rosjat, N., Popovych, S., Wang, B. A., Yeldesbay, A., Toth, T. I., ... Daun, S. (2017). Age-related changes in oscillatory power affect motor action. *PLOS ONE*, *12*(11), 0187911. doi: 10.1371/journal.pone.0187911

Llinás, R., & Yarom, Y. (1986). Oscillatory properties of guinea-pig inferior olivary neurones and their pharmacological modulation: an in vitro study. *The Journal of Physiology*, *376*(1), 163–182. doi: 10.1113/jphysiol.1986.sp016147

Lobo, I. A., & Harris, R. A. (2008). GABAA receptors and alcohol. *Pharmacology Biochemistry and Behavior*, *90*(1), 90–94. doi: 10.1016/j.pbb.2008.03.006

Lotte, F., Congedo, M., Lécuyer, A., Lamarche, F., & Arnaldi, B. (2007). A review of classification algorithms for EEG-based brain-computer interfaces. *Journal of Neural Engineering*, *4*(2), R1–R13. doi: 10.1088/1741-2560/4/2/r01

Lovick, T. A., Griffiths, J. L., Dunn, S. M. J., & Martin, I. L. (2005, jan). Changes in GABAA receptor subunit expression in the midbrain during the oestrous cycle in Wistar rats. *Neuroscience*, *131*(2), 397–405. doi: 10.1016/j.neuroscience.2004.11.010

Luck, S. J. (2014). *An introduction to the event-related potential technique* (Second ed.). Boston, MA: MIT Press.

Luppino, G., Matelli, M., Camarda, R., & Rizzolatti, G. (1993). Corticocortical connections of area F3 (SMA-proper) and area F6 (pre-SMA) in the macaque monkey. *Journal of Comparative Neurology*, *338*(1), 114–140. doi: 10.1002/cne.903380109

Luppino, G., Matelli, M., Camarda, R., & Rizzolatti, G. (1994). Corticospinal projections from mesial frontal and cingulate areas in the monkey. *Neuroreport*, *5*(18), 2545–2548. doi: 10.1097/00001756-199412000-00035

Luppino, G., Matelli, M., Camarda, R. M., Gallese, V., & Rizzolatti, G. (1991). Multiple representations of body movements in mesial area 6 and the adjacent cingulate cortex: an intracortical microstimulation study in the macaque monkey. *Journal of Comparative Neurology*, *311*(4), 463–482. doi: 10.1002/cne.903110403

MacDonald, D. B., Skinner, S., Shils, J., & Yingling, C. (2013). Intraoperative motor evoked potential monitoring - a position statement by the american society of neurophysiological monitoring. *Clinical Neurophysiology*, *124*(12), 2291–2316. doi: 10.1016/j.clinph.2013.07.025

Macdonell, R. A. L., Jackson, G. D., Curatolo, J. M., Abbott, D. F., Berkovic, S. F., Carey, L. M., ... Scheffer, I. E. (1999). Motor cortex localization using functional MRI and transcranial magnetic stimulation. *Neurology*, *53*(7), 1462–1462. doi: 10.1212/wnl.53.7.1462

MacKay, D. M. (1983). On-line source-density computation with a minimum of electrodes. *Electroencephalography and Clinical Neurophysiology*, *56*(6), 696–698. doi: 10.1016/0013-4694(83)90040-8

MacLeod, C. E., Zilles, K., Schleicher, A., Rilling, J. K., & Gibson, K. R. (2003, apr). Expansion of the neocerebellum in hominoidea. *Journal of Human Evolution*, *44*(4), 401–429. doi: 10.1016/s0047-2484(03)00028-9

Maguire, J. L., Stell, B. M., Rafizadeh, M., & Mody, I. (2005, may). Ovarian cycle–linked changes in GABAA receptors mediating tonic inhibition alter seizure susceptibility and anxiety. *Nature Neuroscience*, *8*(6), 797–804. doi: 10.1038/nn1469

Mäki, H., & Ilmoniemi, R. J. (2010). EEG oscillations and magnetically evoked motor potentials reflect motor system excitability in overlapping neuronal populations. *Clinical Neurophysiology*, *121*(4), 492–501. doi: 10.1016/j.clinph.2009.11.078

Maldonado, P. E., Friedman-Hill, S., & Gray, C. M. (2000). Dynamics of striate cortical activity in the alert macaque: II. Fast time scale synchronization. *Cerebral Cortex*, *10*(11), 1117–1131. doi: 10.1093/cercor/10.11.1117

Manganotti, P., Gerloff, C., Toro, C., Katsuta, H., Sadato, N., Zhuang, P., ... Hallett, M. (1998). Task-related coherence and task-related spectral power changes during sequential finger movements. *Electroencephalography and Clinical Neurophysiology/Electromyography and Motor Control*, *109*(1), 50–62. doi: 10.1016/s0924-980x(97)00074-x

Marder, E., & Bucher, D. (2001). Central pattern generators and the control of rhythmic movements. *Current Biology*, *11*(23), 986–996. doi: 10.1016/S0960-9822(01)00581-4

Matsuzaka, Y., Aizawa, H., & Tanji, J. (1992). A motor area rostral to the supplementary motor area (presupplementary motor area) in the monkey: neuronal activity during a learned motor task. *Journal of Neurophysiology*, *68*(3), 653–662. doi: 10.1152/jn.1992.68.3.653

Mattay, V. S., Fera, F., Tessitore, A., Hariri, A. R., Das, S., Callicott, J. H., & Weinberger, D. R. (2002). Neurophysiological correlates of age-related changes in human motor function. *Neurology*, *58*(4), 630–635. doi: 10.1212/wnl.58.4.630

McAllister, C. J., Ronnqvist, K. C., Stanford, I. M., Woodhall, G. L., Furlong, P. L., & Hall, S. D. (2013). Oscillatory beta activity mediates neuroplastic effects of motor cortex stimulation in humans. *Journal of Neuroscience*, *33*(18), 7919–7927. doi: 10.1523/jneurosci.5624-12.2013

McFarland, D. J. (2000). Mu and beta rhythm topographies during motor imagery and actual movements. *Brain Topography*, *12*(3), 177–186. doi: 10.1023/a:1023437823106

McFarland, N. R., & Haber, S. N. (2002). Thalamic relay nuclei of the basal ganglia form both reciprocal and nonreciprocal cortical connections, linking multiple frontal cortical areas. *Journal of Neuroscience*, *22*(18), 8117–8132. doi: 10.1523/jneurosci.22-18-08117.2002

Meckler, C., Allain, S., Carbonnell, L., Hasbroucq, T., Burle, B., & Vidal, F. (2010). Motor inhibition and response expectancy: a laplacian ERP study. *Biological Psychology*, *85*(3), 386–392. doi: 10.1016/j.biopsycho.2010.08.011

Medendorp, W. P., Goltz, H. C., Vilis, T., & Crawford, J. D. (2003). Gaze-centered updating of visual space in human parietal cortex. *Journal of Neuroscience*, *23*(15), 6209–6214. doi: 10.1523/jneurosci.23-15-06209.2003

Merchant, H., Naselaris, T., & Georgopoulos, A. P. (2008). Dynamic sculpting of directional tuning in the primate motor cortex during three-dimensional reaching. *Journal of Neuroscience*, *28*(37), 9164–9172. doi: 10.1523/JNEUROSCI.1898-08.2008

Merlet, I., Birot, G., Salvador, R., Molaee-Ardekani, B., Mekonnen, A., Soria-Frish, A., ... Wendling, F. (2013). From oscillatory transcranial current stimulation to scalp EEG changes: a biophysical and physiological modeling study. *PLoS ONE*, *8*(2), 57330. doi: 10.1371/journal.pone.0057330

Merton, P. A., & Morton, H. B. (1980). Stimulation of the cerebral cortex in the intact human subject. *Nature*, *285*(5762), 227–227. doi: 10.1038/285227a0

Michalareas, G., Vezoli, J., Van Pelt, S., Schoffelen, J.-M., Kennedy, H., & Fries, P. (2016). Alpha-beta and gamma rhythms subserve feedback and feedforward influences among human visual cortical areas. *Neuron*, *89*(2), 384–397. doi: 10.1016/j.neuron.2015.12.018

Miller, K. J., Schalk, G., Fetz, E. E., Den Nijs, M., Ojemann, J. G., & Rao, R. P. N. (2010). Cortical activity during motor execution, motor imagery, and imagery-based online feedback. *Proceedings of the National Academy of Sciences*, *107*(9), 4430–4435. doi: 10.1073/pnas.0913697107

Miller, K. J., Zanos, S., Fetz, E. E., den Nijs, M., & Ojemann, J. G. (2009). Decoupling the cortical power spectrum reveals real-time representation of individual finger movements in humans. *Journal of Neuroscience*, *29*(10), 3132–3137. doi: 10.1523/jneurosci.5506-08.2009

Miller, R. (2007). Theory of the normal waking EEG: From single neurones to waveforms in the alpha, beta and gamma frequency ranges. *International Journal of Psychophysiology*, *64*(1), 18–23. doi: 10.1016/j.ijpsycho.2006.07.009

Mitz, A. R., & Wise, S. P. (1987). The somatotopic organization of the supplementary motor area: intracortical microstimulation mapping. *Journal of Neuroscience*, *7*(4), 1010–1021. doi: 10.1523/jneurosci.07-04-01010.1987

Molinari, M. (2002). Cerebellum. In V. S. Ramachandran (Ed.), *Encyclopedia of the human brain* (pp. 611–628). Elsevier. doi: 10.1016/B0-12-227210-2/00084-4

Molnár, Z., & Cheung, A. F. P. (2006). Towards the classification of subpopulations of layer V pyramidal projection neurons. *Neuroscience Research*, *55*(2), 105–115. doi: 10.1016/j.neures.2006.02.008

Morecraft, R. J., Schroeder, C. M., & Keifer, J. (1996). Organization of face representation in the cingulate cortex of the rhesus monkey. *Neuroreport*, *7*(8), 1343–1348. doi: 10.1097/00001756-199605310-00002

Moreno-Duarte, I., Gebodh, N., Schestatsky, P., Guleyupoglu, B., Reato, D., Bikson, M., & Fregni, F. (2014). Transcranial electrical stimulation. In *The stimulated brain* (pp. 35–59). Elsevier. doi: 10.1016/b978-0-12-404704-4.00002-8

Morgan, R. J., & Soltesz, I. (2008). Nonrandom connectivity of the epileptic dentate gyrus predicts a major role for neuronal hubs in seizures. *Proceedings of the National Academy of Sciences*, *105*(16), 6179–6184. doi: 10.1073/pnas.0801372105

Murakami, S., & Okada, Y. (2006). Contributions of principal neocortical neurons to magnetoencephalography and electroencephalography signals. *The Journal of Physiology*, *575*(3), 925–936. doi: 10.1113/jphysiol.2006.105379

Murata, A., Gallese, V., Luppino, G., Kaseda, M., & Sakata, H. (2000). Selectivity for the shape, size, and orientation of objects for grasping in neurons of monkey parietal area AIP. *Journal of Neurophysiology*, *83*(5), 2580–2601. doi: 10.1152/jn.2000.83.5.2580

Müri, R. M., Iba-Zizen, M. T., Derosier, C., Cabanis, E. A., & Pierrot-Deseilligny, C. (1996). Location of the human posterior eye field with functional magnetic resonance imaging. *Journal of Neurology, Neurosurgery & Psychiatry*, *60*(4), 445–448. doi: 10.1136/jnnp.60.4.445

Murthy, V. N., & Fetz, E. E. (1992). Coherent 25-to 35-Hz oscillations in the sensorimotor cortex of awake behaving monkeys. *Proceedings of the National Academy of Sciences*, *89*(12), 5670–5674. doi: 10.1073/pnas.89.12.5670

Muthalib, M., Besson, P., Rothwell, J., Ward, T., & Perrey, S. (2016). Effects of anodal high-definition transcranial direct current stimulation on bilateral sensorimotor cortex activation during sequential finger movements: an fNIRS study. In *Advances in experimental medicine and biology* (pp. 351–359). Springer New York. doi: 10.1007/978-1-4939-3023-4_44

Muthukumaraswamy, S. D. (2010). Functional properties of human primary motor cortex gamma oscillations. *Journal of Neurophysiology*, *104*(5), 2873–2885. doi: 10.1152/jn.00607.2010

Muthukumaraswamy, S. D., Myers, J. F. M., Wilson, S. J., Nutt, D. J., Lingford-Hughes, A., Singh, K. D., & Hamandi, K. (2013). The effects of elevated endogenous GABA levels on movement-related network oscillations. *NeuroImage*, *66*, 36–41. doi: 10.1016/j.neuroimage.2012.10.054

Nachev, P., Kennard, C., & Husain, M. (2008). Functional role of the supplementary and pre-supplementary motor areas. *Nature Reviews Neuroscience*, *9*(11), 856. doi: 10.1038/nrn2478

Nakajima, K., Maier, M. A., Kirkwood, P. A., & Lemon, R. N. (2000, aug). Striking differences in transmission of corticospinal excitation to upper limb motoneurons

in two primate species. *Journal of Neurophysiology*, *84*(2), 698–709. doi: 10.1152/jn.2000.84.2.698

Nambu, A., Takada, M., Inase, M., & Tokuno, H. (1996). Dual somatotopical representations in the primate subthalamic nucleus: evidence for ordered but reversed body-map transformations from the primary motor cortex and the supplementary motor area. *Journal of Neuroscience*, *16*(8), 2671–2683. doi: 10.1523/jneurosci.16-08-02671.1996

Neuling, T., Rach, S., & Herrmann, C. S. (2013). Orchestrating neuronal networks: sustained after-effects of transcranial alternating current stimulation depend upon brain states. *Frontiers in Human Neuroscience*, *7*. doi: 10.3389/fnhum.2013.00161

Neuper, C., & Pfurtscheller, G. (2001a). Event-related dynamics of cortical rhythms: frequency-specific features and functional correlates. *International Journal of Psychophysiology*, *43*(1), 41–58. doi: 10.1016/s0167-8760(01)00178-7

Neuper, C., & Pfurtscheller, G. (2001b). Evidence for distinct beta resonance frequencies in human EEG related to specific sensorimotor cortical areas. *Clinical Neurophysiology*, *112*(11), 2084–2097. doi: 10.1016/s1388-2457(01)00661-7

Nikouline, V. V., Linkenkaer-Hansen, K., Wikström, H., Kesäniemi, M., Antonova, E. V., Ilmoniemi, R. J., & Huttunen, J. (2000). Dynamics of mu-rhythm suppression caused by median nerve stimulation: a magnetoencephalographic study in human subjects. *Neuroscience Letters*, *294*(3), 163–166. doi: 10.1016/s0304-3940(00)01562-7

Nitsche, M. A., Cohen, L. G., Wassermann, E. M., Priori, A., Lang, N., Antal, A., ... Pascual-Leone, A. (2008). Transcranial direct current stimulation: state of the art 2008. *Brain Stimulation*, *1*(3), 206–223. doi: 10.1016/j.brs.2008.06.004

Nitsche, M. A., Doemkes, S., Karaköse, T., Antal, A., Liebetanz, D., Lang, N., ... Paulus, W. (2007). Shaping the effects of transcranial direct current stimulation of the human motor cortex. *Journal of Neurophysiology*, *97*(4), 3109–3117. doi: 10.1152/jn.01312.2006

Nitsche, M. A., Fricke, K., Henschke, U., Schlitterlau, A., Liebetanz, D., Lang, N., ... Paulus, W. (2003). Pharmacological modulation of cortical excitability shifts induced by transcranial direct current stimulation in humans. *The Journal of Physiology*, *553*(1), 293–301. doi: 10.1113/jphysiol.2003.049916

Nitsche, M. A., & Paulus, W. (2011). Transcranial direct current stimulation - update 2011. *Restorative Neurology and Neuroscience*, *29*(6), 463–492. doi: 10.3233/rnn-2011-0618

Noh, N. A., Fuggetta, G., Manganotti, P., & Fiaschi, A. (2012). Long lasting modulation of cortical oscillations after continuous theta burst transcranial magnetic stimulation. *PLoS ONE*, *7*(4), 35080. doi: 10.1371/journal.pone.0035080

Nomura, T., Takeshima, T., & Nakashima, K. (2001). Reduced pre-movement facilitation of motor evoked potentials in spinocerebellar degeneration. *Journal of the Neurological Sciences*, *187*(1-2), 41–47. doi: 10.1016/s0022-510x(01)00522-6

Nudo, R. J., Milliken, G. W., Jenkins, W. M., & Merzenich, M. M. (1996). Use-dependent alterations of movement representations in primary motor cortex of adult squirrel monkeys. *Journal of Neuroscience*, *16*(2), 785–807. doi: 10.1523/jneurosci.16-02-00785.1996

Nunez, P. L., & Srinivasan, R. (2006). *Electric fields of the brain: The neurophysics of EEG*. New York: Oxford University Press. doi: 10.1093/acprof:oso/9780195050387.001.0001

Oberman, L. (2014). Repetitive transcranial magnetic stimulation (rTMS) protocols. In A. Rotenberg, J. Horvath, & A. Pascual-Leone (Eds.), *Transcranial magnetic stimulation* (Vol. 89, pp. 129–139). New York: Springer New York. doi: 10.1007/978-1-4939-0879-0_7

Ohara, S., Ikeda, A., Kunieda, T., Yazawa, S., Baba, K., Nagamine, T., ... Shibasaki, H. (2000). Movement-related change of electrocorticographic activity in human supplementary motor area proper. *Brain*, *123*(6), 1203–1215. doi: 10.1093/brain/123.6.1203

Oliviero, A., Profice, P., Tonali, P. A., Pilato, F., Saturno, E., Dileone, M., ... Lazzaro, V. D. (2006). Effects of aging on motor cortex excitability. *Neuroscience Research*, *55*(1), 74–77. doi: 10.1016/j.neures.2006.02.002

Olman, C. A., Pickett, K. A., Schallmo, M.-P., & Kimberley, T. J. (2012). Selective BOLD responses to individual finger movement measured with fMRI at 3T. *Human brain mapping*, *33*(7), 1594–1606. doi: 10.1002/hbm.21310

Oostenveld, R., Fries, P., Maris, E., & Schoffelen, J. M. (2011). FieldTrip: Open source software for advanced analysis of MEG, EEG and invasive electrophysiological data. *Computational Intelligence and Neuroscience*. doi: 10.1155/2011/156869

Opitz, A., Legon, W., Rowlands, A., Bickel, W. K., Paulus, W., & Tyler, W. J. (2013). Physiological observations validate finite element models for estimating subject-specific electric field distributions induced by transcranial magnetic stimulation of the human motor cortex. *NeuroImage*, *81*, 253–264. doi: 10.1016/j.neuroimage.2013.04.067

Oppenheim, A. V., & Schafer, R. W. (2013). *Discrete-time signal processing* (International ed.). Harlow, UK: Pearson Higher Ed. doi: 10.1016/b978-075067291-7/50030-3

Orban, G. A., Essen, D. V., & Vanduffel, W. (2004, jul). Comparative mapping of higher visual areas in monkeys and humans. *Trends in Cognitive Sciences*, *8*(7), 315–324. doi: 10.1016/j.tics.2004.05.009

Orth, M., & Rothwell, J. C. (2004). The cortical silent period: intrinsic variability and relation to the waveform of the transcranial magnetic stimulation pulse. *Clinical Neurophysiology*, *115*(5), 1076–1082. doi: 10.1016/j.clinph.2003.12.025

Paik, S.-B., Kumar, T., & Glaser, D. A. (2009). Spontaneous local gamma oscillation selectively enhances neural network responsiveness. *PLoS Computational Biology*, *5*(3). doi: 10.1371/journal.pcbi.1000342

Parent, A., & Hazrati, L.-N. (1995). Functional anatomy of the basal ganglia. I. The cortico-basal ganglia-thalamo-cortical loop. *Brain Research Reviews*, *20*(1), 91–127. doi: 10.1002/mds.10138

Park, M. C., Belhaj-Saïf, A., Gordon, M., & Cheney, P. D. (2001). Consistent features in the forelimb representation of primary motor cortex in rhesus macaques. *Journal of Neuroscience*, *21*(8), 2784–2792. doi: 10.1523/jneurosci.21-08-02784.2001

Parkes, L. M., Bastiaansen, M. C. M., & Norris, D. G. (2006). Combining EEG and fMRI to investigate the post-movement beta rebound. *NeuroImage*, *29*(3), 685–696. doi: 10.1016/j.neuroimage.2005.08.018

Pascual-Leone, A., Freitas, C., Oberman, L., Horvath, J. C., Halko, M., Eldaief, M., ... Rotenberg, A. (2011). Characterizing brain cortical plasticity and network dynamics across the age-span in health and disease with TMS-EEG and TMS-fMRI. *Brain Topography*, *24*(3-4), 302–315. doi: 10.1007/s10548-011-0196-8

Pastötter, B., Hanslmayr, S., & Bäuml, K.-H. (2008). Inhibition of return arises from inhibition of response processes: an analysis of oscillatory beta activity. *Journal of Cognitive Neuroscience*, *20*(1), 65–75. doi: 10.1162/jocn.2008.20010

Patterson, N., Richter, D. J., Gnerre, S., Lander, E. S., & Reich, D. (2006, may). Genetic evidence for complex speciation of humans and chimpanzees. *Nature*, *441*(7097), 1103–1108. doi: 10.1038/nature04789

Paulus, W. (2011). Transcranial electrical stimulation (tES-tDCS; tRNS, tACS) methods. *Neuropsychological Rehabilitation*, *21*(5), 602–617. doi: 10.1080/09602011.2011.557292

Paus, T. (2001). Primate anterior cingulate cortex: where motor control, drive and cognition interface. *Nature Reviews Neuroscience*, *2*(6). doi: 10.1038/35077500

Paus, T., Sipila, P. K., & Strafella, A. P. (2001). Synchronization of neuronal activity in the human primary motor cortex by transcranial magnetic stimulation: an EEG study. *Journal of Neurophysiology*, *86*(4), 1983–1990. doi: 10.1152/jn.2001.86.4.1983

Pellizzer, G., & Hedges, J. H. (2003). Motor planning: effect of directional uncertainty with discrete spatial cues. *Experimental Brain Research*, *150*(3), 276–289. doi: 10.1007/s00221-003-1453-1

Pellizzer, G., Hedges, J. H., & Villanueva, R. R. (2006). Time-dependent effects of discrete spatial cues on the planning of directed movements. *Experimental Brain Research*, *172*(1), 22–34. doi: 10.1007/s00221-005-0317-2

Penfield, W., & Boldrey, E. (1937). Somatic motor and sensory representation in the cerebral cortex of man as studied by electrical stimulation. *Brain: A Journal of Neurology*. doi: 10.1093/brain/60.4.389

Penfield, W., & Rasmussen, T. (1950). *The cerebral cortex of man; a clinical study of localization of function*. Oxford: Macmillan.

Perenin, M.-T., & Vighetto, A. (1988). Optic ataxia: A specific disruption in visuomotor mechanisms: I. Different aspects of the deficit in reaching for objects. *Brain*, *111*(3), 643–674. doi: 10.1093/brain/111.3.643

Perrin, F., Bertrand, O., & Pernier, J. (1987). Scalp current density mapping: value and estimation from potential data. *IEEE Transactions on Biomedical Engineering*, *BME-34*(4), 283–288. doi: 10.1109/tbme.1987.326089

Petrides, M., & Pandaya, D. N. (1994). Comparative architectonic analysis of the human and the macaque frontal cortex. In F. Boller & J. Grafman (Eds.), *Handbook of neuropsychology* (pp. 77–58). Amsterdam: Elsevier.

Pfurtscheller, G. (1992). Event-related synchronization (ERS): an electrophysiological correlate of cortical areas at rest. *Electroencephalography and Clinical Neurophysiology*, *83*(1), 62–69. doi: 10.1016/0013-4694(92)90133-3

Pfurtscheller, G., & Andrew, C. (1999). Event-related changes of band power and coherence: methodology and interpretation. *Journal of Clinical Neurophysiology*, *16*(6), 512. doi: 10.1097/00004691-199911000-00003

Pfurtscheller, G., & Aranibar, A. (1979). Evaluation of event-related desynchronization (ERD) preceding and following voluntary self-paced movement. *Electroencephalography and Clinical Neurophysiology*, *46*(2), 138–146. doi: 10.1016/0013-4694(79)90063-4

Pfurtscheller, G., & Berghold, A. (1989). Patterns of cortical activation during planning of voluntary movement. *Electroencephalography and Clinical Neurophysiology*, *72*(3), 250–258. doi: 10.1016/0013-4694(89)90250-2

Pfurtscheller, G., & Lopes Da Silva, F. H. (1999). Event-related EEG/MEG synchronization and desynchronization: basic principles. *Clinical Neurophysiology*, *110*(11), 1842–1857. doi: 10.1016/S1388-2457(99)00141-8

Pfurtscheller, G., & Neuper, C. (1994). Event-related synchronization of mu rhythm in the EEG over the cortical hand area in man. *Neuroscience Letters*, *174*(1), 93–96. doi: 10.1016/0304-3940(94)90127-9

Pfurtscheller, G., & Neuper, C. (1997). Motor imagery activates primary sensorimotor area in humans. *Neuroscience Letters*, *239*(2-3), 65–68. doi: 10.1016/s0304-3940(97)00889-6

Pfurtscheller, G., Neuper, C., Brunner, C., & da Silva, F. L. (2005). Beta rebound after different types of motor imagery in man. *Neuroscience Letters*, *378*(3), 156–159. doi: 10.1016/j.neulet.2004.12.034

Pfurtscheller, G., Stancak, A., & Edlinger, G. (1997). On the existence of different types of central beta rhythms below 30 Hz. *Electroencephalography and Clinical Neurophysiology*, *102*(4), 316–325. doi: 10.1016/S0013-4694(96)96612-2

Pfurtscheller, G., Stancák, A., & Neuper, C. (1996). Post-movement beta synchronization. A correlate of an idling motor area? *Electroencephalography and Clinical Neurophysiology*, *98*(4), 281. doi: 10.1016/0013-4694(95)00258-8

Pfurtscheller, G., Woertz, M., Müller, G., Wriessnegger, S., & Pfurtscheller, K. (2002). Contrasting behavior of beta event-related synchronization and somatosensory evoked potential after median nerve stimulation during finger manipulation in man. *Neuroscience Letters*, *323*(2), 113–116. doi: 10.1016/S0304-3940(02)00119-2

Picard, N., & Strick, P. L. (1996). Motor areas of the medial wall: a review of their location and functional activation. *Cerebral Cortex*, *6*(3), 342–353. doi: 10.1093/cercor/6.3.342

Picard, N., & Strick, P. L. (2001). Imaging the premotor areas. *Current Opinion in Neurobiology*, *11*(6), 663–672. doi: 10.1016/S0959-4388(01)00266-5

Pierrot-Deseilligny, C., Milea, D., & Müri, R. M. (2004). Eye movement control by the cerebral cortex. *Current Opinion in Neurology*, *17*(1), 17–25. doi: 10.1097/00019052-200402000-00005

Pierrot-Deseilligny, C. H., Rivaud, S., Gaymard, B., & Agid, Y. (1991). Cortical control of reflexive visually-guided saccades. *Brain*, *114*(3), 1473–1485. doi: 10.1093/brain/114.3.1473

Pistohl, T., Schulze-Bonhage, A., Aertsen, A., Mehring, C., & Ball, T. (2012). Decoding natural grasp types from human ECoG. *NeuroImage*, *59*(1), 248–260. doi: 10.1016/j.neuroimage.2011.06.084

Pogosyan, A., Gaynor, L. D., Eusebio, A., & Brown, P. (2009). Boosting cortical activity at beta-band frequencies slows movement in humans. *Current Biology*, *19*(19), 1637–1641. doi: 10.1016/j.cub.2009.07.074

Pollok, B., Gross, J., Kamp, D., & Schnitzler, A. (2008). Evidence for anticipatory motor control within a cerebello-diencephalic-parietal network. *Journal of Cognitive Neuroscience*, *20*(5), 828–840. doi: 10.1162/jocn.2008.20506

Pollok, B., Krause, V., Butz, M., & Schnitzler, A. (2009). Modality specific functional interaction in sensorimotor synchronization. *Human Brain Mapping*, *30*(6), 1783–1790. doi: 10.1002/hbm.20762

Pollok, B., Krause, V., Martsch, W., Wach, C., Schnitzler, A., & S udmeyer, M. (2012). Motor-cortical oscillations in early stages of Parkinson's disease. *The Journal of Physiology*, *590*(13), 3203–3212. doi: 10.1113/jphysiol.2012.231316

Press, C., Cook, J., Blakemore, S.-J., & Kilner, J. (2011). Dynamic modulation of human motor activity when observing actions. *Journal of Neuroscience*, *31*(8), 2792–2800. doi: 10.1523/jneurosci.1595-10.2011

Pringsheim, T., Jette, N., Frolkis, A., & Steeves, T. D. L. (2014). The prevalence of Parkinson's disease: a systematic review and meta-analysis. *Movement Disorders*, *29*(13), 1583–1590. doi: 10.1002/mds.25945

Priori, A. (2003). Brain polarization in humans: a reappraisal of an old tool for prolonged non-invasive modulation of brain excitability. *Clinical Neurophysiology*, *114*(4), 589–595. doi: 10.1016/s1388-2457(02)00437-6

Prokic, E. J., Weston, C., Yamawaki, N., Hall, S. D., Jones, R. S. G., Stanford, I. M., ... Woodhall, G. L. (2015). Cortical oscillatory dynamics and benzodiazepine-site modulation of tonic inhibition in fast spiking interneurons. *Neuropharmacology*, *95*, 192–205. doi: 10.1016/j.neuropharm.2015.03.006

Purpura, D. P., & McMurtry, J. G. (1965). Intracellular activities and evoked potential changes during polarization of motor cortex. *Journal of Neurophysiology*, *28*(1), 166–185. doi: 10.1152/jn.1965.28.1.166

Rangaswamy, M., Porjesz, B., Chorlian, D. B., Wang, K., Jones, K. A., Bauer, L. O., ... Begleiter, H. (2002). Beta power in the EEG of alcoholics. *Biological Psychiatry*, *52*(8), 831–842. doi: 10.1016/s0006-3223(02)01362-8

Ray, N. J., Jenkinson, N., Wang, S., Holland, P., Brittain, J. S., Joint, C., ... Aziz, T. (2008). Local field potential beta activity in the subthalamic nucleus of patients with Parkinson's disease is associated with improvements in bradykinesia after dopamine and deep brain stimulation. *Experimental Neurology*, *213*(1), 108–113. doi: 10.1016/j.expneurol.2008.05.008

Rhodes, E., Gaetz, W. C., Marsden, J., & Hall, S. D. (2018). Transient alpha and beta synchrony underlies preparatory recruitment of directional motor networks. *Journal of Cognitive Neuroscience*, *30*(6), 867–875. doi: 10.1162/jocn_a_01250

Riddle, C. N., & Baker, S. N. (2006). Digit displacement, not object compliance, underlies task dependent modulations in human corticomuscular coherence. *NeuroImage*, *33*(2), 618–627. doi: 10.1016/j.neuroimage.2006.07.027

Rilling, J. K., & Insel, T. R. (1999, aug). The primate neocortex in comparative perspective using magnetic resonance imaging. *Journal of Human Evolution*, *37*(2), 191–223. doi: 10.1006/jhev.1999.0313

Rivara, C.-B., Sherwood, C. C., Bouras, C., & Hof, P. R. (2003). Stereologic characterization and spatial distribution patterns of Betz cells in the human primary motor cortex. *The Anatomical Record*, *270*(2), 137–151. doi: 10.1002/ar.a.10015

Rizzolatti, G., Luppino, G., & Matelli, M. (1998). The organization of the cortical motor system: new concepts. *Electroencephalography and Clinical Neurophysiology*, *106*(4), 283–296. doi: 10.1016/S0013-4694(98)00022-4

Rodriguez, E., George, N., Lachaux, J.-P., Martinerie, J., Renault, B., & Varela, F. J. (1999). Perception's shadow: long-distance synchronization of human brain activity. *Nature*, *397*(6718), 430–433. doi: 10.1038/17120

Rönnqvist, K. C., McAllister, C. J., Woodhall, G. L., Stanford, I. M., & Hall, S. D. (2013). A multimodal perspective on the composition of cortical oscillations. *Frontiers in Human Neuroscience*, *7*. doi: 10.3389/fnhum.2013.00132

Roopun, A. K., Kramer, M. A., Carracedo, L. M., Kaiser, M., Davies, R. D., C. H.and Traub, Kopell, N. J., & Whittington, M. A. (2008). Period concatenation underlies interactions between gamma and beta rhythms in neocortex. *Frontiers in Cellular Neuroscience*, *2*. doi: 10.3389/neuro.03.001.2008

Roopun, A. K., Middleton, S. J., Cunningham, M. O., LeBeau, F. E. N., Bibbig, A., Whittington, M. A., & Traub, R. D. (2006). A beta2-frequency (20-30 Hz) oscillation in nonsynaptic networks of somatosensory cortex. *Proceedings of the National Academy of Sciences*, *103*(42), 15646–15650. doi: 10.1073/pnas.0607443103

Rosanova, M., Casali, A., Bellina, V., Resta, F., Mariotti, M., & Massimini, M. (2009). Natural frequencies of human corticothalamic circuits. *Journal of Neuroscience*, *29*(24), 7679–7685. doi: 10.1523/jneurosci.0445-09.2009

Rossini, P. M., Burke, D., Chen, R., Cohen, L. G., Daskalakis, Z., Iorio, R. D., … Ziemann, U. (2015). Non-invasive electrical and magnetic stimulation of the brain, spinal cord, roots and peripheral nerves: Basic principles and procedures for routine clinical and research application. An updated report from an I.F.C.N. committee. *Clinical Neurophysiology*, *126*(6), 1071–1107. doi: 10.1016/j.clinph.2015.02.001

Rossini, P. M., & Rossi, S. (1998). Clinical applications of motor evoked potentials. *Electroencephalography and Clinical Neurophysiology*, *106*(3), 180–194. doi: 10.1016/s0013-4694(97)00097-7

Rossini, P. M., Zarola, F., Stalberg, E., & Caramia, M. (1988). Pre-movement facilitation of motor-evoked potentials in man during transcranial stimulation of the central motor pathways. *Brain Research*, *458*(1), 20–30. doi: 10.1016/0006-8993(88)90491-x

Rossiter, H. E., Davis, E. M., Clark, E. V., Boudrias, M.-H., & Ward, N. S. (2014). Beta oscillations reflect changes in motor cortex inhibition in healthy ageing. *NeuroImage*, *91*, 360–365. doi: 10.1016/j.neuroimage.2014.01.012

Rotenberg, A., Horvath, J. C., & Pascual-Leone, A. (2014). The transcranial magnetic stimulation (TMS) device and foundational techniques. In A. Rotenberg, J. Horvath, & A. Pascual-Leone (Eds.), *Transcranial magnetic stimulation* (Vol. 89, pp. 3–13). New York: Springer New York. doi: 10.1007/978-1-4939-0879-0_1

Roth, B. J., Pascual-Leone, A., Cohen, L. G., & Hallett, M. (1992). The heating of metal electrodes during rapid-rate magnetic stimulation: a possible safety hazard. *Electroencephalography and Clinical Neurophysiology/Evoked Potentials Section*, *85*(2), 116–123. doi: 10.1016/0168-5597(92)90077-O

Rothwell, J. C. (1997). Techniques and mechanisms of action of transcranial stimulation of the human motor cortex. *Journal of Neuroscience Methods*, *74*(2), 113–122. doi: 10.1016/s0165-0270(97)02242-5

Rouiller, E. M., Tanne, J., Moret, V., & Boussaoud, D. (1999). Origin of thalamic inputs to the primary, premotor, and supplementary motor cortical areas and to area 46 in macaque monkeys: a multiple retrograde tracing study. *Journal of Comparative Neurology*, *409*(1), 131–152. doi: 10.1002/(sici)1096-9861(19990621)409:1<131::aid-cne10>3.0.co;2-a

Ruohonen, J. (2003). Background physics for magnetic stimulation. In *Transcranial magnetic stimulation and transcranial direct current stimulation, proceedings of the 2nd international transcranial magnetic stimulation (TMS) and transcranial direct current stimulation (tDCS) symposium* (pp. 3–12). Elsevier. doi: 10.1016/s1567-424x(09)70204-1

Sakai, K., Ugawa, Y., Terao, Y., Hanajima, R., Furubayashi, T., & Kanazawa, I. (1997). Preferential activation of different I waves by transcranial magnetic stimulation with a figure-of-eight-shaped coil. *Experimental Brain Research*, *113*(1), 24–32. doi: 10.1007/bf02454139

Sakamoto, M., Muraoka, T., Mizuguchi, N., & Kanosue, K. (2009). Combining observation and imagery of an action enhances human corticospinal excitability. *Neuroscience Research*, *65*(1), 23–27. doi: 10.1016/j.neures.2009.05.003

Salami, M., Itami, C., Tsumoto, T., & Kimura, F. (2003). Change of conduction velocity by regional myelination yields constant latency irrespective of distance between thalamus and cortex. *Proceedings of the National Academy of Sciences*, *100*(10), 6174–6179. doi: 10.1073/pnas.0937380100

Salmelin, R., Forss, N., Knuutila, J., & Hari, R. (1995a). Bilateral activation of the human somatomotor cortex by distal hand movements. *Electroencephalography and Clinical Neurophysiology*, *95*(6), 444–452. doi: 10.1016/0013-4694(95)00193-x

Salmelin, R., Hámáaláinen, M., Kajola, M., & Hari, R. (1995b). Functional segregation of movement-related rhythmic activity in the human brain. *NeuroImage*, *2*(4), 237–243. doi: 10.1006/nimg.1995.1031

Salmelin, R., & Hari, R. (1994). Spatiotemporal characteristics of sensorimotor neuromagnetic rhythms related to thumb movement. *Neuroscience*, *60*(2), 537–550. doi: 10.1016/0306-4522(94)90263-1

Sanchez, B., Pacheck, A., & Rutkove, S. B. (2016). Guidelines to electrode positioning for human and animal electrical impedance myography research. *Scientific Reports*, *6*(1). doi: 10.1038/srep32615

Sanes, J. N., & Donoghue, J. P. (1993). Oscillations in local field potentials of the primate motor cortex during voluntary movement. *Proceedings of the National Academy of Sciences*, *90*(10), 4470–4474. doi: 10.1073/pnas.90.10.4470

Sanes, J. N., & Donoghue, J. P. (2000). Plasticity and primary motor cortex. *Annual Review of Neuroscience*, *23*(1), 393–415. doi: 10.1146/annurev.neuro.23.1.393

Saramäki, T. (1993). Finite impulse response filter design. In S. K. Mitra & J. F. Kaiser (Eds.), *Handbook for digital signal processing* (pp. 155–277). Wiley-Interscience.

Sauseng, P., Klimesch, W., Gerloff, C., & Hummel, F. C. (2009). Spontaneous locally restricted EEG alpha activity determines cortical excitability in the motor cortex. *Neuropsychologia*, *47*(1), 284–288. doi: 10.1016/j.neuropsychologia.2008.07.021

Sawaguchi, T., Matsumura, M., & Kubota, K. (1989). Depth distribution of neuronal activity related to a visual reaction time task in the monkey prefrontal cortex. *Journal of Neurophysiology*, *61*(2), 435–446. doi: 10.1152/jn.1989.61.2.435

Sawaki, L., Yaseen, Z., Kopylev, L., & Cohen, L. G. (2003). Age-dependent changes in the ability to encode a novel elementary motor memory. *Annals of Neurology*, *53*(4), 521–524. doi: 10.1002/ana.10529

Saygin, A. P., & Sereno, M. I. (2008, jan). Retinotopy and attention in human occipital, temporal, parietal, and frontal cortex. *Cerebral Cortex*, *18*(9), 2158–2168. doi: 10.1093/cercor/bhm242

Schieber, M. H., & Hibbard, L. S. (1993). How somatotopic is the motor cortex hand area? *Science*, *261*(5120), 489–493. doi: 10.1126/science.8332915

Schnitzler, A., & Gross, J. (2005). Normal and pathological oscillatory communication in the brain. *Nature Reviews Neuroscience*, *6*(4), 285. doi: 10.1038/nrn1650

Schnitzler, A., Salenius, S., Salmelin, R., Jousmäki, V., & Hari, R. (1997). Involvement of primary motor cortex in motor imagery: a neuromagnetic study. *NeuroImage*, *6*(3), 201–208. doi: 10.1006/nimg.1997.0286

Schoffelen, J.-M., Oostenveld, R., & Fries, P. (2008). Imaging the human motor system's beta-band synchronization during isometric contraction. *NeuroImage*, *41*(2), 437–447. doi: 10.1016/j.neuroimage.2008.01.045

Schönle, P. W., Isenberg, C., Crozier, T. A., Dressler, D., Machetanz, J., & Conrad, B. (1989). Changes of transcranially evoked motor responses in man by midazolam, a short acting benzodiazepine. *Neuroscience Letters*, *101*(3), 321–324. doi: 10.1016/0304-3940(89)90553-3

Sejnowski, T. J., & Paulsen, O. (2006). Network oscillations: emerging computational principles. *Journal of Neuroscience*, *26*(6), 1673–1676. doi: 10.1523/jneurosci.3737-05d.2006

Seror, P., Maisonobe, T., & Bouche, P. (2011). A new electrode placement for recording the compound motor action potential of the first dorsal interosseous muscle. *Neurophysiologie Clinique/Clinical Neurophysiology*, *41*(4), 173–180. doi: 10.1016/j.neucli.2011.06.003

Sherrington, C. S., & Leyton, A. S. (1924). Excitable cortex of the chimpanzee, orang-utan, and gorilla. *The Journal of Nervous and Mental Disease*, *60*(4), 401–403. doi: 10.1097/00005053-192410000-00040

Shima, K., Isoda, M., Mushiake, H., & Tanji, J. (2007). Categorization of behavioural sequences in the prefrontal cortex. *Nature*, *445*(7125), 315. doi: 10.1038/nature05470

Shima, K., & Tanji, J. (2000). Neuronal activity in the supplementary and presupplementary motor areas for temporal organization of multiple movements. *Journal of Neurophysiology*, *84*(4), 2148–2160. doi: 10.1152/jn.2000.84.4.2148

Shipp, S. (2005). The importance of being agranular: a comparative account of visual and motor cortex. *Philosophical Transactions of the Royal Society of London B: Biological Sciences*, *360*(1456), 797–814. doi: 10.1098/rstb.2005.1630

Shorter, E., & Healy, D. (2007). *Shock therapy: a history of electroconvulsive treatment in mental illness*. New York: Rutgers University Press.

Siebner, H., & Rothwell, J. (2003). Transcranial magnetic stimulation: new insights into representational cortical plasticity. *Experimental Brain Research*, *148*(1), 1–16. doi: 10.1007/s00221-002-1234-2

Silberstein, P., Pogosyan, A., Kühn, A. A., Hotton, G., Tisch, S., Kupsch, A., ... Brown, P. (2005). Cortico-cortical coupling in Parkinson's disease and its modulation by therapy. *Brain*, *128*(6), 1277–1291. doi: 10.1093/brain/awh480

Silva, F. H. L. D., & Leeuwen, W. S. V. (1977, nov). The cortical source of the alpha rhythm. *Neuroscience Letters*, *6*(2-3), 237–241. doi: 10.1016/0304-3940(77)90024-6

Silva, L., Amitai, Y., & Connors, B. (1991, jan). Intrinsic oscillations of neocortex generated by layer 5 pyramidal neurons. *Science*, *251*(4992), 432–435. doi: 10.1126/science.1824881

Singer, W., & Gray, C. M. (1995). Visual feature integration and the temporal correlation hypothesis. *Annual Review of Neuroscience*, *18*(1), 555–586. doi: 10.1146/annurev.ne.18.030195.003011

Skinner, F. K., Kopell, N., & Marder, E. (1994). Mechanisms for oscillation and frequency control in reciprocally inhibitory model neural networks. *Journal of Computational Neuroscience*, *1*(1-2), 69–87. doi: 10.1007/BF00962719

Smith, C. D., Umberger, G. H., Manning, E. L., Slevin, J. T., Wekstein, D. R., Schmitt, F. A., ... Gash, D. M. (1999). Critical decline in fine motor hand movements in human aging. *Neurology*, *53*(7), 1458–1458. doi: 10.1212/wnl.53.7.1458

Smith, Y., Bevan, M. D., Shink, E., & Bolam, J. P. M. (1998). Microcircuitry of the direct and indirect pathways of the basal ganglia. *Neuroscience*, *86*, 353–387. doi: 10.1016/S0306-4522(98)00004-9

Sohn, J.-W., & Lee, D. (2007). Order-dependent modulation of directional signals in the supplementary and presupplementary motor areas. *Journal of Neuroscience*, *27*(50), 13655–13666. doi: 10.1523/JNEUROSCI.2982-07.2007

Solis-Escalante, T., Müller-Putz, G. R., Pfurtscheller, G., & Neuper, C. (2012). Cue-induced beta rebound during withholding of overt and covert foot movement. *Clinical Neurophysiology*, *123*(6), 1182–1190. doi: 10.1016/j.clinph.2012.01.013

Song, S., Sjöström, P. J., Reigl, M., Nelson, S., & Chklovskii, D. B. (2005). Highly nonrandom features of synaptic connectivity in local cortical circuits. *PLoS Biology*, *3*(3), 68. doi: 10.1371/journal.pbio.0030068

Speckmann, E.-J., Elger, C. E., & Gorji, A. (2011). Neurophysiologic basis of EEG and DC potentials. In D. L. Schomer & F. H. Lopes da Silva (Eds.), *Niedermeyer's electroencephalography: Basic principles, clinical applications, and related fields* (Sixth ed., pp. 17–32). Philadelphia, PA: Wolters Kluwer.

Spinks, R. L., Kraskov, A., Brochier, T., Umilta, M. A., & Lemon, R. N. (2008). Selectivity for grasp in local field potential and single neuron activity recorded simultaneously from M1 and F5 in the awake macaque monkey. *Journal of Neuroscience*, *28*(43), 10961–10971. doi: 10.1523/jneurosci.1956-08.2008

Srinivasan, R. (1999). Methods to improve the spatial resolution of EEG. *International Journal of Bioelectromagnetism*, *1*(1), 102–111. Retrieved from http://ijbem.ws.hosei.ac.jp/volume1/number1/pdf/ijbem_a102-111.pdf

Stagg, C. J. (2014). The physiological basis of brain stimulation. In *The stimulated brain* (pp. 145–177). Elsevier. doi: 10.1016/b978-0-12-404704-4.00006-5

Stagg, C. J., Bachtiar, V., Amadi, U., Gudberg, C. A., Ilie, A. S., Sampaio-Baptista, C., ... Johansen-Berg, H. (2014). Local GABA concentration is related to network-level resting functional connectivity. *eLife*, *3*. doi: 10.7554/elife.01465

Stagg, C. J., Bachtiar, V., & Johansen-Berg, H. (2011). The role of GABA in human motor learning. *Current Biology*, *21*(6), 480–484. doi: 10.1016/j.cub.2011.01.069

Stagg, C. J., Best, J. G., Stephenson, M. C., O'Shea, J., Wylezinska, M., Kincses, Z. T., ... Johansen-Berg, H. (2009). Polarity-sensitive modulation of cortical neurotransmitters by transcranial stimulation. *Journal of Neuroscience*, *29*(16), 5202–5206. doi: 10.1523/jneurosci.4432-08.2009

Stagg, C. J., Bestmann, S., Constantinescu, A. O., Moreno, L. M., Allman, C., Mekle, R., ... Rothwell, J. C. (2011). Relationship between physiological measures of excitability and levels of glutamate and GABA in the human motor cortex. *The Journal of Physiology*, *589*(23), 5845–5855. doi: 10.1113/jphysiol.2011.216978

Stagg, C. J., & Nitsche, M. A. (2011). Physiological basis of transcranial direct current stimulation. *The Neuroscientist*, *17*(1), 37–53. doi: 10.1177/1073858410386614

Stagg, C. J., Wylezinska, M., Matthews, P. M., Johansen-Berg, H., Jezzard, P., Rothwell, J. C., & Bestmann, S. (2009). Neurochemical effects of theta burst stimulation as assessed by magnetic resonance spectroscopy. *Journal of Neurophysiology*, *101*(6), 2872–2877. doi: 10.1152/jn.91060.2008

Stančák, A., Feige, B., Lücking, C. H., & Kristeva-Feige, R. (2000). Oscillatory cortical activity and movement-related potentials in proximal and distal movements. *Clinical Neurophysiology*, *111*(4), 636–650. doi: 10.1016/s1388-2457(99)00310-7

Stancák, A., & Pfurtscheller, G. (1995). Desynchronization and recovery of β rhythms during brisk and slow self-paced finger movements in man. *Neuroscience Letters*, *196*(1), 21–24. doi: 10.1016/0304-3940(95)11827-J

Stancák, A., & Pfurtscheller, G. (1996a). Event-related desynchronisation of central beta-rhythms during brisk and slow self-paced finger movements of dominant and nondominant hand. *Cognitive Brain Research*, *4*(3), 171–183. doi: 10.1016/s0926-6410(96)00031-6

Stancák, A., & Pfurtscheller, G. (1996b). Mu-rhythm changes in brisk and slow self-paced finger movements. *Neuroreport*, *7*(6), 1161–1164. doi: 10.1097/00001756-199604260-00013

Stančák, A., Riml, A., & Pfurtscheller, G. (1997). The effects of external load on movement-related changes of the sensorimotor EEG rhythms. *Electroencephalography and Clinical Neurophysiology*, *102*(6), 495–504. doi: 10.1016/s0013-4694(96)96623-0

Starr, A., Caramia, M., Zarola, F., & Rossini, P. M. (1988). Enhancement of motor cortical excitability in humans by non-invasive electrical stimulation appears prior to voluntary movement. *Electroencephalography and Clinical Neurophysiology*, *70*(1), 26–32. doi: 10.1016/0013-4694(88)90191-5

Starr, M. S., & Summerhayes, M. (1983). Role of the ventromedial nucleus of the thalamus in motor behaviour II. Effects of lesions. *Neuroscience*, *10*(4), 1171–1183. doi: 10.1016/0306-4522(83)90106-9

Steiper, M. E., Young, N. M., & Sukarna, T. Y. (2004, nov). Genomic data support the hominoid slowdown and an early oligocene estimate for the hominoid-cercopithecoid divergence. *Proceedings of the National Academy of Sciences*, *101*(49), 17021–17026. doi: 10.1073/pnas.0407270101

Stepanyants, A., Hirsch, J. A., Martinez, L. M., Kisvárday, Z. F., Ferecskó, A. S., & Chklovskii, D. B. (2007). Local potential connectivity in cat primary visual cortex. *Cerebral Cortex*, *18*(1), 13–28. doi: 10.1093/cercor/bhm027

Stoney, S. D., Thompson, W. D., & Asanuma, H. (1968). Excitation of pyramidal tract cells by intracortical microstimulation: effective extent of stimulating current. *Journal of Neurophysiology*, *31*(5), 659–669. doi: 10.1152/jn.1968.31.5.659

Sun, W., & Dan, Y. (2009, oct). Layer-specific network oscillation and spatiotemporal receptive field in the visual cortex. *Proceedings of the National Academy of Sciences*, *106*(42), 17986–17991. doi: 10.1073/pnas.0903962106

Surmeier, D. J., Mercer, J. N., & Chan, C. S. (2005). Autonomous pacemakers in the basal ganglia: who needs excitatory synapses anyway? *Current Opinion in Neurobiology*, *15*(3), 312–318. doi: 10.1016/j.conb.2005.05.007

Svane, C., Forman, C. R., Nielsen, J. B., & Geertsen, S. S. (2018). Characterization of corticospinal activation of finger motor neurons during precision and power grip in humans. *Experimental Brain Research*, *236*(3), 745–753. doi: 10.1007/s00221-018-5171-0

Swann, N., Poizner, H., Houser, M., Gould, S., Greenhouse, I., Cai, W., ... Aron, A. R. (2011). Deep brain stimulation of the subthalamic nucleus alters the cortical profile of response inhibition in the beta frequency band: a scalp EEG study in Parkinson's disease. *Journal of Neuroscience*, *31*(15), 5721–5729. doi: 10.1523/jneurosci.6135-10.2011

Taira, M., Mine, S., Georgopoulos, A. P., Murata, A., & Sakata, H. (1990). Parietal cortex neurons of the monkey related to the visual guidance of hand movement. *Experimental Brain Research*, *83*(1), 29–36. doi: 10.1007/BF00232190

Takemi, M., Masakado, Y., Liu, M., & Ushiba, J. (2013). Event-related desynchronization reflects downregulation of intracortical inhibition in human primary motor cortex. *Journal of Neurophysiology*, *110*, 1158–1166. doi: 10.1152/jn.01092.2012

Tallgren, P., Vanhatalo, S., Kaila, K., & Voipio, J. (2005). Evaluation of commercially available electrodes and gels for recording of slow EEG potentials. *Clinical Neurophysiology*, *116*(4), 799–806. doi: 10.1016/j.clinph.2004.10.001

Tallon-Baudry, C., & Bertrand, O. (1999). Oscillatory gamma activity in humans and its role in object representation. *Trends in Cognitive Sciences*, *3*(4), 151–162. doi: 10.1016/S1364-6613(99)01299-1

Tallon-Baudry, C., Mandon, S., Freiwald, W. A., & Kreiter, A. K. (2004). Oscillatory synchrony in the monkey temporal lobe correlates with performance in a visual short-term memory task. *Cerebral Cortex*, *14*(7), 713–720. doi: 10.1093/cercor/bhh031

Tan, H., Wade, C., & Brown, P. (2016, feb). Post-movement beta activity in sensorimotor cortex indexes confidence in the estimations from internal models. *The Journal of Neuroscience*, *36*(5), 1516–1528.

Tanji, J., & Kurata, K. I. Y. O. S. H. I. (1982). Comparison of movement-related activity in two cortical motor areas of primates. *Journal of Neurophysiology*, *48*(3), 633–653. doi: 10.1152/jn.1982.48.3.633

Tanji, J., & Shima, K. (1994). Role for supplementary motor area cells in planning several movements ahead. *Nature*, *371*(6496), 413–416. doi: 10.1038/371413a0

Taylor, J. L., & Loo, C. K. (2007). Stimulus waveform influences the efficacy of repetitive transcranial magnetic stimulation. *Journal of Affective Disorders*, *97*(1-3), 271–276. doi: 10.1016/j.jad.2006.06.027

Tecchio, F., Zappasodi, F., Pasqualetti, P., Tombini, M., Caulo, M., Ercolani, M., & Rossini, P. M. (2006a). Long-term effects of stroke on neuronal rest activity in rolandic cortical areas. *Journal of Neuroscience Research*, *83*(6), 1077–1087. doi: 10.1002/jnr.20796

Tecchio, F., Zappasodi, F., Tombini, M., Oliviero, A., Pasqualetti, P., Vernieri, F., ... Rossini, P. M. (2006b). Brain plasticity in recovery from stroke: an MEG assessment. *NeuroImage*, *32*(3), 1326–1334. doi: 10.1016/j.neuroimage.2006.05.004

Thompson, R. F. (1967). *Foundations of physiological psychology*. New York: Harper and Row. doi: 10.2307/1421208

Thomson, A. M., & Lamy, C. (2007). Functional maps of neocortical local circuitry. *Frontiers in Neuroscience*, *1*(1), 19. doi: 10.3389/neuro.01.1.1.002.2007

Thut, G., Ives, J. R., Kampmann, F., Pastor, M. A., & Pascual-Leone, A. (2005). A new device and protocol for combining TMS and online recordings of EEG and evoked potentials. *Journal of Neuroscience Methods*, *141*(2), 207–217. doi: 10.1016/j.jneumeth.2004.06.016

Thut, G., Schyns, P. G., & Gross, J. (2011a). Entrainment of perceptually relevant brain oscillations by non-invasive rhythmic stimulation of the human brain. *Frontiers in Psychology*, *2*. doi: 10.3389/fpsyg.2011.00170

Thut, G., Veniero, D., Romei, V., Miniussi, C., Schyns, P., & Gross, J. (2011b). Rhythmic TMS causes local entrainment of natural oscillatory signatures. *Current Biology*, *21*(14), 1176–1185. doi: 10.1016/j.cub.2011.05.049

Tofts, P. S. (1990). The distribution of induced currents in magnetic stimulation of the nervous system. *Physics in Medicine & Biology*, *35*(8), 1119. doi: 10.1088/0031-9155/35/8/008

Toledo, D. R., Manzano, G. M., Barela, J. A., & Kohn, A. F. (2016). Cortical correlates of response time slowing in older adults: ERP and ERD/ERS analyses during passive ankle movement. *Clinical Neurophysiology*, *127*(1), 655–663. doi: 10.1016/j.clinph.2015.05.003

Tomberg, C., & Caramia, M. D. (1991). Prime mover muscle in finger lift or finger flexion reaction times: identification with transcranial magnetic stimulation. *Electroencephalography and Clinical Neurophysiology/Evoked Potentials Section*, *81*(4), 319–322. doi: 10.1016/0168-5597(91)90019-t

Toth, M., Kiss, A., Kosztolanyi, P., & Kondakor, I. (2007). Diurnal alterations of brain electrical activity in healthy adults: a LORETA study. *Brain Topography*, *20*(2), 63–76. doi: 10.1007/s10548-007-0032-3

Towers, S. K., & Hestrin, S. (2008). D1-like dopamine receptor activation modulates GABAergic inhibition but not electrical coupling between neocortical fast-spiking interneurons. *Journal of Neuroscience*, *28*(10), 2633–2641. doi: 10.1523/JNEUROSCI.5079-07.2008

Traub, R. D., Jefferys, J. G. R., & Whittington, M. A. (1997). Simulation of gamma rhythms in networks of interneurons and pyramidal cells. *Journal of Computational Neuroscience*, *4*(2), 141–150. doi: 10.1023/A:1008839312043

Traub, R. D., Miles, R., & Wong, R. K. S. (1989). Model of the origin of rhythmic population oscillations in the hippocampal slice. *Science*, *243*(4896), 1319–1325. doi: 10.1126/science.2646715

Traub, R. D., Whittington, M. A., Colling, S. B., Buzsaki, G. X. J. J. G., & Jefferys, J. G. (1996b). Analysis of gamma rhythms in the rat hippocampus in vitro and in vivo. *The Journal of Physiology*, *493*(2), 471–484. doi: 10.1113/jphysiol.1996.sp021397

Traub, R. D., Whittington, M. A., Stanford, I. M., & Jefferys, J. G. R. (1996a). A mechanism for generation of long-range synchronous fast oscillations in the cortex. *Nature*, *383*(6601), 621. doi: 10.1038/383621a0

Turkmen, S., Backstrom, T., Wahlstrom, G., Andreen, L., & Johansson, I.-M. (2010, dec). Tolerance to allopregnanolone with focus on the GABA-Areceptor. *British Journal of Pharmacology*, *162*(2), 311–327. doi: 10.1111/j.1476-5381.2010.01059.x

Tyssowski, K. M., DeStefino, N. R., Cho, J.-H., Dunn, C. J., Poston, R. G., Carty, C. E., ... Gray, J. M. (2018). Different neuronal activity patterns induce different gene expression programs. *Neuron*. doi: 10.1016/j.neuron.2018.04.001

Tzagarakis, C., Ince, N. F., Leuthold, A. C., & Pellizzer, G. (2010). Beta-band activity during motor planning reflects response uncertainty. *Journal of Neuroscience*, *30*(34), 11270–11277. doi: 10.1523/JNEUROSCI.6026-09.2010

Van Der Werf, Y. D., & Paus, T. (2006). The neural response to transcranial magnetic stimulation of the human motor cortex. I. intracortical and cortico-cortical contributions. *Experimental Brain Research*, *175*(2), 231–245. doi: 10.1007/s00221-006-0551-2

van Lier, H., Drinkenburg, W. H. I. M., van Eeten, Y. J. W., & Coenen, A. M. L. (2004, aug). Effects of diazepam and zolpidem on EEG beta frequencies are behavior-specific in rats. *Neuropharmacology*, *47*(2), 163–174. doi: 10.1016/j.neuropharm.2004.03.017

Van Vreeswijk, C., Abbott, L. F., & Ermentrout, G. B. (1994). When inhibition not excitation synchronizes neural firing. *Journal of Computational Neuroscience*, *1*(4), 313–321. doi: 10.1007/BF00961879

van Wijk, B. C. M., Beek, P. J., & Daffertshofer, A. (2012). Neural synchrony within the motor system: what have we learned so far? *Frontiers in Human Neuroscience*, *6*. doi: 10.3389/fnhum.2012.00252

Van Wijk, B. C. M., Daffertshofer, A., Roach, N., & Praamstra, P. (2008). A role of beta oscillatory synchrony in biasing response competition? *Cerebral Cortex*, *19*(6), 1294–1302. doi: 10.1093/cercor/bhn174

Villamar, M. F., Wivatvongvana, P., Patumanond, J., Bikson, M., Truong, D. Q., Datta, A., & Fregni, F. (2013). Focal modulation of the primary motor cortex in fibromyalgia using

4x1-ring high-definition transcranial direct current stimulation (HD-tDCS): immediate and delayed analgesic effects of cathodal and anodal stimulation. *The Journal of Pain*, *14*(4), 371–383. doi: 10.1016/j.jpain.2012.12.007

Volgushev, M., Chistiakova, M., & Singer, W. (1998). Modification of discharge patterns of neocortical neurons by induced oscillations of the membrane potential. *Neuroscience*, *83*(1), 15–25. doi: 10.1016/S0306-4522(97)00380-1

von Bonin, G. (1949). Architecture of the precentral motor cortex and some adjacent areas. In P. C. Bucy (Ed.), *The precentral motor cortex* (pp. 7–82). The University of Illinois Press.

von Stein, A., & Sarnthein, J. (2000). Different frequencies for different scales of cortical integration: from local gamma to long range alpha/theta synchronization. *International Journal of Psychophysiology*, *38*(3), 301–313. doi: 10.1016/s0167-8760(00)00172-0

Wagner, T., Valero-Cabre, A., & Pascual-Leone, A. (2007). Noninvasive human brain stimulation. *Annual Review of Biomedical Engineering*, *9*(1), 527–565. doi: 10.1146/annurev.bioeng.9.061206.133100

Wang, X.-J. (2010). Neurophysiological and computational principles of cortical rhythms in cognition. *Physiological Reviews*, *90*(3), 1195–1268. doi: 10.1152/physrev.00035.2008

Wang, X.-J., & Buzsáki, G. (1996). Gamma oscillation by synaptic inhibition in a hippocampal interneuronal network model. *Journal of Neuroscience*, *16*(20), 6402–6413. doi: 10.1523/jneurosci.16-20-06402.1996

Wang, X. J., Golomb, D., & Rinzel, J. (1995). Emergent spindle oscillations and intermittent burst firing in a thalamic model: specific neuronal mechanisms. *Proceedings of the National Academy of Sciences*, *92*(12), 5577–5581. doi: 10.1073/pnas.92.12.5577

Wang, X.-J., & Rinzel, J. (1993). Spindle rhythmicity in the reticularis thalami nucleus: synchronization among mutually inhibitory neurons. *Neuroscience*, *53*(4), 899–904. doi: 10.1016/0306-4522(93)90474-T

Wang, Y., Shima, K., Sawamura, H., & Tanji, J. (2001). Spatial distribution of cingulate cells projecting to the primary, supplementary, and pre-supplementary motor areas: a retrograde multiple labeling study in the macaque monkey. *Neuroscience Research*, *39*(1), 39–49. doi: 10.1016/S0168-0102(00)00198-X

Watts, D. J., & Strogatz, S. H. (1998). Collective dynamics of 'small-world' networks. *Nature*, *393*(6684), 440–442. doi: 10.1038/30918

Weddell, G., Feinstein, B., & Pattle, R. E. (1943). The clinical application of electromyography. *The Lancet*, *241*(6234), 236–239. doi: 10.1016/s0140-6736(00)42228-2

Weinberger, M., Mahant, N., Hutchison, W. D., Lozano, A. M., Moro, E., Hodaie, M., ... Dostrovsky, J. O. (2006). Beta oscillatory activity in the subthalamic nucleus and its relation to dopaminergic response in Parkinson's disease. *Journal of Neurophysiology*, *96*(6), 3248–3256. doi: 10.1152/jn.00697.2006

Weinrich, C. A., Brittain, J.-S., Nowak, M., Salimi-Khorshidi, R., Brown, P., & Stagg, C. J. (2017). Modulation of long-range connectivity patterns via frequency-specific stimulation of human cortex. *Current Biology*, *27*(19), 3061–3068.e3. doi: 10.1016/j.cub.2017.08.075

White, J. A., Chow, C. C., Rit, J., Soto-Treviño, C., & Kopell, N. (1998). Synchronization and oscillatory dynamics in heterogeneous, mutually inhibited neurons. *Journal of Computational Neuroscience*, *5*(1), 5–16. doi: 10.1023/A:1008841325921

Whittington, M. A., Faulkner, H. J., Doheny, H. C., & Traub, R. D. (2000). Neuronal fast oscillations as a target site for psychoactive drugs. *Pharmacology & Therapeutics*, *86*(2), 171–190. doi: 10.1016/S0163-7258(00)00038-3

Whittington, M. A., Traub, R. D., & Jefferys, J. G. R. (1995). Synchronized oscillations in interneuron networks driven by metabotropic glutamate receptor activation. *Nature*, *373*(6515), 612. doi: 10.1038/373612a0

Wichmann, T., & Soares, J. (2006). Neuronal firing before and after burst discharges in the monkey basal ganglia is predictably patterned in the normal state and altered in Parkinsonism. *Journal of Neurophysiology*, *95*(4), 2120–2133. doi: 10.1152/jn.01013.2005

Williams, D., Kühn, A., Kupsch, A., Tijssen, M., van Bruggen, G., Speelman, H., ... Brown, P. (2003). Behavioural cues are associated with modulations of synchronous oscillations in the human subthalamic nucleus. *Brain*, *126*(9), 1975–1985. doi: 10.1093/brain/awg194

Williams, D., Kühn, A., Kupsch, A., Tijssen, M., van Bruggen, G., Speelman, H., ... Brown, P. (2005). The relationship between oscillatory activity and motor reaction time in the parkinsonian subthalamic nucleus. *European Journal of Neuroscience*, *21*(1), 249–258. doi: 10.1111/j.1460-9568.2004.03817.x

Williams, D., Tijssen, M., Van Bruggen, G., Bosch, A., Insola, A., Lazzaro, V. D., ... Brown, P. (2002). Dopamine-dependent changes in the functional connectivity between basal ganglia and cerebral cortex in humans. *Brain*, *125*(7), 1558–1569. doi: 10.1093/brain/awf156

Wilson, H. R., & Cowan, J. D. (1972). Excitatory and inhibitory interactions in localized populations of model neurons. *Biophysical Journal*, *12*(1), 1–24. doi: 10.1016/S0006-3495(72)86068-5

Wilson, T. W., Heinrichs-Graham, E., & Becker, K. M. (2014a). Circadian modulation of motor-related beta oscillatory responses. *NeuroImage*, *102*, 531–539. doi: 10.1016/j.neuroimage.2014.08.013

Wilson, T. W., Kurz, M. J., & Arpin, D. J. (2014b). Functional specialization within the supplementary motor area: a fNIRS study of bimanual coordination. *NeuroImage*, *85*, 445–450. doi: 10.1016/j.neuroimage.2013.04.112

Wilson, T. W., Slason, E., Asherin, R., Kronberg, E., Reite, M. L., Teale, P. D., & Rojas, D. C. (2010). An extended motor network generates beta and gamma oscillatory perturbations during development. *Brain and Cognition*, *73*(2), 75–84. doi: 10.1016/j.bandc.2010.03.001

Wilson, T. W., Slason, E., Asherin, R., Kronberg, E., Teale, P. D., Reite, M. L., & Rojas, D. C. (2011). Abnormal gamma and beta MEG activity during finger movements in early-onset psychosis. *Developmental Neuropsychology*, *36*(5), 596–613. doi: 10.1080/87565641.2011.555573

Wise, S. P. (1985). The primate promoter cortex fifty years after Fulton. *Behavioural Brain Research*, *18*(2), 79–88. doi: 10.1016/0166-4328(85)90064-6

Wise, S. P. (1996). Corticospinal efferents of the supplementary sensorimotor area in relation to the primary motor area. *Advances in Neurology*, *70*, 57–69.

Wolf, P. A. (2004). Epidemiology of stroke. In J. P. Mohr, D. W. Choi, J. C. Grotta, B. Weir, & P. A. Wolf (Eds.), *Stroke - pathophysiology, diagnosis, and management* (Fourth ed., pp. 13–34). Philadelphia: Churchill Livingstone. doi: 10.1016/b0-44-306600-0/50005-5

Wolpaw, J. R., Birbaumer, N., Heetderks, W. J., McFarland, D. J., Peckham, P. H., Schalk, G., ... Vaughan, T. M. (2000). Brain-computer interface technology: a review of the first international meeting. *IEEE Transactions on Rehabilitation Engineering*, *8*(2), 164–173. doi: 10.1109/tre.2000.847807

Wolpaw, J. R., Birbaumer, N., McFarland, D. J., Pfurtscheller, G., & Vaughan, T. M. (2002). Brain-computer interfaces for communication and control. *Clinical Neurophysiology*, *113*(6), 767–791. doi: 10.1016/s1388-2457(02)00057-3

Woolsey, C. N., Settlage, P. H., Meyer, D. R., Sencer, W., Pinto, H. T., & Travis, A. M. (1952). Patterns of localization in precentral and" supplementary" motor areas and their relation to the concept of a premotor area. *Research publications-Association for Research in Nervous and Mental Disease*, *30*, 238–264.

World Medical Association, T. (2013). World medical association declaration of Helsinki: ethical principles for medical research involving human subjects. *JAMA*, *310*(20), 2191. doi: 10.1001/jama.2013.281053

Wüllmer, U., Klockgether, T., Schwarz, M., & Sontag, K. H. (1987). Behavioral actions of baclofen in the rat ventromedial thalamic nucleus: antagonism by delta-aminovalerate. *Brain Research*, *422*(1), 129–136. doi: 10.1016/0006-8993(87)90547-6

Yamada, H., Inokawa, H., Hori, Y., Pan, X., Matsuzaki, R., Nakamura, K., ... Minamimoto, T. (2016). Characteristics of fast-spiking neurons in the striatum of behaving monkeys. *Neuroscience Research*, *105*, 2–18. doi: 10.1016/j.neures.2015.10.003

Yamawaki, N., Borges, K., Suter, B. A., Harris, K. D., & Shepherd, G. M. G. (2014). A genuine layer 4 in motor cortex with prototypical synaptic circuit connectivity. *Elife*, *3*, 05422. doi: 10.7554/eLife.05422

Yamawaki, N., Stanford, I. M., Hall, S. D., & Woodhall, G. L. (2008). Pharmacologically induced and stimulus evoked rhythmic neuronal oscillatory activity in the primary motor cortex in vitro. *Neuroscience*, *151*(2), 386–395. doi: 10.1016/j.neuroscience.2007.10.021

Yanagisawa, T., Yamashita, O., Hirata, M., Kishima, H., Saitoh, Y., Goto, T., ... Kamitani, Y. (2012). Regulation of motor representation by phase-amplitude coupling in the sensorimotor cortex. *Journal of Neuroscience*, *32*(44), 15467–15475. doi: 10.1523/jneurosci.2929-12.2012

Yang, L., Shen, L., Nan, W., Tang, Q., Wan, F., Zhu, F., & Hu, Y. (2017). Time course of EEG activities in continuous tracking task: a pilot study. *Computer Assisted Surgery*, *22*(sup1), 1–8. doi: 10.1080/24699322.2017.1378604

Yu, S., Huang, D., Singer, W., & Nikolić, D. (2008). A small world of neuronal synchrony. *Cerebral Cortex*, *18*(12), 2891–2901. doi: 10.1093/cercor/bhn047

Yuan, H., Perdoni, C., & He, B. (2010). Relationship between speed and EEG activity during imagined and executed hand movements. *Journal of Neural Engineering*, *7*(2), 026001. doi: 10.1088/1741-2560/7/2/026001

Zaehle, T., Rach, S., & Herrmann, C. S. (2010). Transcranial alternating current stimulation enhances individual alpha activity in human EEG. *PLoS ONE*, *5*(11), 13766. doi: 10.1371/journal.pone.0013766

Zaehle, T., Sandmann, P., Thorne, J. D., Jäncke, L., & Herrmann, C. S. (2011). Transcranial direct current stimulation of the prefrontal cortex modulates working memory performance: combined behavioural and electrophysiological evidence. *BMC Neuroscience*, *12*(1), 2. doi: 10.1186/1471-2202-12-2

Zaghi, S., Acar, M., Hultgren, B., Boggio, P. S., & Fregni, F. (2009). Noninvasive brain stimulation with low-intensity electrical currents: putative mechanisms of action for direct and alternating current stimulation. *The Neuroscientist*, *16*(3), 285–307. doi: 10.1177/1073858409336227

Zarkowski, P., Shin, C. J., Dang, T., Russo, J., & Avery, D. (2006). EEG and the variance of motor evoked potential amplitude. *Clinical EEG and Neuroscience*, *37*(3), 247–251. doi: 10.1177/155005940603700316

Zeharia, N., Hertz, U., Flash, T., & Amedi, A. (2015). New whole-body sensory-motor gradients revealed using phase-locked analysis and verified using multivoxel pattern analysis and functional connectivity. *Journal of Neuroscience*, *35*(7), 2845–2859. doi: 10.1523/jneurosci.4246-14.2015

Zhang, Y., Chapman, A.-M., Plested, M., Jackson, D., & Purroy, F. (2012). The incidence, prevalence, and mortality of stroke in France, Germany, Italy, Spain, the

UK, and the US: a literature review. *Stroke Research and Treatment*, *2012*, 1–11. doi: 10.1155/2012/436125

Zhang, Y., Chen, Y., Bressler, S. L., & Ding, M. (2008). Response preparation and inhibition: the role of the cortical sensorimotor beta rhythm. *Neuroscience*, *156*(1), 238–246. doi: 10.1016/j.neuroscience.2008.06.061

Ziemann, U., Reis, J., Schwenkreis, P., Rosanova, M., Strafella, A., Badawy, R., & Müller-Dahlhaus, F. (2015). TMS and drugs revisited 2014. *Clinical Neurophysiology*, *126*(10), 1847–1868. doi: 10.1016/j.clinph.2014.08.028

Zilles, K., & Amunts, K. (2010). Centenary of Brodmann's map — conception and fate. *Nature Reviews Neuroscience*, *11*(2), 139–145. doi: 10.1038/nrn2776

Zilles, K., & Amunts, K. (2011). Architecture of the cerebral cortex. In M. Juergen K & G. Paxinos (Eds.), *The human nervous system* (pp. 836–896). London: Elsevier Science. doi: 10.1016/B978-0-12-374236-0.10023-9

Zilles, K., Schlaug, G., Matelli, M., Luppino, G., Schleicher, A., Qü, M., ... Roland, P. E. (1995). Mapping of human and macaque sensorimotor areas by integrating architectonic, transmitter receptor, MRI and PET data. *Journal of Anatomy*, *187*(Pt 3), 515. Retrieved from https://www.ncbi.nlm.nih.gov/pmc/articles/PMC1167457/pdf/janat00131-0004.pdf